Correlated Trajectories in Semiclassical Approaches to Quantum Chaos

Jack Anton Kuipers

School of Mathematics

March 2008

A dissertation submitted to the University of Bristol in accordance with the requirements of the degree of Doctor of Philosophy in the Faculty of Science

Word count: thirty-nine thousand

Abstract

This thesis is concerned with the application and extension of semiclassical methods, involving correlated trajectories, that were recently developed to explain the observed universal statistics of classically chaotic quantum systems. First we consider systems that depend on an external parameter that does not change the symmetry of the system. We study correlations between the spectra at different values of the parameter, a scaled distance x apart, via the parametric spectral form factor $K(\tau, x)$. Using a semiclassical periodic orbit expansion, we obtain a small τ expansion that agrees with random matrix theory for systems with and without time reversal symmetry. Then we consider correlations of the Wigner time delay in open systems. We study a form factor $K(\tau, x, y, M)$ that depends on the number of scattering channels M, the non-symmetry breaking parameter difference x and also a symmetry breaking parameter y. The Wigner time delay can be expressed semiclassically in terms of the trapped periodic orbits of the system, and using a periodic orbit expansion we obtain several terms in the small τ expansion of the form factor that are identical to those calculated from random matrix theory. The Wigner time delay can also be expressed in terms of scattering trajectories that enter and leave the system. Starting from this picture, we derive all terms in the periodic orbit formula and therefore show how the two pictures of the time delay are related on a semiclassical level. A new type of trajectory correlation is derived which recreates the terms from the trapped periodic orbits. This involves two trajectories approaching the same trapped periodic orbit closely - one trajectory approaches the orbit and follows it for several traversals, while its partner approaches in almost the same way but follows the periodic orbit an additional number of times.

Acknowledgements

I would like to thank my supervisor, Martin Sieber, for all his help and guidance over the last few years, as well as his comments on this manuscript. I am also indebted to Jon Keating, Francesco Mezzadri, Sebastian Müller and Jon Robbins for useful discussions and encouragement. I wish to thank Alfredo Ozorio de Almeida and Raúl Vallejos for their hospitality during my visit to the CBPF.

I am grateful to my mum and Paul for their help with editing this manuscript. I am also profoundly thankful to my parents for all they have done for me.

Finally I wish to thank Giusi, not only for her careful reading of this thesis and helpful suggestions for improving its readability, and her help producing the Figures, but also for her immeasurable support.

Author's Declaration

I declare that the work in this dissertation was carried out in accordance with the Regulations of the University of Bristol. The work is original except where indicated by special reference in the text. No part of the dissertation has been submitted for any other academic award. All views expressed in the dissertation are those of the Author.

SIGNATURE

DATE

Contents

List of Tables

List of Figures

Introduction

Chaotic systems are typified by a sensitivity to initial conditions so that small changes or perturbations grow exponentially, possibly leading to significantly different outcomes. When the system is bound, so that trajectories cannot escape, any region in the available space, if evolved for a sufficiently long time, will become spread (evenly) over the available space. Also, any uncertainty in the past is magnified so that the future effectively becomes random. Physically, any measurement has an uncertainty, such that while it may be possible to calculate the evolution for a certain time, this eventually gives way to randomness. However, this randomness is also liberating in the sense that it is a universal property of all chaotic systems. Therefore, instead of concentrating on the local, system-dependent, behaviour of trajectories, we can examine global properties of all systems.

When we study a quantum system whose classical counterpart is chaotic we face the issue that quantum mechanics involves linear operators that do not generate chaos. However, the correspondence principle states that quantum mechanics should reproduce classical mechanics in the limit of large quantum numbers. The linear operators, like the energy operator (the Hamiltonian), turn the quantum mechanics into an eigenvalue problem where the eigenvalues provide the range of values we could possibly measure for the quantity of interest. For bound systems the eigenvalues are discrete, and the energy eigenvalues essentially encode the quantum evolution. Quantum chaos is concerned with the task of understanding how the chaotic behaviour of a system's classical counterpart manifests itself in the system's linear quantum mechanics. The two regimes are linked by the semiclassical

limit $\hbar \to 0$, and in this limit, we can explore the quantum mechanics in terms of entirely classical quantities. The semiclassical approximation, embodied in the trace formula of Gutzwiller (1971), allows us to express the energy spectrum, a feature of a quantum system, in terms of periodic orbits (features of a classically chaotic system).

Periodic orbits repeat the same motion over again after each period. This regularity seems to run contrary to chaotic behaviour, but periodic orbits are an essential feature of classical chaos. Although they have zero measure, being infinitely outnumbered by aperiodic trajectories, their number grows exponentially with their period and they are dense. This means that we can find a periodic orbit arbitrarily close to any point on the energy shell (the available phase space). Periodic orbits are unstable, so if we examine the evolution of a trajectory that passes through a given point and a periodic orbit passing nearby, then the difference between them grows in time. However, then we will be able to find a new periodic orbit close to the trajectory. Because of this, we can approximate any trajectory by 'stitching' together pieces of many different periodic orbits. In some sense, the periodic orbits encode the dynamics of the system and, in the semiclassical limit, via the trace formula, also provide information about the quantum energy spectrum.

In classical chaos, uncertainties can result from physical measurements or a lack of numerical precision, hence the exponential expansion of differences in the evolution of the system will practically make the future random. If there were no uncertainties, and we knew the conditions of some point exactly, we could then follow its deterministic evolution forever. In quantum mechanics, uncertainties are inherent due to the Heisenberg uncertainty principle, which means that there is a minimum size beyond which we cannot measure or investigate. The time scale by which this minimum size expands enough for the classical behaviour to be effectively treated as random is called the Ehrenfest time, and beyond it we can study the global universal behaviour. The idea that all quantum chaotic systems display universal properties is embodied in a conjecture of Bohigas et al. (1984). This conjecture states that the statistics of quantum chaotic systems will agree with the statistics of random

matrices that possess a symmetry corresponding to the physical symmetry of the system. Each quantum operator can be expressed as a matrix and its spectrum is given by the eigenvalues of the matrix. This conjecture then means that the exact dynamics of the system and the entries of the matrix are unimportant to the statistics, and only the symmetries matter. We examine this background to quantum chaos in Chapter 1.

As well as being able to describe the statistics of quantum chaotic systems by comparison to random matrices, we can also use trace formulae to describe them in terms of periodic orbits. The statistics of the energy levels can be described by correlation functions and, semiclassically, these are given by multiple sums over periodic orbits. In particular, the two-point correlation function, and its Fourier transform the spectral form factor $K(\tau)$, are given by double sums over periodic orbits. To recreate results from Random Matrix Theory (RMT), we need to consider pairs of orbits that are linked in some way. Orbits are clearly linked to themselves and the contribution of these pairs was calculated by Berry (1985) and gave the leading order RMT result for small values of the parameter τ of the form factor. Orbits with 'self-encounters' discovered by Sieber and Richter (2001) provided the next order term, and they involve an orbit that approaches itself closely in an encounter. Outside of the encounter, the orbit consists of two long loops that connect the parts of the orbit that are close together in the encounter. A partner orbit could be constructed that crosses the encounter in a different way, so that it follows one loop in the same direction and the other loop in the opposite direction to the original orbit. Such a partner can only exist with time reversal symmetry, but because it follows the rest of the orbit almost exactly (up to time reversal) it is highly correlated with the original orbit. Extending this idea, Müller et al. (2004, 2005) derived the full expansion, semiclassically, of the form factor. This expansion was for small values of the variable $\tau < 1$, corresponding to correlation lengths greater than the average spacing between energy levels.

As the work of this thesis is based on correlations between periodic orbits of classically chaotic systems and how they relate to quantum statistics, we consider

the calculation of the form factor in some detail in Chapter 2. This will complete our review of the background we need for the rest of the thesis. Hence we will have the elements we need to consider the application of these methods in novel situations.

The first such situation we examine covers parametric correlations due to varying an external parameter of the system (that preserves its symmetry). This application is covered in Chapter 3, where we show that we find exact agreement with small τ RMT results, and this work was published in Kuipers and Sieber (2007a). In Appendix A we present a derivation of the agreement to all orders for systems without time reversal symmetry. We also present an alternative derivation of this agreement in Appendix B, which relates to the work on quantum transport (Chapter 5).

We then apply similar ideas to open systems, for example to chaotic cavities which have scattering leads attached. We consider a particular quantity, the Wigner time delay, for which semiclassical methods provide two descriptions. One in terms of trajectories that enter and then leave the system, and the other in terms of periodic orbits that remain trapped inside. In Chapter 4 we consider the description in terms of the trapped periodic orbits. In Section 4.1 we examine the form factor for the time delay and in Section 4.2 we cover parametric correlations. We also consider the effect of a parameter that breaks the symmetry of the system. This is covered in Section 4.3 and involves including the ideas of Saito and Nagao (2006) and Nagao et al. (2007). This final result encompasses, in the right limits, all the other results of Chapters 3 and 4, which all agree with the small τ expansion of RMT results discussed in Section 4.4. These results for the time delay were published in Kuipers and Sieber (2007b).

We then, in Chapter 5, turn our attention to the description in terms of scattering trajectories. Besides the Wigner time delay, this framework is capable of describing other scattering quantities like the conductance. We introduce this framework by studying parametric correlations of the conductance in Section 5.2 before considering the Wigner time delay again. The contribution of correlated trajectories with self-encounters allows us to recreate the average time delay in Section 5.3. Furthermore we consider a correlation function of the time delay. Finally, in Section 5.4, we

show how the two pictures for the time delay are equivalent semiclassically by recreating the periodic orbit form from the scattering trajectory picture. This requires a new type of correlation markedly different from trajectories with self-encounters. Instead, trajectories which are captured by a trapped periodic orbit, and follow it for several traversals before leaving, are shown to be highly correlated with (partner) trajectories that follow the orbit an additional number of times. This work has been submitted for publication (Kuipers and Sieber, 2007c).

1 Quantum Chaos

In this thesis we consider quantum systems whose classical counterparts are chaotic. Chaotic systems are deterministic, but small differences between trajectories grow exponentially, so that their long term behaviour can effectively be considered as stochastic. We consider the properties of chaotic systems in Section 1.1 before exploring their quantum mechanical counterparts in Section 1.2. Moreover, in the semiclassical limit, quantum quantities can be related to the classical motion, as we see in Section 1.3. This background is comprehensively reviewed by Gutzwiller (1990) and Cvitanović et al. (2005), and here we focus on those parts that are relevant for this thesis. In Section 1.4 we see how the quantum mechanics of a system can also be expressed using a Hermitian matrix, which must be symmetric if the system has time reversal symmetry. Some properties of quantum systems are related to the eigenvalues of these matrices, and the behaviour of the eigenvalues can then be modelled in terms of random matrices, which we consider in Section 1.5. An overview of the use of both RMT and semiclassics for quantum chaotic systems is provided by Haake (2000), while random matrices are covered by Mehta (2004). These concepts will thus be outlined below rather than reviewed in detail.

1.1 Classical chaotic motion

In order to introduce the properties of chaotic systems, we will consider a classical dynamical system with f degrees of freedom which is a Hamiltonian flow. The dynamics is determined by the Hamiltonian $H(\boldsymbol{q}, \boldsymbol{p})$ and Hamilton's equations of motion

$$\dot{q}_i = \frac{\partial H}{\partial p_i}, \quad \dot{p}_i = -\frac{\partial H}{\partial q_i}, \quad i = 1 \dots f \qquad (1.1.1)$$

where $\boldsymbol{q} = (q_1, \dots, q_f)$ is a vector of the configuration space coordinates, and $\boldsymbol{p} = (p_1, \dots, p_f)$ the conjugate momenta. The solutions to these equations consist of trajectories, through the $2f$-dimensional phase space $\boldsymbol{x} = (\boldsymbol{q}, \boldsymbol{p})$, which have the form $\zeta = \boldsymbol{x}(t)$. When there is no time dependence in the Hamiltonian, the energy E of the system is conserved and the solutions live in the $(2f - 1)$-dimensional energy surface (shell) defined by

$$H(\boldsymbol{q}, \boldsymbol{p}) = E \qquad (1.1.2)$$

Along each trajectory, at each point $\boldsymbol{x}(t)$ we can define a Poincaré surface of section, which is $(2f - 2)$-dimensional. In order to focus on the behaviour of the system near the trajectory we pick a surface of section which is 'orthogonal' to the trajectory, and we investigate the local motion in the surface as it is moved along the trajectory. This allows us to examine one of the characterizing properties of chaotic systems, hyperbolicity.

1.1.1 Hyperbolicity

To describe the hyperbolicity of a chaotic system we analyse the linearized motion about a given trajectory. If the trajectory starts at a point $\boldsymbol{x}(0)$ and we let it evolve for a certain time t to the point $\boldsymbol{x}(t)$, then a small displacement $\delta\boldsymbol{x}(0)$ in the Poincaré surface at $\boldsymbol{x}(0)$ is mapped to a small displacement $\delta\boldsymbol{x}(t)$ in the Poincaré section at $\boldsymbol{x}(t)$ according to the following equation

$$\delta\boldsymbol{x}(t) \approx M(\boldsymbol{x}(0), t)\delta\boldsymbol{x}(0) \qquad (1.1.3)$$

This first order approximation of the motion involves the stability matrix $M(\boldsymbol{x}(0), t)$, with entries defined as

$$M_{ij}(\boldsymbol{x}(0), t) = \frac{\partial(\delta x_i(t))}{\partial(\delta x_j(0))}\bigg|_{\boldsymbol{x}(0)}, \quad i, j = 1 \dots 2f - 2 \qquad (1.1.4)$$

8

The $(2f - 2)$ eigenvalues, $\Lambda(\boldsymbol{x}(0), t)$, of this stability matrix determine the local dynamical behaviour of the system, and for Hamiltonian flows, they come in $(f - 1)$ pairs

$$\Lambda_i(\boldsymbol{x}(0), t), \Lambda_i(\boldsymbol{x}(0), t)^{-1}, \quad i = 1 \ldots f - 1 \tag{1.1.5}$$

where $|\Lambda_i(\boldsymbol{x}(0), t)| > 1$ for chaotic systems. This property is called hyperbolicity, and it indicates that it is possible to find $(f-1)$ pairs of stable and unstable coordinates, where the local motion in each pair follows a hyperbola. The $|\Lambda_i(\boldsymbol{x}(0), t)|$ are called stretching factors and the Lyapunov exponents can be defined in terms of these stretching factors as

$$\lambda_i(\boldsymbol{x}(0)) = \lim_{t \to \infty} \frac{1}{t} \ln(|\Lambda_i(\boldsymbol{x}(0), t)|) \tag{1.1.6}$$

so that $|\Lambda_i(\boldsymbol{x}(0), t)| \sim e^{\lambda_i(\boldsymbol{x}(0))t}$. As we will see in section 1.1.3, chaotic systems also have the property of ergodicity, which means that the Lyapunov exponents will coincide with global values λ_i for almost all trajectories. The largest exponent λ dominates the local stretching for long times (for almost all trajectories).

1.1.2 Periodic orbits

A periodic orbit γ is a trajectory in the energy shell that repeats its motion after some time T, so that

$$\boldsymbol{x}(t) = \boldsymbol{x}(t + T) \tag{1.1.7}$$

holds for all times t. The minimum (positive) time T_γ for which this holds, is the period of the orbit. The orbit follows a closed loop in the energy shell returning to the same point after each period, and this provides us with a natural time scale to study motion near the periodic orbit. We take a point along the orbit and place a Poincaré section orthogonal to the trajectory there. The system evolves in such a way that a local neighbourhood of the orbit is transported around the whole periodic orbit until it returns to the Poincaré section. Because it passes along every point of the periodic orbit, the eigenvalues of the stability matrix of this transport, M_γ, do not depend on the starting point, and they are an invariant property of the orbit.

9

They provide the $(f-1)$ pairs $|\Lambda_{\gamma,i}|$, $|\Lambda_{\gamma,i}|^{-1}$ of stretching and contracting factors of the orbit. Hence we can find the Lyapunov exponents $\lambda_{\gamma,i}$ of the periodic orbit following $|\Lambda_{\gamma,i}| = e^{\lambda_{\gamma,i}T_\gamma}$.

For systems with only 2 degrees of freedom, in the linearized approximation, the eigenvectors of M_γ define a pair of unstable and stable directions. After being transported around the periodic orbit once, a point with coordinates (u,s) in those directions, hits the Poincaré section again at the point (u',s'). These two points can be related to each other through the stability matrix as

$$u' = \Lambda_\gamma u, \quad s' = \Lambda_\gamma^{-1}s \tag{1.1.8}$$

and it is clear that the points follow the hyperbolic motion associated with chaos. Due to hyperbolicity, the two eigenvalues, which as we have seen are the inverse of each other, need to be real. If they are negative we obtain a reflection about the axes after each traversal of the periodic orbit and the intersection points switch from one half of the hyperbola to the other. The analysis above for the linearized approximation can be extended to general dynamical systems where the stable and unstable manifolds are not straight lines but complicated curves. Due to the Birkhoff-Moser theorem (see Ozorio de Almeida, 1988, for example), we can make a change of coordinates to normal form coordinates which lie along the stable and unstable manifolds. In terms of these coordinates, the hyperbolic mapping from the Poincaré section to itself still has the simple form

$$u' = \Lambda_\gamma[U(s,u)]u, \quad s' = \Lambda_\gamma^{-1}[U(s,u)]^{-1}s \tag{1.1.9}$$

where the U is a measure of the non-linearity and tends to 1 as $su \to 0$, meaning that we recover true hyperbolae as we approach the axes.

When we consider systems with higher degrees of freedom $(f > 2)$ in the linearized approximation, the eigenvalues of M_γ need no longer be real. We still have $(f-1)$ pairs of eigenvalues, but if an eigenvalue Λ is complex, then it is part of a

loxodromic quartet because Λ^*, $\frac{1}{\Lambda}$ and $\frac{1}{\Lambda^*}$ must also be eigenvalues.

For a particular loxodromic quartet j, we can write the four eigenvalues in the form $\mathrm{e}^{\pm\lambda_{\gamma,j}T_\gamma \pm \mathrm{i}\phi_{\gamma,j}}$, where $\lambda_{\gamma,j} > 0$. The eigenvectors are also complex and come in conjugate pairs, so to make the motion clear we split the quartet into a stable and unstable part. The eigenvalues $\mathrm{e}^{\lambda_{\gamma,j}T_\gamma \pm \mathrm{i}\phi_{\gamma,j}}$ and one of their eigenvector pair give the unstable part, and their inverses the stable part. In the following we focus (as in Ozorio de Almeida, 1988) on the eigenvector associated to the unstable eigenvalue $\mathrm{e}^{\lambda_{\gamma,j}T_\gamma + \mathrm{i}\phi_{\gamma,j}}$ with a positive sign in front of the phase $\phi_{\gamma,j}$. Its real and imaginary part span the two-dimensional unstable plane. In this plane, after each iteration of the periodic orbit, all points increase their distance from the origin by a factor of $|\Lambda_{\gamma,j}|$, as well as rotating clockwise by an angle of $\phi_{\gamma,j}$. The points then spiral out in this plane at the same time as they spiral inwards in the stable plane. We can define (non-invariant) stable and unstable directions that rotate (at the same rate as points in the planes) as we move around the periodic orbit (Turek et al., 2005). In a system of coordinates along these directions, points would move along straight lines in each plane as they are transported around the periodic orbit, and we can separate the quartet into two pairs of stable and unstable directions. In fact, this rotation also happens when an eigenvalue is real and negative, but then the rotation is given by π.

Remaining in the linearized approximation, for each loxodromic quartet of eigenvalues we have a stable and unstable plane, and for each real pair of eigenvalues a stable and unstable eigenvector. The stable manifold of the periodic orbit is the space spanned by all the stable planes and eigenvectors, while the unstable manifold is the $(f-1)$ dimensional hyperplane spanned by the unstable equivalents. Returning to general dynamics, the stable and unstable manifolds are no longer flat hyperplanes but complicated curved surfaces, but again we can rectify them using normal form coordinates. Then we can span this normal form space with $(f-1)$ pairs of (possibly rotating) coordinates. The mapping from the Poincaré section to itself for a point $(\boldsymbol{u}, \boldsymbol{s})$ in these coordinates has a simple hyperbolic form for each of its component parts (u_i, s_i).

1.1.3 Ergodicity and mixing

As well as hyperbolicity, chaotic systems are also characterized by the property of ergodicity (see Cvitanović et al., 2005; Ozorio de Almeida, 1988, for example). This means that a typical trajectory in the system will explore the whole of the available phase space. Moreover, it will do so uniformly (with respect to an invariant measure of the system). The probability that a trajectory enters a particular region of the energy shell (in a certain time interval) is independent of the position of the region. Also, starting from a given region, the position of the trajectory after a sufficiently long time can be considered as a uniform random variable over the available phase space. In a certain sense, this is equivalent to saying that the past is irrelevant for the present, even though given the deterministic nature of the evolution they are clearly related.

A system with a certain measure is ergodic if all sets invariant under time evolution have full or zero measure. The natural measure for Hamiltonian systems is the Liouville measure $\mathrm{d}\boldsymbol{y} = \mathrm{d}\boldsymbol{x}\delta(H(\boldsymbol{x}) - E)$ where $\boldsymbol{y}$ is a coordinate in the energy shell. The volume of the energy shell is $\Omega = \int \mathrm{d}\boldsymbol{y}$, and the Liouville measure is uniform on it. The whole energy shell is invariant, as the evolution is volume preserving, and obviously has full measure. The periodic orbits are also invariant, because they repeat the same motion each period, but they have zero measure.

An important consequence of the ergodicity of chaotic systems is that, due to the ergodic theorem, the averages over long trajectories are simplified. Firstly, if we measure some function $F(\boldsymbol{x})$ along the trajectory $\boldsymbol{x}(t)$, then the time average

$$\frac{1}{T} \int_0^T \mathrm{d}t \, F(\boldsymbol{x}(t)) \tag{1.1.10}$$

should be independent of the starting point $\boldsymbol{x}(0)$ in the limit as $T \to \infty$. Secondly, since almost all trajectories explore the available phase space uniformly, then for them, this average should be the same as an energy shell average over the Liouville measure. Ergodicity implies that both averages are equivalent

$$\lim_{T \to \infty} \frac{1}{T} \int_0^T \mathrm{d}t \, F(\boldsymbol{x}(t)) = \frac{1}{\Omega} \int \mathrm{d}\boldsymbol{y} \, F(\boldsymbol{y}) \qquad (1.1.11)$$

However, this property only holds for almost all trajectories, and it does not hold for the trajectories we are interested in, the periodic orbits (which as noted before have zero measure). Individual periodic orbits, by definition, cyclically repeat a given closed path and this is the only part of the energy shell that they can explore. If, however, we examine orbits of a similar period, as a group they will tend to explore the energy shell uniformly as their period (and hence their number) increases. In order to average over this ensemble of orbits (with a proper weighting) we can use the uniform distribution of orbits on the energy shell, in the form of the sum rule of Hannay and Ozorio de Almeida (1984) and its generalisation, the equidistribution theorem, and replace the average over the orbits with an energy shell average. We will examine this in more detail in section 1.3.4.

As well as ergodicity, chaotic systems have a stronger property called mixing. In this thesis, we only consider 'hard' or fully chaotic systems which have all of these properties. An important consequence of mixing is that a small region around a typical trajectory will also, after long times, cover the energy shell uniformly. In essence, points in a given region can go anywhere in the energy shell and could have come from anywhere, so information about their history and future is unimportant.

Moreover, if we take any (open) set in our phase space A_1 and evolve it for time t to the set $A_1(t)$ then as $t \to \infty$ this set will be uniform across phase space (with respect to the invariant measure). The size of its intersection with any other (open) set A_2 thus depends only on the size of A_1 and the fraction of the size of A_2 relative to the whole phase space volume Ω. With respect to the Liouville measure this is

$$\lim_{t \to \infty} \frac{1}{\Omega} \int_{A_2 \cap A_1(t)} \mathrm{d}\boldsymbol{y} = \frac{1}{\Omega} \int_{A_2} \mathrm{d}\boldsymbol{y} \, \frac{1}{\Omega} \int_{A_1} \mathrm{d}\boldsymbol{y} \qquad (1.1.12)$$

If we set $A_2 = A_1$, we can see how time evolution decorrelates the set from its future image, and how a trajectory and its neighbourhood effectively forget the past over long time scales.

As opposed to hyperbolicity which determines the local evolution, it is clear from the discussion above that ergodicity and mixing are global properties. Locally we know the exact evolution of a region - it is compressed and stretched according to hyperbolicity - but once this stretching makes the region longer than the typical length scales of the system, the information about the past loses its importance and, depending on the situation, we might equally well treat the evolution as a stochastic process.

1.2   Quantum mechanics

When we consider the quantum version of a classical system, we replace our trajectory in the classical phase space by a trajectory in the complex Hilbert space of the system. The state of the system $|\psi(t)\rangle$, defined only up to a phase factor, evolves in time under the quantum Hamiltonian operator $\hat{H}$ following the Schrödinger equation

$$i\hbar \frac{\mathrm{d}}{\mathrm{d}t}|\psi(t)\rangle = \hat{H}|\psi(t)\rangle \tag{1.2.1}$$

If, as we assumed for the classical case, the Hamiltonian operator does not depend on time, then we can separate out the time dependence, and just consider the time-independent Schrödinger equation

$$\hat{H}|\phi\rangle = E|\phi\rangle \tag{1.2.2}$$

This is simply an eigenvalue problem, where the eigenvectors form the basis of the Hilbert space and the eigenvalues represent the energy of the system. To get a handle on the problem, we can consider a particular representation, for example, the position representation. With this change of viewpoint, the state vectors become functions of the position $\boldsymbol{q}$, and we look for the eigenfunctions and eigenvalues of

$$\hat{H}\phi_n(\boldsymbol{q}) = E_n\phi_n(\boldsymbol{q}) \tag{1.2.3}$$

Finding the quantum Hamiltonian involves substituting $-i\hbar\partial_{\boldsymbol{q}}$ for the momentum $\boldsymbol{p}$ in the classical Hamiltonian. However, this does not commute with the position, so we must select a suitable order of products in the Hamiltonian, for example the Weyl ordering. Starting from a classical system then, we find the differential operator $\hat{H}$ using this substitution and try to obtain the solutions to the eigenvalue problem which satisfy physically sensible boundary and continuity conditions. The time evolution of each eigenfunction is given by

$$\psi_n(\boldsymbol{q}, t) = e^{-\frac{i}{\hbar}E_n t}\phi_n(\boldsymbol{q}) \tag{1.2.4}$$

In the classical setting we had a compact energy shell, which corresponds to a bound quantum system. The eigenvalue spectrum is then discrete, and we can normalise the eigenfunctions which form an orthogonal and complete set. The eigenvalues of the Hamiltonian operator are the energy levels of the system. Other physical observables are also represented by Hermitian operators, and have their own eigenvalues that give the possible outcomes of a physical measurement.

1.2.1 Density of states

We now focus on a particular observable, the energy E, whose discrete spectrum gives a set of real values, E_n. The counting (or spectral staircase) function $N(E)$ is defined as the number of states less than the real energy variable

$$N(E) = \#\{n : E_n < E\} = \sum_n \Theta(E - E_n) \tag{1.2.5}$$

where Θ is the Heaviside step function. The staircase function $N(E)$ will have a step at each energy level E_n and is represented in Figure 1.1.

'Differentiating' the counting function, with respect to energy, we obtain the density of states which is thus given by a Dirac delta function at each of the values of E_n

$$d(E) = \sum_n \delta(E - E_n) \tag{1.2.6}$$
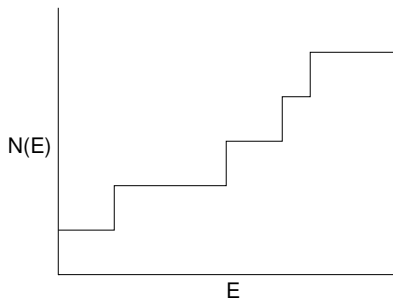
Figure 1.1: Representation of the counting function $N(E)$.
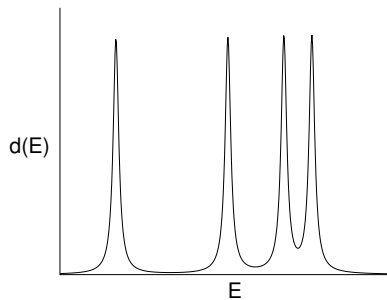
Figure 1.2: Representation of the density of states $d(E)$. The delta functions have been smoothed for clarity.

This is qualitatively represented in Figure 1.2, and can be considered to consist of two parts: a smooth part $\bar{d}(E)$ and an oscillating part $d^{\mathrm{osc}}(E)$

$$d(E) = \bar{d}(E) + d^{\mathrm{osc}}(E) \tag{1.2.7}$$

The smooth part of the density of states is the local average density of energy levels, while the oscillating part gives the fluctuations around this average.

1.2.2 Spectral form factor

One way of comparing energy level statistics of different systems is to consider correlation functions of the density of states. In order to compare different systems we need to rescale the energy parameter to be system independent. To do this we define a new energy parameter $\tilde{E}$ as the mean part of the counting function

$$\tilde{E} = \bar{N}(E) \tag{1.2.8}$$

In terms of this new variable, the unfolded density of states $\tilde{d}(\tilde{E})$ has a mean value of one. For universal correlation functions, we compare the unfolded density of states at energies a distance ω apart. For example, the two-point correlation function could be defined as

$$R_2'(\omega) = \left\langle \tilde{d}\left(\tilde{E} + \frac{\omega}{2}\right) \tilde{d}\left(\tilde{E} - \frac{\omega}{2}\right) \right\rangle_{\tilde{E}} \tag{1.2.9}$$

Because of the delta functions in the density of states, we have to average over a range of energies $\Delta \tilde{E}$ around the energy $\tilde{E}$ to obtain a useful function (see Berry, 1985). The delta functions are either zero or infinite spikes, so in order to smooth the correlation function, we need to average over a (semiclassically) large number of energy levels. As the unfolded levels are on average 1 apart, this requirement can be expressed as $\Delta \tilde{E} \gg 1$. If we average over too large an energy range, however, we lose the local information that we are interested in. In addition, for the semiclassical approximations we will use, we require that classical quantities do not vary too much over the energy range, or that the energy range is classically small ($\Delta \tilde{E} \ll \tilde{E}$). A problem with the definition of the two-point correlation function as given in equation (1.2.9) is that it diverges at small ω. In fact we have a product of two delta functions so even after the energy averaging it diverges like the delta function

$$\delta(\omega) \left\langle \tilde{d} \right\rangle_{\tilde{E}} = \delta(\omega) \tag{1.2.10}$$

This divergence can be removed by subtracting this term, and we define the two-point correlation function as

$$R_2(\omega) = \left\langle \tilde{d} \left(\tilde{E} + \frac{\omega}{2} \right) \tilde{d} \left(\tilde{E} - \frac{\omega}{2} \right) \right\rangle_{\tilde{E}} - \delta(\omega) \tag{1.2.11}$$

If we write the density of states as a sum of its smooth and oscillating parts (equation (1.2.7)), and substitute into equation (1.2.11), we can use the fact that

$$\left\langle \tilde{d}^{\mathrm{osc}}(\tilde{E}) \right\rangle_{\tilde{E}} = 0 \tag{1.2.12}$$

to simplify the correlation function to

$$R_2(\omega) = 1 + \left\langle \tilde{d}^{\mathrm{osc}} \left(\tilde{E} + \frac{\omega}{2} \right) \tilde{d}^{\mathrm{osc}} \left(\tilde{E} - \frac{\omega}{2} \right) \right\rangle_{\tilde{E}} - \delta(\omega) \tag{1.2.13}$$

This form of the correlation function contains the constant 1 from the smooth part squared, the delta function to remove the divergence and the irreducible two-point correlation function

$$\tilde{R}_2(\omega) = \left\langle \tilde{d}^{\text{osc}}\left(\tilde{E} + \frac{\omega}{2}\right) \tilde{d}^{\text{osc}}\left(\tilde{E} - \frac{\omega}{2}\right) \right\rangle_{\tilde{E}} \tag{1.2.14}$$

The unfolded density of states is related to the original density of states by

$$\tilde{d}(\tilde{E}) = \frac{\partial N(E)}{\partial E}\frac{\partial E}{\partial \tilde{E}} = \frac{d(E)}{\bar{d}(E)} \tag{1.2.15}$$

We can therefore express the irreducible two-point correlation function in terms of the original density of states and energy variable as

$$\tilde{R}_2(\omega) = \left\langle \frac{d^{\text{osc}}\left(E + \frac{\omega}{2\bar{d}}\right) d^{\text{osc}}\left(E - \frac{\omega}{2\bar{d}}\right)}{\bar{d}^2} \right\rangle_E \tag{1.2.16}$$

In the original energy variable E, the average is over a range ΔE around E satisfying $E \gg \Delta E \gg \frac{1}{\bar{d}(E)}$. We also consider the Fourier transform of the irreducible two-point correlation function, known as the spectral form factor

$$K(\tau) = \int d\omega \, \tilde{R}_2(\omega) e^{-2\pi i\omega\tau} \tag{1.2.17}$$

which can also be written in terms of the two-point correlation function as

$$K(\tau) = 1 + \int d\omega \, (R_2(\omega) - 1) e^{-2\pi i\omega\tau} \tag{1.2.18}$$

where the 1 cancels the Fourier transform of the subtracted delta function. The variable τ in the transform is conjugate to the unfolded energy separation ω and corresponds to a dimensionless time quantity scaled by the Heisenberg time, which is given by $T_{\text{H}} = 2\pi\hbar\bar{d}(E)$. A time corresponding to the Heisenberg time ($\tau = 1$), is therefore conjugate to the mean level spacing. As we have a pair of Fourier

conjugate variables, the behaviour of the correlation function at large correlation distances (compared to the mean level separation) corresponds to the behaviour of the form factor at small τ and likewise short correlation distances to large τ. We shall see that these two regimes are different in the semiclassical limit. If we make the substitution $\omega = \bar{d}\eta$, we can also express the form factor in terms of an unscaled energy distance η as

$$K(\tau) = \left\langle \int \mathrm{d}\eta \, \frac{d^{\mathrm{osc}}\left(E + \frac{\eta}{2}\right) d^{\mathrm{osc}}\left(E - \frac{\eta}{2}\right)}{\bar{d}} \mathrm{e}^{\frac{-\mathrm{i}\eta}{\hbar}\tau T_{\mathrm{H}}} \right\rangle \tag{1.2.19}$$

1.2.3 Propagator and Green's function

Returning to quantum evolution, we follow Cvitanović et al. (2005) and explore a different description to set the stage for the semiclassical approximations in the next section. In the position representation, for a time-independent Hamiltonian, an arbitrary wavefunction $\psi(\boldsymbol{q}', t)$ can be expanded in the eigenfunction basis as

$$\psi(\boldsymbol{q}', t) = \sum_n c_n \mathrm{e}^{-\frac{\mathrm{i}}{\hbar}E_n t} \phi_n(\boldsymbol{q}') \tag{1.2.20}$$

where the evolution of each eigenfunction was given in equation (1.2.4). The c_n are the coefficients of the initial wavefunction $\psi(\boldsymbol{q}, 0)$ in the eigenfunction basis $\phi_n(\boldsymbol{q})$ given by the inner product

$$c_n = \int \mathrm{d}\boldsymbol{q} \, \phi_n^*(\boldsymbol{q}) \psi(\boldsymbol{q}, 0) \tag{1.2.21}$$

We can use these equations to express the quantum evolution, in terms of the propagator $K(\boldsymbol{q}', \boldsymbol{q}, t)$, as

$$\psi(\boldsymbol{q}', t) = \int \mathrm{d}\boldsymbol{q} \, K(\boldsymbol{q}', \boldsymbol{q}, t) \psi(\boldsymbol{q}, 0) \tag{1.2.22}$$

which propagates the initial state to the state at time t. By substituting equation (1.2.21) into equation (1.2.20) we get the following formula for the propagator

19

in terms of the eigenfunctions of the system

$$K(\boldsymbol{q}', \boldsymbol{q}, t) = \sum_n \phi_n^*(\boldsymbol{q}) e^{-\frac{i}{\hbar} E_n t} \phi_n(\boldsymbol{q}') \qquad (1.2.23)$$

The propagator satisfies the Schrödinger equation, and also a boundary condition representing the fact that the state remains on its starting position if it is evolved for no time

$$\lim_{t \to 0} K(\boldsymbol{q}', \boldsymbol{q}, t) = \sum_n \phi_n^*(\boldsymbol{q}) \phi_n(\boldsymbol{q}') = \delta(\boldsymbol{q}' - \boldsymbol{q}) \qquad (1.2.24)$$

where the last step follows from the completeness of the eigenfunctions. The propagator corresponds to taking a state concentrated at a point $\boldsymbol{q}$, evolving it forward for time t and finding the new concentration at position $\boldsymbol{q}'$. If we evolve a state for time t_1 and then time t_2, the propagator for the total time $t = t_1 + t_2$ is given by

$$K(\boldsymbol{q}', \boldsymbol{q}, t) = \int \mathrm{d}\boldsymbol{q}_1 \, K(\boldsymbol{q}', \boldsymbol{q}_1, t_2) K(\boldsymbol{q}_1 \boldsymbol{q}, t_1) \qquad (1.2.25)$$

so that it evolves the state from $\boldsymbol{q}$ to an intermediary point $\boldsymbol{q}_1$ and then to the final position $\boldsymbol{q}'$ and we integrate over all possible intermediary points.

With no time dependence in the Hamiltonian, it is more instructive to switch to the energy picture by making a Laplace transform and considering the Green's function

$$G(\boldsymbol{q}', \boldsymbol{q}, E) = \frac{1}{i\hbar} \int_0^\infty \mathrm{d}t \, e^{\frac{i}{\hbar} E t} K(\boldsymbol{q}', \boldsymbol{q}, t) \qquad (1.2.26)$$

where we can add a small positive imaginary part $i\epsilon$ to the energy E to ensure the convergence of the integral.

We can write this Green's function in terms of the eigenfunctions of the system using the formula for the propagator in equation (1.2.23) to obtain

$$G(\boldsymbol{q}', \boldsymbol{q}, E) = \sum_n \frac{\phi_n^*(\boldsymbol{q}) \phi_n(\boldsymbol{q}')}{E - E_n} \qquad (1.2.27)$$

It is easy to see that if we take the trace of this Green's function we obtain a

pole at each of the energy levels

$$\text{Tr } G(E) = \int d\boldsymbol{q}\, G(\boldsymbol{q}, \boldsymbol{q}, E) = \sum_n \frac{1}{E - E_n} \tag{1.2.28}$$

due to the completeness of the eigenstates. In this form, the Green's function can now be related to the density of states. Observing that a Lorentzian of width ϵ

$$f(x) = \frac{\epsilon}{\pi} \frac{1}{[x^2 + \epsilon^2]} \tag{1.2.29}$$

approximates a Dirac delta function in the limit as ϵ tends to 0, and by writing the Lorentzian in a different way, we get the relation

$$\delta(x) = \lim_{\epsilon \to 0} -\frac{1}{\pi} \text{Im} \frac{1}{x + i\epsilon} \tag{1.2.30}$$

This allows us to express the density of states in terms of the trace of the Green's function

$$d(E) = \lim_{\epsilon \to 0} -\frac{1}{\pi} \text{Im Tr } G(E + i\epsilon) \tag{1.2.31}$$

1.3 Semiclassical approximations

In general, the full quantum mechanics of a system cannot be solved analytically, but we can gain insight into the behaviour by looking at the semiclassical regime. In the quantum mechanical equations we take the limit $\hbar \to 0$, and we can see that the differential evolution equations have a non-analytic singularity. However, due to the correspondence principle, we should arrive at classical mechanics on the other side of the singularity. In the semiclassical regime, as we shall see, the essence of the quantum mechanics is described by entirely classical quantities. Of course, $\hbar$ is a fixed physical constant, therefore in practice when taking the limit $\hbar \to 0$, we are studying the regime in which physical quantities, like the action, become large compared to $\hbar$.

1.3.1 Propagator and Green's function

To obtain the semiclassical approximation to the propagator, we start (see, for example, Gutzwiller, 1990) from Feynman's path integral form. The propagator can be obtained by combining propagators of shorter time as in equation (1.2.25), and Feynman (1948) considered splitting the time interval into N short steps, which we will assume to be equally long and denoted by t_ϵ (with $t = Nt_\epsilon$). This gives the following relation for the propagator

$$K(\boldsymbol{q}', \boldsymbol{q}, t) = \int \mathrm{d}\boldsymbol{q}_1 \ldots \mathrm{d}\boldsymbol{q}_{N-1} \, K(\boldsymbol{q}', \boldsymbol{q}_{N-1}, t_\epsilon) \ldots K(\boldsymbol{q}_1 \boldsymbol{q}, t_\epsilon) \tag{1.3.1}$$

where we integrate over the $N-1$ intermediate positions. In the limit where N becomes large, and the time of each step small, we can make a short time approximation for each propagator. For a particle of mass m moving under a potential $V(\boldsymbol{q})$, in Cartesian coordinates, the Hamiltonian is

$$\hat{H} = -\frac{\hbar^2}{2m}\Delta + V(\boldsymbol{q}) \tag{1.3.2}$$

where Δ is the Laplacian. The short time propagator is then given by

$$K(\boldsymbol{q}', \boldsymbol{q}, t_\epsilon) \approx \left(\frac{m}{2\pi \mathrm{i}\hbar t_\epsilon}\right)^{\frac{f}{2}} \mathrm{e}^{\frac{\mathrm{i}}{\hbar}\left(\frac{m(\boldsymbol{q}'-\boldsymbol{q})^2}{t_\epsilon} - V(\boldsymbol{q})t_\epsilon\right)} \tag{1.3.3}$$

where we have made approximations up to linear order in the small time step. These approximations include that the particle remains near the point $\boldsymbol{q}$ during the short time step, so the potential can be considered as constant over the small region, that the velocity is approximated by $\frac{\boldsymbol{q}'-\boldsymbol{q}}{t_\epsilon}$, and that we can commute the Laplacian and the potential.

When we substitute the short time propagator into equation (1.3.1) we obtain

$$K(\boldsymbol{q}', \boldsymbol{q}, t) \approx \int \mathrm{d}\boldsymbol{q}_1 \ldots \mathrm{d}\boldsymbol{q}_{N-1} \left(\frac{m}{2\pi \mathrm{i}\hbar t_\epsilon}\right)^{\frac{fN}{2}} \mathrm{e}^{\frac{\mathrm{i}t_\epsilon}{\hbar}\sum_{i=1}^{N}\left[\frac{m}{2}\left(\frac{\boldsymbol{q}_i - \boldsymbol{q}_{i-1}}{2t_\epsilon}\right)^2 - V(\boldsymbol{q}_{i-1})\right]}$$

$$\tag{1.3.4}$$

where $\boldsymbol{q}_0 = \boldsymbol{q}$ and $\boldsymbol{q}_N = \boldsymbol{q}'$. The term in the complex exponential includes the approximation to Hamilton's principle function (full action) evaluated along a polygonal path through all the intermediate points $\boldsymbol{q}_i$ at their respective times. The principle function is given by the integral

$$R(\boldsymbol{q}', \boldsymbol{q}, t) = \int_0^t \mathrm{d}t'\, L(\dot{\boldsymbol{q}}, \boldsymbol{q}), \quad L(\dot{\boldsymbol{q}}, \boldsymbol{q}) = \dot{\boldsymbol{q}}\boldsymbol{p} - H(\boldsymbol{q}, \boldsymbol{p}) \tag{1.3.5}$$

where $L(\dot{\boldsymbol{q}}, \boldsymbol{q})$ is the Lagrangian. Taking the limit $N \to \infty$, the integrals of equation (1.3.4) can be evaluated using a stationary phase approximation, and the stationary points of the principle function are trajectories travelling from $\boldsymbol{q}$ to $\boldsymbol{q}'$ in time t. Evaluating the integrals (Gutzwiller, 1967), we obtain the Van Vleck propagator

$$K(\boldsymbol{q}', \boldsymbol{q}, t) \approx \frac{1}{(2\pi\mathrm{i}\hbar)^{\frac{f}{2}}} \sum_\zeta |D_R|^{\frac{1}{2}} \mathrm{e}^{\frac{\mathrm{i}}{\hbar} R_\zeta(\boldsymbol{q}', \boldsymbol{q}, t) - \frac{\mathrm{i}\pi}{2} \tilde{\nu}_\zeta} \tag{1.3.6}$$

which is a sum over all classical trajectories ζ connecting $\boldsymbol{q}$ and $\boldsymbol{q}'$ in time t. D_R is the determinant of the matrix formed by the second derivative of the principle function with respect to the final and initial positions, or equivalently

$$D_R = \det \frac{\partial \boldsymbol{p}'}{\partial \boldsymbol{q}} \tag{1.3.7}$$

A geometrical interpretation of this determinant can be given as follows. Consider our classical trajectories starting at the point $\boldsymbol{q}$, with unfixed momentum due to the uncertainty principle. When a region of trajectories spanning a small volume $\delta\boldsymbol{p}$ in the momentum space is transported by the classical dynamics for a time t the trajectories end up spread over the volume $\delta\boldsymbol{q}$ in the position space around the point $\boldsymbol{q}'$. The ratio of the initial and final volume is the determinant in equation (1.3.7). The approximation for the semiclassical propagator fails, however, if D_R becomes too large along the trajectory ζ, or equivalently if its inverse becomes 0. The inverse depends on the Jacobean

$$J = \frac{\partial \boldsymbol{q}''}{\partial \boldsymbol{p}'} \tag{1.3.8}$$

23

which we evaluate for the moment up to an intermediate point $\boldsymbol{q}''$. Every time we reach a conjugate point, where more than one trajectory (from the initial momentum neighbourhood) has the same position coordinate $\boldsymbol{q}''$, at the same time, the determinant of this matrix becomes zero and the semiclassical approximation diverges. The divergence can be avoided by making a change of coordinates (eg changing some position coordinates to momentum ones) before the conjugate point, and changing back afterwards. This results in multiplying the propagator by the phase factor $\mathrm{e}^{-\frac{\mathrm{i}\pi}{2}}$ a number of times equal to the loss in rank of J (namely once for each coordinate change necessary). We add this phase for every conjugate point along the trajectory from $\boldsymbol{q}$ to $\boldsymbol{q}'$ and record it via a topological index $\tilde{\nu}_\zeta$.

To obtain the semiclassical approximation to the Green's function, we now take the Laplace transform of the semiclassical approximation to the propagator. For long times we can again approximate the integral using the stationary phase approximation. The result is that we can write the semiclassical Green's function in terms of all the classical trajectories linking the two end points as follows

$$G(\boldsymbol{q}', \boldsymbol{q}, E) \approx \frac{1}{\mathrm{i}\hbar \left(2\pi\mathrm{i}\hbar\right)^{\frac{f-1}{2}}} \sum_\zeta |D_S|^{\frac{1}{2}} \mathrm{e}^{\frac{\mathrm{i}}{\hbar} S_\zeta(\boldsymbol{q}', \boldsymbol{q}, E) - \frac{\mathrm{i}\pi}{2}\nu_\zeta} \tag{1.3.9}$$

where the sum is over all trajectories ζ linking $\boldsymbol{q}$ and $\boldsymbol{q}'$ at the energy E. $S_\zeta(\boldsymbol{q}', \boldsymbol{q}, E)$ is the classical action of the trajectory ζ and is given by the integral of the momentum along the path

$$S_\zeta(\boldsymbol{q}', \boldsymbol{q}, E) = \int_{\boldsymbol{q}}^{\boldsymbol{q}'} \mathrm{d}\boldsymbol{q}'' \, \boldsymbol{p}_\zeta(\boldsymbol{q}'', \boldsymbol{q}, E) \tag{1.3.10}$$

The topological index ν_ζ in equation (1.3.9) counts the number of conjugate points along the trajectory ζ (at the energy E). D_S is the determinant of the matrix formed by the second derivative of the action with respect to the final and initial positions, and the energy

$$D_S = \det \begin{pmatrix} \frac{\partial^2 S}{\partial \boldsymbol{q} \partial \boldsymbol{q}'} & \frac{\partial^2 S}{\partial \boldsymbol{q} \partial E} \\ \frac{\partial^2 S}{\partial \boldsymbol{q}' \partial E} & \frac{\partial^2 S}{\partial E^2} \end{pmatrix} \tag{1.3.11}$$

This determinant can be simplified by using a coordinate system where one axis

points along the trajectory and the others are orthogonal. The semiclassical approximation for the Green's function given by equation (1.3.9) is only valid as long as q and q' remain separate in position or time, and is referred to as a 'long' trajectory approximation. However, the propagator diverges for short times (as a delta function) and the Laplace transform of the short time form of the propagator (equation (1.3.3)) can be expressed as (see Cvitanović et al., 2005)

$$G_0(q', q, E) = -\frac{im}{2\hbar^2} \left(\frac{p}{2\pi\hbar|q'-q|} \right)^{\frac{f-2}{2}} H^+_{\frac{f-2}{2}} \left(\frac{p|q'-q|}{\hbar} \right) \qquad (1.3.12)$$

where H^+ is a Hankel function of the first kind and $p = \sqrt{2m(E - V(q))}$. This semiclassical approximation for the Green's function is only valid as long as q and q' remain close in position and time and is known as a 'short' trajectory approximation. Both approximations are important in what follows.

1.3.2 Trace formula

For the semiclassical approximation to the density of states, we need to take the trace of the semiclassical Green's function

$$\text{Tr } G(E) = \int dq \, G(q, q, E) \qquad (1.3.13)$$

by integrating over all position space. Inside the integral, the two positions in the Green's function are identical, so we use the short trajectory form of the semiclassical approximation of equation (1.3.12) (alternatively one can proceed directly from the propagator in equation (1.3.3)). Performing this integral, using the asymptotics of the Hankel function of the first kind for small argument, we obtain Weyl's formula and recover the average density of states

$$\bar{d}(E) \approx \frac{1}{(2\pi\hbar)^f} \int dx \, \delta(E - H(x)) = \frac{\Omega(E)}{(2\pi\hbar)^f} \qquad (1.3.14)$$

25

which is now expressed in terms of the classical volume of the energy shell. This result has the following interpretation. Because of the Heisenberg uncertainty principle, the smallest resolvable space is a (Planck) cell of size $(2\pi\hbar)^f$ in phase space. If each cell can support a quantum state, then the average number of states $\bar{N}(E)$ can be estimated by simply counting the number of cells that will fit in the phase space volume below the energy E. This estimate gives the above result for the mean density of states.

The idea of Planck cells allows us to provide a better picture of the separation between local and global properties of a quantum chaotic system. For the purely classical motion, once a small region around the trajectory is stretched (and compressed) so as to become as large as the typical size of the system, the evolution starts to become ergodic (and mixing) and, depending on the application, can be treated as a random variable. The time this takes depends on the size of the region and can be made longer by shrinking the initial region. Quantum mechanically, however, there is a shortest possible length scale given by the sides of a Planck cell. The time this takes to grow to the typical size of the system is called the Ehrenfest time T_{E}. Because the stretching is dominated by the largest Lyapunov exponent λ, the Ehrenfest time is such that

$$(2\pi\hbar)\mathrm{e}^{\lambda T_{\mathrm{E}}} \approx 1, \quad T_{\mathrm{E}} \approx \frac{1}{\lambda}\ln\left(\frac{1}{2\pi\hbar}\right) \tag{1.3.15}$$

Semiclassically then, below this time scale we can concentrate on the local hyperbolic motion, while above it we can focus on the global ergodic behaviour.

The 'zero-length' trajectories in the trace considered above are not the only ones that can connect the point $\boldsymbol{q}$ to itself. Any trajectory that passes through the same point twice will count, and, as long as they are separated in time, we use the long trajectory form of the Green's function. The integral over position space is performed using a stationary phase approximation. The condition that the trajectory is a stationary point turns out to be equivalent to the requirement that the momentum is the same each time it passes through $\boldsymbol{q}$, meaning that the

trajectory must be periodic. The result of the integral then gives the oscillating part of the density of states as a sum over the periodic orbits of the system (Gutzwiller, 1971)

$$d^{\mathrm{osc}}(E) \approx \mathrm{Re}\frac{1}{\pi\hbar}\sum_{\gamma,r} A_{\gamma,r}\mathrm{e}^{\frac{\mathrm{i}}{\hbar}rS_{\gamma}(E)} \tag{1.3.16}$$

where γ labels the primitive periodic orbits, and r their repetitions. The orbits have classical action S_{γ} and the amplitude is given by

$$A_{\gamma,r} = \frac{T_{\gamma}\mathrm{e}^{-\frac{\mathrm{i}\pi}{2}r\mu_{\gamma}}}{\sqrt{|\det(M_{\gamma}^r - 1)|}} \tag{1.3.17}$$

which incorporates the period T_{γ}, the stability matrix M_{γ} and the Maslov index μ_{γ}. The latter counts the number of conjugate point along the periodic orbit, but also has a geometrical interpretation due to Creagh et al. (1990) and Robbins (1991). The stable and unstable manifold of the periodic orbit can rotate as they are transported along the periodic orbit, and the Maslov index is the number of times the manifolds rotate by half a turn along the orbit. After each loop along the periodic orbit, the manifolds must be back where they started, so the Maslov index will be an integer. If the system involves reflections on hard walls (with Dirichlet boundary conditions), then we also need to add twice the number of reflections to the Maslov index.

1.3.3 Form factor

From the trace formula for the density of states we can obtain the semiclassical approximation for the form factor by substituting the expression for the oscillating part of the density of states in terms of periodic orbits (equation (1.3.16)) into the form factor equation (1.2.19). When we make this substitution, we also make some simplifications and assumptions. We ignore any differences in the slowly varying prefactor and we expand the action as a Taylor series up to first order as

$$S_{\gamma}\left(E \pm \frac{\eta}{2}\right) \approx S_{\gamma}(E) \pm \frac{\eta}{2}\frac{\mathrm{d}S_{\gamma}(E)}{\mathrm{d}E} = S_{\gamma}(E) \pm \frac{\eta}{2}T_{\gamma}(E) \tag{1.3.18}$$

27

Because the sum over orbits in the density of states includes the complex conjugate, we obtain terms with action sums and action differences in the form factor. The terms with action sums will add destructively, and should average to zero, so we only retain terms with an action difference. Now when we substitute into the form factor we obtain

$$K(\tau) = \frac{1}{2\pi\hbar T_{\mathrm{H}}} \left\langle \int \mathrm{d}\eta \sum_{\substack{\gamma,r \\ \gamma',r'}} \left[A_{\gamma,r} A^*_{\gamma',r'} \mathrm{e}^{\frac{\mathrm{i}}{\hbar}(rS_\gamma - r'S_{\gamma'})} \mathrm{e}^{\frac{\mathrm{i}\eta}{2\hbar}(rT_\gamma + r'T_{\gamma'})} + \mathrm{c.c.} \right] \mathrm{e}^{\frac{-\mathrm{i}\eta}{\hbar}\tau T_{\mathrm{H}}} \right\rangle$$

(1.3.19)

This is the quantity we wish to consider in the semiclassical limit $\hbar \to 0$. When we perform the integral the result is

$$K(\tau) = \frac{1}{T_{\mathrm{H}}} \left\langle \sum_{\substack{\gamma,r \\ \gamma',r'}} A_{\gamma,r} A^*_{\gamma',r'} \mathrm{e}^{\frac{\mathrm{i}}{\hbar}(rS_\gamma - r'S_{\gamma'})} \delta\left(\tau T_{\mathrm{H}} - \frac{rT_\gamma + r'T_{\gamma'}}{2} \right) \right\rangle$$

(1.3.20)

Since the orbits have positive periods T_γ, and because τ is positive, we retain only the delta function that contributes. We will examine the semiclassical evaluation of this quantity for closed systems, in the regime $\tau < 1$, in Chapter 2.

1.3.4 Equidistribution

In section 1.1.3 we considered the ergodic property of almost all trajectories in a classical chaotic system. So far, however, we have refrained from exploring similar properties of long periodic orbits, which are crucial for the semiclassical evaluation of the form factor in terms of periodic orbits. As we have seen, ergodicity does not hold for the periodic orbits, but as a group, the long orbits should still spread evenly over the energy shell. In fact, the ensemble of (weighted) long periodic orbits is uniformly distributed over the energy shell, and sums over the ensemble can be replaced with an energy shell average.

This uniformity of the long periodic orbits is reflected in the sum rule of Hannay and Ozorio de Almeida (1984). They considered the time average of a (smoothed) delta function for a typical trajectory. Due to ergodicity (see equation (1.1.11)), in

the limit of long times, the time average is equivalent to an energy shell average. Integrating both sides of this equivalence over the energy shell (see also Ozorio de Almeida, 1988), the delta function picks out the periodic orbits and gives them a weight that depends on their stability. This led to a sum rule over the periodic orbits

$$\lim_{T \to \infty} \frac{1}{T} \sum_{\substack{\gamma, r \\ rT_\gamma < T}} \frac{T_\gamma}{|\det(M_\gamma^r - 1)|} = 1 \qquad (1.3.21)$$

The fraction in this sum is very similar to the stability amplitudes (see equation (1.3.17)), and in fact coincides with $\frac{|A_{\gamma, r}|^2}{T_\gamma}$. We now rearrange this result to get the form of the Hannay–Ozorio de Almeida sum rule that we will use later. Looking at the large time asymptotics of the sum, the contribution of the repetitions of the periodic orbits can be neglected as their number is exponentially smaller than that of the primitive orbits. We can 'differentiate' to obtain

$$\sum_\gamma |A_\gamma|^2 \delta_\epsilon (T - T_\gamma) \sim T, \quad T \to \infty \qquad (1.3.22)$$

where the delta function is smoothed by the width ϵ so that we average over a small range of time. In this formula, the exponential growth in the number of orbits essentially balances the exponential decay of their amplitudes.

The Hannay–Ozorio de Almeida sum rule is in fact an example of a more general equidistribution theorem (Bowen, 1972; Parry and Pollicott, 1990). Imagine that we measure some function $F(\boldsymbol{x})$ along a periodic orbit γ

$$F_\gamma = \frac{1}{T_\gamma} \int_0^{T_\gamma} \mathrm{d}t \, F(\boldsymbol{x}(t)) \qquad (1.3.23)$$

where the point $\boldsymbol{x}(0)$ is on the periodic orbit γ. If we sum over all primitive periodic orbits weighted as before, we can replace the sum with a phase space average

$$\sum_\gamma |A_\gamma|^2 F_\gamma \delta_\epsilon (T - T_\gamma) \sim \frac{T}{\Omega} \int \mathrm{d}\boldsymbol{y} \, F(\boldsymbol{y}) = T \langle F \rangle, \quad T \to \infty \qquad (1.3.24)$$

This result is similar to the property of ergodicity in equation (1.1.11), and will allow us to simplify periodic orbit sums later. The upshot of this result is that we can effectively replace the function F_γ for each orbit with the phase space average value $\langle F \rangle$ (from the right hand side). The equidistribution theorem will therefore be important in the evaluation of the semiclassical form factor that we consider in Chapter 2.

1.4 Time reversal symmetry

So far we have considered both the classical and quantum mechanics of a general chaotic system and its semiclassical approximation. In classical mechanics, the motion was given by the classical Hamiltonian $H(\boldsymbol{q}, \boldsymbol{p})$ and Hamilton's equations of motion (1.1.1). The solutions were trajectories $\zeta = \boldsymbol{x}(t) = (\boldsymbol{q}(t), \boldsymbol{p}(t))$ restricted to the energy surface. However, the classical system may have additional properties or symmetries, and an important example is time reversal symmetry (see Haake, 2000, for example). We will use the conventional definition that a system has time reversal symmetry if, for any trajectory ζ, we can reverse the direction of the momentum and travel back along the 'same' trajectory (with the same position and reversed momentum). If we reverse the momentum at time t', this time reversed trajectory $\overline{\zeta} = (\boldsymbol{q}(t' - t), -\boldsymbol{p}(t' - t))$ must also be a solution of the Hamiltonian. Of course changing the momentum at different times t' leads to the same time reversed trajectory, simply with a different starting point, so we can choose $t' = 0$. In a more formal way, we can represent time reversal as an operator $\tilde{T}$ acting on the phase space coordinate $\boldsymbol{x}$, which changes the sign of the momentum, so that $\tilde{T}(\boldsymbol{q}, \boldsymbol{p}) = (\boldsymbol{q}, -\boldsymbol{p})$ The time reversal of any trajectory $\zeta = \boldsymbol{x}(t)$ is given by $\overline{\zeta} = \tilde{T}\boldsymbol{x}(-t)$. When the system has time reversal symmetry, the Hamiltonian is an even function of the momentum $H(\boldsymbol{q}, \boldsymbol{p}) = H(\boldsymbol{q}, -\boldsymbol{p})$, and any periodic orbit γ has a time-reversed partner $\overline{\gamma}$ traversed in the opposite direction. In fact, an equivalent definition of conventional time reversal is that the Hamiltonian is invariant under time reversal $H(\boldsymbol{q}, \boldsymbol{p}) = \tilde{T}H(\boldsymbol{q}, \boldsymbol{p})$, or that it is an even function of the momentum.

We now consider time reversal symmetry in the quantum mechanical setting. In the position representation, the conventional definition is that a system has time reversal symmetry if, for each solution $\psi(\boldsymbol{q}, t)$ of the Schrödinger equation, its time reversed partner $\overline{\psi} = \psi^*(\boldsymbol{q}, -t)$ is also a solution. The time reversal operator $\hat{T}$ is the operator of complex conjugation (and we also reverse the direction of time), and in analogy with the classical situation, any solution $\psi(\boldsymbol{q}, t)$ leads to a second solution $\overline{\psi}(\boldsymbol{q}, t) = \hat{T}\psi(\boldsymbol{q}, -t)$ linked by time reversal. The time reversal operator then commutes with the Hamiltonian $[\hat{T}, \hat{H}] = \hat{T}\hat{H} - \hat{H}\hat{T} = 0$, making the Hamiltonian real. This property provides an equivalent definition of time reversal invariance for quantum mechanical systems.

Conventional time reversal symmetry is an example of a more general antiunitary symmetry (or non-conventional time reversal symmetry). A system has antiunitary symmetry if the Hamiltonian commutes with any antiunitary operator $\hat{T}'$. Antiunitarity means that

$$\left\langle \hat{T}'\psi_2 | \hat{T}'\psi_1 \right\rangle = \langle \psi_2 | \psi_1 \rangle^* = \langle \psi_1 | \psi_2 \rangle \tag{1.4.1}$$

where $\langle \psi_1 | \psi_2 \rangle$ is the inner product of the two states. This differs only in complex conjugation from the action of a unitary operator $\hat{U}$

$$\left\langle \hat{U}\psi_2 | \hat{U}\psi_1 \right\rangle = \langle \psi_2 | \psi_1 \rangle \tag{1.4.2}$$

More importantly, all possible antiunitary operators $\hat{T}'$, which can represent a time reversal operator, can be generated from a unitary transform $\hat{U}$ acting on the operator $\hat{T}$ as

$$\hat{T}' = \hat{U}\hat{T} \tag{1.4.3}$$

If we apply time reversal twice, we should recreate the initial wavefunction (up to the phase), which leads (along with the unitarity of $\hat{U}$) to the requirement that $\hat{T}'^2 = \pm 1$. The case where $\hat{T}'^2 = -1$ represents physical systems with an odd number of spin-$\frac{1}{2}$ particles. We will not consider this case and will only include time reversal symmetry operators which square to 1, which implies that the unitary

transform $\hat{U}$ is symmetric as $\hat{U}\hat{U}^* = 1$.

As we have seen from the time-independent Schrödinger equation, the quantum mechanics reduces to an eigenvalue problem, with the eigenvectors forming a basis of the Hilbert space. Any operator on an element of the Hilbert space can be thought of as an infinite dimensional square matrix. The Hamiltonian, because it represents a physical observable, can be represented as a Hermitian matrix. A unitary transformation changes the basis in the Hilbert space and the Hamiltonian matrix, but leaves the eigenvalues (which are the physically observable values of the energy) unchanged. With time reversal symmetry, the Hamiltonian matrix must also be real and symmetric, and this property is unchanged under orthogonal (matrix) transformations. As the energy spectrum is given by the eigenvalues of the Hamiltonian matrix, the study of these matrices provides insights into the eigenvalue statistics.

1.5   Random matrix theory

Random matrix theory (RMT, see Mehta, 2004) is the study of the properties of matrices whose elements are random variables following a given probability distribution. Interest in it increased in the 1950s as it gave a way of describing the spectra of atomic nuclei. At low energies, soluble approximations to the quantum mechanics are capable of describing the states, but as the energy increases the inaccuracies and the number of states grow so as to render these approximations inapplicable. Wigner hypothesized that, at high energies, the energy levels of particular nuclei have the same statistics as the eigenvalues of random matrices. As the Hamiltonian of a nucleus can be written as a Hermitian matrix (which also satisfies any symmetry of the system) this hypothesis means that the exact details of the entries are unimportant and can effectively be chosen at random. Though the eigenvalues depend on the particular matrix, their statistics can be shown to be the same for almost any member of the ensemble of matrices with the same symmetry, and hence universal for that symmetry class.

A heavy atomic nucleus, with many nucleons, could well be a quantum chaotic

system. The fact that quantum systems might have differing spectral statistics depending on whether they are chaotic or not was first voiced by Percival (1973). The energy spectrum of completely non-chaotic (integrable) systems was considered by Berry and Tabor (1977) and shown generally to have Poissonian statistics, or in other words that the levels are uncorrelated. Although they did not investigate chaotic systems, Berry and Tabor (1977) suggested that their levels might be correlated and repel each other. Interestingly, they noted that this behaviour also occurs for the eigenvalues of random matrices. Numerical evidence of this level repulsion was found for the stadium billiard (McDonald and Kaufman, 1979; Casati et al., 1980) and for the Sinai billiard (Berry, 1981). Further consideration of the Sinai billiard by Bohigas et al. (1984) led them to conjecture that all quantum chaotic systems should have universal spectral statistics given by the relevant random matrix ensemble. The spectral statistics then only depend on the symmetries of the system. This link between RMT and quantum chaos is covered by Haake (2000), and a review of the experimental support is provided by Stöckmann (1999).

We have already seen an example of universality in classical chaotic systems, namely ergodicity. Once the time scales are long enough to be in the ergodic limit, the actual dynamics of the system are of secondary importance and give way to a general stochastic behaviour. It does not seem to be so strange then that the exact details of a quantum chaotic system also become unimportant and only the symmetries remain. The time scale delineating the local and universal behaviour has a simpler interpretation in the quantum chaotic case, and, as we have seen, is given by the Ehrenfest time T_E. More precisely, we can expect the statistics of a quantum chaotic system to agree with the universal RMT results on time scales longer than T_E, while local system specific behaviour might dominate for shorter times.

1.5.1 Form factor

We now consider how random matrix theory allows us to calculate eigenvalue statistics. The Hamiltonian matrices are (generally) infinite dimensional, so the first step is to approximate them with a finite $N \times N$ square matrix and then take the limit

$N \to \infty$. The matrix elements are then filled with random variables that are independent and identically distributed with zero mean and non-zero (finite) variance. Without time reversal symmetry, the matrix is Hermitian, so the elements above and below the diagonal are related by complex conjugation $H_{ij} = H_{ji}^*$ and the diagonal elements are real. We only need to fill the diagonal with N real random variables, and the upper (or lower) triangle with $\frac{1}{2}N(N-1)$ complex random variables, to define the whole matrix. With time reversal symmetry the matrix is also symmetric so all the elements are real, and we only need to fill the diagonal and upper triangle with $\frac{1}{2}N(N+1)$ real random numbers.

However, the set of random matrices formed in this way will not be representative of a general Hamiltonian matrix because it lacks invariance. Without time reversal symmetry, we saw that a unitary transformation corresponds to a change of basis of the Hilbert space, and does not affect the eigenvalues. The set of random matrices should also be invariant under a unitary transform $H' = U^{-1}HU$, for any unitary matrix U. To achieve this, each matrix H is given a weight $P(H)$ so that the invariance $P(H')\mathrm{d}H' = P(H)\mathrm{d}H$ holds (where $\mathrm{d}H$ is a product of infinitesimals of the free elements of H). With this invariance, and the independence of the (free) matrix elements, the weight function is a Gaussian function $P(H) = \mathrm{e}^{-\mathrm{Tr}f(H)}$ where $f(H)$ is a quadratic function of the matrix H. This invariance implies that the matrix elements themselves have a Gaussian distribution. The set of random matrices with this weighting is known as the Gaussian Unitary Ensemble (GUE). With time reversal symmetry, the random matrices should be invariant under an orthogonal transformation $H' = O^{-1}HO$, for any orthogonal matrix O. The set of random matrices, with a weight to achieve this invariance, is known as the Gaussian Orthogonal Ensemble (GOE), and the weight function is again a Gaussian.

From the ensembles it is possible to calculate the joint probability distribution of the eigenvalues. For the GOE, we make a change of variables from the $\frac{1}{2}N(N+1)$ independent real matrix elements to the N eigenvalues, and $\frac{1}{2}N(N-1)$ remaining parameters. For the GUE, the independent matrix elements were made up of $\frac{1}{2}N(N-1)$ complex elements and N real ones. We can express each complex variable

in terms of two real variables (the real and imaginary part), so we make a change of variable to the N eigenvalues, and $N(N-1)$ remaining real parameters. To find the joint probability distribution of the eigenvalues, we integrate over the remaining parameters in both cases.

To arrive at the two-point correlation function, we can then integrate over all but two of the eigenvalues. When we take the large N limit, we get the following RMT result for the GUE case

$$R_2(\omega) = 1 - \left(\frac{\sin(\pi\omega)}{\pi\omega}\right)^2 \tag{1.5.1}$$

and for the GOE case

$$R_2(\omega) = 1 - \left(\frac{\sin(\pi\omega)}{\pi\omega}\right)^2 + \left(\frac{\mathrm{Si}(\pi\omega)}{\pi} - \frac{\mathrm{sgn}(\omega)}{2}\right)\left(\frac{\cos(\pi\omega)}{\omega} - \frac{\sin(\pi\omega)}{\pi\omega^2}\right) \tag{1.5.2}$$

where

$$\mathrm{Si}(\pi\omega) = \int_0^{\pi\omega} \mathrm{d}x\, \frac{\sin(x)}{x}, \quad \mathrm{sgn}(\omega) = \begin{cases} 1 & \omega > 0 \\ 0 & \omega = 0 \\ -1 & \omega < 0 \end{cases} \tag{1.5.3}$$

From here, we are able to take the Fourier transform (cf equation (1.2.18)) to get the RMT result for the spectral form factor. As the correlation functions are even, so too are the Fourier transforms, and therefore we need only consider $\tau > 0$. For the GUE (without time reversal symmetry) case we obtain

$$K(\tau) = \begin{cases} \tau & \tau \le 1 \\ 1 & \tau > 1 \end{cases} \tag{1.5.4}$$

and for the GOE (with time reversal symmetry) case the spectral form factor is

$$K(\tau) = \begin{cases} 2\tau - \tau \ln(1 + 2\tau) = 2\tau + \sum\limits_{n=2}^{\infty} \frac{(-2)^{n-1}}{n-1}\tau^n & \tau \leq 1 \\ 2 - \tau \ln\left(\frac{2\tau+1}{2\tau-1}\right) & \tau > 1 \end{cases} \qquad (1.5.5)$$

These results give us the typical distribution of the eigenvalues of matrices from the GUE or GOE that can represent Hamiltonian matrices of systems with and without time reversal symmetry. The conjecture of Bohigas et al. (1984) is that individual quantum chaotic systems should have the same statistics in the semiclassical limit. Namely, that systems without time reversal symmetry should exhibit GUE statistics, while systems with time reversal symmetry (or any antiunitary symmetry) should exhibit GOE statistics. We shall examine, in the next Chapter, a semiclassical explanation of this by considering correlated periodic orbit pairs in the semiclassical approximation of the form factor.

2 Periodic orbit correlations

We have seen how the form factor, which describes the distribution of the energy eigenvalues of a quantum system, can be approximated semiclassically by a double sum over periodic orbits of the corresponding classical system. Furthermore, the quantum result has a universal form that depends only on the symmetries of the system and can be derived from RMT. A semiclassical evaluation of the double sum over periodic orbits should therefore yield the same result as RMT. The first step towards showing this was the evaluation of the 'diagonal' approximation by Berry (1985). Berry paired periodic orbits with themselves (and their time reversals for systems with time reversal symmetry) and was able to evaluate their contribution with the sum rule arguments of Hannay and Ozorio de Almeida (1984). These orbits gave the leading order term of the RMT result for small τ.

In order to go beyond the diagonal approximation, we need to find correlated pairs of periodic orbits whose action difference $|S_\gamma - S_{\gamma'}|$ is small on the scale of $\hbar$. The first such pair was found by Sieber and Richter (2001) (and also detailed in Sieber, 2002) for a system with uniformly hyperbolic dynamics. This pair is depicted in Figure 2.1, and consists of an orbit with a small angle self crossing and a partner that follows almost the same trajectory. The partner, however, avoids crossing, and completes the trajectory back to the crossing in the opposite direction, so it can only exist in systems with time reversal symmetry.

By considering long periodic orbits as uniform on the energy shell, Sieber and Richter (2001) calculated the expected number of such orbits with a crossing as a function of the crossing angle. By linearizing the motion, it can be argued that
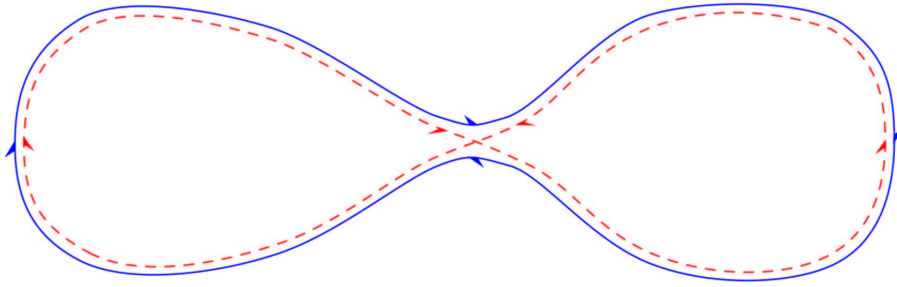
Figure 2.1: The type of periodic orbit pair that gives the first off-diagonal contribution to the form factor for systems with time reversal symmetry.

a)   b)
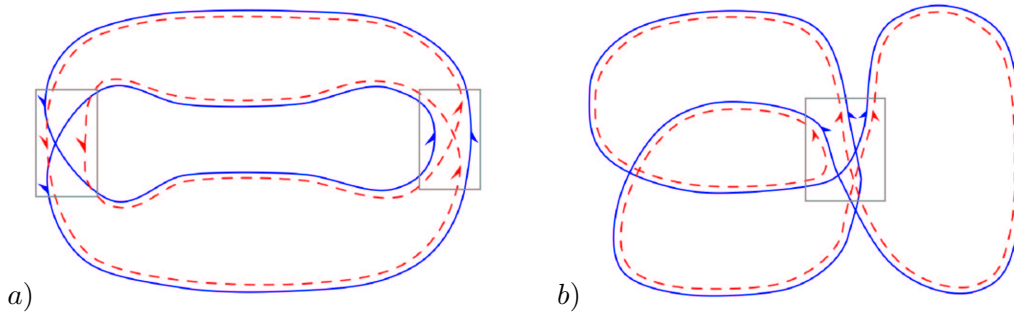
Figure 2.2: The types of periodic orbit pair that give the first off-diagonal contributions to the form factor for systems without time reversal symmetry. The encounter regions are indicated by the rectangles.

the partner orbit must exist, and so they were able to give the first off-diagonal correction to the form factor in a system with uniformly hyperbolic dynamics and time reversal symmetry. This correction agreed with the second order term of the GOE random matrix results.

To facilitate the extension of this method to include orbits with more crossings, in order to obtain higher order terms in the form factor expansion, these ideas were reformulated in terms of phase space coordinates instead of crossing angles. This was done simultaneously by Spehner (2003) and by Turek and Richter (2003), and later for higher dimensional systems (Turek et al., 2005). Not long after this reformulation, the orbit pairs responsible for the next order correction were identified by Heusler et al. (2004), and their contribution shown to agree with the next term in the RMT result. Of these orbit pairs, those that are possible for systems without time reversal symmetry are depicted in Figure 2.2

Examining the orbit in Figure 2.2a, we can see that it has two regions where the

orbit gets close to itself, namely the areas in the Figure indicated by the rectangles. These regions are known as 'self-encounters', and the sections of the orbit inside the encounter regions are called encounter stretches. The partner orbit (dashed) traverses each of the encounter regions differently, but follows the rest of the original orbit almost exactly, albeit in a different order. The long sections of the orbit, joining together the encounter regions, are called 'links' (previously they were called 'loops'), and an encounter region that involves l encounter stretches is called an l-encounter. It is worth mentioning that when we discuss encounters we really mean 'active' encounters where the partner orbit traverses the encounter region differently. The long links may come close to themselves or each other many times, but these meetings are inconsequential as long as the partner orbit traverses them in the same way as the original orbit.

The periodic orbit in Figure 2.2b has a single important region where the orbit gets close to itself, but now the encounter involves three orbit stretches, so that the periodic orbit has a single 3-encounter. The partner orbit again traverses the encounter region differently, while following the rest of the orbit almost exactly. For systems without time reversal symmetry, these two types of periodic orbit pair give contributions in the semiclassical limit which sum to zero. For systems with time reversal symmetry, links and encounter stretches can also be traversed in opposite directions, and this leads to a larger number of possible types of correlated orbit pairs.

These ideas and calculations were further extended by Müller et al. (2004, 2005) to cover orbits with an arbitrary number of encounters each involving an arbitrary number of stretches. The probability that such an orbit exists is again estimated using the uniformity of long periodic orbits over the energy shell. The number of different configurations of orbit pairs, called 'structures', can be found by considering all possible configurations of encounter regions, and all possible ways of reconnecting links within the encounter region (via different encounter stretches) in such a way that we still have a complete orbit that respects the symmetry of the dynamics. By combining the number of structures, the action difference, the probability of

existence and the equidistribution theorem, Müller et al. (2004) were able to generate all terms of the small τ RMT expansion. More details about the calculation are given in Müller et al. (2005), and a completely detailed treatment in Müller (2005). We review this work in Section 2.2 so that we can apply it to parametric correlations in Chapter 3 and open systems in Chapter 4.

2.1 Diagonal approximation

In order to introduce the diagonal approximation, we recall the semiclassical approximation to the form factor that is given by a double sum over periodic orbits (equation (1.3.20))

$$K(\tau) = \frac{1}{T_{\mathrm{H}}} \left\langle \sum_{\substack{\gamma,r \\ \gamma',r'}} A_{\gamma,r} A_{\gamma',r'}^* \mathrm{e}^{\frac{\mathrm{i}}{\hbar}(rS_\gamma - r'S_{\gamma'})} \delta\left(\tau T_{\mathrm{H}} - \frac{rT_\gamma + r'T_{\gamma'}}{2}\right) \right\rangle \qquad (2.1.1)$$

The simplest pairs of orbits to evaluate in the sum are the 'diagonal' pairs where an orbit is paired with itself (and its time reversal if the system has time reversal symmetry). Upon using the diagonal approximation $\gamma = \gamma'$ (Berry, 1985), the form factor becomes

$$K^{\mathrm{diag}}(\tau) = \frac{\kappa}{T_{\mathrm{H}}} \left\langle \sum_{\gamma,r} |A_{\gamma,r}|^2 \delta\left(\tau T_{\mathrm{H}} - rT_\gamma\right) \right\rangle \qquad (2.1.2)$$

where κ is 1 if the system does not have time reversal symmetry and 2 if it does, to account for the above mentioned symmetry. In order to evaluate this, we use the sum rule of Hannay and Ozorio de Almeida (1984). This sum rule is derived from the uniformity of the long periodic orbits on the energy shell and is given by (see equation (1.3.22))

$$\sum_\gamma |A_\gamma|^2 \delta_\epsilon\left(T - T_\gamma\right) \sim T, \quad T \to \infty \qquad (2.1.3)$$

The contribution of the repetitions of the periodic orbits can be ignored as it is exponentially smaller than that of the primitive orbits, and we remove the repetitions from this sum. Using the sum rule, the diagonal approximation simply becomes
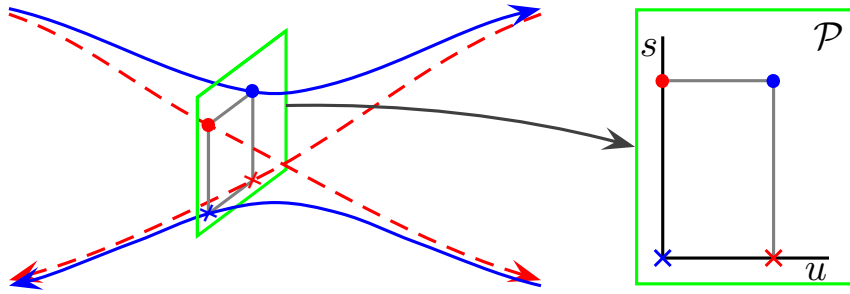
Figure 2.3: A close up of a 2-encounter and the piercing points of the encounter stretches (or their time reversals) in a Poincaré section.

$$K^{\text{diag}}(\tau) = \kappa\tau \tag{2.1.4}$$

This gives the first term in the small τ expansion of the RMT results (see equations (1.5.4) and (1.5.5)).

2.2 Full form factor for $\tau < 1$

In order to go beyond the leading order and obtain the full form factor, Müller et al. (2004, 2005) considered correlated periodic orbits with self-encounters, as described in the introduction to this Chapter.

For a periodic orbit with a single 2-encounter, as shown in Figure 2.1 we have two orbit links that join the encounter region. For now we will consider a system with 2 degrees of freedom, and we enlarge the encounter region in Figure 2.3, where the solid lines represent the encounter stretches of the original orbit.

To better understand the partner orbit, it is useful to look at a Poincaré section at a point along the encounter. The two encounter stretches traverse the encounter region in different directions. For this reason, in order to have the piercing points close in the Poincaré section we consider the piercing points of encounter stretches travelling from left to right and the time reversal of the encounter stretches that travel from right to left. The piercing points of time reversed stretches are indicated by crosses in Figure 2.3. We set the origin of the Poincaré section at the piercing point of the time reversal of the lower encounter stretch of the original orbit. The

41

two encounter stretches of the original orbit should be close to each other, and in this case the second encounter stretch will have some small components s and u along the stable and unstable manifolds respectively and pierce the Poincaré section at the point (u, s).

In Figure 2.3, the encounter stretches of the partner orbit are indicated by dashed lines. In the linearized approximation, the coordinates of the piercing points of these encounter stretches (or their time reversal) lie at opposite corners of a rectangle formed by the piercing points of the original orbit, and this is also depicted in Figure 2.3. This can be understood in the following way.

If we start following the partner orbit, as depicted in Figure 2.1, from a point in the link on the left, we see that it reaches the encounter at almost the same point as the upper encounter stretch of the original orbit. To create a partner, we wish to traverse the encounter differently and arrive at almost the start of the lower encounter stretch. A trajectory that does exactly this must have approximately the same stable component s, such that it follows the left link back in time. It will also have an approximately zero unstable component, so that it leaves the encounter region along the same link as the time reversed lower encounter stretch. Following this trajectory, we traverse the right orbit link in the opposite direction, and arrive at the end of the upper encounter stretch. If the trajectory traverses the encounter region so that its time reverse pierces the Poincaré section at coordinates $\approx (u, 0)$, then it will leave the encounter region along the same link as the lower encounter stretch and complete a periodic orbit by following the left link.

We return to systems with f degrees of freedom and in order to consider more complicated self-encounters, we can keep in mind the picture of the orbit links being joined together by the stretches in the encounter region. The partner orbit will contain the same links (possibly traversed in a different direction), but they will be connected together differently in the encounter region. To examine this in more detail we consider a periodic orbit with a single 3-encounter, depicted in Figure 2.2b. Since all the encounter stretches are traversed in the same direction, this pair also exists for systems without time reversal symmetry. In Figure 2.4 we draw a schematic
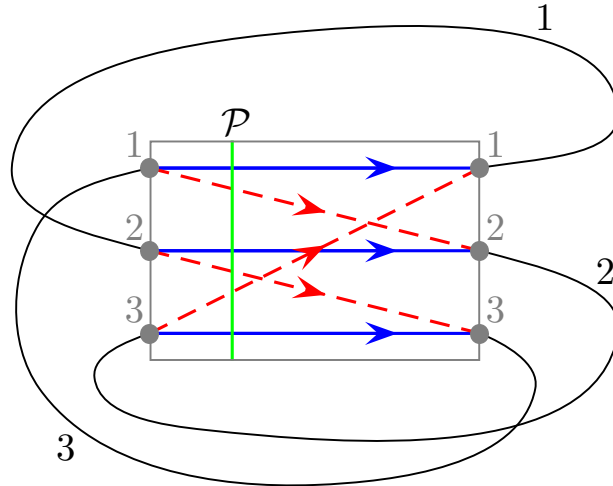
Figure 2.4: A schematic diagram of a periodic orbit with a single 3-encounter and its partner formed by reconnecting the encounter stretches.

representation of this orbit and we focus on the encounter region which is highlighted in the picture by a rectangle.

As the orbit travels along each of the three encounter stretches it enters the encounter region and then leaves, and we can consider the places where the orbit enters as entrance 'ports' and the points where the orbit leaves as exit ports. The encounter stretches each connect a single entrance port to an exit port, and after following each stretch the orbit then follows a link until it re-enters the encounter region. In Figure 2.4, the encounter stretches are represented by the solid straight lines. We follow the original orbit, starting at the top entrance port which we number 1. The first part of the orbit is the first encounter stretch which leaves the encounter region through exit port 1 and then follows the link which we also number 1. This link re-enters the encounter region at the entrance port numbered 2, and then the orbit follows the second encounter stretch. We continue along the orbit, numbering links and encounter stretches, until we complete the periodic orbit by returning to the first encounter stretch.

For the partner orbit, we reconnect the entrance and exit ports with different encounter stretches. For the example in Figure 2.4, where the encounter stretches of the partner orbit are represented by the dashed straight lines, the first encounter

stretch of the partner orbit connects the entrance port 1 to the exit port 2. From there, we follow link 2 to entrance port 3 and then the next encounter stretch which leaves the encounter region through exit port 1, and so on until we complete the orbit.

With time reversal symmetry, the encounter stretches may be traversed in different directions, which complicates the idea of entrance and exit ports. Instead we can think of each encounter stretch joining a port on the left to a port on the right. When we consider a general l-encounter, we have an intersection point in the Poincaré section for each of the l encounter stretches (or their time reverse), at coordinates $(\boldsymbol{u}_i, \boldsymbol{s}_i)$ for $i = 1 \ldots l$, say. We could set the origin of the section on one of these piercing points, generally the first, such that $(\boldsymbol{u}_1, \boldsymbol{s}_1) = 0$, but we will keep the coordinates arbitrary for the moment. The encounter stretches then join the l ports on the left to the l ports on the right, which we number by the order in which the stretches pierce the Poincaré section. To obtain the partner orbit, we change the encounter stretches so that they reconnect the ports. We can represent the reconnections in a permutation matrix

$$
\begin{pmatrix}
1 & 2 & \ldots & l \\
\pi(1) & \pi(2) & \ldots & \pi(l)
\end{pmatrix}
\tag{2.2.1}
$$

where each column records the fact that the encounter stretch (or its time reverse) of the partner orbit entering left port i exits through right port $\pi(i)$. In order to find the coordinates of the partner encounter stretches, we note that to come from the same left port i, any family of trajectories must have approximately the same stable component $\boldsymbol{s}_i$, while to leave from the same right port j, they must have approximately the same unstable component $\boldsymbol{u}_j$. The partner orbit must then have encounter stretches whose (possibly time reversed) piercing points in the Poincaré section are given by $\approx (\boldsymbol{u}_{\pi(i)}, \boldsymbol{s}_i)$.

In our example of Figure 2.4, the permutation matrix is simply
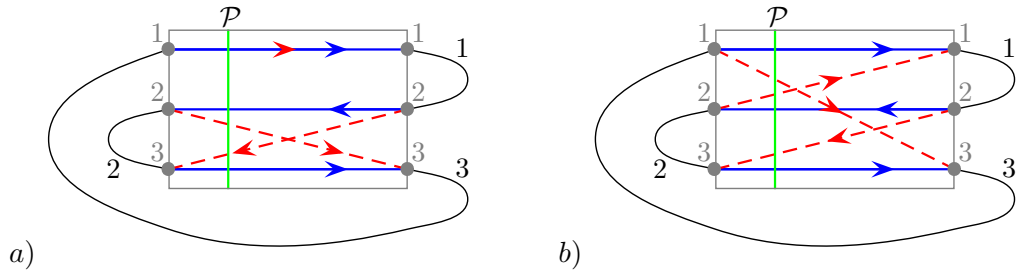
Figure 2.5: Examples of encounter reconnections that do not lead to suitable partner orbits.

$$\begin{pmatrix} 1 & 2 & 3 \\ 2 & 3 & 1 \end{pmatrix} \qquad (2.2.2)$$

and the coordinates of the encounter stretches follow immediately. We can try and generate periodic orbit pairs starting from permutation matrices, but not all those possible lead to a suitable partner orbit. In order that the l-encounter does not break up into separate or smaller encounters, the permutation corresponding to that encounter must consist of a single cycle of length l. For example, we consider a periodic orbit with a single 3-encounter for a system with time reversal symmetry in Figure 2.5. A reconnection which involves only 2 encounter stretches, corresponding to the permutation matrix

$$\begin{pmatrix} 1 & 2 & 3 \\ 1 & 3 & 2 \end{pmatrix} \qquad (2.2.3)$$

is drawn in Figure 2.5a. This reconnection leads to a periodic orbit pair with a single 2-encounter, which is already included as such.

We must also make sure that the partner does not break up into smaller periodic orbits. As we need pairs of closely related orbits for the double sum, if one of the pair breaks up it can no longer be included. When we follow the links between the reconnected encounter stretches, the partner must remain a single complete periodic orbit. For example, the reconnections described by

$$\begin{pmatrix} 1 & 2 & 3 \\ 3 & 1 & 2 \end{pmatrix} \qquad (2.2.4)$$

45

in Figure 2.5b leads to the partner forming two orbits. In fact, one passes from left port 1 to right port 3 during the encounter, and then follows link 3 to complete the orbit. The other starts following link 1, traverses the encounter region from right to left passing through left port 3 and follows link 2 in the opposite direction back to left port 2. Finally it crosses the encounter region again, leaving through right port 1 to complete the orbit. Now that we have considered some examples of periodic orbits pairs with self-encounters, we examine how we can generate and count such pairs using permutation matrices.

2.2.1 Number of orbit pairs

We can treat more complicated orbits along the same lines as described in the previous section. A general orbit can have V encounters, where each encounter α involves l_α orbit stretches. The orbit pairs will be described by a certain 'structure', which describes the links and encounter stretches of the original orbit, and how they are reconnected to form the partner orbit. The restriction that the partner must remain a single orbit still holds.

If we define a vector $\boldsymbol{v}$, where the components v_l specify how many l-encounters the orbit has, it is easy to see that

$$V = \sum_{l \geq 2} v_l \qquad L = \sum_{\alpha} l_\alpha = \sum_{l \geq 2} l v_l \qquad (2.2.5)$$

where L is the total number of orbit links, or encounter stretches. For each vector $\boldsymbol{v}$ there may be many different structures, depending on the symmetry of the dynamics, but we will see later that each structure with the same $\boldsymbol{v}$ gives the same contribution to the form factor, so an important step will be the evaluation of the number of structures $N(\boldsymbol{v})$ associated with a given vector $\boldsymbol{v}$.

For a particular vector, finding the number of possible structures, which give a permissible periodic orbit pair, is a combinatorial problem. This problem can be simplified by relating structures to permutation matrices, and full details are given by Müller (2005). The situation is simpler for systems without time reversal symmetry,

46

because all encounter stretches traverse each encounter in the same direction, and the orbit links all join a right port to a left port. A permutation matrix represents a structure as long as it satisfies the properties mentioned in the previous section. Specifically, to represent a structure with a corresponding vector $\boldsymbol{v}$, the permutation must consist of v_l l-cycles for $l \geq 2$, with each cycle corresponding to one of the V encounters. Of course, the partner orbit must be a single complete orbit as described before. Without time reversal symmetry, each orbit link starting on right port j leads to left port $j + 1$. For the partner, if we start on left port i we cross the encounter region leaving from right port $\pi(i)$ and then follow an orbit link to the left port $\pi(i) + 1$. We can define a second permutation matrix that describes in which sequence the left ports of the partner are traversed.

$$
\begin{pmatrix}
1 & 2 & \ldots & L \\
\pi(1) + 1 & \pi(2) + 1 & \ldots & \pi(L) + 1
\end{pmatrix}'
\tag{2.2.6}
$$

The prime is to show that this permutation matrix connects left ports to left ports. This permutation must be a single L-cycle for the partner to be a complete orbit. The number of structures corresponding to $\boldsymbol{v}$ is then given by the number of permutation matrices that satisfy both of these properties.

From our example in Figure 2.4, the permutation matrix linking one left port to another is

$$
\begin{pmatrix}
1 & 2 & 3 \\
3 & 1 & 2
\end{pmatrix}'
\tag{2.2.7}
$$

which is indeed a 3-cycle. In fact the permutation matrix of equation (2.2.2) is the only one that satisfies both properties. Therefore, there is only one structure corresponding to a single 3-encounter for systems without time reversal symmetry.

For systems with time reversal symmetry, the situation is complicated by the fact that orbit links can connect any combination of left and right ports, and the encounter stretches can travel in either direction. Müller (2005) reverted to a picture of entrance and exit ports and crucially considered both the orbit and its time reverse

together. Together, the orbit and its time reverse contain all the encounter stretches and orbit links traversed in both directions. The entrance ports of the time reversed orbit are the time reverse of the exit ports of the original orbit. The reconnection of the encounters can be recorded in a double permutation matrix that describes the reconnection of both the partner orbit and its time reverse

$$
\begin{pmatrix}
1 & 2 & \ldots & L & \overline{1} & \overline{2} & \ldots & \overline{L} \\
\pi(1) & \pi(2) & \ldots & \pi(L) & \pi(\overline{1}) & \pi(\overline{2}) & \ldots & \pi(\overline{L})
\end{pmatrix}
\tag{2.2.8}
$$

where the overbar denotes time reversal of the ports. The result of the permutation $\pi(i)$ can be either a port j or its time reversal $\overline{j}$. The reconnection is subject to the restriction that if an encounter stretch takes the port m to $\pi(m) = n$, then the time reversed stretch takes the port $\overline{n}$ back to $\overline{m} = \overline{\pi^{-1}(n)}$, where m and n are any port or its time reversal (ie they are elements of $1, \ldots, L, \overline{1}, \ldots, \overline{L}$). Note also that a port obviously cannot be connected to its own time reversal.

To represent a structure with a given vector $\boldsymbol{v}$, the permutation must consist of v_l pairs of l-cycles. The cycles in each pair are mutually time reversed and correspond to one of the V encounters in both the partner and its time reversal. The orbit links of the original orbit take the port j to the port $j+1$, while the orbit links of the time reverse take the port $\overline{j}$ to the port $\overline{j-1}$. When we combine the encounter stretches with the following link (traversed in the correct direction), the resulting permutation matrix must consist of two L-cycles corresponding to the partner orbit and its time reversal. The number of permutation matrices that satisfy these properties is the number of structures corresponding to $\boldsymbol{v}$.

The number of structures for each symmetry class can then be calculated numerically by counting the permutation matrices that satisfy the requirements, and these numbers are tabulated in Müller (2005). Müller et al. (2004, 2005) took this further, and derived a recursion relation for the number of structures for a given vector $\boldsymbol{v}$. To obtain this relation, they considered the effect of removing one link from an orbit. By establishing the number of possible ways of recovering orbits with

fewer links, the required recursion relation was obtained.

For systems without time reversal symmetry, the number of structures can be calculated explicitly by using the following formula (Müller, 2003), re-expressed in terms of our notation

$$N(\boldsymbol{v}) = \frac{1}{L+1} \sum_{\boldsymbol{v}' \leq \boldsymbol{v}} \frac{(-1)^{L'-V'} L'! \, (L-L')!}{\prod_{n \geq 2} n^{v_n} v_n'! \, (v_n - v_n')!} \qquad (2.2.9)$$

The sum here is over all integer vectors $\boldsymbol{v}'$ whose components satisfy $0 \leq v_n' \leq v_n$ for all n. L' and V' are the number of links and encounters of the vector $\boldsymbol{v}'$ given by $L' = \sum_{n \geq 2} n v_n'$ and $V' = \sum_{n \geq 2} v_n'$.

In Chapter 3, we apply the semiclassical calculation described in this Section (Müller et al., 2004, 2005) to parametric correlations, and we compare our results with those obtained from RMT. For systems without time reversal symmetry, the RMT integral can be obtained in closed form. To be able to compare our expansion to all orders in τ, we will later need the number of orbits calculated with this formula. For systems with time reversal symmetry, and for the correlation functions for open systems that we consider in Chapter 4, closed form final RMT results are as yet unknown. Instead we compare terms of a small τ expansion calculated semiclassically with those from the RMT integrals. For this purpose, the number of orbit pairs tabulated in Müller (2005) suffices.

2.2.2 Action differences

One important quantity in the semiclassical calculation is the action difference between the orbit and its partner $(S_\gamma - S_{\gamma'})$. For the periodic orbit with a single 2-encounter shown in Figure 2.1 we have two orbit links that join the encounter region. We focussed on the encounter region in Figure 2.3, and we saw that the encounter stretches (or their time reversals) of the orbit and its partner pierce the Poincaré section at the corners of a rectangle in the linearized approximation. The action does not depend on the direction that the encounter stretches are traversed in (for systems with time reversal symmetry), so we can consider the action difference

49
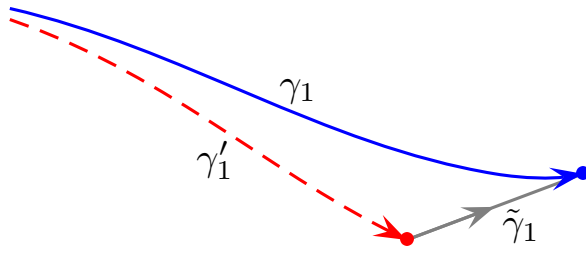
Figure 2.6: An encounter stretch and its partner from a left port to the Poincaré section.

when the four encounter stretches pass in the same direction from the two ports on the left to the two on the right.

To calculate the action difference between the orbit pair, we further split the encounter stretches and their partners into four regions linking the Poincaré section to the four left and right ports. For example, from the upper left port to the Poincaré section we have an original encounter stretch piercing at $(\boldsymbol{u}, \boldsymbol{s})$ and the partner stretch piercing at approximately $(0, \boldsymbol{s})$. We enlarge again, label the stretches γ_1 and γ_1' and depict them in Figure 2.6.

To calculate the action difference between these two stretches, we use a result described by Ozorio de Almeida (1988) which follows from the Poincaré–Cartan theorem. A one parameter family of trajectories (in the energy shell of the system) forms a two dimensional surface. The action integral from some start point to some end point in this surface, is independent of the path in the surface, so that it is the same along any arbitrary curve, embedded in the two dimensional surface, which connects the same start and end points. In our case, we have a family described by varying the unstable component, so that

$$\int_{\gamma_1} \boldsymbol{p} \, \mathrm{d}\boldsymbol{q} = \int_{\gamma_1'} \boldsymbol{p} \, \mathrm{d}\boldsymbol{q} + \int_{\tilde{\gamma}_1} \boldsymbol{p} \, \mathrm{d}\boldsymbol{q} \qquad (2.2.10)$$

The action difference is then given by the integral over the curve $\tilde{\gamma}_1$ joining the two piercing points in the Poincaré section. To be exact, we can extend the stretches back into a link where they become exponentially close, and thus ignore any difference

in their starting points. We can also consider, in a similar manner, the encounter stretches from the other left port to the Poincaré section, and the stretches from the Poincaré section to the two right ports. The total action difference is given by the action integral around the edge of the curve bounded by the piercing points in the Poincaré section. As noted previously, this is a rectangle in the linearized approximation. In systems with f degrees of freedom, as we have seen in Section 1.1, the Poincaré section can be separated into $(f-1)$ sets of (u, s) coordinates, and the piercing points form a rectangle in each. The closed loop action around each rectangle is simply its symplectic area, and the total action integral is then given by the sum of the $(f-1)$ areas. This area is invariant under time evolution of the system.

The linearized action difference of the 2-encounter is the symplectic area $\boldsymbol{su}$ which depends solely on the relative positions of the piercing points of the original encounter stretches. If the Poincaré section is shifted through the encounter region, the coordinates increase and decrease exponentially, but the area remains invariant. This is as expected, since the action difference is unrelated to the choice of the section.

When we consider a general l-encounter, labelled by α, we have l piercing points of the encounter stretches (or their time reverse) in the Poincaré section, at coordinates $(\boldsymbol{u}_i, \boldsymbol{s}_i)$. The partner orbit has encounter stretches whose (possibly time reversed) piercing points in the Poincaré section are given by $(\boldsymbol{u}_{\pi(i)}, \boldsymbol{s}_i)$. The action difference is calculated by integrating between piercing points along the curves in the Poincaré section described by a family of trajectories that leave from each left port, and a family that enter the right port. In all, we must integrate around a complicated path that consists of straight lines in the linearized approximation. This path will enclose an area corresponding to the action difference.

It is simpler however to calculate the action difference by making the reconnection in a series of exchanges of two encounter stretches. We start with the l encounter stretches (or their time reversal) of the original orbit, and with stretch number 1 (which connects left port 1 to right port 1). We find encounter stretches

that make a 2-encounter with the encounter stretch $\pi(1)$ which have piercing coordinates $(\boldsymbol{u}_{\pi(1)}, \boldsymbol{s}_1)$ and $(\boldsymbol{u}_1, \boldsymbol{s}_{\pi(1)})$. We would then have one stretch that passes from left port 1 to right port $\pi(1)$ (which we want in the final configuration of the partner orbit), and a 'dummy' stretch that passes from port $\pi(1)$ to port 1. The action difference is simply that of a 2-encounter, and is given by $(\boldsymbol{s}_{\pi(1)} - \boldsymbol{s}_1)(\boldsymbol{u}_{\pi(1)} - \boldsymbol{u}_1)$. Then we proceed by taking the dummy stretch and making a new 2-encounter with the original orbit stretch $\pi^2(1)$. If we repeat this process $l - 1$ times, we will arrive at the final configuration of the partner orbit. The action difference from each stage is simply summed to obtain the action difference between the periodic orbit and its partner from the l-encounter, and is given by

$$\Delta S_\alpha = \sum_{j=1}^{l-1} (\boldsymbol{s}_{\pi^j(1)} - \boldsymbol{s}_{\pi^{(j-1)}(1)})(\boldsymbol{u}_{\pi^j(1)} - \boldsymbol{u}_1) \tag{2.2.11}$$

Note that each dummy stretch keeps the unstable coordinate of right port 1, hence the asymmetry in the equation. We make a change of variables to the stable and unstable differences of the two stretches involved in each exchange as follows

$$\boldsymbol{s}_{\alpha j} = \boldsymbol{s}_{\pi^j(1)} - \boldsymbol{s}_{\pi^{(j-1)}(1)}, \quad \boldsymbol{u}_{\alpha j} = \boldsymbol{u}_{\pi^j(1)} - \boldsymbol{u}_1 \tag{2.2.12}$$

In these coordinates the action difference from each exchange is $\boldsymbol{s}_{\alpha j} \boldsymbol{u}_{\alpha j}$, so the total action difference from the encounter is

$$\Delta S_\alpha = \sum_{j=1}^{l-1} \boldsymbol{s}_{\alpha j} \boldsymbol{u}_{\alpha j} \tag{2.2.13}$$

The encounter region is defined as being the region in which all of these stable and unstable components are smaller than some small constant c. The encounter time t_{enc}^α is the time spent by the orbit in each traversal of the encounter region and so it depends on the stable and unstable components as follows

$$t_{\text{enc}}^\alpha \approx \frac{1}{\lambda} \ln \frac{c^2}{\max_{i,m} |s_{\alpha i,m}| \times \max_{j,n} |u_{\alpha j,n}|} \tag{2.2.14}$$

52

where m and n label the components of $\boldsymbol{s}_{\alpha i}$ and $\boldsymbol{u}_{\alpha j}$ in the $(f-1)$ sets of (s, u) coordinates. In the semiclassical limit, we are interested in orbit pairs with an action difference that is small on the scale of $\hbar$. The action difference is the sum of products of the form $s_{\alpha j,n} u_{\alpha j,n}$, so the denominator in the above equation should be of the order of $\hbar$. The encounter times are therefore of the order of the Ehrenfest time (cf equation (1.3.15)).

In general, we can have many l-encounters, and the total action difference between an orbit described by $\boldsymbol{v}$ and its partner is the sum of the action differences from each encounter

$$\Delta S = \sum_{\alpha=1}^{V} \sum_{j=1}^{l_\alpha - 1} \boldsymbol{s}_{\alpha j} \boldsymbol{u}_{\alpha j} = \sum_{\alpha, j} \boldsymbol{s}_{\alpha j} \boldsymbol{u}_{\alpha j} = \tilde{\boldsymbol{s}} \tilde{\boldsymbol{u}} \qquad (2.2.15)$$

where $\tilde{\boldsymbol{s}}$ is a vector whose entries record the stable phase space separations and $\tilde{\boldsymbol{u}}$ records the unstable separations.

2.2.3 Probability of encounters

For an orbit and its partner, with a certain structure, the phase space separations $(\tilde{\boldsymbol{u}}, \tilde{\boldsymbol{s}})$ of the encounter stretches determine the action difference of the pair. To calculate the contribution of this type of orbit pair to the form factor, we examine the average probability density that an orbit with the given structure and encounter stretch separations exists. To do this we treat the long periodic orbits as uniform so that the probability that an orbit stretch pierces a region of a Poincaré section of size $\mathrm{d}\boldsymbol{u}\mathrm{d}\boldsymbol{s}$ in a time interval $\mathrm{d}t$ is a uniform probability given by

$$\frac{\mathrm{d}\boldsymbol{u}\mathrm{d}\boldsymbol{s}\mathrm{d}t}{\Omega} \qquad (2.2.16)$$

so the weight of a certain structure, with given phase space separations $\tilde{\boldsymbol{s}}, \tilde{\boldsymbol{u}}$, of period T is

$$\frac{w_T(\tilde{\boldsymbol{s}}, \tilde{\boldsymbol{u}})}{L} = \frac{\int_0^T \mathrm{d}t_L \int_0^{T-t_{\mathrm{enc}}} \mathrm{d}t_{L-1} \ldots \int_0^{T-t_{\mathrm{enc}}-t_{L-1}\ldots-t_2} \mathrm{d}t_1}{L\Omega^{L-V} \prod_\alpha t_{\mathrm{enc}}^\alpha} \qquad (2.2.17)$$

53

This weight is derived by picking a starting point t_L on the orbit and considering the times of the piercing points of the orbit in the various Poincaré sections of the encounter regions following the order described by the particular structure. To obtain the weight of a particular structure, we integrate over all the possible piercing times, but in the equation above we have made a change of variable to the link times (denoted by t_i for $i = 1 \ldots L-1$). The limits are determined by the fact that the total time of the L links is the orbit time minus the total encounter time $t_{\text{enc}} = \sum_\alpha l_\alpha t_{\text{enc}}^\alpha$, as each encounter α involves l_α encounter stretches that each take a time t_{enc}^α to traverse. Only $L - 1$ integrals are performed over the possible link times, as the L-th link time will be determined by the other link times and the time of the orbit. The remaining integral over t_L is over the possible starting points. Most of the factors in the denominator compensate for overcounting. The factor L effectively compensates for overcounting the L possible and equivalent choices of the starting orbit stretch in the structure. The Poincaré section of each encounter is positioned at first piercing point of that encounter in the structure. Changing the time of the piercing point means moving the Poincaré section through the encounter region, but this does not affect the structure. Therefore, when we integrate over the time of the piercing point (or equivalently the link time) we have counted all possible positions of the section, and the encounter region is actually overcounted by its encounter time. For the weight, we integrate over all piercing times (or link times) so the total overcounting factor is $\prod_\alpha t_{\text{enc}}^\alpha$.

When we perform the integrals, the weight becomes

$$\frac{w_T(\tilde{\boldsymbol{s}}, \tilde{\boldsymbol{u}})}{L} = \frac{T(T - \sum_\alpha l_\alpha t_{\text{enc}}^\alpha)^{L-1}}{L! \Omega^{L-V} \prod_\alpha t_{\text{enc}}^\alpha} \tag{2.2.18}$$

This result is independent of the structure considered, so we can consider all structures with the same vector $\boldsymbol{v}$ together, and simply multiply by their number $N(\boldsymbol{v})$. With this weight we can define the density $P_{\boldsymbol{v}}(\Delta S)$ of the number of orbits with a certain vector and action difference ΔS. This is given by

$$P_{\boldsymbol{v}}(\Delta S) = N(\boldsymbol{v}) \int \mathrm{d}\tilde{\boldsymbol{s}} \, \mathrm{d}\tilde{\boldsymbol{u}} \, \delta\left(\Delta S - \tilde{\boldsymbol{s}}\tilde{\boldsymbol{u}}\right) \frac{w_T(\tilde{\boldsymbol{s}}, \tilde{\boldsymbol{u}})}{L} \tag{2.2.19}$$

where the integrals are over the $L - V$ stable and unstable separations

$$\mathrm{d}\tilde{\boldsymbol{s}} \, \mathrm{d}\tilde{\boldsymbol{u}} = \mathrm{d}^{L-V}\boldsymbol{s} \, \mathrm{d}^{L-V}\boldsymbol{u} = \prod_{\alpha=1}^{V} \prod_{j=1}^{l_\alpha - 1} \mathrm{d}\boldsymbol{s}_{\alpha j} \, \mathrm{d}\boldsymbol{u}_{\alpha j} \tag{2.2.20}$$

In the next section, we will show how using this average density, we can approximate the sum over orbit pairs by an integral over the action difference and obtain their contribution to the form factor.

2.2.4 Final contribution

Recalling equation (1.3.20), with the repetition of primitive orbits removed, we will examine the contribution to the form factor of orbits defined by a vector $\boldsymbol{v}$, which is given by

$$K_{\boldsymbol{v}}(\tau) = \frac{1}{T_{\mathrm{H}}} \left\langle \sum_{\gamma,\gamma'}^{\text{fixed } \boldsymbol{v}} A_\gamma A_{\gamma'}^* \mathrm{e}^{\frac{\mathrm{i}}{\hbar}(S_\gamma - S_{\gamma'})} \delta\left(\tau T_{\mathrm{H}} - \frac{T_\gamma + T_{\gamma'}}{2}\right) \right\rangle \tag{2.2.21}$$

Here, the orbit pairs we are considering traverse the same links, and the encounter stretches are close together, so they should have the same Maslov indices ($\mu_\gamma = \mu_{\gamma'}$). We can use the equidistribution theorem to sum over the orbits and we separate the weighted sum from the expected number of correlated orbits. We then approximate the expected number by an integral over action differences, with the density $P_{\boldsymbol{v}}(\Delta S)$, to express the contribution to the form factor as

$$K_{\boldsymbol{v}}(\tau) \approx \kappa\tau \int \mathrm{d}\Delta S \, P_{\boldsymbol{v}}(\Delta S) \mathrm{e}^{\frac{\mathrm{i}}{\hbar}\Delta S} \tag{2.2.22}$$

When we use the definition of $P_{\boldsymbol{v}}(\Delta S)$ from equation (2.2.19), the previous equation reduces to

$$K_{\boldsymbol{v}}(\tau) \approx \kappa\tau N(\boldsymbol{v}) \int \mathrm{d}\tilde{\boldsymbol{s}} \, \mathrm{d}\tilde{\boldsymbol{u}} \, \frac{w_T(\tilde{\boldsymbol{s}}, \tilde{\boldsymbol{u}})}{L} \mathrm{e}^{\frac{\mathrm{i}}{\hbar}\tilde{\boldsymbol{s}}\tilde{\boldsymbol{u}}} \tag{2.2.23}$$

When we substitute the expression for the weight of equation (2.2.18), we obtain

$$K_{\boldsymbol{v}}(\tau) \approx \kappa\tau N(\boldsymbol{v}) \int \mathrm{d}\tilde{\boldsymbol{s}}\,\mathrm{d}\tilde{\boldsymbol{u}}\, \frac{T(T - \sum_\alpha l_\alpha t_{\mathrm{enc}}^\alpha)^{L-1}}{L!\Omega^{L-V}\prod_\alpha t_{\mathrm{enc}}^\alpha} \mathrm{e}^{\frac{\mathrm{i}}{\hbar}\tilde{\boldsymbol{s}}\tilde{\boldsymbol{u}}} \qquad (2.2.24)$$

The main ingredient that simplifies the semiclassical calculation is the fact that, in the semiclassical limit, for a given encounter α we find

$$\int \prod_j \mathrm{d}\boldsymbol{s}_{\alpha j}\,\mathrm{d}\boldsymbol{u}_{\alpha j}\,(t_{\mathrm{enc}}^\alpha)^m \mathrm{e}^{\frac{\mathrm{i}}{\hbar}\sum_j \boldsymbol{s}_{\alpha j}\boldsymbol{u}_{\alpha j}} \approx \begin{cases} 0 & \text{if } m = -1 \\ (2\pi\hbar)^{(l_\alpha-1)(f-1)} & \text{if } m = 0 \end{cases} \qquad (2.2.25)$$

where we need to keep in mind that the encounter time depends on the stable and unstable coordinates. For $m = -1$, the result of the integral behaves like $\sin\left(\frac{1}{\hbar}\right)$, which oscillates in the limit $\hbar \to 0$, and so these terms should be removed by the energy averaging. For $m \geq 1$, the final semiclassical result involves powers of $\frac{T_{\mathrm{E}}}{T_{\mathrm{H}}}$, which behaves like $\hbar\ln(\hbar)$. This vanishes in the limit $\hbar \to 0$, and so these terms can also be ignored.

This means that we can expand the multinomial term in equation (2.2.24), and keep only the terms where the t_{enc}^α in the numerator exactly cancel those in the denominator. In general, to find the contribution of orbits of the type $\boldsymbol{v}$, we simply need to expand the weight function $\frac{w_T(\tilde{\boldsymbol{s}},\tilde{\boldsymbol{u}})}{L}$, keep the terms where the encounter times all cancel, and substitute the result of the above integral.

When we do this, we find that the only term remaining here is

$$K_{\boldsymbol{v}}(\tau) \approx \kappa\tau N(\boldsymbol{v}) \int \mathrm{d}\tilde{\boldsymbol{s}}\,\mathrm{d}\tilde{\boldsymbol{u}}\, \frac{T^{L-V}\prod_\alpha(-l_\alpha)}{L(L-V-1)!\Omega^{L-V}} \mathrm{e}^{\frac{\mathrm{i}}{\hbar}\tilde{\boldsymbol{s}}\tilde{\boldsymbol{u}}} \qquad (2.2.26)$$

When we perform the $(L - V)$ double integrals using equation (2.2.25), we get a factor of $(2\pi\hbar)^{(L-V)(f-1)}$ so the contribution becomes

$$K_{\boldsymbol{v}}(\tau) \approx \kappa\tau N(\boldsymbol{v}) \left(\frac{T(2\pi\hbar)^{f-1}}{\Omega}\right)^{L-V} \frac{(-1)^V\prod_\alpha(l_\alpha)}{L(L-V-1)!} \qquad (2.2.27)$$

56

The original sum was over orbits with periods $T = \tau T_{\mathrm{H}}$, so when we recall the definition of the Heisenberg time $T_{\mathrm{H}} = \frac{\Omega}{(2\pi\hbar)^{f-1}}$, the form factor contribution is given by

$$K_{\boldsymbol{v}}(\tau) \approx \kappa \tau^{L-V+1} N(\boldsymbol{v}) \frac{(-1)^V \prod_{\alpha}(l_{\alpha})}{L(L-V-1)!} \qquad (2.2.28)$$

We can see that the power of τ in the contribution of each vector depends on the value of $L - V + 1$. To find the coefficient of τ^n in the semiclassical form factor we can then sum over all vectors where $L - V + 1 = n$, so that the coefficient is given by

$$K_n(\tau) = \sum_{\boldsymbol{v}}^{L-V+1=n} \kappa N(\boldsymbol{v}) \frac{(-1)^V \prod_{\alpha}(l_{\alpha})}{L(L-V-1)!} \qquad (2.2.29)$$

As a last step, Müller et al. (2004, 2005) use the recursion relation on the number of orbit pairs to perform this sum. For systems without time reversal symmetry, the result is 0 for $n \geq 2$ meaning that all off-diagonal terms vanish, and the final result is in line with the small τ RMT result in equation (1.5.4)

$$K(\tau) \approx \tau \qquad (2.2.30)$$

For systems with time reversal symmetry, the coefficients are given by

$$K_n(\tau) = \frac{(-2)^{n-1}}{n-1}, \quad n \geq 2 \qquad (2.2.31)$$

so that the semiclassical form factor is given by

$$K(\tau) \approx 2\tau + \sum_{n=2}^{\infty} \frac{(-2)^{n-1}}{n-1} \tau^n \qquad (2.2.32)$$

which agrees with the small τ RMT result (equation (1.5.5)), for each term and to all orders.

2.2.5 Semiclassical recipe

In the next two Chapters, we extend this method and consider parametric correlations and correlations of the Wigner time delay for open systems. The semiclassical expression for the form factor of these correlations again involves a double sum over pairs of periodic orbits. Using similar semiclassical arguments, we will be able to express the contribution of orbits labelled by $\boldsymbol{v}$ to the form factor as (cf equation (2.2.23))

$$K_{\boldsymbol{v}}(\tau,\dots) \approx \kappa\tau N(\boldsymbol{v}) \int \mathrm{d}\tilde{\boldsymbol{s}}\,\mathrm{d}\tilde{\boldsymbol{u}}\, \frac{z_T(\tilde{\boldsymbol{s}},\tilde{\boldsymbol{u}})}{L} \mathrm{e}^{\frac{\mathrm{i}}{\hbar}\tilde{\boldsymbol{s}}\tilde{\boldsymbol{u}}} \tag{2.2.33}$$

where $z_T(\tilde{\boldsymbol{s}},\tilde{\boldsymbol{u}})$ is a product of the weight $w_T(\tilde{\boldsymbol{s}},\tilde{\boldsymbol{u}})$ and a factor depending on the exact type of correlation we are considering. The factor will include all the extra terms due to the type of correlation, and we can consider $z_T(\tilde{\boldsymbol{s}},\tilde{\boldsymbol{u}})$ as an 'augmented' weight.

As this expression is very similar to equation (2.2.23), we can calculate the contribution in the same way as before, and extract a recipe for it. Only terms in $z_T(\tilde{\boldsymbol{s}},\tilde{\boldsymbol{u}})$ where the $t_{\mathrm{enc}}^{\alpha}$ cancel in the numerator and denominator contribute in the integral of equation (2.2.25) in the semiclassical limit. As we know the number of structures $N(\boldsymbol{v})$, we can calculate the contribution just from knowing $z_T(\tilde{\boldsymbol{s}},\tilde{\boldsymbol{u}})$ by expanding the numerator and finding the coefficient of $\prod_{\alpha} t_{\mathrm{enc}}^{\alpha}$. This coefficient will have T to a power of at least $L-V$, so we factorise this out and define the coefficient following

$$T^{L-V}C(T,\boldsymbol{v}) \tag{2.2.34}$$

This will be the only term that contributes, so we can replace $\frac{z_T(\tilde{\boldsymbol{s}},\tilde{\boldsymbol{u}})}{L}$ in the integral in equation (2.2.33) by

$$\frac{T^{L-V}C(T,\boldsymbol{v})}{L!\,\Omega^{L-V}} \tag{2.2.35}$$

When we perform the double $(L-V)$ integrals according to equation (2.2.25), the contribution to the form factor for this type of orbit becomes

58

$$K_{\boldsymbol{v}}(\tau, \ldots) \approx \kappa \tau^{L-V+1} \frac{N(\boldsymbol{v}) C(\tau T_{\mathrm{H}}, \boldsymbol{v})}{L!} \qquad (2.2.36)$$

Thus in order to find the contribution of orbits of the type $\boldsymbol{v}$ to the form factor, we simply need to find the coefficient of $\prod_\alpha t_{\mathrm{enc}}^\alpha$ in the numerator of $\frac{z_T(\tilde{\boldsymbol{s}}, \tilde{\boldsymbol{u}})}{L}$ and follow these steps.

2.3   Discussion

The steps and approximations we have taken up to this point have allowed us to see which kinds of correlated orbits are responsible for each of the terms of the small τ expansion of the form factor obtained from RMT. Unfortunately the procedure lacks a rigorous justification, although it gains *a postiori* credibility from the fact that it reproduces the RMT results.

In the following we give a few details and considerations related to the main steps and approximations of the semiclassical calculation. Consider, for example, the use of the equidistribution theorem, which comes from the uniform distribution of the long periodic orbits on the energy shell. We take into account particular correlated orbits and the average probability that they exist in the ensemble of long orbits is evaluated with the equidistribution theorem. This evaluation requires that typical links in an orbit are long enough that their ends can be treated as uncorrelated. This then allows the use of the property of mixing to approximate the phase space average of the weight function with a product of averages over the link ends, which in turn picks out orbits with the required piercing points. Similarly, we assume that we can decouple the parts of the orbit that are involved in the local behaviour of encounters from the links that wander ergodically. These parts must connect to each other, and the connection involves parts of the orbit of order of the Ehrenfest time, which is the time scale that separates the two behaviours. Müller (2005) examined the effect of the 'fringes' of the encounter regions, where some of the encounter stretches remain close also for times of the order of the Ehrenfest time. In the limit $\hbar \to 0$, the Ehrenfest time is vanishingly small compared to the time scale of the orbits we

59

are considering, the Heisenberg time, and so these corrections do not affect the form factor. A sharp cut off between the encounters and the links makes sense in this limit, and justifies the decoupling assumption. Likewise, the links are of the order of the Heisenberg time, so the assumption that they are long enough to decorrelate seems reasonable.

Small corrections due to the encounters that are of the order of the Ehrenfest time are important as a result of the semiclassical integral in equation (2.2.25). Terms with inverse powers of encounter times oscillate rapidly in the limit $\hbar \to 0$, and should be removed by the energy averaging. Terms with powers of encounter times give a result that includes the ratio of the Ehrenfest time to the Heisenberg time, and also vanish in the limit. Only terms where all encounter times cancel give a reliable contribution, and the asymptotic contribution of the integral comes from the origin $(\boldsymbol{u}, \boldsymbol{s}) = (0, 0)$. This means that, near the origin, many of the approximations made become more exact, and provides a justification for their use.

Including corrections to the approximations makes the calculations more difficult. These corrections were considered by Heusler (2003) (see also Sieber, 2003; Müller, 2005) in relation to orbits with a single 2-encounter on a surface with constant negative curvature. They looked at the next order correction to the amplitudes, action difference and the weight function and showed that the sum of all these contributions cancel. This result lends support to the use of the approximations, but for non-uniformly hyperbolic systems it is not known if corrections to the approximations do cancel. We can also test the assumptions and approximations discussed in this Chapter by applying them to new situations. If using the same methods we can recover RMT results in novel situations, this would lend support to the method. We shall consider applying this method to parametric correlations and open systems in the next two Chapters.

It could be said that this method captures the heart of the semiclassical calculations, and in doing so it provides us with an explanation in terms of classical orbits of the energy statistics of quantum chaotic systems. Alternatively, it may simply provide us with another way to expand RMT integrals. At the moment we lack a

rigorous justification, which is a technically demanding challenge, but it does seem that with its link to classical periodic orbits, this method offers an explanation of the statistics described by RMT.

For closed systems, this agreement is partly due to the fact that any error from the parts of the orbit involved in the transition from the encounters (and the local hyperbolic motion we consider for them) to the links (and their global ergodic behaviour) are of the order of the Ehrenfest time, and can be ignored compared to the Heisenberg time. For open systems however, there is a third relevant time scale, the dwell time which is the average time spent in the system. If this is longer than the Ehrenfest time, we can still expect average trajectories to become ergodic between any encounters and to remain in a regime describable by RMT. When the Ehrenfest time gets longer than the average trajectory time, we never really leave local behaviour during the trajectories' stay in the system, and errors of the order of the Ehrenfest time become important. When applying these methods in this regime (see for example Whitney and Jacquod, 2006; Brouwer and Rahav, 2006), it is unclear that the approximations, especially concerning the decoupling of the encounters and the rest of the trajectory, are still justified. Moreover, in the absence of RMT results as a guide, it is harder to assess whether all contributions have been included correctly. We will briefly consider these different regimes in Chapter 5.

A major challenge for a rigorous justification is to show that no other periodic orbits give a contribution. However, in order for the form factor to recreate RMT results for $\tau > 1$, a minimum requirement is that there must be other correlated pairs to cancel the divergent diagonal approximation. Fundamentally, for $\tau > 1$, or times longer than the Heisenberg time, an ergodic trajectory would pass through every Planck cell on average more than once, and there would be an enormous number of encounters (for example between all adjacent Planck cells on the trajectory entered at separate times). With the weight function approach we have considered in this Chapter, we concentrate on one particular structure with a fixed number of encounters at a time. We reconnect the encounters to create a partner orbit and ignore any other encounters that may occur in the links between them. This ap-

proach still holds for times longer than the Heisenberg time (the links just become longer). However, in a different sense these orbits rarely leave the encounter regions, but pass from one to the next without long links in between. If we allowed all possible encounters and reconnections, the weight function approach would no longer apply without the ergodic links. The Heisenberg time represents the border between shorter orbits with long wandering links that occasionally come close to each other, and longer orbits with the property that they are often close to another part of themselves. It is interesting to wonder whether a different type of correlated orbit pair can arise from this property, but it is not clear how to treat this eventuality semiclassically.

Recently though, progress in the regime $\tau > 1$ has come from the methods of Müller et al. (2004, 2005) that we have explored in this Chapter. Heusler et al. (2007) considered a generating function of the correlation function using spectral determinants. This allowed them to express the correlation function in terms of a sum over four sets of periodic orbits (also known as pseudo or composite orbits) and to recreate the full form factor for all τ. Implicit in this is a use of resummation (Keating and Müller, 2007) which re-expresses the sum over long periodic orbits in terms of shorter ones, and the correlations of orbits longer than the Heisenberg time in terms of those that are shorter. Treating the correlations between the long periodic orbits directly remains one of the challenges of the study of correlated trajectories in quantum chaos.

3   Parametric correlations

With parametric correlations we consider systems that no longer only depend on the energy, but also on some external parameter. This parameter could be anything, for example the temperature or a magnetic field, but in this Chapter we are only interested in physical situations where changing this parameter does not change the symmetry of the system. If the symmetry is changed then we have a different class of problem, one such example is the GOE-GUE transition. A recent semiclassical analysis of this transition between symmetry classes, due to the influence of a magnetic field, has been considered by Saito and Nagao (2006), where they derive terms in the form factor up to the third order. More recently, Nagao et al. (2007) extended this to seventh order. In this paper they also considered parametric correlations due to a magnetic field for systems without time reversal symmetry and arrived at the same results we present in this Chapter. We consider the GOE-GUE transition for open systems in Section 4.3, but since for many physical processes the system remains in one symmetry class as the parameter of interest is varied, we focus only on the effect of this type of variation in this Chapter. Because this covers a wide range of physical situations, the effects of parametric variation can be observed and tested experimentally. A review of parametric correlations is given by Ozorio de Almeida et al. (1998), with a focus on the semiclassical approach. Here we introduce the ideas we need for our semiclassical analysis and discuss some experiments where these effects can be observed.

Some of the first considerations of the statistical properties of parametric variations appeared in Wilkinson (1988). In that paper, and in Wilkinson (1989, 1990),

the author studied the dependence of the dissipation of the system on the rate of varying the external parameter, and he also modelled the dissipation using random matrices. Examining the level curvature instead, Gaspard et al. (1990) were able to show that the tail of its distribution followed results from RMT (the exact RMT results for level curvature distributions were derived later by von Oppen, 1994, 1995). Gaspard et al. (1990) rescaled the level curvatures to compare different systems, and on the basis of their theoretical and numerical results, they suggested that the level curvature distribution should have a universal form, only dependent on the symmetry of the system.

At roughly the same time, Goldberg et al. (1991) studied a new parametric correlation function, the parametric number variance, both semiclassically and numerically. The semiclassical analysis involved the diagonal approximation and included the important insight that the parametric velocities of orbit actions (the derivatives of the action with respect to the parameter) are uncorrelated with the orbit actions and follow a Gaussian distribution. In this Chapter we extend these ideas when we derive the off-diagonal contributions. Goldberg et al. (1991) also argued that the parametric number variance should show universal behaviour when the parameter difference is small. This idea of universal behaviour was also considered by Szafer and Altshuler (1993). They considered parametric velocity correlations for disordered, ring (annulus) and cylindrical shaped, systems with a magnetic flux passing through the hole. For small fluctuations of the magnetic flux (but bigger than some cutoff value) they derived a universal quantity and compared it with numerical simulations. A numerical comparison of chaotic billiards on a cylindrical surface with the universal quantity, although less close, led them to suggest that the same behaviour should be observed for all systems of this type. More precisely, systems whose level statistics follow RMT predictions (when the parameter difference is removed) should possess this universal quantity for parametric correlations.

The papers by Simons and Altshuler (1993a,b) clarified and illuminated these concepts. They showed that, with the correct rescaling of the external parameter, the parametric correlations take a universal form. They examined disordered ring

systems and chaotic billiards, but as they noticed that only the rescaling is system dependent, they speculated that the results should generalize to other chaotic systems. They also derived universal forms from RMT by adding an extra term corresponding to parametric correlations. These new RMT results are, like the previous ones, universal and depend only on the symmetry of the underlying dynamics. Using rescaling, it is then possible to compare semiclassical methods, RMT predictions and numerical and experimental results. The comparison between semiclassical methods and RMT predictions is covered by the rest of this Chapter, while we briefly examine the comparison with numerical and experimental results in the rest of this introduction.

The papers of Goldberg et al. (1991); Szafer and Altshuler (1993); Simons and Altshuler (1993a,b) have numerical results that (usually) show good agreement, in the applicable regimes, to the universal predictions. Results obtained by numerical methods that had been shown to agree with experiments, allowed for the first indirect comparison with experimental results. As such, Simons et al. (1993) showed the effectiveness of rescaling for the spectra of hydrogen in a magnetic field (a case also studied numerically by Goldberg et al., 1991). They looked at a range of correlation functions including the parametric number variance and the two-point parametric velocity correlation function, and showed very good agreement with the RMT predictions, especially at small values of the parameter difference. Similar results were obtained a year later by Mucciolo et al. (1994) for the energy spectra of crystals. The first experiments designed specifically to test the universality of parametric correlations came in 1999. Microwave billiard experiments from Barth et al. (1999) and Hlushchuk et al. (2000) showed very good agreement for the Sinai billiard, and slightly worse agreement at larger parameter differences for the annular ray-splitting billiard. Barth et al. (1999) also looked at a different type of correlation, for a rectangular billiard with scattering disks, that resulted from a parameter change that affects the system only locally. A completely different type of experiment was performed by Bertelsen et al. (1999). They looked at the spectra of a quartz block, with an octant corner removed, as the temperature was varied. Their results, like oth-

ers before, showed good agreement at small values of the parameter difference, but significant discrepancies elsewhere. Finally, with similar results, was an experiment performed by Schaadt and Kudrolli (1999) on the vibrational eigenfrequencies of an aluminium plate as the length of one side was varied. This system is a macroscopic analogue of a quantum chaotic one, and they found very close agreement between the experimental results and RMT theory.

The papers which compare various correlation functions numerically and experimentally to RMT type predictions showed good agreement for small values of the parameter difference, and varying degrees of agreement for larger values. Aside from the problems of gathering sufficient data of the correct type and calculating derivatives from the data, part of the difficulty seems to be in the exact nature of the rescaling. Leboeuf and Sieber (1999) showed that the rescaling introduced by Simons and Altshuler (1993a,b) is, in general, not invariant under reparameterization. They introduce a rescaling that is invariant, and which has the property that the velocity variance of the new parameter is identical to unity. For other correlation quantities it seems that the average (in some sense) of the rescaled parameter should be one. However, for numerical or experimental results, care must be taken that the average satisfies this property in practice. Indeed when Hussein et al. (2002) imposed the condition that the average of the absolute value of the level curvature should be equal to one on the data from Bertelsen et al. (1999) the agreement with RMT predictions was shown to be remarkable. Likewise, Pato et al. (2005) imposed the same condition on data from four experiments and, when rescaled appropriately, found extremely close agreement between theory and experiment.

For the comparison of numerical and experimental results with RMT and semiclassical calculations, the correct rescaling is essential. In the rest of this Chapter we show how, using the ideas developed by Müller et al. (2004, 2005) we can get the same results as from RMT using a semiclassical argument. One last ingredient we need is the rescaling factor itself (Simons and Altshuler, 1993a,b). By using arguments with a similar flavour to the semiclassical sum rule, a direct semiclassical evaluation of the variance of matrix elements was derived by Eckhardt et al. (1995)

and for the variance of the velocities by Leboeuf and Sieber (1999). This is the rescaling factor we need, and with everything in place, we can now derive the RMT results using a semiclassical argument.

3.1 Parametric form factor

Previously our density of states depended solely on the energy E, but here we consider that our system is also influenced by some external parameter X, so that the density of states depends on both E and X. Along with the energy unfolding described in section 1.3.3, to obtain universal correlation functions we also need to unfold the external parameter. Following Simons and Altshuler (1993a,b) and Leboeuf and Sieber (1999), we introduce a new parameter

$$\tilde{X} = \int_{X_0}^{X} dX' \, \sigma(X') \tag{3.1.1}$$

where X_0 is the value of the parameter X at which we wish $\tilde{X}$ to correspond to 0, and $\sigma(X)$ is defined by the following

$$\sigma(X) = \left\langle \left[\frac{\partial \tilde{E}_n(X)}{\partial X} \right]^2 \right\rangle^{\frac{1}{2}} \tag{3.1.2}$$

where $\frac{\partial \tilde{E}_n}{\partial X}$ are the level velocities and the average is performed over the energy levels in the interval $\Delta \tilde{E}$. In terms of the unfolded variables, the mean level density and the variance of the level velocities are both 1. With the unfolded density of states $\tilde{d}(\tilde{E}, \tilde{X})$, the (irreducible) parametric two-point correlation function is given by

$$\tilde{R}_2(\omega, x) = \left\langle \tilde{d}^{\mathrm{osc}} \left(\tilde{E} + \frac{\omega}{2}, \tilde{X} + \frac{x}{2} \right) \tilde{d}^{\mathrm{osc}} \left(\tilde{E} - \frac{\omega}{2}, \tilde{X} - \frac{x}{2} \right) \right\rangle_{\tilde{E}, \tilde{X}} \tag{3.1.3}$$

The averaging is now performed both over a range of energies $\Delta \tilde{E}$ as well as a parameter interval $\Delta \tilde{X}$. These ranges are small on the classical scale, and so, by linearizing the unfolding relations, we can express the parametric two-point correlation

function in terms of the original density of states.

$$\tilde{R}_2(\omega, x) \sim \left\langle \frac{d^{\mathrm{osc}}\left(E + \frac{\omega}{2\bar{d}} + \frac{x\rho}{2\sigma}, X + \frac{x}{2\sigma}\right) d^{\mathrm{osc}}\left(E - \frac{\omega}{2\bar{d}} - \frac{x\rho}{2\sigma}, X - \frac{x}{2\sigma}\right)}{\bar{d}^2} \right\rangle_{E,X} \quad (3.1.4)$$

Here σ is evaluated at the parameter value X and $\bar{d}$ at the values of E and X. Compared to the non-parametric case, the extra term $\frac{x\rho}{2\sigma}$ is due to the change of the energy when X is changed at fixed $\tilde{E}$

$$\rho = \left. \frac{\partial E}{\partial X} \right|_{\tilde{E}} = -\frac{\partial \bar{N}/\partial X}{\partial \bar{N}/\partial E} \quad (3.1.5)$$

As well as the two-point correlation function, we can also consider its Fourier transform, the parametric form factor. We make the substitution $\omega = \bar{d}\eta$ to arrive at

$$K(\tau, x) = \int \mathrm{d}\eta \, \frac{d^{\mathrm{osc}}\left(E + \frac{\eta}{2} + \frac{x\rho}{2\sigma}, X + \frac{x}{2\sigma}\right) d^{\mathrm{osc}}\left(E - \frac{\eta}{2} - \frac{x\rho}{2\sigma}, X - \frac{x}{2\sigma}\right)}{\bar{d}} \mathrm{e}^{\frac{-\mathrm{i}\eta\tau T_{\mathrm{H}}}{\hbar}} \quad (3.1.6)$$

where the Heisenberg time is given by $T_{\mathrm{H}} = 2\pi\hbar\bar{d}$. We recall that the oscillating part of the density of states can be written as a sum over periodic orbits (see equation (1.3.16))

$$d^{\mathrm{osc}}(E, X) = \frac{1}{2\pi\hbar} \sum_{\gamma, r} \left[A_{\gamma, r} \mathrm{e}^{\frac{\mathrm{i}}{\hbar} r S_\gamma(E, X)} + \mathrm{c.c.} \right] \quad (3.1.7)$$

where γ labels the primitive periodic orbits and r their repetitions, and the orbits have action S_γ and amplitude A_γ (which includes the period T_γ and the Maslov index). We can substitute this into the form factor making the same simplifications as before, i.e. we ignore differences in the slowly varying prefactor and we only consider terms in the double sum where the actions of the two orbits have a different sign. For convenience we will also remove the repetitions of primitive orbits, as their contribution is exponentially smaller than that of the primitive orbits. When we expand the action up to first order we obtain

$$S_\gamma \left(E \pm \frac{\eta}{2} \pm \frac{x\rho}{2\sigma}, X \pm \frac{x}{2\sigma} \right) \approx S_\gamma(E, X) \pm \frac{\eta}{2} T_\gamma(E, X) \pm \frac{x}{2\sigma} Q_\gamma(E, X) \qquad (3.1.8)$$

where Q_γ is the parametric velocity of the orbit γ and is given by

$$Q_\gamma = \left. \frac{\partial S_\gamma}{\partial X} \right|_{\tilde{E}} = \rho \frac{\partial S_\gamma}{\partial E} + \frac{\partial S_\gamma}{\partial X} \qquad (3.1.9)$$

The form factor then becomes

$$K(\tau, x) = \frac{1}{2\pi\hbar T_{\mathrm{H}}} \int \mathrm{d}\eta \sum_{\gamma, \gamma'} \left[A_\gamma A_{\gamma'}^* \mathrm{e}^{\frac{\mathrm{i}}{\hbar}(S_\gamma - S_{\gamma'})} \mathrm{e}^{\frac{\mathrm{i}x}{2\sigma\hbar}(Q_\gamma + Q_{\gamma'})} \mathrm{e}^{\frac{\mathrm{i}\eta}{2\hbar}(T_\gamma + T_{\gamma'})} + \mathrm{c.c.} \right] \mathrm{e}^{\frac{-\mathrm{i}\eta}{\hbar}\tau T_{\mathrm{H}}}$$

$$(3.1.10)$$

If we perform the integral over η and keep only the contributing delta function, then the parametric form factor can be expressed as

$$K(\tau, x) = \frac{1}{T_{\mathrm{H}}} \left\langle \sum_{\gamma, \gamma'} A_\gamma A_{\gamma'}^* \mathrm{e}^{\frac{\mathrm{i}}{\hbar}(S_\gamma - S_{\gamma'})} \mathrm{e}^{\frac{\mathrm{i}x}{2\sigma\hbar}(Q_\gamma + Q_{\gamma'})} \delta \left(\tau T_{\mathrm{H}} - \frac{T_\gamma + T_{\gamma'}}{2} \right) \right\rangle \qquad (3.1.11)$$

3.1.1   Diagonal approximation

For the diagonal approximation ($\gamma = \gamma'$) the parametric form factor is

$$K^{\mathrm{diag}}(\tau, x) = \frac{1}{T_{\mathrm{H}}} \left\langle \sum_\gamma |A_\gamma|^2 \mathrm{e}^{\frac{\mathrm{i}x}{\sigma\hbar} Q_\gamma} \delta \left(\tau T_{\mathrm{H}} - T_\gamma \right) \right\rangle \qquad (3.1.12)$$

where κ is 2 if the system has time reversal symmetry, because we can also pair an orbit with its time reversal, and κ is 1 if the system does not have time reversal symmetry. In order to be able to perform this sum we need to know how the average (over orbits of a similar period T) of $\mathrm{e}^{\frac{\mathrm{i}x}{\sigma\hbar} Q_\gamma}$ behaves. Following the argument in Ozorio de Almeida et al. (1998) we assume that the Q_γ have a Gaussian distribution (Goldberg et al., 1991). This assumption can be understood intuitively by considering the effect along the orbit of making a small change to the external parameter. Each small section of the orbit will be shifted slightly, leading to a slight change in the action. The total change in the action will be the sum of all the small and

essentially random changes along the orbit, and so can be expected to tend towards following a Gaussian distribution via the central limit theorem. We can therefore evaluate the required average as

$$\left\langle e^{\frac{ix}{\sigma\hbar}Q_\gamma} \right\rangle = e^{-\frac{x^2}{2\sigma^2\hbar^2}\overline{Q^2}} \tag{3.1.13}$$

by integrating over a Gaussian probability distribution. The right hand side can be evaluated, in line with the equidistribution theorem, as an energy shell integral and this leads to the result $\overline{Q^2} = aT$ as given in Goldberg et al. (1991). Again this result can be understood intuitively as follows. Since the number of small orbit sections, and their accompanying random shifts in the action, grows linearly with the period, the variance of the resulting distribution grows likewise. If we define β as $\frac{ax^2}{2\sigma^2\hbar^2}$ then the average over Q_γ is given by

$$\left\langle e^{\frac{ix}{\sigma\hbar}Q_\gamma} \right\rangle = e^{-\beta T} \tag{3.1.14}$$

We can effectively replace the parametric velocity term in equation (3.1.12) by this average when we perform the sum over periodic orbits using the equidistribution theorem. For closed systems, for all orbits of period T, this means

$$\sum_\gamma |A_\gamma|^2 e^{\frac{ix}{\sigma\hbar}Q_\gamma} \delta_\epsilon (T - T_\gamma) \sim T e^{-\beta T}, \quad T \to \infty \tag{3.1.15}$$

When we substitute this result into equation (3.1.12), we find that our diagonal approximation is simply

$$K^{\mathrm{diag}}(\tau, x) = \kappa\tau e^{-B\tau} \tag{3.1.16}$$

where we have defined B as βT_{H}. If we use the relation $\sigma^2 = \frac{\kappa a \bar{d}}{2\pi\hbar}$ (see Leboeuf and Sieber, 1999) we know that β is given by

$$\beta = \frac{2\pi^2 x^2}{\kappa T_H} \tag{3.1.17}$$

70

And more importantly for our comparison with RMT results, B is given by

$$B = \frac{2\pi^2 x^2}{\kappa} \tag{3.1.18}$$

In the following we extend the calculations of Müller et al. (2004, 2005) discussed in Chapter 2 to include parametric correlations and compare to RMT predictions.

3.1.2 Off-diagonal terms

In this section we will present our first novel results of this thesis. We explore the effect of parametric correlations, for a general symmetry preserving parameter, on correlated periodic orbit pairs with self-encounters. The calculation, discussed in Chapter 2, of Müller et al. (2005) for the non-parametric form factor is performed using the uniformity of long periodic orbits via the equidistribution theorem. A naïve extension to the parametric case, including the average of Q_γ from equation (3.1.14) directly, and treating it as independent, would simply multiply their result by $\mathrm{e}^{-B\tau}$. However, when considering orbit pairs with self-encounters, in each encounter region we have orbit stretches that follow almost identical paths, and so cannot be considered as independent or uncorrelated. The change in action as the parameter is varied will be almost identical for all the encounter stretches, and this must be taken into account when performing the Gaussian average. This correction constitutes the novelty of what we present in this section, and means that we should consider the average over Q_γ for the links and encounter regions separately.

For orbit pairs with structures described by a certain vector $\boldsymbol{v}$, there are V encounters, α, each with l_α encounter stretches that last t_{enc}^α. The time that the orbit spends in the links is simply the orbit time minus the total time it spends in the encounters

$$T_{\mathrm{links}} = T_\gamma - \sum_\alpha l_\alpha t_{\mathrm{enc}}^\alpha \tag{3.1.19}$$

The contribution from the parametric velocities of the uncorrelated links of γ is on average

$$\left\langle \mathrm{e}^{\frac{\mathrm{i}x}{\sigma\hbar}Q_\gamma^{\mathrm{links}}} \right\rangle = \mathrm{e}^{-\beta(T-\sum_\alpha l_\alpha t_{\mathrm{enc}}^\alpha)} \tag{3.1.20}$$

For each encounter region α, however, we have l_α stretches that are close together and will be affected by the external parameter variations in the same way. As the links are correlated in this way, when we perform the Gaussian average over the encounter, the variance of the parametric velocities of the l_α encounter stretches will be approximately l_α^2 times the variance of a single stretch. The contribution from crossing the encounter region l_α times is then

$$\left\langle \mathrm{e}^{\frac{\mathrm{i}x}{\sigma\hbar}l_\alpha Q_{\mathrm{enc}}^\alpha} \right\rangle = \mathrm{e}^{-\beta l_\alpha^2 t_{\mathrm{enc}}^\alpha} \tag{3.1.21}$$

meaning that the contribution from the parametric velocity over the whole periodic orbit is now approximated by

$$\left\langle \mathrm{e}^{\frac{\mathrm{i}x}{\sigma\hbar}Q_\gamma} \right\rangle = \mathrm{e}^{-\beta T}\mathrm{e}^{-\beta \sum_\alpha l_\alpha(l_\alpha-1)t_{\mathrm{enc}}^\alpha} \tag{3.1.22}$$

To calculate the semiclassical contribution, the important quantity is the augmented weight (see section 2.2.5). This includes the weight of encounters and for parametric correlations also the factor from the parametric velocities given above. In total the weight is given by (cf equation (2.2.18))

$$\frac{z_T(\tilde{\boldsymbol{s}}, \tilde{\boldsymbol{u}})}{L} = \frac{\mathrm{e}^{-\beta T}T(T-\sum_\alpha l_\alpha t_{\mathrm{enc}}^\alpha)^{L-1}\prod_\alpha \mathrm{e}^{-\beta l_\alpha(l_\alpha-1)t_{\mathrm{enc}}^\alpha}}{L!\Omega^{L-V}\prod_\alpha t_{\mathrm{enc}}^\alpha} \tag{3.1.23}$$

where α labels the V different encounters, each being a l_α-encounter, and $L = \sum_\alpha l_\alpha$. Only terms where the encounter times in the numerator and denominator cancel exactly contribute in the semiclassical limit, so we can expand the exponentials as a power series up to first order and the augmented weight becomes

$$\frac{z_T(\tilde{\boldsymbol{s}}, \tilde{\boldsymbol{u}})}{L} \approx \frac{\mathrm{e}^{-\beta T}T(T-\sum_\alpha l_\alpha t_{\mathrm{enc}}^\alpha)^{L-1}\prod_\alpha(1-l_\alpha(l_\alpha-1)\beta t_{\mathrm{enc}}^\alpha)}{L!\Omega^{L-V}\prod_\alpha t_{\mathrm{enc}}^\alpha} \tag{3.1.24}$$

The contribution of orbits with different types of encounters can then be calculated

72

following the methods in Müller et al. (2005) using the recipe given in section 2.2.5. In essence, for each vector $\boldsymbol{v}$, we find the terms in the augmented weight where all the encounter times cancel exactly and use the semiclassical result of the integral in equation (2.2.25) to find the contribution. The contribution to the form factor, for all orbits with $L - V \leq 4$, is summarized in Table 3.1. We use a shorthand notation for the vectors where each term in brackets, $(l)^{v_l}$, means that the vector has v_l l-encounters. The central column is the contribution of each structure, so

$\boldsymbol{v}$	L	V	$\frac{K_{\boldsymbol{v}}(\tau,x)}{\kappa N(\boldsymbol{v})}$	$N(\boldsymbol{v})$ no TRS	$N(\boldsymbol{v})$ TRS
$(2)^1$	2	1	$-\mathrm{e}^{-B\tau}\left(\tau^2 + B\tau^3\right)$	-	1
$(2)^2$	4	2	$\mathrm{e}^{-B\tau}\left(\tau^3 + B\tau^4 + \frac{B^2\tau^5}{6}\right)$	1	5
$(3)^1$	3	1	$-\mathrm{e}^{-B\tau}\left(\tau^3 + B\tau^4\right)$	1	4
$(2)^3$	6	3	$-\mathrm{e}^{-B\tau}\left(\frac{2\tau^4}{3} + \frac{2B\tau^5}{3} + \frac{B^2\tau^6}{6} + \frac{B^3\tau^7}{90}\right)$	-	41
$(2)^1(3)^1$	5	2	$\mathrm{e}^{-B\tau}\left(\frac{3\tau^4}{5} + \frac{3B\tau^5}{5} + \frac{B^2\tau^6}{10}\right)$	-	60
$(4)^1$	4	1	$-\mathrm{e}^{-B\tau}\left(\frac{\tau^4}{2} + \frac{B\tau^5}{2}\right)$	-	20
$(2)^4$	8	4	$\mathrm{e}^{-B\tau}\left(\frac{\tau^5}{3} + \frac{B\tau^6}{3} + \frac{B^2\tau^7}{10} + \frac{B^3\tau^8}{90} + \frac{B^4\tau^9}{2520}\right)$	21	509
$(2)^2(3)^1$	7	3	$-\mathrm{e}^{-B\tau}\left(\frac{2\tau^5}{7} + \frac{2B\tau^6}{7} + \frac{B^2\tau^7}{14} + \frac{B^3\tau^8}{210}\right)$	49	1092
$(2)^1(4)^1$	6	2	$\mathrm{e}^{-B\tau}\left(\frac{2\tau^5}{9} + \frac{2B\tau^6}{9} + \frac{B^2\tau^7}{30}\right)$	24	504
$(3)^2$	6	2	$\mathrm{e}^{-B\tau}\left(\frac{\tau^5}{4} + \frac{B\tau^6}{4} + \frac{B^2\tau^7}{20}\right)$	12	228
$(5)^1$	5	1	$-\mathrm{e}^{-B\tau}\left(\frac{\tau^5}{6} + \frac{B\tau^6}{6}\right)$	8	148

Table 3.1: Contribution of different types of orbit pairs to the form factor for parametric correlations, along with the number of structures for systems with and without time reversal symmetry (TRS).

to find the contribution to the form factor of each vector, we now multiply the contribution of each type of orbit by the number of structures $N(\boldsymbol{v})$ and κ. If we do that for all orbits with $L - V \leq 6$, and add the diagonal contribution, we obtain the following result, up to 9th order, for the form factor for systems without time reversal symmetry ($\kappa = 1$)

$$K(\tau, x) = \mathrm{e}^{-B\tau}\left[\tau + \frac{B^2\tau^5}{6} + \frac{B^4\tau^9}{120} + \ldots\right] \qquad (3.1.25)$$

It is noticeable that, when we sum over all vectors with the same value of $L - V$, all

terms cancel apart from the highest order term of the orbits with only 2-encounters. In fact we can show that they do cancel, to all orders, using a recurrence relation argument which is presented in the Appendix of Kuipers and Sieber (2007a) and repeated here in Appendix A. We also consider a different proof starting from the parametric correlation function in Appendix B. For orbits with V 2-encounters, $L = 2V$ and the only term remaining (the highest order one) gives a contribution of

$$\tau^{2V+1} \frac{(2B)^V N(\boldsymbol{v})}{(2V)!} \mathrm{e}^{-B\tau} \tag{3.1.26}$$

To calculate the number of orbits corresponding to vectors that only have V 2-encounters we can use equation (2.2.9). In this case, the only non-vanishing component of $\boldsymbol{v}$ is $v_2 = V$, and the sum is over all vectors with component $v_2' = m$ where $m = 0, \ldots, V$. The result is

$$N(\boldsymbol{v}) = \frac{1}{2V+1} \sum_{m=0}^{V} \frac{(-1)^m (2m)! (2V-2m)!}{2^V m! (V-m)!} = \frac{(2V)!}{2^V (V+1)!} \frac{1+(-1)^V}{2} \tag{3.1.27}$$

so that we can easily see that the contribution is

$$\tau^{2V+1} \frac{B^V}{(V+1)!} \mathrm{e}^{-B\tau} \tag{3.1.28}$$

for even V and zero for odd V. In fact because we have the contribution for all V we can get the form factor explicitly (including the diagonal term which corresponds to $V = 0$) as

$$K(\tau, x) = \sum_{m=0}^{\infty} \tau^{4m+1} \frac{B^{2m}}{(2m+1)!} \mathrm{e}^{-B\tau} = \frac{\sinh(B\tau^2)}{B\tau} \mathrm{e}^{-B\tau} \tag{3.1.29}$$

For systems with time reversal symmetry, we have the same contribution from each structure (as given in Table 3.1), but a different number of structures corresponding to each vector. By multiplying the contribution by the number of structures and by a factor of $\kappa = 2$, because we can also pair each orbit with its time reversal, we get the contribution of each vector $\boldsymbol{v}$. By summing over all vectors $\boldsymbol{v}$

74

with $L - V \leq 6$ we can obtain the result for the form factor for systems with time reversal symmetry ($\kappa = 2$) up to 7th order, which is given by

$$
\begin{aligned}
K(\tau, x) \quad = \mathrm{e}^{-B\tau} \quad & \left[2\tau - 2\tau^2 - (2B - 2)\tau^3 + \left(2B - \frac{8}{3} \right) \tau^4 \right. \\
& + \left(\frac{5B^2}{3} - \frac{8B}{3} + 4 \right) \tau^5 - \left(\frac{5B^2}{3} - 4B + \frac{32}{5} \right) \tau^6 \\
& \left. - \left(\frac{41B^3}{45} - \frac{11B^2}{5} + \frac{32B}{5} - \frac{32}{3} \right) \tau^7 + \dots \right] \qquad (3.1.30)
\end{aligned}
$$

3.2 RMT results

The two-point correlation function integrals are given in Simons and Altshuler (1993a,b) in terms of the rescaled parameter x. Here we take the Fourier transform, so the RMT prediction for the GUE (no time reversal symmetry) case is given by the following integral

$$
K^{\mathrm{GUE}}(\tau, x) = \frac{1}{2} \int_{-1}^{1} \mathrm{d}\lambda \int_{1}^{\infty} \mathrm{d}\lambda_1 \int_{-\infty}^{\infty} \mathrm{d}\omega \, \cos(\pi\omega(\lambda_1 - \lambda)) \mathrm{e}^{-\frac{\pi^2 x^2 (\lambda_1{}^2 - \lambda^2)}{2}} \mathrm{e}^{-2\pi\mathrm{i}\omega\tau}
$$
$$(3.2.1)$$

The result is given in Sieber (2000), and for $\tau < 1$ it is calculated as follows. First the integral over ω is performed which gives

$$
K^{\mathrm{GUE}}(\tau, x) = \frac{1}{2} \int_{-1}^{1} \mathrm{d}\lambda \int_{1}^{\infty} \mathrm{d}\lambda_1 \, \mathrm{e}^{-\frac{\pi^2 x^2 (\lambda_1{}^2 - \lambda^2)}{2}} \left[\delta(\lambda_1 - \lambda - 2\tau) + \delta(\lambda_1 - \lambda + 2\tau) \right]
$$
$$(3.2.2)$$

Because τ is positive and $\lambda_1 \geq \lambda$ the second delta function does not contribute. From the first delta function we get the relation $2\tau = \lambda_1 - \lambda$. As we are considering the case where $\tau < 1$, the domain of integration for λ_1 is reduced to $1 \leq \lambda_1 \leq 1 + 2\tau$. We also have the relation $\lambda_1{}^2 - \lambda^2 = 4\tau\lambda_1 - 4\tau^2$ so that when we perform the integral over λ we are left with

$$
K^{\mathrm{GUE}}(\tau, x) = \frac{1}{2} \int_{1}^{1+2\tau} \mathrm{d}\lambda_1 \, \mathrm{e}^{2\pi^2 x^2 \tau^2 - 2\pi^2 x^2 \tau \lambda_1} \qquad (3.2.3)
$$

We can make the substitution $\lambda_1 = 1 + \tau y_1$ to arrive at

$$K^{\text{GUE}}(\tau, x) = \frac{\text{e}^{2\pi^2 x^2 \tau^2} \text{e}^{-2\pi^2 x^2 \tau}}{2} \int_0^2 \text{d}y_1 \; \tau \text{e}^{-2\pi^2 x^2 \tau^2 y_1} \qquad (3.2.4)$$

which can be rewritten as

$$K^{\text{GUE}}(\tau, x) = \frac{\sinh(2\pi^2 x^2 \tau^2)}{2\pi^2 x^2 \tau} \text{e}^{-2\pi^2 x^2 \tau} \qquad (3.2.5)$$

By comparing with equation (3.1.29) we can see that this is exactly the contribution we obtained from considering periodic orbits in section 3.1.2, because $B = 2\pi^2 x^2$ for the GUE case (see equation (3.1.18)).

The RMT result for the situation with time reversal symmetry, the GOE case, is given by

$$
\begin{aligned}
K^{\text{GOE}}(\tau, x) \;=\; & \int_{-1}^{1} \text{d}\lambda \int_{1}^{\infty} \text{d}\lambda_1 \int_{1}^{\infty} \text{d}\lambda_2 \int_{-\infty}^{\infty} \text{d}\omega \; \cos(\pi\omega(\lambda - \lambda_1\lambda_2))\text{e}^{-2\pi\text{i}\omega\tau} \\
& \times \exp\left\{ -\frac{\pi^2 x^2}{4}(2\lambda_1{}^2\lambda_2{}^2 - \lambda^2 - \lambda_1{}^2 - \lambda_2{}^2 + 1) \right\} \\
& \times \frac{(1-\lambda^2)(\lambda - \lambda_1\lambda_2)^2}{(2\lambda\lambda_1\lambda_2 - \lambda^2 - \lambda_1{}^2 - \lambda_2{}^2 + 1)^2}
\end{aligned}
\qquad (3.2.6)
$$

The integral over ω gives

$$
\begin{aligned}
K^{\text{GOE}}(\tau, x) \;=\; & \int_{-1}^{1} \text{d}\lambda \int_{1}^{\infty} \text{d}\lambda_1 \int_{1}^{\infty} \text{d}\lambda_2 \; [\delta(\lambda - \lambda_1\lambda_2 - 2\tau) + \delta(\lambda - \lambda_1\lambda_2 + 2\tau)] \\
& \times \exp\left\{ -\frac{\pi^2 x^2}{4}(2\lambda_1{}^2\lambda_2{}^2 - \lambda^2 - \lambda_1{}^2 - \lambda_2{}^2 + 1) \right\} \\
& \times \frac{(1-\lambda^2)(\lambda - \lambda_1\lambda_2)^2}{(2\lambda\lambda_1\lambda_2 - \lambda^2 - \lambda_1{}^2 - \lambda_2{}^2 + 1)^2}
\end{aligned}
\qquad (3.2.7)
$$

Since τ is positive and $\lambda_1\lambda_2 \geq \lambda$ only the second delta function contributes, giving the relation $\lambda = \lambda_1\lambda_2 - 2\tau$. As we are considering the case when $\tau < 1$ our domain of integration for the other two variables is given by $1 \leq \lambda_1 \leq 1 + 2\tau$ and $1 \leq \lambda_2 \leq \frac{1+2\tau}{\lambda_1}$. When we perform the integral over λ we are left with

$$K^{\text{GOE}}(\tau, x) = \int_1^{1+2\tau} d\lambda_1 \int_1^{\frac{1+2\tau}{\lambda_1}} d\lambda_2 \, \frac{4\tau^2(1 - \lambda_1^2\lambda_2^2 + 4\tau\lambda_1\lambda_2 - 4\tau^2)}{(1 + \lambda_1^2\lambda_2^2 - \lambda_1^2 - \lambda_2^2 - 4\tau^2)^2}$$
$$\times \exp\left\{ -\frac{\pi^2 x^2}{4}(1 + \lambda_1^2\lambda_2^2 - \lambda_1^2 - \lambda_2^2 + 4\tau\lambda_1\lambda_2 - 4\tau^2) \right\} \tag{3.2.8}$$

In order to evaluate this integral as a series in τ it is useful to remove the τ dependence from the limits. First we make a change of variables $y_1' = \lambda_1$ and $y_2' = \lambda_1\lambda_2$ to obtain

$$K^{\text{GOE}}(\tau, x) = \int_1^{1+2\tau} dy_1' \int_{y_1'}^{1+2\tau} dy_2' \, \frac{1}{y_1'} \frac{4\tau^2(1 - y_2'^2 + 4\tau y_2' - 4\tau^2)}{(1 + y_2'^2 - y_1'^2 - \frac{y_2'^2}{y_1'^2} - 4\tau^2)^2}$$
$$\times \exp\left\{ -\frac{\pi^2 x^2}{4}(1 + y_2'^2 - y_1'^2 - \frac{y_2'^2}{y_1'^2} + 4\tau y_2' - 4\tau^2) \right\} \tag{3.2.9}$$

Then we make the change of variables defined by $y_1' = 1 + \tau y_1$ and $y_2' = 1 + \tau y_2$, which removes all τ dependency from the limits. To conclude we expand the integrand as a series in τ, though here we only include the first two terms for clarity

$$K^{\text{GOE}}(\tau, x) = \int_0^2 dy_1 \int_{y_1}^2 dy_2 \, \frac{2 - y_2}{2(1 - y_1 y_2 + y_1^2)^2}\tau$$
$$+ \left[\frac{y_1(y_2 - 2)(4 - y_1 y_2 + 2y_1^2 - y_2^2)}{2(1 - y_1 y_2 + y_1^2)^3} \right.$$
$$\left. + \frac{(2 - y_2)(2 + 2\pi^2 x^2 - 6y_1 - y_2)}{4(1 - y_1 y_2 + y_1^2)^2} \right] \tau^2 + \ldots \tag{3.2.10}$$

When we perform the integral term by term, we get the following series

$$K^{\text{GOE}}(\tau, x) = 2\tau - (2\pi^2 x^2 + 2)\tau^2 + (\pi^4 x^4 + 2)\tau^3 - \left(\frac{\pi^6 x^6}{3} - \pi^4 x^4 + \frac{8}{3} \right)\tau^4$$
$$+ \left(\frac{\pi^8 x^8}{12} - \frac{2\pi^6 x^6}{3} + \frac{2\pi^4 x^4}{3} + 4 \right)\tau^5$$
$$- \left(\frac{\pi^{10} x^{10}}{60} - \frac{\pi^8 x^8}{4} + \pi^6 x^6 + \frac{\pi^4 x^4}{3} + \frac{32}{5} \right)\tau^6$$
$$+ \left(\frac{\pi^{12} x^{12}}{360} - \frac{\pi^{10} x^{10}}{15} + \frac{7\pi^8 x^8}{12} - \frac{2\pi^6 x^6}{15} + \frac{\pi^4 x^4}{5} + \frac{32}{3} \right)\tau^7$$
$$+ \ldots \tag{3.2.11}$$

If we extract an exponential factor and set $B = \pi^2 x^2$ (see equation (3.1.18)), then the result is

$$
\begin{aligned}
K^{\text{GOE}}(\tau, x) \quad = \mathrm{e}^{-B\tau} \quad & \left[2\tau - 2\tau^2 - (2B - 2)\tau^3 + \left(2B - \frac{8}{3} \right) \tau^4 \right. \\
& + \left(\frac{5B^2}{3} - \frac{8B}{3} + 4 \right) \tau^5 - \left(\frac{5B^2}{3} - 4B + \frac{32}{5} \right) \tau^6 \\
& \left. - \left(\frac{41B^3}{45} - \frac{11B^2}{5} + \frac{32B}{5} - \frac{32}{3} \right) \tau^7 + \ldots \right]
\end{aligned}
\qquad (3.2.12)
$$

This is exactly the same as the terms obtained semiclassically from periodic orbits in equation (3.1.30). We have now shown how the small τ RMT results can be obtained semiclassically for parametric correlations. In the next Chapter we consider how we can apply this method when the system is open.

4 Trapped orbits in open systems

In open systems trajectories are allowed to escape, representing dynamics that occurs in many physical situations, including molecular and nuclear interactions and transport through semiconductors. In these systems effects due to the chaotic dynamics are of practical interest and can be measured experimentally. On a larger scale we can study microwave scattering from open chaotic cavities. An interesting property of open systems is that the trapped set of orbits typically has a fractal nature. The volume of the region that remains inside the system will decay, through the opening, on average exponentially with time. This exponential decay is due to the hyperbolicity and ergodicity of the chaotic system, which also means that the parts of the region escaping over time will come from areas evenly spread across the region. The space covered by the parts remaining inside the system will tend towards a fractal (like a Cantor set) in a decreasing neighbourhood around the trapped periodic orbits.

In this Chapter we consider chaotic cavities with leads attached and for them we focus on one particular physical quantity, namely the Wigner time delay (and its autocorrelation functions). It is interesting that a semiclassical description of this quantity can be obtained by considering either trajectories that enter and subsequently leave the system or the periodic orbits that are trapped. Our calculation involves the periodic orbits in a way analogous to the method used in the previous Chapter for parametric correlations, but, for open systems, the bulk of relevant work

is based on scattering trajectories, which we will consider in the next Chapter.

Open systems were first considered within the framework of scattering problems, which are typically described by a quantum mechanical scattering matrix. A semiclassical treatment then gives scattering properties in terms of open trajectories linking an entrance and exit for example. The semiclassical evaluation of the contribution of correlated trajectories that goes beyond the diagonal approximation has been performed in terms of open trajectories (Richter and Sieber, 2002; Heusler et al., 2006; Braun et al., 2006; Müller et al., 2007), and thinking in terms of trajectories gives an intuitive picture of the process, but we shall leave this description for Chapter 5. In this Chapter, however, we apply an important idea from this work to periodic orbits, namely that as encounter stretches are close together, the probability that they escape from the system is interdependent since if one encounter stretch survives then all of the encounter stretches should survive.

The duality between the open trajectories and the trapped periodic orbits was noticed by Blümel and Smilansky (1990). They realised that the semiclassical scattering matrix was the quantum analogue of the Poincaré scattering map introduced by Jung (1986). For open systems this is a modification of the Poincaré map for closed systems, but for open systems the map only acts on the preserved trapped set (which is a fractal set for chaotic systems, see Jung and Scholz, 1987). Blümel and Smilansky (1990) then expressed the trace of powers of the scattering matrix of an open system in terms of the trapped periodic orbits. They also considered the two-point correlation function, and by taking the diagonal approximation (which requires modification of the Hannay–Ozorio de Almeida sum rule) got the first analytical and numerical results suggesting adherence to RMT results. The required modification of the Hannay–Ozorio de Almeida sum rule was made more explicit by Cvitanović and Eckhardt (1991) by including a term corresponding to the exponential decay of trajectories remaining inside the system. The decay can be thought of as the volume of phase space not covered by backwards iteration of the opening, and because of hyperbolicity and ergodicity, will be asymptotically exponential.

The time delay was first expressed, via its relation to a density of states, in terms

of a sum over the trapped periodic orbits by Balian and Bloch (1974). For a particular example system of scattering between three disks Eckhardt (1993) calculated the two-point correlation function of the time delay. By giving a Lorentzian width to the resonances and by using the diagonal approximation, he was able to obtain a first approximation of the correlation function. The same result had also been found in the case of a leaky surface of constant negative curvature by Wardlaw and Jaworski (1989). By including an analogue of a conjecture on the pair correlation function of the zeros of the Riemann zeta function Shushin and Wardlaw (1992) were able to extend this result and they obtained a function that agrees with the first order asymptotic expansion of the RMT result (Fyodorov et al., 1997). The expression of the time delay in terms of a periodic orbit sum was derived by Vallejos et al. (1998) for the particular case of a chaotic cavity. Vallejos et al. (1998) also considered a two point correlation function of the time delay in the crossover regime between broken and preserved time reversal symmetry (including both extremes). They calculated the diagonal approximation and showed agreement with the first term in the RMT results for dynamical systems with either broken or preserved time reversal symmetry. We can now expand this treatment to go beyond the diagonal approximation by using the ideas we discussed in Chapter 2. This allows us to obtain the RMT expressions, semiclassically for time delay correlations, which we do in Section 4.1.

First we briefly consider some of the experimental work in this area. The semiclassical results described in terms of classical trajectories or periodic orbits are for clean chaotic cavities. For semiconductor transport however, the medium can be considered as disordered with the electrons scattering off the defects. The theoretical treatment is then done stochastically, but, in the proper regime, gives effectively the same results as the semiclassical treatment of clean chaotic cavities (see Lewenkopf and Weidenmüller, 1991, for example). The first experimental results came from Doron et al. (1990) where they studied microwave scattering from a chaotic cavity experimentally, numerically and theoretically. The experiment allowed them to measure the scattering matrix and derive its autocorrelation function, which showed good agreement with the theoretical and numerical curves. The comparison of these

experimental results with RMT was performed later by Lewenkopf et al. (1992). Close agreement was found, but the data were not detailed enough to determine whether the complete RMT result or the diagonal semiclassical result followed the data more accurately. Of course with the recent semiclassical improvements over the diagonal approximation, which we describe in this Chapter, the distinction becomes obsolete for the behaviour at large correlation lengths or small τ.

To examine parametric correlations in open systems, Dietz et al. (2006) measured, for a superconducting microwave cavity, parametric correlations related to a rotatable scatterer. The angle of the obstacle was the external parameter, and with it fixed they found good agreement with the GOE RMT results. Looking at parametric correlations, however, they found agreement with a model of a RMT result for open systems. In section 4.2, we consider parametric correlations in open systems, in the setting of the time delay, and our semiclassical derivation shows exact agreement with RMT for small τ.

4.1 Wigner time delay correlations

In this Chapter, we consider chaotic cavities and to make our system open we can imagine attaching a lead that carries M scattering channels or quantized states to the cavity. The incoming and outgoing wave in the lead are related by the $M \times M$ scattering matrix $S(E)$ which incorporates all the dynamics of the scattering process. The Wigner time delay, which represents the extra time spent in the scattering process compared to free motion, is defined in terms of the scattering matrix by (Wigner, 1955; Smith, 1960)

$$\tau_{\mathrm{W}}(E) = -\frac{\mathrm{i}\hbar}{M}\mathrm{Tr}\left[S^{\dagger}(E)\frac{\mathrm{d}}{\mathrm{d}E}S(E)\right] = -\frac{\mathrm{i}\hbar}{M}\frac{\mathrm{d}}{\mathrm{d}E}\ln\det S(E) \qquad (4.1.1)$$

This time delay can be expressed semiclassically both in terms of the trapped set of periodic orbits of the open system, and in terms of the open scattering trajectories that enter and exit through the lead. In this Chapter we will look at the semiclassical
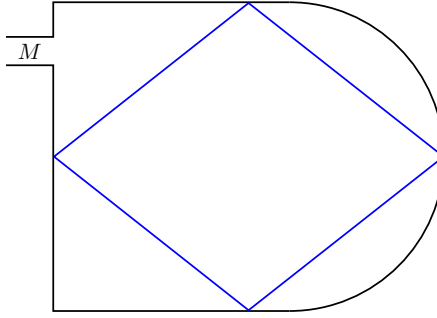
Figure 4.1: Representation of a chaotic cavity with an attached lead carrying M channels, and a trapped periodic orbit.

approximation in terms of the trapped periodic orbits. A representation of an open scattering cavity is given in Figure 4.1.

The description of the Wigner time delay in terms of trapped periodic orbits comes from its relation to a density of states, which is the difference between the level density of the open scattering system and a free system (Friedel, 1952)

$$\tau_{\mathrm{W}}(E) = \frac{2\pi\hbar}{M}d(E) \approx \frac{2\pi\hbar}{M}\bar{d}(E) + \frac{2\pi\hbar}{M}d^{\mathrm{osc}}(E) \tag{4.1.2}$$

where the density of states $d(E)$ can be separated into a mean part $\bar{d}(E)$ and a fluctuating part $d^{\mathrm{osc}}(E)$, each of which has a semiclassical approximation in a similar way as for closed systems. The approximation for the mean density of states comes from Weyl's law for the corresponding closed system ($\bar{d}(E) \sim \Omega/(2\pi\hbar)^f$, where Ω is the volume of the shell of constant energy E and f is the number of degrees of freedom). The fluctuating part can be expressed, like in the Gutzwiller trace formula (see section 1.3.2), as a sum over periodic orbits. The difference with closed systems is that the sum only includes periodic orbits that are trapped in the system (Balian and Bloch, 1974; Vallejos et al., 1998). Using these approximations, we can write the time delay as

$$\tau_{\mathrm{W}}(E) \approx \frac{T_{\mathrm{H}}}{M} + \frac{1}{M}\sum_{\gamma,r}\left[A_{\gamma,r}e^{\frac{\mathrm{i}}{\hbar}rS_{\gamma}(E)} + \mathrm{c.c.}\right] \tag{4.1.3}$$

where the Heisenberg time is related to the average level density by $T_{\mathrm{H}} = 2\pi\hbar\bar{d}$.

The first term is the average time spent in the cavity $\bar{\tau}_{\mathrm{W}}$. In the sum, γ labels the trapped primitive periodic orbits and r their repetitions. The orbits have action S_γ and their stability amplitude $A_{\gamma,r}$ can be expressed in terms of the stability matrix M_γ, the period T_γ and the Maslov index μ_γ as in equation (1.3.17).

The irreducible two-point correlation function of the time delay (with the energy unfolding) is given by

$$\tilde{R}_2(\omega, M) = \left\langle \frac{\tau_{\mathrm{W}}^{\mathrm{osc}}\left(E + \frac{\omega}{2\bar{d}}\right) \tau_{\mathrm{W}}^{\mathrm{osc}}\left(E - \frac{\omega}{2\bar{d}}\right)}{\bar{\tau}_{\mathrm{W}}^2} \right\rangle_E \qquad (4.1.4)$$

which, because of the relation between the time delay and the density of states, can also be expressed as

$$\tilde{R}_2(\omega, M) = \left\langle \frac{d^{\mathrm{osc}}\left(E + \frac{\omega}{2\bar{d}}\right) d^{\mathrm{osc}}\left(E - \frac{\omega}{2\bar{d}}\right)}{\bar{d}^2} \right\rangle_E \qquad (4.1.5)$$

We again consider the form factor and with the substitution $\omega = \bar{d}\eta$ we obtain

$$K(\tau, M) = \int \mathrm{d}\eta \, \frac{d^{\mathrm{osc}}\left(E + \frac{\eta}{2}\right) d^{\mathrm{osc}}\left(E - \frac{\eta}{2}\right)}{\bar{d}} \mathrm{e}^{\frac{-\mathrm{i}\eta}{\hbar}\tau T_{\mathrm{H}}} \qquad (4.1.6)$$

which can be written in terms of the sum over orbits, using equation (4.1.3), keeping only terms where the actions of the two orbits have a different sign. For convenience we also ignore repetitions of primitive orbits and obtain

$$K(\tau, M) = \frac{1}{2\pi\hbar T_{\mathrm{H}}} \int \mathrm{d}\eta \sum_{\gamma,\gamma'} \left[A_\gamma A_{\gamma'}^* \mathrm{e}^{\frac{\mathrm{i}}{\hbar}(S_\gamma - S_{\gamma'})} \mathrm{e}^{\frac{\mathrm{i}\eta}{2\hbar}(T_\gamma + T_{\gamma'})} + \mathrm{c.c.} \right] \mathrm{e}^{\frac{-\mathrm{i}\eta}{\hbar}\tau T_{\mathrm{H}}} \qquad (4.1.7)$$

This is now the quantity we wish to examine, with the proviso that the sum is only over trapped orbits. If we perform the integral over η and remove the delta function that does not contribute, we can rewrite the form factor as

$$K(\tau, M) = \frac{1}{T_{\mathrm{H}}} \left\langle \sum_{\gamma,\gamma'} A_\gamma A_{\gamma'}^* \mathrm{e}^{\frac{\mathrm{i}}{\hbar}(S_\gamma - S_{\gamma'})} \delta\left(\tau T_{\mathrm{H}} - \frac{T_\gamma + T_{\gamma'}}{2}\right) \right\rangle \qquad (4.1.8)$$

84

4.1.1 Diagonal approximation

Upon using the diagonal approximation, $\gamma = \gamma'$, the form factor of equation (4.1.8) becomes

$$K^{\mathrm{diag}}(\tau, M) = \frac{\kappa}{T_{\mathrm{H}}} \left\langle \sum_{\gamma} |A_{\gamma}|^2 \delta\left(\tau T_{\mathrm{H}} - T_{\gamma}\right) \right\rangle \qquad (4.1.9)$$

where κ is 1 if the system does not have time reversal symmetry and 2 if it does. For open systems we need to modify the Hannay–Ozorio de Almeida sum rule to take into account the probability that an orbit escapes. If μ is the escape rate, then when we sum over all orbits of period T (Cvitanović and Eckhardt, 1991) we have

$$\sum_{\gamma} |A_{\gamma}|^2 \delta_{\epsilon}\left(T - T_{\gamma}\right) \sim T \mathrm{e}^{-\mu T}, \quad T \to \infty \qquad (4.1.10)$$

which follows from the equidistribution theorem. This effectively means that each orbit has, on average, a probability of surviving of $\mathrm{e}^{-\mu T}$. This escape rate μ is a classical property of the system and is the inverse of the mean time spent in the cavity, the dwell time T_{d}. For chaotic systems, this dwell time is equal to the average time delay (Lewenkopf and Vallejos, 2004b) so that we have $\mu = \frac{M}{T_H}$. If we now substitute this sum rule into equation (4.1.9), we find that our diagonal approximation is simply given by

$$K^{\mathrm{diag}}(\tau, M) = \kappa \tau \mathrm{e}^{-M\tau} \qquad (4.1.11)$$

4.1.2 Off-diagonal terms

The calculation of off-diagonal terms that we discussed in Chapter 2 is performed using the uniformity of the long periodic orbits. If we repeated this calculation for the open case, by directly applying the open sum rule of equation (4.1.10), we would simply multiply the result by $\mathrm{e}^{-M\tau}$. However Heusler et al. (2006) notice that, for trajectories with self-encounters, if one encounter stretch does not escape during the encounter, then all the stretches in the encounter will survive as they are close to each other. For each encounter α, which is an l_{α}-encounter, then the effective time

that the l_α orbit stretches spend where they can escape is given by the time of just a single crossing t_{enc}^α. The effective time that the whole orbit spends during which it can escape is thus reduced from the orbit time T to

$$T_{\text{exp}} = T - \sum_\alpha (l_\alpha - 1) t_{\text{enc}}^\alpha \tag{4.1.12}$$

where α labels the V different encounters. This means that the probability of survival is now given by

$$\mathrm{e}^{-\mu T} \mathrm{e}^{\sum\limits_\alpha \mu(l_\alpha - 1) t_{\text{enc}}^\alpha} \tag{4.1.13}$$

The important quantity to calculate is the augmented weight of encounters (see section 2.2.5), and for open systems with the survival probability included this is given by (cf equation (2.2.18))

$$\frac{z_T(\tilde{\boldsymbol{s}}, \tilde{\boldsymbol{u}})}{L} = \frac{\mathrm{e}^{-\mu T} T (T - \sum_\alpha l_\alpha t_{\text{enc}}^\alpha)^{L-1} \prod_\alpha \mathrm{e}^{\mu(l-1) t_{\text{enc}}^\alpha}}{L! \Omega^{L-V} \prod_\alpha t_{\text{enc}}^\alpha} \tag{4.1.14}$$

where $L = \sum_\alpha l_\alpha$. We should note that we are taking a semiclassical limit where the Ehrenfest time remains small compared to the dwell time, which removes any effect from their ratio. We discuss this in Chapter 5 and here we can imagine keeping the number of channels, M, fixed. With this choice, only terms where the encounter times in the numerator and denominator cancel exactly contribute in the semiclassical limit so we can expand the exponentials as a power series and only consider terms up to first order. The augmented weight can then be written as

$$\frac{z_T(\tilde{\boldsymbol{s}}, \tilde{\boldsymbol{u}})}{L} \approx \frac{\mathrm{e}^{-\mu T} T (T - \sum_\alpha l_\alpha t_{\text{enc}}^\alpha)^{L-1} \prod_\alpha (1 + (l_\alpha - 1) \mu t_{\text{enc}}^\alpha)}{L! \Omega^{L-V} \prod_\alpha t_{\text{enc}}^\alpha} \tag{4.1.15}$$

The contribution of orbits with different types of encounters can then be calculated following the methods in Müller et al. (2004, 2005), using the recipe given in section 2.2.5, where the main semiclassical ingredient is the integral of equation (2.2.25). The contribution to the form factor, for orbits with $L - V \leq 4$, is summarized in Table 4.1, where we have again used a shorthand notation for the vectors $\boldsymbol{v}$. To find

$\boldsymbol{v}$	L	V	$\dfrac{K_{\boldsymbol{v}}(\tau,M)}{\kappa N(\boldsymbol{v})}$	$N(\boldsymbol{v})$ no TRS	$N(\boldsymbol{v})$ TRS
$(2)^1$	2	1	$\mathrm{e}^{-M\tau}\left(-\tau^2 + \frac{M\tau^3}{2}\right)$	-	1
$(2)^2$	4	2	$\mathrm{e}^{-M\tau}\left(\tau^3 - \frac{M\tau^4}{2} + \frac{M^2\tau^5}{24}\right)$	1	5
$(3)^1$	3	1	$\mathrm{e}^{-M\tau}\left(-\tau^3 + \frac{M\tau^4}{3}\right)$	1	4
$(2)^3$	6	3	$\mathrm{e}^{-M\tau}\left(-\frac{2\tau^4}{3} + \frac{M\tau^5}{3} - \frac{M^2\tau^6}{24} + \frac{M^3\tau^7}{720}\right)$	-	41
$(2)^1(3)^1$	5	2	$\mathrm{e}^{-M\tau}\left(\frac{3\tau^4}{5} - \frac{7M\tau^5}{30} + \frac{M^2\tau^6}{60}\right)$	-	60
$(4)^1$	4	1	$\mathrm{e}^{-M\tau}\left(-\frac{\tau^4}{2} + \frac{M\tau^5}{8}\right)$	-	20
$(2)^4$	8	4	$\mathrm{e}^{-M\tau}\left(\frac{\tau^5}{3} - \frac{M\tau^6}{6} + \frac{M^2\tau^7}{40} - \frac{M^3\tau^8}{720} + \frac{M^4\tau^9}{40320}\right)$	21	509
$(2)^2(3)^1$	7	3	$\mathrm{e}^{-M\tau}\left(-\frac{2\tau^5}{7} + \frac{5M\tau^6}{42} - \frac{11M^2\tau^7}{840} + \frac{M^3\tau^8}{2520}\right)$	49	1092
$(2)^1(4)^1$	6	2	$\mathrm{e}^{-M\tau}\left(\frac{2\tau^5}{9} - \frac{5M\tau^6}{72} + \frac{M^2\tau^7}{240}\right)$	24	504
$(3)^2$	6	2	$\mathrm{e}^{-M\tau}\left(\frac{\tau^5}{4} - \frac{M\tau^6}{12} + \frac{M^2\tau^7}{180}\right)$	12	228
$(5)^1$	5	1	$\mathrm{e}^{-M\tau}\left(-\frac{\tau^5}{6} + \frac{M\tau^6}{30}\right)$	8	148

Table 4.1: Contribution of different types of orbit pair to the form factor of the time delay for systems with and without time reversal symmetry (TRS).

the contribution to the form factor we now multiply the contribution of each type of orbit (described by a vector $\boldsymbol{v}$) by κ and by the number of structures corresponding to the vector. If we do that for all orbits with $L - V \leq 6$, and add the diagonal contribution, we can obtain the following result, up to 9th order, for the form factor for systems without time reversal symmetry ($\kappa = 1$)

$$
\begin{aligned}
K(\tau, M) \;=\; \mathrm{e}^{-M\tau} \Bigg[&\tau - \frac{M\tau^4}{6} + \frac{M^2\tau^5}{24} - \frac{M\tau^6}{15} + \frac{M^2\tau^7}{20} - \frac{7M^3\tau^8}{720} \\
&- \frac{M\tau^8}{28} + \frac{M^4\tau^9}{1920} + \frac{401M^2\tau^9}{10080} + \dots \Bigg]
\end{aligned}
\tag{4.1.16}
$$

From the same orbits we can also obtain the result for the form factor for systems with time reversal symmetry ($\kappa = 2$) up to 7th order

$$
\begin{aligned}
K(\tau, M) \;=\; \mathrm{e}^{-M\tau} \Bigg[&2\tau - 2\tau^2 + (M+2)\tau^3 - \left(\frac{7M}{3} + \frac{8}{3}\right)\tau^4 \\
&+ \left(\frac{5M^2}{12} + \frac{13M}{3} + 4\right)\tau^5 - \left(\frac{17M^2}{12} + \frac{39M}{5} + \frac{32}{5}\right)\tau^6 \\
&+ \left(\frac{41M^3}{360} + \frac{43M^2}{12} + \frac{212M}{15} + \frac{32}{3}\right)\tau^7 + \dots \Bigg]
\end{aligned}
\tag{4.1.17}
$$

4.2 Parametric correlations

We can easily include parametric correlations by simply combining the arguments of sections 3.1 and 4.1. The semiclassical approximation to the parametric form factor for the time delay is given by

$$K(\tau, x, M) = \frac{1}{T_{\mathrm{H}}} \left\langle \sum_{\gamma,\gamma'} A_\gamma A_{\gamma'}^* e^{\frac{i}{\hbar}(S_\gamma - S_{\gamma'})} e^{\frac{ix}{2\sigma\hbar}(Q_\gamma + Q_{\gamma'})} \delta\left(\tau T_{\mathrm{H}} - \frac{T_\gamma + T_{\gamma'}}{2} \right) \right\rangle$$

(4.2.1)

where the sum is again only over trapped orbits. For the diagonal approximation ($\gamma = \gamma'$) this becomes

$$K^{\mathrm{diag}}(\tau, x, M) = \frac{\kappa}{T_{\mathrm{H}}} \left\langle \sum_\gamma |A_\gamma|^2 e^{\frac{ix}{\sigma\hbar}Q_\gamma} \delta\left(\tau T_{\mathrm{H}} - T_\gamma \right) \right\rangle$$

(4.2.2)

This sum can be performed using the equidistribution theorem by including the survival probability of periodic orbits in open systems and using the assumption that the parametric velocities have a Gaussian distribution. For this we use the open sum rule of equation (4.1.10), along with the Gaussian average in equation (3.1.14). Using the notation of sections 3.1.1 and 4.1.1, we find that our diagonal approximation for parametric correlations in open systems is simply

$$K^{\mathrm{diag}}(\tau, x, M) = \kappa \tau e^{-(B+M)\tau}$$

(4.2.3)

To calculate the off-diagonal terms we again use the methods described in Chapter 2 (Müller et al., 2005), combined with our arguments for open systems and parametric correlations (see sections 3.1.2 and 4.1.2). For an orbit of period T, with V encounters α that each have l_α encounter stretches lasting t_{enc}^α, the contribution to the form factor is modified to include the probability of survival and the parametric velocity correlations as the following additional factor

$$e^{-(\beta+\mu)T} e^{-\sum_\alpha (\beta l_\alpha - \mu)(l_\alpha - 1) t_{\mathrm{enc}}^\alpha}$$

(4.2.4)

where we have made the assumption that we can treat the two effects independently. The important quantity to calculate, as already noticed, is the augmented weight of encounters, and for parametric correlations of open systems we include the above factor. Again, only terms where the encounter times in the numerator and denominator cancel exactly contribute in the semiclassical limit, so we can expand the exponentials as a power series and only consider terms up to first order. Doing so, we obtain (cf equation (2.2.18))

$$\frac{z_T(\tilde{\boldsymbol{s}}, \tilde{\boldsymbol{u}})}{L} \approx \frac{\mathrm{e}^{-(\beta+\mu)T} T (T - \sum_\alpha l_\alpha t_{\mathrm{enc}}^\alpha)^{L-1} \prod_\alpha (1 - (\beta l_\alpha - \mu)(l_\alpha - 1) t_{\mathrm{enc}}^\alpha)}{L! \Omega^{L-V} \prod_\alpha t_{\mathrm{enc}}^\alpha} \qquad (4.2.5)$$

with α labelling the V different encounters, and $L = \sum_\alpha l_\alpha$. The contribution of orbits with different types of encounters can then be calculated following the methods in Müller et al. (2005), and for orbits with $L - V \leq 4$, is summarized in Table 4.2. To find the contribution to the form factor we now multiply the contribution of each

$\boldsymbol{v}$	$\dfrac{K_{\boldsymbol{v}}(\tau,x,M)\mathrm{e}^{(B+M)\tau}}{\kappa N(\boldsymbol{v})}$	$N(\boldsymbol{v})$, no TRS	$N(\boldsymbol{v})$ TRS
$(2)^1$	$-\tau^2 - \frac{1}{2}\left(2B - M\right)\tau^3$	-	1
$(2)^2$	$\tau^3 + \frac{1}{2}\left(2B - M\right)\tau^4 + \frac{1}{24}\left(2B - M\right)^2 \tau^5$	1	5
$(3)^1$	$-\tau^3 - \frac{1}{3}\left(3B - M\right)\tau^4$	1	4
$(2)^3$	$-\frac{2}{3}\tau^4 - \frac{1}{3}\left(2B - M\right)\tau^5 - \frac{1}{24}\left(2B - M\right)^2 \tau^6$ $-\frac{1}{720}\left(2B - M\right)^3 \tau^7$	-	41
$(2)^1(3)^1$	$\frac{3}{5}\tau^4 + \left(\frac{3B}{5} - \frac{7M}{30}\right)\tau^5 + \left(\frac{B^2}{10} - \frac{BM}{12} + \frac{M^2}{60}\right)\tau^6$	-	60
$(4)^1$	$-\frac{1}{2}\tau^4 - \frac{1}{8}\left(4B - M\right)\tau^5$	-	20
$(2)^4$	$\frac{1}{3}\tau^5 + \frac{1}{6}\left(2B - M\right)\tau^6 + \frac{1}{40}\left(2B - M\right)^2 \tau^7$ $+\frac{1}{720}\left(2B - M\right)^3 \tau^8 + \frac{1}{40320}\left(2B - M\right)^4 \tau^9$	21	509
$(2)^2(3)^1$	$-\frac{2}{7}\tau^5 - \left(\frac{2B}{7} - \frac{5M}{42}\right)\tau^6 - \left(\frac{B^2}{14} - \frac{13BM}{210} + \frac{11M^2}{840}\right)\tau^7$ $-\left(\frac{B^3}{210} - \frac{2B^2 M}{315} + \frac{BM^2}{360} - \frac{M^3}{2520}\right)\tau^8$	49	1092
$(2)^1(4)^1$	$\frac{2}{9}\tau^5 + \left(\frac{2B}{9} - \frac{5M}{72}\right)\tau^6 + \left(\frac{B^2}{30} - \frac{BM}{40} + \frac{M^2}{240}\right)\tau^7$	24	504
$(3)^2$	$\frac{1}{4}\tau^5 + \frac{1}{12}\left(3B - M\right)\tau^6 + \frac{1}{180}\left(3B - M\right)^2 \tau^7$	12	228
$(5)^1$	$-\frac{1}{6}\tau^5 - \frac{1}{30}\left(5B - M\right)\tau^6$	8	148

Table 4.2: Contribution of different types of orbit pairs to the parametric form factor of the time delay.

vector by the number of structures corresponding to that vector (and κ). If we do

this for all orbits with $L - V \le 6$, and add the diagonal contribution, we can get the following result, up to 9th order, for the form factor for systems without time reversal symmetry ($\kappa = 1$)

$$
\begin{aligned}
K(\tau, x, M) \quad = \mathrm{e}^{-(B+M)\tau} \quad & \left[\tau - \frac{M}{6}\tau^4 + \frac{(2B-M)^2}{24}\tau^5 - \frac{M}{15}\tau^6 - \left(\frac{BM}{15} - \frac{M^2}{20} \right) \tau^7 \right. \\
& - \left(\frac{7M(2B-M)^2}{720} + \frac{M}{28} \right) \tau^8 \\
& \left. + \left(\frac{(2B-M)^4}{1920} - \frac{BM}{28} + \frac{401M^2}{10080} \right) \tau^9 + \dots \right]
\end{aligned} \qquad (4.2.6)
$$

If we set $M = 0$, this reproduces the result for parametric correlations in section 3.1.2. Likewise, if we set $B = 0$, then this reproduces the result for open systems in section 4.1.2, as we would expect. From the same orbits we can also get the result for the form factor for systems with time reversal symmetry ($\kappa = 2$) up to 7th order

$$
\begin{aligned}
K(\tau, x, M) \quad = \mathrm{e}^{-(B+M)\tau} \quad & \left[2\tau - 2\tau^2 - (2B - M - 2)\tau^3 + \left(2B - \frac{7M}{3} - \frac{8}{3} \right) \tau^4 \right. \\
& + \left(\frac{5(2B-M)^2}{12} - \frac{8B}{3} + \frac{13M}{3} + 4 \right) \tau^5 \\
& - \left(\frac{5B^2}{3} - \frac{11BM}{3} + \frac{17M^2}{12} - 4B + \frac{39M}{5} + \frac{32}{5} \right) \tau^6 \\
& - \left(\frac{41(2B-M)^3}{360} - \frac{11B^2}{5} + 7BM - \frac{43M^2}{12} \right. \\
& \left. \left. + \frac{32B}{5} - \frac{212M}{15} - \frac{32}{3} \right) \tau^7 + \dots \right]
\end{aligned} \qquad (4.2.7)
$$

which again reproduces the results from sections 3.1.2 and 4.1.2 if we set $M = 0$ or $B = 0$.

4.3 GOE-GUE transition

For the transition between symmetry classes, we introduce a (second) parameter Y, a magnetic field, that takes a time reversal invariant system (at $Y = 0$) and breaks the symmetry as it is increased ($Y \to \infty$). This magnetic field adds a term

$\theta_\gamma(Y) = \int_\gamma \boldsymbol{A} \mathrm{d}\boldsymbol{q}$ to the action, where $\boldsymbol{A}$ is the potential of the magnetic field (Saito and Nagao, 2006). The form factor, after performing the transform and keeping the only delta function that contributes, becomes

$$
\begin{aligned}
K(\tau, x, y, M) \;=\; & \frac{1}{T_\mathrm{H}} \left\langle \sum_{\gamma,\gamma'} A_\gamma A_{\gamma'}^* \mathrm{e}^{\frac{\mathrm{i}}{\hbar}(S_\gamma - S_{\gamma'})} \mathrm{e}^{\frac{\mathrm{i}}{\hbar}(\theta_\gamma - \theta_{\gamma'})} \mathrm{e}^{\frac{\mathrm{i}x}{2\sigma\hbar}(Q_\gamma + Q_{\gamma'})} \right. \\
& \left. \times\, \delta\left(\tau T_\mathrm{H} - \frac{T_\gamma + T_{\gamma'}}{2}\right) \right\rangle
\end{aligned}
\tag{4.3.1}
$$

The sum here is over the periodic orbits of the open system, and we have included the term from parametric correlations due to the difference x in our first parameter X. The effects discussed before for open systems and parametric correlations should hold regardless of the magnetic field, which is a classically small effect. In particular we observed that for open systems the average probability that an orbit survives should be included, while for parametric correlations the difference between the orbits at different parameter values acts like Gaussian noise. Importantly, there are also small corrections due to the encounters for both of these effects.

The evaluation of the extra term from the phases due to transition parameter is similar to our previous treatment of parametric correlations, in that we assume that it follows a Gaussian distribution. The difference is that the sign of the phase of an orbit (or orbit stretch) now depends on the direction in which the orbit (stretch) is traversed. To evaluate the form factor we need to be able to evaluate the average over the phase difference of the orbit pair

$$
\left\langle \mathrm{e}^{\frac{\mathrm{i}}{\hbar}(\theta_\gamma - \theta_{\gamma'})} \right\rangle
\tag{4.3.2}
$$

For the diagonal approximation we pair an orbit γ with itself and its time reverse $\overline{\gamma}$ (which exists by the assumption that we start with a time reversal invariant system and then proceed to break the symmetry), so we obtain

$$
K^{\mathrm{diag}}(\tau, x, y, M) = \frac{1}{T_\mathrm{H}} \left\langle \sum_\gamma |A_\gamma|^2 \left[1 + \mathrm{e}^{\frac{\mathrm{i}}{\hbar}(\theta_\gamma - \theta_{\overline{\gamma}})}\right] \mathrm{e}^{\frac{\mathrm{i}x}{\sigma\hbar}Q_\gamma} \delta\left(\tau T_\mathrm{H} - T_\gamma\right) \right\rangle
\tag{4.3.3}
$$

91

When we pair an orbit with itself, the two orbits follow the same path (in the same direction), the phases are the same and cancel giving one. When we compare an orbit with its time reverse however, the orbits follow the same path in the opposite direction, the phases are equal and opposite, and we have to evaluate

$$\left\langle e^{\frac{2i}{\hbar}\theta_\gamma} \right\rangle = e^{-y'T_\gamma} \tag{4.3.4}$$

Here we have used a Gaussian average (Saito and Nagao, 2006), where y' is given by $\frac{4Y^2 D}{\hbar^2}$ for a constant D. This Gaussian average is similar to our treatment for the parameter x. We can see that the parameter Y provides an average contribution of $e^{-y'T'}$ where T' is the amount of time the two orbits in a pair travel in opposite directions (along the same path). To get the diagonal approximation we use the equidistribution theorem in the form of the open sum rule (equation (4.1.10)) combined by the effect of both parameters (with the assumption that these are independent of each other and the probability of survival). If we set $y = y'T_H$, then we arrive at the following expression for the form factor

$$K^{\text{diag}}(\tau, x, y, M) = \tau e^{-(B+M)\tau} \left(1 + e^{-y\tau}\right) \tag{4.3.5}$$

To go beyond the diagonal approximation, we need to include the contribution of the symmetry breaking parameter in the calculations we have done so far based on Müller et al. (2004, 2005) and Müller (2005). The calculation is complicated by the fact that the amount of time the orbit pair spend travelling in different directions depends on their exact structure. We can no longer sum over the vectors $\boldsymbol{v}$, but we have to go back one step and sum over the individual structures. The main steps and combinatorics, however, are all presented in Nagao et al. (2007). First we need to return to the definition of $w_T(\tilde{\boldsymbol{s}}, \tilde{\boldsymbol{u}})$ (equation (2.2.17)). It can be expressed as an integral over the remaining $L-1$ non-vanishing links (with times t_i) in an orbit with L links after the integral over the starting point has been performed

$$w_T(\tilde{\boldsymbol{s}}, \tilde{\boldsymbol{u}}) = \frac{T \int_0^{T-t_{\text{enc}}} \mathrm{d}t_{L-1} \cdots \int_0^{T-t_{\text{enc}}-t_{L-1}\ldots-t_2} \mathrm{d}t_1}{\Omega^{L-V} \prod_\alpha t_{\text{enc}}^\alpha} \tag{4.3.6}$$

where $t_{\text{enc}} = \sum_\alpha l_\alpha t_{\text{enc}}^\alpha$ is the sum of all the encounter times. For each vector $\boldsymbol{v}$ we have a number of different structures, each with different numbers of links and encounter regions traversed in opposite directions. If we have, say, N links traversed in different directions then there will be a contribution of $\mathrm{e}^{-y'(t_1+\ldots+t_N)}$ from the magnetic phases. The augmented weight will therefore include the factor

$$z_T'(\tilde{\boldsymbol{s}}, \tilde{\boldsymbol{u}}) = \frac{T \int_0^{T-t_{\text{enc}}} \mathrm{d}t_{L-1} \cdots \int_0^{T-t_{\text{enc}}-t_{L-1}\ldots-t_2} \mathrm{d}t_1 \mathrm{e}^{-y'(t_1+\ldots+t_N)}}{\Omega^{L-V} \prod_\alpha t_{\text{enc}}^\alpha} \tag{4.3.7}$$

These integrals can easily be obtained, but now depend on N as well. The crux of the semiclassical calculations is the encounter time corrections. For each l-encounter, we also need to know the number of encounter traversals that are traversed in the opposite direction in the partner orbit. This number, n, can vary between 0 and l, and we need to include this contribution in our calculations. The l encounter stretches are correlated, and so

$$\left\langle \mathrm{e}^{\frac{2\mathrm{i}}{\hbar} n\theta_{\text{enc}}} \right\rangle = \mathrm{e}^{-n^2 y' t_{\text{enc}}} \tag{4.3.8}$$

in exactly the same way as for parametric correlations due to the parameter X. For the contribution of each structure to the form factor, we therefore include this term. If each l_α has a corresponding n_α then we have to multiply $z_T'(\tilde{\boldsymbol{s}}, \tilde{\boldsymbol{u}})$ by the factor below corresponding to all three effects

$$z_T(\tilde{\boldsymbol{s}}, \tilde{\boldsymbol{u}}) = z_T'(\tilde{\boldsymbol{s}}, \tilde{\boldsymbol{u}}) \times \mathrm{e}^{-(\beta+\mu)T} \prod_\alpha \mathrm{e}^{-(\beta l_\alpha-\mu)(l_\alpha-1)t_{\text{enc}}^\alpha} \mathrm{e}^{-n_\alpha^2 y' t_{\text{enc}}^\alpha} \tag{4.3.9}$$

to obtain the full augmented weight $z_T(\tilde{\boldsymbol{s}}, \tilde{\boldsymbol{u}})$. In the above we have included terms corresponding to the survival probability and the parametric correlations. For these we recall that the survival probability of an encounter is increased by the closeness of the encounter stretches and that they are dependent for the Gaussian averaging of

the parameter x. We can expand this product to first order in the encounter times

$$\mathrm{e}^{-(\beta+\mu)T} \prod_\alpha (1 - [(\beta l_\alpha - \mu)(l_\alpha - 1) + n_\alpha^2 y'] t_{\mathrm{enc}}^\alpha) \tag{4.3.10}$$

Then it is simple to calculate the contribution to the form factor for each structure. Nagao et al. (2007) include a Table of the number of each structure, and the values of l,n and N for the structure. With these values we can sum over all structures with the same vector $\boldsymbol{v}$ to get the entries in Table 4.3, where we have let $\tilde{y} = y\tau$ for compactness.

$\boldsymbol{v}$	$K_{\boldsymbol{v}}(\tau, x, y, M)\mathrm{e}^{(B+M)\tau}$
$(2)^1$	$-2\mathrm{e}^{-\tilde{y}}\tau^2 - (2B - M)\left(\frac{1-\mathrm{e}^{-\tilde{y}}}{\tilde{y}}\right)\tau^3$
$(2)^2$	$\left(2 + 6\mathrm{e}^{-\tilde{y}} + \frac{2-2\mathrm{e}^{-\tilde{y}}}{\tilde{y}} + \tilde{y}\mathrm{e}^{-\tilde{y}} + \frac{\tilde{y}^2\mathrm{e}^{-\tilde{y}}}{6}\right)\tau^3$ $+ (2B - M)\left(\frac{1+\mathrm{e}^{-\tilde{y}}}{2} + \frac{4-4\mathrm{e}^{-\tilde{y}}+2\tilde{y}-6\tilde{y}\mathrm{e}^{-\tilde{y}}}{\tilde{y}^2} + \frac{\tilde{y}\mathrm{e}^{-\tilde{y}}}{6}\right)\tau^4$ $+ (2B - M)^2\left(\frac{1+\mathrm{e}^{-\tilde{y}}}{24} + \frac{4\mathrm{e}^{-\tilde{y}}-4+2\tilde{y}+2\tilde{y}\mathrm{e}^{-\tilde{y}}}{\tilde{y}^3}\right)\tau^5$
$(3)^1$	$-\left(2 + 4\mathrm{e}^{-\tilde{y}} + \frac{2-2\mathrm{e}^{-\tilde{y}}}{\tilde{y}} + \tilde{y}\mathrm{e}^{-\tilde{y}}\right)\tau^3 - \left(3B - M\right)\left(\frac{1+\mathrm{e}^{-\tilde{y}}}{3} + \frac{2-2\mathrm{e}^{-\tilde{y}}}{\tilde{y}}\right)\tau^4$
$(2)^3$	$-\left(\frac{50\mathrm{e}^{-\tilde{y}}}{3} + \frac{20-20\mathrm{e}^{-\tilde{y}}+28\tilde{y}-48\tilde{y}\mathrm{e}^{-\tilde{y}}}{\tilde{y}^2} + 4\tilde{y}\mathrm{e}^{-\tilde{y}} + \frac{\tilde{y}^2\mathrm{e}^{-\tilde{y}}}{3}\right)\tau^4$ $+ (2B - M)\left(2\mathrm{e}^{-\tilde{y}} + \frac{4-4\mathrm{e}^{-\tilde{y}}-34\tilde{y}+30\tilde{y}\mathrm{e}^{-\tilde{y}}-13\tilde{y}^2+45\tilde{y}^2\mathrm{e}^{-\tilde{y}}}{\tilde{y}^3} - \frac{\tilde{y}\mathrm{e}^{-\tilde{y}}}{6}\right)\tau^5$ $+ (2B - M)^2\left(\frac{\mathrm{e}^{-\tilde{y}}}{12} + \frac{192-192\mathrm{e}^{-\tilde{y}}-24\tilde{y}-168\tilde{y}\mathrm{e}^{-\tilde{y}}-21\tilde{y}^2-51\tilde{y}^2\mathrm{e}^{-\tilde{y}}-4\tilde{y}^3+5\tilde{y}^3\mathrm{e}^{-\tilde{y}}}{3\tilde{y}^4}\right)\tau^6$ $+ (2B - M)^3\left(\frac{768-768\mathrm{e}^{-\tilde{y}}-384\tilde{y}-384\tilde{y}\mathrm{e}^{-\tilde{y}}+56\tilde{y}^2-56\tilde{y}^2\mathrm{e}^{-\tilde{y}}}{24\tilde{y}^5}\right.$ $\left. + \frac{4\tilde{y}^3+4\tilde{y}^3\mathrm{e}^{-\tilde{y}}+\tilde{y}^4-\tilde{y}^4\mathrm{e}^{-\tilde{y}}}{24\tilde{y}^5}\right)\tau^7$
$(2)^1$ $(3)^1$	$\left(16\mathrm{e}^{-\tilde{y}} + \frac{24-24\mathrm{e}^{-\tilde{y}}+44\tilde{y}-68\tilde{y}\mathrm{e}^{-\tilde{y}}}{\tilde{y}^2} + \frac{10\tilde{y}\mathrm{e}^{-\tilde{y}}}{3}\right)\tau^4$ $- 4B\left(\frac{2\mathrm{e}^{-\tilde{y}}}{3} + \frac{20-20\mathrm{e}^{-\tilde{y}}-22\tilde{y}+2\tilde{y}\mathrm{e}^{-\tilde{y}}-11\tilde{y}^2+23\tilde{y}^2\mathrm{e}^{-\tilde{y}}}{\tilde{y}^3}\right)\tau^5$ $+ M\left(\mathrm{e}^{-\tilde{y}} + \frac{36-36\mathrm{e}^{-\tilde{y}}-36\tilde{y}-17\tilde{y}^2+35\tilde{y}^2\mathrm{e}^{-\tilde{y}}}{\tilde{y}^3}\right)\tau^5$ $- (2B - M)(3B - M)\left(\frac{12-12\mathrm{e}^{-\tilde{y}}-6\tilde{y}-6\tilde{y}\mathrm{e}^{-\tilde{y}}-\tilde{y}^2+\tilde{y}^2\mathrm{e}^{-\tilde{y}}}{\tilde{y}^3}\right)\tau^6$
$(4)^1$	$-\left(2\mathrm{e}^{-\tilde{y}} + \frac{4-4\mathrm{e}^{-\tilde{y}}+16\tilde{y}-20\tilde{y}\mathrm{e}^{-\tilde{y}}}{\tilde{y}^2}\right)\tau^4$ $+ (4B - M)\left(\frac{12-12\mathrm{e}^{-\tilde{y}}-6\tilde{y}-6\tilde{y}\mathrm{e}^{-\tilde{y}}-9\tilde{y}^2+9\tilde{y}^2\mathrm{e}^{-\tilde{y}}}{2\tilde{y}^3}\right)\tau^5$

Table 4.3: Contribution of different types of orbit pairs to the parametric transition form factor of the time delay.

When we sum over $\boldsymbol{v}$, the contribution of all these orbits gives the transition form factor up to 5th order in τ

$$K(\tau, x, y, M) = \mathrm{e}^{-(B+M)\tau}$$

$$\times \left\{ \left[1 + \mathrm{e}^{-y\tau}\right]\tau - 2\mathrm{e}^{-y\tau}\tau^2 + \left[2\mathrm{e}^{-y\tau} + \frac{y^2\tau^2\mathrm{e}^{-y\tau}}{6} - (2B - M)\left(\frac{1 - \mathrm{e}^{-y\tau}}{y\tau}\right)\right]\tau^3 \right.$$

$$- \left[\frac{8\mathrm{e}^{-y\tau}}{3} + \frac{2y\tau\mathrm{e}^{-y\tau}}{3} + \frac{y^2\tau^2\mathrm{e}^{-y\tau}}{3} + M\left(\frac{1 + \mathrm{e}^{-y\tau}}{6}\right) - (2B - M)\left(\frac{y\tau\mathrm{e}^{-y\tau}}{6}\right)\right.$$

$$\left. -2B\left(\frac{4 - 4\mathrm{e}^{-y\tau} - y\tau - 3y\tau\mathrm{e}^{-y\tau}}{y^2\tau^2}\right) + 4M\left(\frac{1 - \mathrm{e}^{-y\tau} - y\tau\mathrm{e}^{-y\tau}}{y^2\tau^2}\right)\right]\tau^4$$

$$+ \left[4\mathrm{e}^{-y\tau} + \frac{4y\tau\mathrm{e}^{-y\tau}}{3} + \frac{y^2\tau^2\mathrm{e}^{-y\tau}}{3} + \frac{y^4\tau^4\mathrm{e}^{-y\tau}}{120} + (4B - 3M)\frac{\mathrm{e}^{-y\tau}}{3}\right.$$

$$- (2B - M)\frac{y\tau\mathrm{e}^{-y\tau}}{6} + 8B\left(\frac{6\mathrm{e}^{-y\tau} - 6 + y\tau + 5y\tau\mathrm{e}^{-y\tau} + 2y^2\tau^2\mathrm{e}^{-y\tau}}{y^3\tau^3}\right)$$

$$+ M\left(\frac{52 - 52\mathrm{e}^{-y\tau} + 2y\tau - 54y\tau\mathrm{e}^{-y\tau} + y^2\tau^2 - 29y^2\tau^2\mathrm{e}^{-y\tau}}{y^3\tau^3}\right)$$

$$\left.\left. + (2B - M)^2\left(\frac{1 + \mathrm{e}^{-y\tau}}{24} + \frac{4\mathrm{e}^{-y\tau} - 4 + 2y\tau + 2y\tau\mathrm{e}^{-y\tau}}{y^3\tau^3}\right)\right]\tau^5 + \ldots\right\}$$

$$(4.3.11)$$

This result encompasses all previous results, though to lower order. If we take the limits $y = 0$ and $y \to \infty$ we get the GOE and GUE results respectively from the previous section. Setting $B = 0$ removes the parametric correlation, and setting $M = 0$ closes the system. Performing both we get the GOE-GUE transition results found in Saito and Nagao (2006) and Nagao et al. (2007). If we also expand the remaining exponentials for small τ we can compare with the series calculated from the RMT integral in Section 4.4, and we find exact agreement.

4.4 RMT results

The two-point correlation function of the Wigner time delay for the GUE case is derived in Fyodorov and Sommers (1996) (with more detail given in Fyodorov and Sommers, 1997). When we take the Fourier transform, the following integral is the RMT prediction for the GUE form factor

$$K^{\mathrm{GUE}}(\tau, M) = \frac{1}{2}\int_{-1}^{1}\mathrm{d}\lambda \int_{1}^{\infty}\mathrm{d}\lambda_1 \int_{-\infty}^{\infty}\mathrm{d}\omega \, \cos(\pi\omega(\lambda_1 - \lambda))\left(\frac{1 + \lambda}{1 + \lambda_1}\right)^{M}\mathrm{e}^{-2\pi\mathrm{i}\omega\tau}$$

$$(4.4.1)$$

We can evaluate this integral as a series in τ, but we can also include the effect of parametric variation as an extra factor in the integral (Fyodorov and Sommers, 1996)

$$
\begin{aligned}
K^{\text{GUE}}(\tau, x, M) &= \frac{1}{2}\int_{-1}^{1}\mathrm{d}\lambda \int_{1}^{\infty}\mathrm{d}\lambda_1 \int_{-\infty}^{\infty}\mathrm{d}\omega \, \cos(\pi\omega(\lambda_1 - \lambda))\mathrm{e}^{-2\pi\mathrm{i}\omega\tau} \\
&\quad \times \left(\frac{1+\lambda}{1+\lambda_1}\right)^{M}\mathrm{e}^{-\frac{\pi^2 x^2(\lambda_1{}^2 - \lambda^2)}{2}}
\end{aligned}
\tag{4.4.2}
$$

When we set $x = 0$ this recreates the integral without the effect of the external parameter X. Because we expand both integrals in the same way, we will consider this more general case. First, we perform the integral over ω to obtain

$$
K^{\text{GUE}}(\tau, x, M) = \frac{1}{2}\int_{-1}^{1}\mathrm{d}\lambda \int_{1}^{\infty}\mathrm{d}\lambda_1 \, \delta(\lambda_1 - \lambda - 2\tau)\left(\frac{1+\lambda}{1+\lambda_1}\right)^{M}\mathrm{e}^{-\frac{\pi^2 x^2(\lambda_1{}^2 - \lambda^2)}{2}}
\tag{4.4.3}
$$

Because τ is positive and $\lambda_1 \geq \lambda$ the other delta function does not contribute and we exclude it. From the contributing delta function we get the relation $2\tau = \lambda_1 - \lambda$. As we are only considering the case where $\tau < 1$, the domain of integration can be reduced to $1 \leq \lambda_1 \leq 1 + 2\tau$. If we perform the integral over λ we are left with

$$
K^{\text{GUE}}(\tau, x, M) = \frac{1}{2}\int_{1}^{1+2\tau}\mathrm{d}\lambda_1 \left(\frac{1+\lambda_1 - 2\tau}{1+\lambda_1}\right)^{M}\mathrm{e}^{2\pi^2 x^2 \tau(\tau - \lambda_1)}
\tag{4.4.4}
$$

which upon the substitution $\lambda_1 = 1 + \tau y_1$, $B = 2\pi^2 x^2$ (see equation (3.1.18)) becomes

$$
K^{\text{GUE}}(\tau, x, M) = \frac{\tau \mathrm{e}^{-B\tau}}{2}\int_{0}^{2}\mathrm{d}y_1 \left(1 - \frac{2\tau}{2+\tau y_1}\right)^{M}\mathrm{e}^{B\tau^2(1-y_1)}
\tag{4.4.5}
$$

We can expand the integrand to get a series in τ, which we can integrate term by term. If we extract an exponential prefactor, we obtain the following result

$$
\begin{aligned}
K^{\mathrm{GUE}}(\tau, x, M) \;=\; \mathrm{e}^{-(B+M)\tau} \Bigg[&\, \tau - \frac{M}{6}\tau^4 + \frac{(2B-M)^2}{24}\tau^5 - \frac{M}{15}\tau^6 \\
&- \left(\frac{BM}{15} - \frac{M^2}{20} \right)\tau^7 - \left(\frac{7M(2B-M)^2}{720} + \frac{M}{28} \right)\tau^8 \\
&+ \left(\frac{(2B-M)^4}{1920} - \frac{BM}{28} + \frac{401M^2}{10080} \right)\tau^9 + \ldots \Bigg]
\end{aligned}
$$

$$(4.4.6)$$

This is exactly the contribution we obtained from considering periodic orbits in Section 4.2. We can remove the parametric correlations by setting $x = 0$ (or equivalently $B = 0$), giving the result

$$
\begin{aligned}
K^{\mathrm{GUE}}(\tau, M) \;=\; \mathrm{e}^{-M\tau} \Bigg[&\, \tau - \frac{M\tau^4}{6} + \frac{M^2\tau^5}{24} - \frac{M\tau^6}{15} + \frac{M^2\tau^7}{20} - \frac{7M^3\tau^8}{720} \\
&- \frac{M\tau^8}{28} + \frac{M^4\tau^9}{1920} + \frac{401M^2\tau^9}{10080} + \ldots \Bigg]
\end{aligned}
$$

$$(4.4.7)$$

Which is exactly the contribution we obtained from considering the orbits in Section 4.1.2.

With time reversal symmetry, the two-point correlation function can be found in Lehmann et al. (1995). With a Fourier transform, the RMT result for the form factor is, for the GOE case, given by

$$
\begin{aligned}
K^{\mathrm{GOE}}(\tau, M) \;=\; &\int_{-1}^{1} \mathrm{d}\lambda \int_{1}^{\infty} \mathrm{d}\lambda_1 \int_{1}^{\infty} \mathrm{d}\lambda_2 \int_{-\infty}^{\infty} \mathrm{d}\omega \, \cos(\pi\omega(\lambda - \lambda_1\lambda_2)) \mathrm{e}^{-2\pi\mathrm{i}\omega\tau} \\
&\times \frac{(1-\lambda^2)(\lambda - \lambda_1\lambda_2)^2}{(2\lambda\lambda_1\lambda_2 - \lambda^2 - \lambda_1{}^2 - \lambda_2{}^2 + 1)^2} \left(\frac{1+\lambda}{\lambda_1 + \lambda_2} \right)^{M}
\end{aligned}
$$

$$(4.4.8)$$

The effect of parametric variation given by Fyodorov et al. (1997) also adds an extra term to the integral leading to

$$
\begin{aligned}
K^{\mathrm{GOE}}(\tau, x, M) \;=\; &\int_{-1}^{1} \mathrm{d}\lambda \int_{1}^{\infty} \mathrm{d}\lambda_1 \int_{1}^{\infty} \mathrm{d}\lambda_2 \int_{-\infty}^{\infty} \mathrm{d}\omega \, \cos(\pi\omega(\lambda - \lambda_1\lambda_2)) \mathrm{e}^{-2\pi\mathrm{i}\omega\tau} \\
&\times \left(\frac{1+\lambda}{\lambda_1 + \lambda_2} \right)^{M} \exp\left\{ -\frac{\pi^2 x^2}{4}(2\lambda_1{}^2\lambda_2{}^2 - \lambda^2 - \lambda_1{}^2 - \lambda_2{}^2 + 1) \right\} \\
&\times \frac{(1-\lambda^2)(\lambda - \lambda_1\lambda_2)^2}{(2\lambda\lambda_1\lambda_2 - \lambda^2 - \lambda_1{}^2 - \lambda_2{}^2 + 1)^2}
\end{aligned}
$$

$$(4.4.9)$$

This is similar to the integral in Section 3.2 and we proceed in the same way. Firstly, the integral over ω gives

$$
\begin{aligned}
K^{\mathrm{GOE}}(\tau, x, M) \;=\;& \int_{-1}^{1} \mathrm{d}\lambda \int_{1}^{\infty} \mathrm{d}\lambda_1 \int_{1}^{\infty} \mathrm{d}\lambda_2 \, \delta(\lambda - \lambda_1\lambda_2 + 2\tau) \left(\frac{1+\lambda}{\lambda_1 + \lambda_2} \right)^M \\
& \times \exp\left\{ -\frac{\pi^2 x^2}{4}(2\lambda_1{}^2\lambda_2{}^2 - \lambda^2 - \lambda_1{}^2 - \lambda_2{}^2 + 1) \right\} \\
& \times \frac{(1-\lambda^2)(\lambda - \lambda_1\lambda_2)^2}{(2\lambda\lambda_1\lambda_2 - \lambda^2 - \lambda_1{}^2 - \lambda_2{}^2 + 1)^2}
\end{aligned}
\tag{4.4.10}
$$

Again, because τ is positive and $\lambda_1\lambda_2 \geq \lambda$ only one delta function contributes, giving the relation $\lambda = \lambda_1\lambda_2 - 2\tau$. As we are considering the case where $\tau < 1$ our domain of integration for the other two variables is given by $1 \leq \lambda_1 \leq 1 + 2\tau$ and $1 \leq \lambda_2 \leq \frac{1+2\tau}{\lambda_1}$. When we perform the integral over λ we are left with

$$
\begin{aligned}
K^{\mathrm{GOE}}(\tau, x, M) \;=\;& \int_{1}^{1+2\tau} \mathrm{d}\lambda_1 \int_{1}^{\frac{1+2\tau}{\lambda_1}} \mathrm{d}\lambda_2 \, \frac{4\tau^2(1 - \lambda_1{}^2\lambda_2{}^2 + 4\tau\lambda_1\lambda_2 - 4\tau^2)}{(1 + \lambda_1{}^2\lambda_2{}^2 - \lambda_1{}^2 - \lambda_2{}^2 - 4\tau^2)^2} \\
& \times \exp\left\{ -\frac{\pi^2 x^2}{4}(1 + \lambda_1{}^2\lambda_2{}^2 - \lambda_1{}^2 - \lambda_2{}^2 + 4\tau\lambda_1\lambda_2 - 4\tau^2) \right\} \\
& \times \left(\frac{1 + \lambda_1\lambda_2 - 2\tau}{\lambda_1 + \lambda_2} \right)^M
\end{aligned}
\tag{4.4.11}
$$

We now remove the τ dependence from the limits to evaluate this integral as a series in τ. We make a change of variables $y'_1 = \lambda_1$ and $y'_2 = \lambda_1\lambda_2$ to obtain

$$
\begin{aligned}
K^{\mathrm{GOE}}(\tau, x, M) \;=\;& \int_{1}^{1+2\tau} \mathrm{d}y'_1 \int_{y'_1}^{1+2\tau} \mathrm{d}y'_2 \, \frac{1}{y'_1} \frac{4\tau^2(1 - y'_2{}^2 + 4\tau y'_2 - 4\tau^2)}{(1 + y'_2{}^2 - y'_1{}^2 - \frac{y'_2{}^2}{y'_1{}^2} - 4\tau^2)^2} \\
& \times \exp\left\{ -\frac{\pi^2 x^2}{4}(1 + y'_2{}^2 - y'_1{}^2 - \frac{y'_2{}^2}{y'_1{}^2} + 4\tau y'_2 - 4\tau^2) \right\} \\
& \times \left(\frac{1 + y'_2 - 2\tau}{y'_1 + \frac{y'_2}{y'_1}} \right)^M
\end{aligned}
\tag{4.4.12}
$$

Then we make the change of variables $y_1 = 1 + \tau y'_1$ and $y_2 = 1 + \tau y_2$, which removes all τ dependency from the limits. We also make the substitution $B = \pi^2 x^2$ (see equation (3.1.18)) and we expand the integrand as a series in τ, though only the

98

first two terms are included for clarity

$$
\begin{aligned}
K^{\mathrm{GOE}}(\tau, x, M) \;=\; & \int_0^2 \mathrm{d}y_1 \int_{y_1}^2 \mathrm{d}y_2 \, \frac{2 - y_2}{2(1 - y_1 y_2 + y_1{}^2)^2} \tau \\
& + \left[\frac{y_1(y_2 - 2)(4 - y_1 y_2 + 2y_1{}^2 - y_2{}^2)}{2(1 - y_1 y_2 + y_1{}^2)^3} \right. \\
& \left. + \frac{(2 - y_2)(2 + 2B + 2M - 6y_1 - y_2)}{4(1 - y_1 y_2 + y_1{}^2)^2} \right] \tau^2 + \dots \quad (4.4.13)
\end{aligned}
$$

When we perform the integral term by term and extract an exponential we obtain the following series for the result

$$
\begin{aligned}
K^{\mathrm{GOE}}(\tau, x, M) \;=\; & e^{-(B+M)\tau} \left[2\tau - 2\tau^2 - (2B - M - 2)\tau^3 + \left(2B - \frac{7M}{3} - \frac{8}{3} \right)\tau^4 \right. \\
& + \left(\frac{5(2B - M)^2}{12} - \frac{8B}{3} + \frac{13M}{3} + 4 \right)\tau^5 \\
& - \left(\frac{5B^2}{3} - \frac{11BM}{3} + \frac{17M^2}{12} - 4B + \frac{39M}{5} + \frac{32}{5} \right)\tau^6 \\
& - \left(\frac{41(2B - M)^3}{360} - \frac{11B^2}{5} + 7BM - \frac{43M^2}{12} \right. \\
& \left. \left. + \frac{32B}{5} - \frac{212M}{15} - \frac{32}{3} \right)\tau^7 + \dots \right] \quad (4.4.14)
\end{aligned}
$$

which is the same as the terms from periodic orbits in equation (4.2.7). We can again remove the parametric dependence by setting $B = 0$ to give the result

$$
\begin{aligned}
K^{\mathrm{GOE}}(\tau, M) \;=\; & e^{-M\tau} \left[2\tau - 2\tau^2 + (M + 2)\tau^3 - \left(\frac{7M}{3} + \frac{8}{3} \right)\tau^4 \right. \\
& + \left(\frac{5M^2}{12} + \frac{13M}{3} + 4 \right)\tau^5 - \left(\frac{17M^2}{12} + \frac{39M}{5} + \frac{32}{5} \right)\tau^6 \\
& \left. + \left(\frac{41M^3}{360} + \frac{43M^2}{12} + \frac{212M}{15} + \frac{32}{3} \right)\tau^7 + \dots \right] \quad (4.4.15)
\end{aligned}
$$

which is the same as the terms from the orbits in equation (4.1.17).

We have now shown how these RMT results can be obtained semiclassically for both parametric correlations and correlations of the time delay for open systems, and a combination of the two. We should also consider the RMT results for the transition between the GOE and the GUE symmetry classes. The transition adds

another factor to the correlation function of the GOE result (Fyodorov et al., 1997) and hence to our Fourier transform in equation (4.4.9). This factor is given by

$$
\begin{aligned}
G(y) \;\;=\;\; & \exp\left(\frac{y}{8}(\lambda^2 + 1 - 2\lambda_2^2)\right)\left[(1 - \lambda^2)\left(1 + \frac{yR}{4}\right)\cosh\chi + (\lambda_2^2 - \lambda_1^2)\sinh\chi \right. \\
& \left. + \frac{yR}{4}(2\lambda_2^2 + \lambda^2 - 1)\sinh\chi\right]
\end{aligned}
\tag{4.4.16}
$$

where

$$
R = \lambda_1^2 + \lambda_2^2 + \lambda^2 - 2\lambda\lambda_1\lambda_2 - 1 \quad \text{and} \quad \chi = \frac{y}{8}(1 - \lambda^2)
\tag{4.4.17}
$$

Here we have set the two transition parameters y_1 and y_2 from Fyodorov et al. (1997) to $y_1^2 = y_2^2 = y/8$. We follow the same steps as before to obtain the form factor as a series in τ

$$
\begin{aligned}
K(\tau, x, y, M) \;\;=\;\; & \mathrm{e}^{-(B+M)\tau}\left[2\tau - (2 + y)\tau^2 + \left(2 + 2y + \frac{1}{2}y^2 - 2B + M\right)\tau^3 \right. \\
& - \left(\frac{8}{3} + 2y + y^2 + \frac{1}{6}y^3 - 2B - By + \frac{7}{3}M + \frac{1}{2}My\right)\tau^4 \\
& + \left(4 + 2y + \frac{7}{6}y^2 + \frac{1}{3}y^3 + \frac{1}{24}y^4 - \frac{8}{3}B + \frac{13}{3}M \right. \\
& \left.\left. + \frac{5}{12}(2B - M)^2 - \frac{4}{3}(B - M)y - \frac{1}{6}(2B - M)y^2\right)\tau^5 + \dots\right]
\end{aligned}
\tag{4.4.18}
$$

We are, as yet unable to perform the integrals without expanding the $\mathrm{e}^{-y\tau}$ terms, so we cannot see the transition from GOE to GUE with this expansion. Being able to keep any $\mathrm{e}^{-y\tau}$ terms would provide a better check of the agreement between the semiclassical calculation and RMT. However if we also expand these terms in the semiclassical result from equation (4.3.11) the result agrees exactly with this formula. This shows that the semiclassical treatment in terms of periodic orbit correlations can reproduce RMT results even for highly complicated correlation functions. In fact, in this case, the periodic orbit expansion gives more information than the expansion of the RMT integrals.

For the work described in Chapter 3 and Chapter 4, we have used the same

methods and semiclassical approximations discussed in Chapter 2, including the assumptions that the encounters can be decoupled from the links, and that the links can be considered as uncorrelated. Further to this we have assumed that the effect of external parameters on an orbit can be treated independently. This has generated agreement with RMT in all scenarios, and the fact that the same methods provide this agreement in these novel scenarios provides support that these methods are correct in calculating the semiclassical contribution.

In fact, the inclusion of different effects shows an analogy between the semiclassical and the RMT calculations. Each additional effect that we include in the form factor, leads to an additional factor in both the semiclassical orbit sums as well as the RMT integrals. In the semiclassical case, this factor depends crucially on the correlated nature of the stretches in each encounter. Including these factors, we can successfully treat the semiclassical calculation of complicated correlation functions depending on several parameters, and show agreement with RMT.

With this all in place we can now consider applying these types of correlations to the other picture of open systems, the scattering trajectories.

5 Open trajectories

For scattering problems, described by a scattering matrix, we have a semiclassical approximation that gives an intuitive picture of the process. The elements that link a certain incoming and outgoing channel are approximated by the classical trajectories that enter and then leave the system through those channels. One example of a quantity which can be derived from the scattering matrix is the Landauer conductance (as given by Fisher and Lee, 1981). Semiclassically, it is given by a sum over all the open trajectories that start in one lead and end in another. The steps in the semiclassical evaluation of this sum and hence the conductance follow a similar history to those taken for the evaluation of the form factor for closed systems. The diagonal approximation was evaluated by Baranger et al. (1993a) (with more detail given in Baranger et al., 1993b), and the authors also realised that off-diagonal terms were needed to accurately describe the conductance.

The contribution of the first off-diagonal term was found by Richter and Sieber (2002) by applying the method from their work on closed systems (Sieber and Richter, 2001). In order to perform the calculation they used a modified version of the Hannay–Ozorio de Almeida sum rule which takes into account the survival probability of the trajectory (see also Cvitanović and Eckhardt, 1991). Heusler et al. (2006) extended (and corrected) this treatment, in a similar way to their extension (Müller et al., 2004, 2005) of previous work on closed systems (Sieber and Richter, 2001). In their work, Heusler et al. (2006) obtained the full expansion of the conductance in terms of the number of entrance and exit channels of the (clean) chaotic ballistic cavity, and found agreement with the RMT predictions. In fact a small but

significant modification of the survival probability in the open sum rule was needed, that, if an orbit does not escape while traversing an encounter region once it will not escape during any of the traverses. Therefore the effective time when the orbit might escape is slightly reduced and its survival probability slightly increased.

With a similar (though more complicated) calculation, and also using the same modification of the survival probability in the open sum rule, Braun et al. (2006) calculated all orders of the shot noise power which is a higher order correlation function. Interestingly, for the shot noise, and other correlation functions like the conductance variance (Müller et al., 2007), there are off-diagonal terms that contribute at the same order as the diagonal approximation. It therefore follows that we need to include correlated trajectories with encounters to obtain the leading order behaviour. To introduce the semiclassical treatment of correlated trajectories for the conductance we include parametric correlations and consider the parametric conductance variance in section 5.2.2. There we will see exactly which correlated trajectories are needed to obtain the leading order result.

The Wigner time delay can also be expressed in terms of scattering trajectories and we will see how we can apply the methods developed for the conductance to the time delay. This allows us to recreate the average time delay in section 5.3.1, and also in this case we need to consider correlated trajectories for systems with time reversal symmetry. For the two-point correlation function of the time delay, Lewenkopf and Vallejos (2004a) calculated the diagonal approximation by using trajectories and showed that it did not reproduce the leading order term (see section 4.1.1). In section 5.3.2 we include correlated trajectories that contribute at the same order and show how this re-establishes the agreement between the two pictures. The agreement, however, goes further than this - not only should we be able to recreate the average time delay from scattering trajectories, but we should also be able to recreate the trapped periodic orbit terms. To achieve this we introduce a new type of correlated trajectory pair in Section 5.4. The trajectories involved follow a trapped orbit for several traversals, and we will see how their semiclassical contribution allows us to obtain full agreement between the two pictures of the time delay.

Before we look at these calculations we should examine the semiclassical limit we are taking. If we fix the (physical) size of the leads, then the classical escape rate and dwell time are constant. However, as $\hbar \to 0$, the Ehrenfest time grows like $\ln\left(\frac{1}{\hbar}\right)$ and will become larger than the dwell time. This means that trajectories of average length should be considered as following local hyperbolic motion (relative to nearby trajectories) since they are not long enough to use the property of ergodicity or uniformity. In this regime the approximations and arguments we have been using in this thesis break down, and we would need to focus on the system specific behaviour to get a handle on the semiclassics. Instead we want the dwell time to be much longer than the Ehrenfest time so that average length trajectories can be considered as wandering uniformly between any encounters. For example, if we fix the number of channels then the dwell time grows like the Heisenberg time, which behaves like $\frac{1}{\hbar^{f-1}}$. This growth is much faster than the Ehrenfest time, so that in the limit $\hbar \to 0$ we are safely in the RMT regime and can still use all the methods we have been using. Classically, the leads must shrink so that the escape rate decreases. This leaves the problem that we have a different set of trajectories (and trapped orbits) for each value of $\hbar$, and the picture is not so clear as it was for closed systems where we always have the same classical orbits. However, as we are mainly interested in their universal ergodic properties, the actual trajectories themselves are not so important. Taking the limit in the way suggested satisfies the semiclassical assumptions we need and keeps us in the universal regime. In fact we would stay in this regime as long as the dwell time grows more quickly than the Ehrenfest time and we could shrink the leads more slowly to achieve this, which would also change the classical trajectories more slowly.

By shrinking the leads in such a way that the dwell time grows at the same rate as the Ehrenfest time we enter a different regime, on the border between the system specific and the universal. For quantum transport, this regime has been considered, for example, by Whitney and Jacquod (2006) and Brouwer and Rahav (2006) where they examined the first off-diagonal contributions to correlation functions of the conductance. Corrections due to the finite ratio between the Ehrenfest

and dwell times are important and are outside both the universal RMT regime as well as the system specific regime. In fact these corrections, precisely because they give information beyond RMT, are a good testing ground for the usefulness and importance of semiclassical methods. Unfortunately it is not entirely clear how the methods used for correlated trajectories, which require the decoupling of different parts of the same trajectory (the local hyperbolicity of the encounters and the global uniformity of the links), still hold in a regime where the two opposing behaviours of the parts overlap. Justification of the use of different approximations for the encounters and the links is thin and, as the region where they join together is also of the Ehrenfest time, any errors become important and can change the contribution. For example the stretches in an encounter region are close together and they should all stay or leave together, so it is assumed that the survival probability depends just on the time of one stretch. However, by changing the small constant that defines the encounter regions, the encounter time becomes longer or shorter thus changing the approximation for the probability of survival although, for the same trajectory, this should remain the same. The error is a factor of $\mathrm{e}^{-\mu t}$ where t is of the order of the Ehrenfest time, which disappears and can be ignored in the RMT regime but not necessarily when we are calculating Ehrenfest time corrections. These considerations might lead to a correction term which vanishes in the semiclassical limit, as was the case for the next order correction to the contribution of a periodic orbit with a single 2-encounter for closed systems of constant negative curvature (Heusler, 2003; Sieber, 2003). This remains to be shown and we restrict ourselves to the universal regime in the following, even though some results, notably equation (5.4.1), should remain valid outside.

5.1   Semiclassical scattering matrix

In Section 4.1 we mentioned that, for the time delay, when opening our system we imagine attaching a lead capable of supporting M quantum states. A wavefunction entering the system along the lead will be in a superposition of these states and will

scatter around the chaotic system before leaving it as a new superposition of the M states in the lead. The entire scattering process can be encoded in the $M \times M$ scattering matrix $S(E)$ which links the incoming states to the outgoing ones and hence any incoming wave to an outgoing one. This scattering matrix is obviously a quantum object, but when we consider it in the semiclassical limit it can be approximated in terms of open trajectories that enter and later leave the system. One such trajectory is represented in Figure 5.1.

Each element of the scattering matrix S_{ba} represents the transition from a state or channel a to the channel b. The semiclassical approximation is given in terms of classical trajectories that connect the incoming channel to the outgoing one (Miller, 1975; Richter, 2000; Richter and Sieber, 2002)

$$S_{ba}(E) \approx \frac{1}{\sqrt{T_{\mathrm{H}}}} \sum_{\zeta(a \to b)} A_\zeta \mathrm{e}^{\frac{\mathrm{i}}{\hbar} S_\zeta} \mathrm{e}^{-\frac{\mathrm{i}\pi}{2} \nu_\zeta} \tag{5.1.1}$$

where, similarly to semiclassical expressions in terms of periodic orbits, S_ζ is the action of the trajectory ζ, A_ζ is a stability amplitude (whose form is given in Richter, 2000) and ν_ζ is a topological index, like a Maslov index. The sum is then over all classical trajectories that start in channel a and end in channel b. These trajectories start with a fixed (absolute) angle (dependent on a) relative to the entrance lead direction, but with an arbitrary position in the lead, and end with a fixed angle (dependent on b) in the exit lead. From the semiclassical approximation to the scattering matrix elements we can derive both the time delay and the conductance in terms of scattering trajectories.

5.1.1 Wigner time delay

To obtain the semiclassical approximation for the Wigner time delay we substitute the approximation for the scattering matrix elements of equation (5.1.1) into the time delay equation (see equation (4.1.1))

$$\tau_{\mathrm{W}}(E) = -\frac{\mathrm{i}\hbar}{M} \mathrm{Tr} \left[S^\dagger(E) \frac{\mathrm{d}}{\mathrm{d}E} S(E) \right] \tag{5.1.2}$$

When we differentiate the scattering matrix elements, however, we ignore the change in the slowly varying prefactor and only keep the term from the oscillating action exponentials

$$\tau_{\mathrm{W}} \approx \frac{1}{MT_{\mathrm{H}}} \sum_{a,b} \sum_{\zeta,\zeta'(a\to b)} T_\zeta A_\zeta A_{\zeta'}^* \mathrm{e}^{\frac{\mathrm{i}}{\hbar}(S_\zeta - S_{\zeta'})} \mathrm{e}^{-\frac{\mathrm{i}\pi}{2}(\nu_\zeta - \nu_{\zeta'})} \tag{5.1.3}$$

where $T_\zeta = \frac{\partial S_\zeta}{\partial E}$ is the time the trajectory ζ spends inside the system. We can see that the time delay is a sum over trajectory pairs ζ, ζ' both of which start and end in the same channels (a and b respectively), followed by a sum over all the possible channels.

We can also obtain the time delay by considering a correlation function of scattering matrix elements

$$C(\epsilon) = \sum_{a,b} S_{ba}\left(E + \frac{\epsilon}{2}\right) S_{ba}^*\left(E - \frac{\epsilon}{2}\right) \tag{5.1.4}$$

If we set $\epsilon = 0$ the previous equation becomes

$$C(0) = \mathrm{Tr}\left[S(E)S^\dagger(E)\right] \tag{5.1.5}$$

which is simply equal to M as the scattering matrix is unitary. This unitarity means that nothing is lost during scattering, so the magnitudes of the incoming and outgoing waves are the same. By using the semiclassical approximation of the matrix elements from equation (5.1.1) and expanding the action up to first order in energy ($S_\zeta(E + \epsilon) \approx S_\zeta(E) + \epsilon T_\zeta(E)$), the correlation function can be expressed in terms of pairs of scattering trajectories

$$C(\epsilon) \approx \frac{1}{T_{\mathrm{H}}} \sum_{a,b} \sum_{\zeta,\zeta'(a\to b)} A_\zeta A_{\zeta'}^* \mathrm{e}^{\frac{\mathrm{i}}{\hbar}(S_\zeta - S_{\zeta'})} \mathrm{e}^{-\frac{\mathrm{i}\pi}{2}(\nu_\zeta - \nu_{\zeta'})} \mathrm{e}^{\frac{\mathrm{i}\epsilon}{2\hbar}(T_\zeta + T_{\zeta'})} \tag{5.1.6}$$

Here both trajectories ζ, ζ' travel from channel a to channel b and we sum over all channels. From the correlation function we can derive a 'symmetrized' version of

the time delay (Lewenkopf and Vallejos, 2004a).

$$\tau_W = \frac{-i\hbar}{M} \frac{d}{d\epsilon} C(\epsilon)\Big|_{\epsilon=0} = -\frac{i\hbar}{2M} \text{Tr} \left[S^\dagger(E) \frac{dS(E)}{dE} - S(E) \frac{dS^\dagger(E)}{dE} \right] \qquad (5.1.7)$$

Both of the terms give half of the time delay and so this is exactly equivalent to equation (5.1.2). This is due to the unitarity of the scattering matrix and we can see that the two terms are the same, for example, if we differentiate the constant $C(0) = \text{Tr} \left[S(E) S^\dagger(E) \right] = M$ with respect to the energy to obtain

$$0 = \text{Tr} \left[S^\dagger(E) \frac{dS(E)}{dE} \right] + \text{Tr} \left[\frac{dS^\dagger(E)}{dE} S(E) \right] \qquad (5.1.8)$$

and use the fact that the trace is invariant under a cyclical change of a matrix product. If we now use the semiclassical approximation for the correlation function and differentiate at $\epsilon = 0$ we get the semiclassical approximation for the symmetrized time delay

$$\tau_W \approx \frac{1}{M T_H} \sum_{a,b} \sum_{\zeta,\zeta'(a \to b)} \left(\frac{T_\zeta + T_{\zeta'}}{2} \right) A_\zeta A_{\zeta'}^* e^{\frac{i}{\hbar}(S_\zeta - S_{\zeta'})} e^{-\frac{i\pi}{2}(\nu_\zeta - \nu_{\zeta'})} \qquad (5.1.9)$$

where the only difference from equation (5.1.3) is that we now take the average trajectory time. For the trajectory pairs we will consider in section 5.3.1 to obtain the average time delay, both trajectories spend approximately the same time inside the system and both approximations for the time delay are the same. The equivalence is more general as we have seen, and we shall see how this plays out for the two-point correlation function of the time delay in section 5.3.2, where the trajectories considered no longer need to have the same length. The advantage of using the symmetrized form of the time delay is that it allows us to simplify the calculation by separating the contribution into a product of contributions form the encounters and the links, in a similar way to the conductance of a chaotic ballistic device (Heusler et al., 2006).
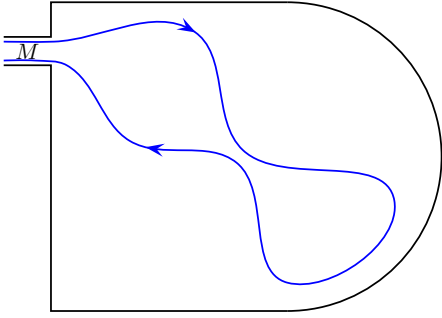
Figure 5.1: An example of a scattering trajectory which enters and leaves the system.
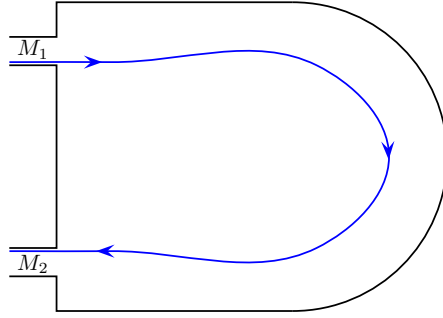
Figure 5.2: An example of a scattering trajectory which enters through lead 1 and leaves through lead 2.

5.1.2 Landauer conductance

For the conductance we imagine attaching two leads, with M_1 and M_2 channels respectively, to the same system we use for the time delay. The scattering matrix is then split into four blocks, each of which consists semiclassically of trajectories between some pair of the two leads

$$S = \begin{pmatrix} r_1 & t^\dagger \\ t & r_2 \end{pmatrix} \qquad (5.1.10)$$

Here r_i represents the reflection amplitude from lead i to itself and t the transmission amplitude from one lead to the other. Each element of the matrix is still approximated by the classical trajectories that pass from one channel to another and an example of a trajectory that contributes to the transmission is shown in Figure 5.2.

The conductance from lead 1 to lead 2 is proportional to the transmission, so if we measure it in units of the quantum conductance $\left(\frac{e^2}{\pi\hbar}\right)$, it is given by

$$G(E) = \text{Tr}[t(E)t^\dagger(E)] = \sum_{a,b} t_{ba} t_{ba}^* \qquad (5.1.11)$$

which is a sum over channels a in lead 1 and channels b in lead 2. As each matrix element t_{ba} can be written semiclassically as a sum over trajectories that start in

110

channel a of lead 1 and end in channel b of lead 2, the conductance can then be written as a double sum over trajectories

$$G(E) \approx \frac{1}{T_{\mathrm{H}}} \sum_{a,b} \sum_{\zeta,\zeta'(a \to b)} A_\zeta A_{\zeta'}^* \mathrm{e}^{\frac{\mathrm{i}}{\hbar}(S_\zeta - S_{\zeta'})} \mathrm{e}^{-\frac{\mathrm{i}\pi}{2}(\nu_\zeta - \nu_{\zeta'})} \qquad (5.1.12)$$

where both ζ and ζ' go from channel a to channel b and then we sum over all possible channel combinations. We can now see how this is very similar to the correlation function of the scattering matrix elements $C(\epsilon)$. The conductance, however, is restricted only to trajectories that enter through one lead and leave through another and so has a different sum over channels. The correlation function $C(\epsilon)$ also has an extra exponential factor due to the energy difference, but still the similarity to the conductance allows us to take advantage of the work that has been done on the latter.

5.2   Parametric quantum transport

To introduce the calculations we will later perform for the time delay and its correlation function we will examine the corresponding calculations done for quantum transport by Müller et al. (2007). As well as giving a brief overview of the method we shall also add parametric correlations using the methods we have developed in the previous two Chapters. We will first consider a parametric correlation of transmission amplitudes and then the observable parametric conductance variance. To do this we simply include a factor which represents the parametric correlations, as was the case for periodic orbits.

5.2.1   Parametric correlation of transmission amplitudes

Müller et al. (2007) evaluate semiclassically many quantities like the average conductance and higher order correlation functions. They also include the effect of a symmetry breaking parameter. However we will consider a non-symmetry breaking parameter and will first introduce an artificial quantity, the average of a parametric

correlation function of the transmission amplitudes, which we shall define as

$$\left\langle \tilde{G}(E,x) \right\rangle = \left\langle \mathrm{Tr} \left[t \left(E, X + \frac{x}{2} \right) t^\dagger \left(E, X - \frac{x}{2} \right) \right] \right\rangle_E \qquad (5.2.1)$$

to mimic the form of the conductance. The parametric dependence of this quantity would not be directly observable, but the calculation will be useful later when we examine the parametric conductance variance. Semiclassically we have the following double sum over trajectories

$$\left\langle \tilde{G}(E,x) \right\rangle = \left\langle \frac{1}{T_\mathrm{H}} \sum_{a,b} \sum_{\zeta,\zeta'(a \to b)} A_\zeta A_{\zeta'}^* \mathrm{e}^{\frac{\mathrm{i}}{\hbar}(S_\zeta - S_{\zeta'})} \mathrm{e}^{\frac{\mathrm{i}x}{2\sigma\hbar}(Q_\zeta + Q_{\zeta'})} \mathrm{e}^{-\frac{\mathrm{i}\pi}{2}(\nu_\zeta - \nu_{\zeta'})} \right\rangle \qquad (5.2.2)$$

In the following, we evaluate this along the lines of Heusler et al. (2006). We note that for the trajectory pairs we will consider in this Section, the topological indices cancel ($\nu_\zeta = \nu_{\zeta'}$) so we can drop the corresponding exponential factor for convenience. Firstly the diagonal approximation $\zeta = \zeta'$ gives

$$\left\langle \tilde{G}^\mathrm{diag}(E,x) \right\rangle = \left\langle \frac{1}{T_\mathrm{H}} \sum_{a,b} \sum_{\zeta(a \to b)} |A_\zeta|^2 \mathrm{e}^{\frac{\mathrm{i}x}{\sigma\hbar}Q_\zeta} \right\rangle \qquad (5.2.3)$$

For trajectories of a fixed period T_ζ the parametric factor is approximated by using the Gaussian noise assumption as in equation (3.1.14)

$$\left\langle \mathrm{e}^{\frac{\mathrm{i}x}{\sigma\hbar}Q_\zeta} \right\rangle \approx \mathrm{e}^{-\beta T_\zeta} \qquad (5.2.4)$$

The sum over all trajectories connecting channel a to b can be performed by using the analogue of the Hannay–Ozorio de Almeida sum rule for open systems (Richter and Sieber, 2002) by turning the sum into an integral over the trajectory time

$$\sum_{\zeta(a \to b)} |A_\zeta|^2 \ldots = \int_0^\infty \mathrm{d}T_\zeta \, \mathrm{e}^{-\mu T_\zeta} \ldots \qquad (5.2.5)$$
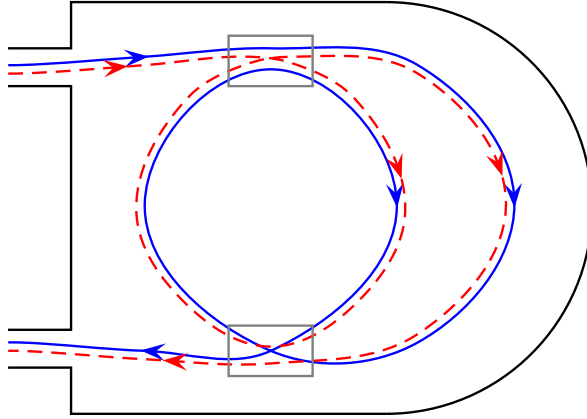
Figure 5.3: An example of a trajectory with two self-encounters and its partner.

where μ is the classical escape rate of the system, or the inverse of the average time delay $(= \frac{M}{T_H})$. The exponential term represents the average probability that a trajectory remains in the system for the time T_ζ. The diagonal approximation then takes the form of the following integral over all trajectory times T

$$\left\langle \tilde{G}^{\mathrm{diag}}(E,x) \right\rangle = \sum_{a,b} \int_0^\infty \mathrm{d}T \, \frac{1}{T_H} \mathrm{e}^{-\mu T} \mathrm{e}^{-\beta T} = \frac{M_1 M_2}{M+B} \tag{5.2.6}$$

where $B = \beta T_H$ and the sum over channels a and b simply gives a factor of $M_1 M_2$ because of the respective number of choices of each channel.

The off-diagonal terms are found by considering trajectory pairs that are correlated and differ only in encounter regions, in a similar way to the calculation for periodic orbit pairs. An example of a trajectory with two self encounters and its partner is shown in Figure 5.3. For open systems we remember that we need to use the exposure time rather than the trajectory time, to reflect the slightly reduced probability of escape due to the encounter regions. For a trajectory pair with encounters described by the vector $\boldsymbol{v}$, the contribution can be written, using the open sum rule, as

$$\left\langle \tilde{G}_{\boldsymbol{v}}(E,x) \right\rangle = \frac{M_1 M_2 N(\boldsymbol{v})}{T_H} \int \mathrm{d}T \int \mathrm{d}\tilde{\boldsymbol{s}} \, \mathrm{d}\tilde{\boldsymbol{u}} \, w_T(\tilde{\boldsymbol{s}}, \tilde{\boldsymbol{u}}) \mathrm{e}^{\frac{\mathrm{i}}{\hbar} \tilde{\boldsymbol{s}} \tilde{\boldsymbol{u}}} \mathrm{e}^{-\mu T_{\mathrm{exp}}} \mathrm{e}^{\frac{\mathrm{i}x}{\sigma \hbar} Q_\zeta} \tag{5.2.7}$$

113

where $N(\boldsymbol{v})$ is the number of trajectory structures corresponding to each vector $\boldsymbol{v}$. The main difference from periodic orbits is that there is an extra link (giving $L+1$ in total) because both ends of the trajectory are free. The weight function changes because of this freedom, and we also no longer overcount by a factor of L because the start and end are fixed in the leads. The restriction on the links is that they all have positive duration, and in terms of an integral the weight is given by

$$w_T(\tilde{\boldsymbol{s}}, \tilde{\boldsymbol{u}}) = \frac{\int_0^{T-t_{\text{enc}}} \mathrm{d}t_L \cdots \int_0^{T-t_{\text{enc}}-t_L \cdots -t_2} \mathrm{d}t_1}{\Omega^{L-V} \prod_\alpha t_{\text{enc}}^\alpha} \tag{5.2.8}$$

we see that now it is simply written as an L-fold integral over different link times $t_i, i = 1 \ldots L$, while the last link time is fixed by the total trajectory time

$$T = \sum_{i=1}^{L+1} t_i \tag{5.2.9}$$

When we perform the sum over trajectories of different lengths we integrate over the trajectory time T, which can be re-expressed as an integral over the last link time. With the weight factor, the contribution now includes integrals over all the links times t_i. Heusler et al. (2006) then rewrite the contribution of a correlated trajectory pair as integrals over the link times and the encounter regions. To do this, we need to decompose the term from the survival probability (cf equation (4.1.13)) as follows

$$\mathrm{e}^{-\mu T_{\text{exp}}} = \mathrm{e}^{-\sum\limits_{i=1}^{L+1} \mu t_i} \mathrm{e}^{-\sum\limits_{\alpha=1}^{V} \mu t_{\text{enc}}^\alpha} \tag{5.2.10}$$

and the parametric correlations (cf equation (3.1.22))

$$\left\langle \mathrm{e}^{\frac{\mathrm{i}x}{\sigma\hbar} Q_\zeta} \right\rangle = \mathrm{e}^{-\sum\limits_{i=1}^{L+1} \beta t_i} \mathrm{e}^{-\sum\limits_{\alpha=1}^{V} \beta l_\alpha^2 t_{\text{enc}}^\alpha} \tag{5.2.11}$$

into terms from the links and encounters. This then gives the following contribution to the average parametric correlation function of the transmission amplitudes

$$\left\langle \tilde{G}_{\boldsymbol{v}}(E,x) \right\rangle = \frac{M_1 M_2 N(\boldsymbol{v})}{T_{\mathrm{H}}} \left(\prod_{i=1}^{L+1} \int \mathrm{d}t_i \, \mathrm{e}^{-\frac{M+B}{T_{\mathrm{H}}}t_i} \right)$$

$$\times \left(\prod_{\alpha=1}^{V} \int \mathrm{d}^{l_\alpha-1}\boldsymbol{s}_{\alpha j} \, \mathrm{d}^{l_\alpha-1}\boldsymbol{u}_{\alpha j} \frac{\mathrm{e}^{-\frac{M+l_\alpha^2 B}{T_{\mathrm{H}}}t_{\mathrm{enc}}^\alpha} \mathrm{e}^{\frac{\mathrm{i}}{\hbar}\sum_j \boldsymbol{s}_{\alpha j}\boldsymbol{u}_{\alpha j}}}{\Omega^{l_\alpha-1}t_{\mathrm{enc}}^\alpha} \right) \quad (5.2.12)$$

We can now see the real advantage of using the correlation function as we can separate the above integral into a product over the links and the encounters. The integral over the links is easily performed and gives a factor of $\frac{T_{\mathrm{H}}}{M+B}$ for each link. Each encounter integral can be expanded to first order in the encounter time and gives a factor of $\frac{M+l_\alpha^2 B}{T_{\mathrm{H}}^{l_\alpha-1}}$. In total all the Heisenberg times cancel and we can view the result as having a factor of $(M+B)^{-1}$ for each link and $(M+l_\alpha^2 B)$ for each encounter. These diagrammatic type rules show the power of separating the contribution into links and encounters (which can also be seen in Appendix B) as they allow us to effectively read off the contribution of trajectories corresponding to any vector $\boldsymbol{v}$.

The number of trajectory structures corresponding to each vector $\boldsymbol{v}$ is the same as for periodic orbits, because of a one-to-one relation between them. In fact, by joining the ends of each trajectory structure (connecting the parts of the trajectory and its partner that leave through the exit lead to the start of the trajectories in the entrance lead) we obtain a periodic orbit structure. Equivalently, we can start with any periodic orbit structure and cut one of its links. By moving the cut ends of the link to the leads we create a trajectory structure (the link must be traversed in the same direction in both orbits, so with time reversal symmetry we must choose either the partner orbit or its time reversal to ensure that this is the case). This effectively creates L trajectory structures, which is why we no longer overcount by L in the weight function. When we sum over the possible trajectories in both symmetry classes we obtain the following result for the situation without time reversal symmetry

$$\left\langle \tilde{G}(E,x) \right\rangle = \frac{M_1 M_2}{M+B} \left[1 + \frac{B(7B-2M)}{(M+B)^4} \right.$$
$$\left. + \frac{B(628B^3 - 888B^2M + 183BM^2 - 2M^3)}{(M+B)^8} + \ldots \right] \quad (5.2.13)$$

115

and for the situation with time reversal symmetry

$$
\begin{aligned}
\left\langle \tilde{G}(E,x) \right\rangle &= \frac{M_1 M_2}{M+B} \left[1 - \frac{(4B+M)}{(M+B)^2} + \frac{(44B^2+M^2)}{(M+B)^4} \right. \\
&\qquad \left. - \frac{(784B^3 - 312B^2 M + 12BM^2 + M^3)}{(M+B)^6} + \ldots \right]
\end{aligned}
\tag{5.2.14}
$$

If we set $B = 0$, we recover the first few terms of the non-parametric result (Heusler et al., 2006).

5.2.2 The parametric conductance variance

In order to understand our calculation later of the correlation function of the Wigner time delay, it is instructive to go through the calculation of the conductance variance as derived in Müller et al. (2007). This calculation is very similar to the calculation of the shot noise power (Braun et al., 2006) but is actually closer to the calculation we will perform. We will also include a parametric term, and we state the expression for the conductance when it depends on a non-symmetry breaking external parameter X

$$
G(E,X) = \text{Tr}[t(E,X)t^{\dagger}(E,X)]
\tag{5.2.15}
$$

We can then define the parametric conductance variance as

$$
\left\langle G\left(E, X + \frac{x}{2}\right) G\left(E, X - \frac{x}{2}\right) \right\rangle - \langle G(E,X) \rangle^2
\tag{5.2.16}
$$

which can be written, semiclassically, as a quadruple sum over trajectories with one pair going from channel a to b and the other from c to d

$$
\left\langle \frac{1}{T_{\text{H}}^2} \sum_{\substack{a,b \\ c,d}} \sum_{\substack{\zeta,\zeta'(a \to b) \\ \xi,\xi'(c \to d)}} A_\zeta A_{\zeta'}^* A_\xi A_{\xi'}^* e^{\frac{i}{\hbar}(S_\zeta - S_{\zeta'} + S_\xi - S_{\xi'})} e^{\frac{ix}{2\sigma\hbar}(Q_\zeta - Q_{\zeta'} - Q_\xi + Q_{\xi'})} \right\rangle
$$
$$
- \left\langle \frac{1}{T_{\text{H}}} \sum_{a,b} \sum_{\zeta,\zeta'(a \to b)} A_\zeta A_{\zeta'}^* e^{\frac{i}{\hbar}(S_\zeta - S_{\zeta'})} \right\rangle^2
\tag{5.2.17}
$$

116

The average conductance $\langle G(E,X) \rangle$ comes from the same correlated pairs of trajectories we considered in the previous section. If we consider terms in the first sum above where ζ and ζ' form a correlated pair with self-encounters (which we will denote by $\zeta \approx \zeta'$), and ξ and ξ' form a separate correlated pair, the factor from the parametric correlations is one and we recreate the second term. We can thus remove the second term in the above equation by removing such pairs from the semiclassical treatment of the first term. In terms of trajectories we then obtain

$$\left\langle \frac{1}{T_{\mathrm{H}}^2} \sum_{\substack{a,b \\ c,d}} \sideset{}{'}\sum_{\substack{\zeta,\zeta'(a\to b) \\ \xi,\xi'(c\to d)}} A_\zeta A_{\zeta'}^* A_\xi A_{\xi'}^* \mathrm{e}^{\frac{\mathrm{i}}{\hbar}(S_\zeta - S_{\zeta'} + S_\xi - S_{\xi'})} \mathrm{e}^{\frac{\mathrm{i}x}{2\sigma\hbar}(Q_\zeta - Q_{\zeta'} - Q_\xi + Q_{\xi'})} \right\rangle \quad (5.2.18)$$

where the trajectories ζ, ζ' go from channel a in the entrance lead (with M_1 channels) to channel b in the exit lead (with M_2 channels). Likewise trajectories ξ, ξ' go from channel c to channel d. Because we have removed terms from correlated trajectories where $\zeta \approx \zeta'$ and $\xi \approx \xi'$ (this restriction is denoted by the prime on the sum) we are left with pairs of correlated trajectories where $\zeta \approx \xi'$ and $\zeta' \approx \xi$, and the case where all four trajectories interact through encounters.

For the pairs of correlated trajectories, $\zeta \approx \xi'$ and $\zeta' \approx \xi$, we can calculate the diagonal term relatively easily. This requires that $a = c$ and $b = d$ so we have a factor of $M_1 M_2$ from the sum over channels. The parametric term separates into the following factors

$$\left\langle \mathrm{e}^{\frac{\mathrm{i}x}{\sigma\hbar}(Q_\zeta - Q_\xi)} \right\rangle = \mathrm{e}^{-\beta T_\zeta} \mathrm{e}^{-\beta T_\xi} \quad (5.2.19)$$

So that when we integrate over the trajectory lengths we get

$$\frac{M_1 M_2}{T_{\mathrm{H}}^2} \int_0^\infty \int_0^\infty \mathrm{d}T_\zeta \mathrm{d}T_\xi \, \mathrm{e}^{-(\mu+\beta)T_\zeta} \mathrm{e}^{-(\mu+\beta)T_\xi} = \frac{M_1 M_2}{(M+B)^2} \quad (5.2.20)$$

Further to the diagonal approximation, each of the two pairs of independently correlated trajectories can have self-encounters leading to higher order terms, and because they are independent we can separate the sum in equation (5.2.18)

117

$$
\left\langle \sum_{a,b} \frac{1}{T_{\mathrm{H}}} \sum_{\zeta \approx \xi'(a \to b)} A_\zeta A_{\xi'}^* \mathrm{e}^{\frac{\mathrm{i}}{\hbar}(S_\zeta - S_{\xi'})} \mathrm{e}^{\frac{\mathrm{i}x}{2\sigma\hbar}(Q_\zeta + Q_{\xi'})} \right.
$$

$$
\left. \times \frac{1}{T_{\mathrm{H}}} \sum_{\zeta' \approx \xi(a \to b)} A_\xi A_{\zeta'}^* \mathrm{e}^{\frac{\mathrm{i}}{\hbar}(S_\xi - S_{\zeta'})} \mathrm{e}^{-\frac{\mathrm{i}x}{2\sigma\hbar}(Q_\xi + Q_{\zeta'})} \right\rangle \tag{5.2.21}
$$

With a change of variable names and performing the sum over channels, we are essentially considering the following

$$
M_1 M_2 \left[\sum_{\boldsymbol{v}} \frac{N(\boldsymbol{v})}{T_{\mathrm{H}}} \sum_\zeta \mathrm{e}^{-\mu T_\zeta} \mathrm{e}^{\frac{\mathrm{i}x}{\sigma\hbar}Q_\zeta} \mathrm{e}^{\frac{\mathrm{i}}{\hbar}\Delta S_\zeta} \right]^2 = \frac{\langle \tilde{G}(E,x) \rangle^2}{M_1 M_2} \tag{5.2.22}
$$

where the term in square brackets is a sum over correlated pairs $\zeta \approx \xi'$, including the diagonal pair. The result is simply related to the mean correlation function of the transmission amplitudes and is

$$
\frac{M_1 M_2}{(M+B)^2} \left[1 + \frac{2B(7B - 2M)}{(M+B)^4} + \dots \right] \tag{5.2.23}
$$

for the unitary case, and

$$
\frac{M_1 M_2}{(M+B)^2} \left[1 - \frac{(8B + 2M)}{(M+B)^2} + \frac{(104B^2 + 8BM + 3M^2)}{(M+B)^4} + \dots \right] \tag{5.2.24}
$$

for the orthogonal case.

When we examine terms where all four trajectories interact then things are no longer so simple. We will consider in detail the first such term where four trajectories meet at a single two encounter. An example of such a situation is shown in Figure 5.4 and we can see that ζ' and ξ' cross over in the encounter so that they leave through the same channels as the trajectories ξ and ζ respectively. This means that $b = d$, giving a channel factor of $M_1^2 M_2$. Because ζ' and ξ' cross over between the start and the end of the interaction (the encounter in this case) such a quadruplet of trajectories is known as an 'x-quadruplet'.

We number the trajectory links in order along ζ then along ξ, as in Figure 5.4, so that the trajectory times are
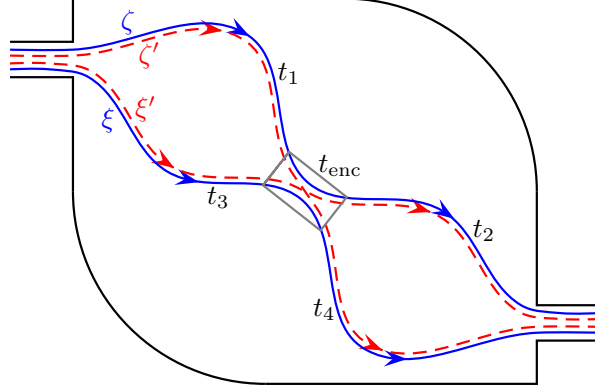
Figure 5.4: An example of two trajectories with a single encounter and two partner trajectories.

$$
\begin{aligned}
T_\zeta &= t_1 + t_{\mathrm{enc}} + t_2 \\
T_{\zeta'} &= t_1 + t_{\mathrm{enc}} + t_4 \\
T_\xi &= t_3 + t_{\mathrm{enc}} + t_4 \\
T_{\xi'} &= t_3 + t_{\mathrm{enc}} + t_2
\end{aligned}
\tag{5.2.25}
$$

An important factor we need to consider is the parametric correlation term

$$
\left\langle e^{\frac{\mathrm{i}x}{2\sigma\hbar}(Q_\zeta - Q_{\zeta'} - Q_\xi + Q_{\xi'})} \right\rangle
\tag{5.2.26}
$$

where we get a contribution when we have trajectories at different values of the parameter X travelling along the same stretches. Before the encounter, ζ and ζ' coincide, and as they are at the same value of the external parameter there will be no parametric contribution from this section (link 1) of the trajectory. However, for link 2, after the encounter, ζ and ξ' coincide and so we get a contribution of $e^{-\beta t_2}$. The same happens for links 3 and 4 giving a factor $e^{-\beta t_4}$, while for the encounter all four encounter stretches are close and provide no contribution. Altogether we get the following for the contribution to the conductance

$$
\frac{M_1^2 M_2}{T_{\mathrm{H}}^2} \int_0^\infty \mathrm{d}t_1 \mathrm{d}t_2 \mathrm{d}t_3 \mathrm{d}t_4 \, e^{-\mu(t_1+t_2+t_3+t_4)} e^{-\beta(t_2+t_4)} \int \mathrm{d}\boldsymbol{s} \, \mathrm{d}\boldsymbol{u} \, \frac{e^{-\mu t_{\mathrm{enc}}}}{\Omega t_{\mathrm{enc}}} e^{\frac{\mathrm{i}}{\hbar}\boldsymbol{s}\boldsymbol{u}}
\tag{5.2.27}
$$

119

which can be evaluated as

$$-\frac{M_1^2 M_2}{M(M+B)^2} \tag{5.2.28}$$

We could also exchange ζ' and ξ', which would require that $a = c$ giving the channel factor $M_1 M_2^2$. For this case we get a parametric correlation from the start of each trajectory, with times t_1 and t_3, which gives a similar result, but with a different channel factor. In total we obtain a contribution of

$$-\frac{M_1^2 M_2 + M_1 M_2^2}{M(M+B)^2} = -\frac{M_1 M_2}{(M+B)^2} \tag{5.2.29}$$

This cancels with the diagonal term calculated previously, and we find that the first term for the parametric conductance variance comes from trajectory quadruplets with more complicated interactions. These quadruplets of trajectories are known as 'd-quadruplets' as ζ and ζ' start and end together like diagonal pairs (as do ξ and ξ') but all four interact inside the cavity. Trajectories ζ and ζ' both start in channel a before the interaction and end in channel b afterwards. Similarly, ξ and ξ' both travel from c to d around the interaction. This gives a channel factor of $M_1^2 M_2^2$ and if $a = c$ and $b = d$ we can also swap ζ' and ξ' obtaining an additional contribution of $M_1 M_2$. The trajectory quadruplets that contribute to the leading order term are drawn in Figure 4 of Müller et al. (2007), where the contribution from 4j was the x-quadruplet example we calculated above which cancels with the diagonal term. In Figure 5.5, we draw a schematic representation of the d-quadruplets that contribute at leading order (these are quadruplets 4c-h in Müller et al., 2007).

By considering which stretches are traversed by trajectories at different parameter values in each of the quadruplets drawn in Figure 5.5, we can calculate the result for each trajectory as given in Table 5.1. For the quadruplets depicted in Figures 5.5b-c and 5.5e-f, there is a second structure that can be formed by reflecting the interaction, and a corresponding factor of 2 has been included in Table 5.1 (reflecting quadruplets 5.5a and 5.5d effectively recreates the same structure).

For systems without time reversal symmetry, where only trajectory quadruplets
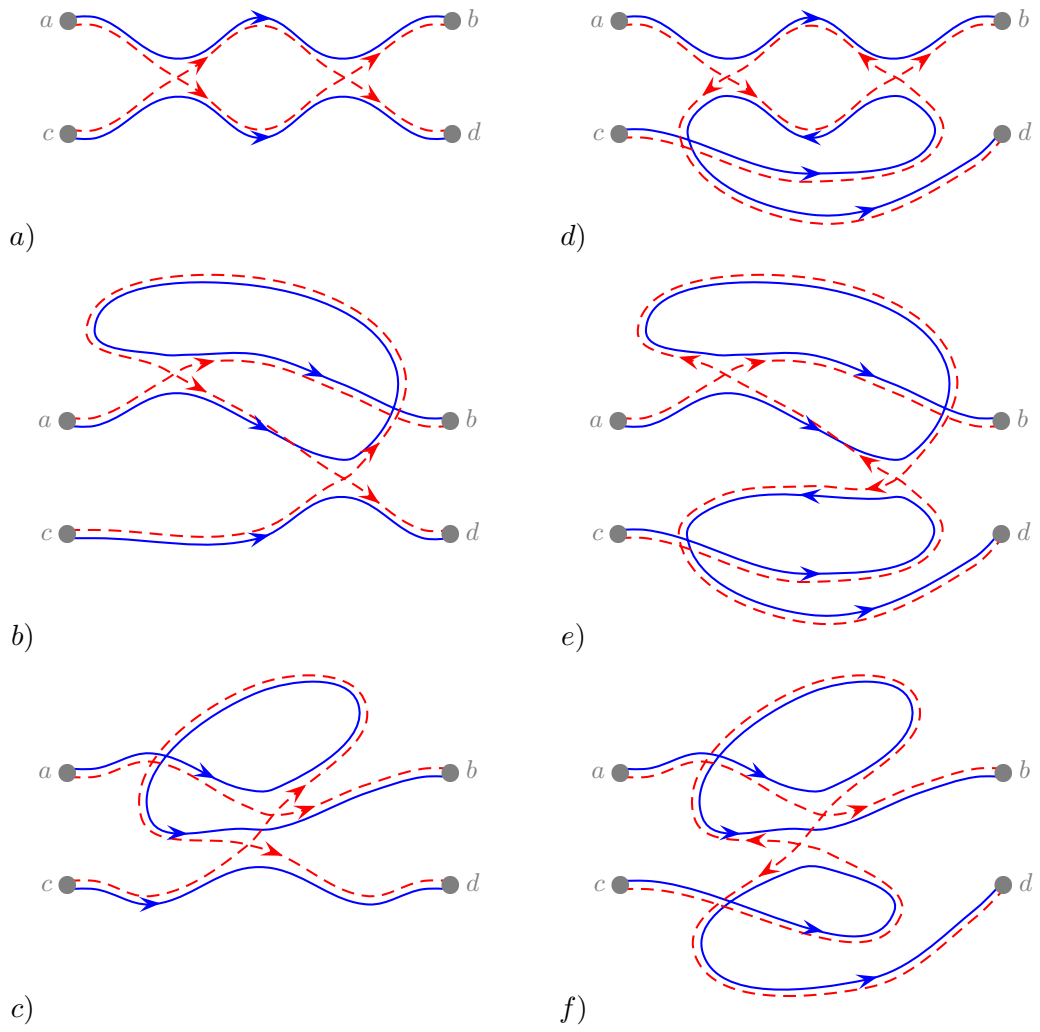
Figure 5.5: A schematic diagram of the trajectory d-quadruplets that contribute at leading order to the parametric conductance variance. For systems without time reversal symmetry only quadruplets a-c exist.

5.5a	5.5b	5.5c
$\frac{1}{M^2(M+B)^2}$	$\frac{2}{M^4}$	$\frac{-2}{M^4}$
5.5d	5.5e	5.5f
$\frac{1}{M^2(M+B)^2}$	$\frac{2}{M^4}$	$\frac{-2}{M^4}$

Table 5.1: Contribution of different types of trajectory quadruplets to the parametric conductance variance.

5.5a-c exist, when we sum their contribution and multiply by the channel factor we obtain the following result

$$\frac{M_1^2 M_2^2}{M^2(M+B)^2} + \frac{M_1 M_2}{M^2(M+B)^2} \tag{5.2.30}$$

while with time reversal symmetry trajectories 5.5d-f also exist giving twice this result. In total the leading order term of the parametric conductance variance is given by

$$\kappa \left(\frac{M_1 M_2}{M(M+B)} \right)^2 \tag{5.2.31}$$

Again if we set $B = 0$ we recover the first term of the non-parametric result (Müller et al., 2007).

5.3   The time delay

The time delay, as derived from the correlation function of scattering matrix elements (equation (5.1.7)) can now be evaluated semiclassically using similar methods. Firstly we recreate the average time delay, where for systems without time-reversal symmetry the diagonal approximation (pairing a trajectory with itself) suffices (cf Lewenkopf and Vallejos, 2004a). For systems with time-reversal symmetry, however, a small correction is needed which comes from correlated trajectories that have close self-encounters. Furthermore, examining the irreducible two-point correlation function of the time delay, the diagonal approximation does not provide the leading order RMT result (Lewenkopf and Vallejos, 2004a), but by considering all correlated trajectory quadruplets that contribute to leading order we can regain agreement with the periodic orbit picture. Considering the semiclassical approximation to the scat-

tering matrix itself, we can also show that unitarity is satisfied if all contributions are included.

5.3.1 The average time delay

To derive the average time delay from correlated trajectory pairs, we shall exploit the use of diagrammatic rules by considering the symmetrized version of the time delay. We concentrate on the correlation function of matrix elements

$$C(\epsilon) \approx \frac{1}{T_{\mathrm{H}}} \sum_{a,b} \sum_{\zeta,\zeta'(a \to b)} A_\zeta A_{\zeta'}^* \mathrm{e}^{\frac{\mathrm{i}}{\hbar}(S_\zeta - S_{\zeta'})} \mathrm{e}^{-\frac{\mathrm{i}\pi}{2}(\nu_\zeta - \nu_{\zeta'})} \mathrm{e}^{\frac{\mathrm{i}\epsilon}{2\hbar}(T_\zeta + T_{\zeta'})} \tag{5.3.1}$$

which, aside from the exponential factor containing the average trajectory time and a different channel sum, is the same as the conductance (from Heusler et al., 2006, for example). Again, the topological indices cancel and we ignore them in the following. The diagonal term, where the two trajectories ζ and ζ' are the same gives a contribution of

$$C^{\mathrm{diag}}(\epsilon) \approx \frac{1}{T_{\mathrm{H}}} \sum_{a,b} \sum_{\zeta(a \to b)} |A_\zeta|^2 \mathrm{e}^{\frac{\mathrm{i}\epsilon}{\hbar}T_\zeta} \tag{5.3.2}$$

The sum over all trajectories connecting channel a to b is performed using the open sum rule in equation (5.2.5), but the sum over channels depends on the symmetry of the dynamics. For systems without time-reversal symmetry ($\kappa = 1$) we can pick both a and b from the M possible channels giving a factor of M^2. For systems with time-reversal symmetry ($\kappa = 2$), however, if the start and end channel are the same ($a = b$) we can also compare the trajectory ζ with its time reversal, giving an additional M possibilities. The diagonal term thus becomes

$$C^{\mathrm{diag}}(\epsilon) \approx \frac{M(M + \kappa - 1)}{T_{\mathrm{H}}} \int_0^\infty \mathrm{d}T_\zeta \, \mathrm{e}^{-(\mu - \frac{\mathrm{i}\epsilon}{\hbar})T_\zeta} = \frac{M(M + \kappa - 1)}{T_{\mathrm{H}} \left(\mu - \frac{\mathrm{i}\epsilon}{\hbar}\right)} \tag{5.3.3}$$

Off-diagonal contributions from the trajectory structures with encounters described by the vector $\boldsymbol{v}$ can be written as

$$C_{\boldsymbol{v}}(\epsilon) \approx \frac{N(\boldsymbol{v})}{T_{\mathrm{H}}} \sum_{a,b} \sum_{\zeta(a \to b)} |A_\zeta|^2 \int \mathrm{d}\tilde{\boldsymbol{s}} \, \mathrm{d}\tilde{\boldsymbol{u}} \, w_T(\tilde{\boldsymbol{s}}, \tilde{\boldsymbol{u}}) \mathrm{e}^{\frac{\mathrm{i}}{\hbar} \tilde{\boldsymbol{s}} \tilde{\boldsymbol{u}}} \mathrm{e}^{\frac{\mathrm{i}\epsilon}{\hbar} T_\zeta} \tag{5.3.4}$$

Since the weight function involves an integral over L links (see equation (5.2.8)) and the sum over all trajectories can be written as an integral over the last link length using the open sum rule, the correlation function can be separated into contributions from the links and encounters in a similar way as for the conductance

$$
\begin{aligned}
C_{\boldsymbol{v}}(\epsilon) &\approx \frac{N(\boldsymbol{v})}{T_{\mathrm{H}}} \sum_{a,b} \left(\prod_{i=1}^{L+1} \int_0^\infty \mathrm{d}t_i \, \mathrm{e}^{-(\mu - \frac{\mathrm{i}\epsilon}{\hbar})t_i} \right) \\
&\quad \times \left(\prod_{\alpha=1}^{V} \int \mathrm{d}^{l_\alpha - 1} \boldsymbol{s}_{\alpha j} \, \mathrm{d}^{l_\alpha - 1} \boldsymbol{u}_{\alpha j} \frac{\mathrm{e}^{-\left(\mu - \frac{\mathrm{i}\epsilon l_\alpha}{\hbar}\right) t_{\mathrm{enc}}^\alpha} \mathrm{e}^{\frac{\mathrm{i}}{\hbar} \sum_j \boldsymbol{s}_{\alpha j} \boldsymbol{u}_{\alpha j}}}{\Omega^{l_\alpha - 1} t_{\mathrm{enc}}^\alpha} \right)
\end{aligned}
\tag{5.3.5}
$$

We can sum over a and b by including the channel factor and sum over all possible vectors to give the total off-diagonal contribution

$$
\begin{aligned}
C^{\mathrm{off}}(\epsilon) &\approx \frac{M(M+\kappa-1)}{T_{\mathrm{H}}} \sum_{\boldsymbol{v}} N(\boldsymbol{v}) \left(\prod_{i=1}^{L+1} \int_0^\infty \mathrm{d}t_i \, \mathrm{e}^{-(\mu - \frac{\mathrm{i}\epsilon}{\hbar})t_i} \right) \\
&\quad \times \left(\prod_{\alpha=1}^{V} \int \mathrm{d}^{l_\alpha - 1} \boldsymbol{s}_{\alpha j} \, \mathrm{d}^{l_\alpha - 1} \boldsymbol{u}_{\alpha j} \frac{\mathrm{e}^{-\left(\mu - \frac{\mathrm{i}\epsilon l_\alpha}{\hbar}\right) t_{\mathrm{enc}}^\alpha} \mathrm{e}^{\frac{\mathrm{i}}{\hbar} \sum_j \boldsymbol{s}_{\alpha j} \boldsymbol{u}_{\alpha j}}}{\Omega^{l_\alpha - 1} t_{\mathrm{enc}}^\alpha} \right)
\end{aligned}
\tag{5.3.6}
$$

When we perform all the integrals we obtain the following

$$C^{\mathrm{off}}(\epsilon) \approx M(M+\kappa-1) \sum_{\boldsymbol{v}} (-1)^V N(\boldsymbol{v}) \frac{\prod_{\alpha=1}^{V} \left(\mu - \frac{\mathrm{i}\epsilon l_\alpha}{\hbar} \right)}{T_{\mathrm{H}}^{L-V-1} \left(\mu - \frac{\mathrm{i}\epsilon}{\hbar} \right)^{L+1}} \tag{5.3.7}$$

If we set $n = L - V + 1$ we can rewrite this as a sum over n, where for each n we sum over all vectors $\boldsymbol{v}$ with $L - V + 1 = n$. We can also include the diagonal term by saying that it corresponds to a trajectory with no encounter ($L = V = 0$) for which $N(\boldsymbol{v}) = 1$. With the diagonal term, all these trajectories give the average contribution to the correlation function

$$C^{\mathrm{ave}}(\epsilon) \approx M(M+\kappa-1) \sum_{n=1}^{\infty} \sum_{\boldsymbol{v}} (-1)^V N(\boldsymbol{v}) \frac{\prod_{\alpha=1}^{V} \left(\mu - \frac{\mathrm{i}\epsilon l_\alpha}{\hbar} \right)}{T_{\mathrm{H}}^n \left(\mu - \frac{\mathrm{i}\epsilon}{\hbar} \right)^{L+1}} \tag{5.3.8}$$

124

We can differentiate at $\epsilon = 0$ to find the contribution to the time delay of these types of trajectories

$$\tau_{\mathrm{W}}^{\mathrm{ave}} = (M + \kappa - 1) \sum_{n=1}^{\infty} \sum_{\boldsymbol{v}} (-1)^V N(\boldsymbol{v}) \frac{L + 1 - \sum_{\alpha} l_{\alpha}}{T_{\mathrm{H}}^n \mu^{n+1}} \qquad (5.3.9)$$

We can use the fact that $\sum_{\alpha} l_{\alpha} = L$ and $\mu T_{\mathrm{H}} = M$ to simplify the result to

$$\tau_{\mathrm{W}}^{\mathrm{ave}} = \bar{\tau}_{\mathrm{W}} (M + \kappa - 1) \sum_{n=1}^{\infty} \frac{1}{M^n} \sum_{\boldsymbol{v}} (-1)^V N(\boldsymbol{v}) \qquad (5.3.10)$$

Now we use the recursion relation (Heusler et al., 2006) to evaluate the sum over the vectors $\boldsymbol{v}$ for $n > 1$ as

$$\sum_{\boldsymbol{v}}^{L - V + 1 = n} (-1)^V N(\boldsymbol{v}) = (1 - \kappa)^{n-1} \qquad (5.3.11)$$

to obtain the final result

$$\tau_{\mathrm{W}}^{\mathrm{ave}} = \bar{\tau}_{\mathrm{W}} \frac{(M + \kappa - 1)}{(M + \kappa - 1)} = \bar{\tau}_{\mathrm{W}} \qquad (5.3.12)$$

This shows that these types of trajectory correlations do indeed recreate the average time delay semiclassically.

5.3.2 Correlation functions of the time delay

We now examine a correlation function of the time delay, and show that it is possible to obtain the same result using open trajectories that can be obtained from periodic orbits. We start with the calculation of the diagonal contribution from Lewenkopf and Vallejos (2004a) and consider the irreducible two point correlation function of the time delay

$$\tilde{R}_2(\omega, M) = \left\langle \frac{\tau_{\mathrm{W}}^{\mathrm{osc}}\left(E + \frac{\omega}{2\bar{d}}\right) \tau_{\mathrm{W}}^{\mathrm{osc}}\left(E - \frac{\omega}{2\bar{d}}\right)}{\bar{\tau}_{\mathrm{W}}^2} \right\rangle_E \qquad (5.3.13)$$

where $\tau_\mathrm{W}^\mathrm{osc}$ is the fluctuating part of the time delay ($\tau_\mathrm{W}^\mathrm{osc} = \tau_\mathrm{W} - \bar{\tau}_\mathrm{W}$). The leading order of the correlation function is given by Eckhardt (1993) and Vallejos et al. (1998), and can be derived from either the RMT or periodic orbit results in Chapter 4

$$\tilde{R}_2^\mathrm{lo}(\eta, M) = \frac{2\kappa}{T_\mathrm{H}^2} \frac{\mu^2 - \left(\frac{\eta}{\hbar}\right)^2}{\left[\mu^2 + \left(\frac{\eta}{\hbar}\right)^2\right]^2} \tag{5.3.14}$$

where we have used the substitution $\omega = \bar{d}\eta$.

Since the fluctuating part of the time delay $\tau_\mathrm{W}^\mathrm{osc}$ is the time delay with the average part removed, we can write the oscillating part of the time delay as a sum over trajectory pairs by simply removing, from the time delay in equation (5.1.3), the trajectories pairs which give the mean delay time (see section 5.3.1). Therefore, when we write the correlation function in terms of trajectories, it becomes

$$\tilde{R}_2(\eta, M) = \frac{1}{T_\mathrm{H}^4} \left\langle \sum_{\substack{a,b \\ c,d}} \sideset{}{'}\sum_{\substack{\zeta,\zeta'(a \to b) \\ \xi,\xi'(c \to d)}} T_\zeta T_\xi A_\zeta A_{\zeta'}^* A_\xi A_{\xi'}^* e^{\frac{\mathrm{i}}{\hbar}(S_\zeta - S_{\zeta'} + S_\xi - S_{\xi'})} e^{\frac{\mathrm{i}\eta}{2\hbar}(T_\zeta - T_{\zeta'} - T_\xi + T_{\xi'})} \right\rangle$$
$$\tag{5.3.15}$$

Here, ζ, ζ' are trajectories from channel a to b and ξ, ξ' are trajectories from channel c to d and we sum over trajectories and channels. We have removed the correlated trajectories where $\zeta \approx \zeta'$ and $\xi \approx \xi'$ because these pairs give the average time delay. For the diagonal approximation therefore we only have $\zeta = \xi'$ (and $\zeta' = \xi$). Without time reversal symmetry this means that channels $a = c$ and $b = d$ so we obtain a factor of M^2 from the sum over the channels. With time reversal symmetry we can also have $a = d$ and $b = c$, and if all channels are the same we can also pair both ζ and ζ' with ξ and ξ' and their time reverse giving a total channel factor of $2M(M + 1)$. To leading order the channel factor is κM^2. We can express the correlation function as an integral over the trajectory times after we perform the channel sum and use the open sum rule

$$\tilde{R}_2^\mathrm{diag}(\eta, M) \approx \frac{\kappa M^2}{T_\mathrm{H}^4} \int_0^\infty \int_0^\infty \mathrm{d}T_\zeta \mathrm{d}T_\xi \, T_\zeta T_\xi e^{-\mu(T_\zeta + T_\xi)} e^{\frac{\mathrm{i}\eta}{\hbar}(T_\zeta - T_\xi)} \tag{5.3.16}$$

which, after integrating, is

$$\tilde{R}_2^{\text{diag}}(\eta, M) \approx \frac{\kappa}{T_{\text{H}}^2} \frac{\mu^2}{\left[\mu^2 + \left(\frac{\eta}{\hbar}\right)^2\right]^2} \tag{5.3.17}$$

We have a factor of two different from the expected result (equation (5.3.14)), and a different functional form. However, as can be seen from the calculation of the parametric conductance variance in section 5.2.2, we expect quadruplets with encounters to contribute at the same order as the diagonal term.

To calculate the leading order we follow a similar procedure as for the parametric conductance variance, but have an additional time factor in the prefactor and a different channel factor. For example we can consider quadruplets like the one with a single 2-encounter depicted in Figure 5.4. The channel factor is simply $2M^3$ for the unitary case as we obtain M^3 from the trajectories where channel $a = c$ and a further M^3 from the case where $b = d$. Each of these cases gives the same contribution so we include them both in the total channel factor. The situation for the channel factor is more complicated for the orthogonal case for systems with time reversal symmetry. When all the possible combinations of pairing trajectories with possible time reversed trajectories are considered, the channel factor can be calculated as $4M^3 + 8M^2 + 4M$. To leading order, the channel factor is thus $2\kappa M^3$.

We again label the trajectory links in order along trajectory ζ then along trajectory ξ as in section 5.2.2 and Figure 5.4. Then we can write the trajectory times in terms of the link and encounter times (as equation (5.2.25)) as follows

$$
\begin{aligned}
T_\zeta &= t_1 + t_{\text{enc}} + t_2 \\
T_{\zeta'} &= t_1 + t_{\text{enc}} + t_4 \\
T_\xi &= t_3 + t_{\text{enc}} + t_4 \\
T_{\xi'} &= t_3 + t_{\text{enc}} + t_2
\end{aligned}
\tag{5.3.18}
$$

The important factor now is the difference in times

$$\frac{1}{2}(T_\zeta - T_{\zeta'} - T_\xi - T_{\xi'}) = t_2 - t_4 \tag{5.3.19}$$

so that the contribution to the correlation function is given by

$$\frac{2\kappa M^3}{T_H^4} \int_0^\infty dt_1 dt_2 dt_3 dt_4 \, e^{-\mu(t_1+t_2+t_3+t_4)} e^{\frac{i\eta}{\hbar}(t_2-t_4)}$$
$$\times \int ds\, du\, (t_1 + t_{enc} + t_2)(t_3 + t_{enc} + t_4) \frac{e^{-\mu t_{enc}}}{\Omega t_{enc}} e^{\frac{i}{\hbar} su} \tag{5.3.20}$$

This can be evaluated as

$$\frac{2\kappa}{T_H^2} \frac{\left(\frac{\eta}{\hbar}\right)^2}{\left[\mu^2 + \left(\frac{\eta}{\hbar}\right)^2\right]^2} \tag{5.3.21}$$

Following a similar procedure we find the contribution from the diagrams in Figure 5.5 and give the main results in Table 5.2 (including the factor 2 for quadruplets with a second structure related by reflection). For the unitary case the channel fac-

5.5a	5.5b	5.5c
$\dfrac{-\mu^2 - 2\left(\frac{\eta}{\hbar}\right)^2}{M^4 T_H^2 \left[\mu^2 + \left(\frac{\eta}{\hbar}\right)^2\right]^2}$	$\dfrac{8\left(\frac{\eta}{\hbar\mu}\right)^2 \left[\mu^2 + \left(\frac{\eta}{\hbar}\right)^2\right]}{M^4 T_H^2 \left[\mu^2 + \left(\frac{\eta}{\hbar}\right)^2\right]^2}$	$\dfrac{2\mu^2 - 2\left(\frac{\eta}{\hbar}\right)^2 - 8\left(\frac{\eta}{\hbar\mu}\right)^2 \left[\mu^2 + \left(\frac{\eta}{\hbar}\right)^2\right]}{M^4 T_H^2 \left[\mu^2 + \left(\frac{\eta}{\hbar}\right)^2\right]^2}$

Table 5.2: Contribution of different types of trajectory quadruplets to the two-point correlation function of the time delay.

tor is simply $M^4 + M^2$. When we now multiply these contributions by the leading order of this channel factor and add the terms calculated above, we arrive at the following result

$$\frac{2}{T_H^2} \frac{\mu^2 - \left(\frac{\eta}{\hbar}\right)^2}{\left[\mu^2 + \left(\frac{\eta}{\hbar}\right)^2\right]^2} \tag{5.3.22}$$

which is indeed the leading order term in equation (5.3.14). For the orthogonal case (systems with time reversal symmetry), the channel factor for the quadruplets 5.5a-c can be calculated as $M^2(M+1)^2 + 2M(M+1)$, which is also M^4 to leading order. However there are additional trajectory quadruplets that contribute (5.5d-f) which are related to the quadruplets 5.5a-c by time reversal of parts of the structure. These additional quadruplets give the same contributions as those in Figures 5.5a-c. Therefore, the leading order contribution is simply twice that for the unitary case,

again in line with equation (5.3.14).

It is worth noting here that to calculate higher order terms it is best to use the symmetrized version of the time delay (equation (5.1.9)). We will consider the calculation of the leading order result for the two-point correlation function of the time delay in this framework. We do this in order to show that we indeed obtain the same result, even though individual trajectory structures give different contributions with respect to the non-symmetrized case. To help perform the calculation, similarities, in particular to Ericson fluctuations (Müller et al., 2007), can be exploited by defining a 'symmetrized' correlation function in terms of the correlation function of the scattering matrix elements

$$\tilde{C}_2(\eta, M) = \left\langle C^{\text{osc}}\left(\epsilon_1, E + \frac{\eta}{2}\right) C^{\text{osc}}\left(\epsilon_2, E - \frac{\eta}{2}\right)\right\rangle_E \tag{5.3.23}$$

where $C^{\text{osc}}(\epsilon, E)$ is the fluctuating part of the correlation function of the scattering matrix elements at energy E. The semiclassical approximation therefore has the trajectory pairs responsible for the average part removed, so that we have the following semiclassical expression

$$\tilde{C}_2(\eta, M) \approx \frac{1}{T_{\text{H}}^2} \left\langle \sum_{\substack{a,b \\ c,d}} \sideset{}{'}\sum_{\substack{\zeta,\zeta'(a\to b) \\ \xi,\xi'(c\to d)}} A_\zeta A_{\zeta'}^* A_\xi A_{\xi'}^* e^{\frac{i}{\hbar}(S_\zeta - S_{\zeta'} + S_\xi - S_{\xi'})}\right.$$
$$\left. \times e^{\frac{i\eta}{2\hbar}(T_\zeta - T_{\zeta'} - T_\xi + T_{\xi'})} e^{\frac{i\epsilon_1}{2\hbar}(T_\zeta + T_{\zeta'})} e^{\frac{i\epsilon_2}{2\hbar}(T_\xi + T_{\xi'})}\right\rangle \tag{5.3.24}$$

The correlation function of the time delay can then be derived by differentiating the above expression

$$\tilde{R}_2(\eta, M) = \frac{-\hbar^2}{T_{\text{H}}^2} \frac{\mathrm{d}^2}{\mathrm{d}\epsilon_1 \mathrm{d}\epsilon_2} \left. \tilde{C}_2(\eta, M)\right|_{\epsilon_1 = \epsilon_2 = 0} \tag{5.3.25}$$

This gives the semiclassical approximation to the correlation function that comes directly from using the symmetrized time delay

$$\tilde{R}_2(\eta, M) = \frac{1}{T_{\mathrm{H}}^4} \left\langle \sum_{\substack{a,b \\ c,d}} \sum_{\substack{\zeta,\zeta'(a \to b) \\ \xi,\xi'(c \to d)}}' \left(\frac{T_\zeta + T_{\zeta'}}{2}\right) \left(\frac{T_\xi + T_{\xi'}}{2}\right) A_\zeta A_{\zeta'}^* A_\xi A_{\xi'}^* \right.$$

$$\left. \times\ \mathrm{e}^{\frac{\mathrm{i}}{\hbar}(S_\zeta - S_{\zeta'} + S_\xi - S_{\xi'})} \mathrm{e}^{\frac{\mathrm{i}\eta}{2\hbar}(T_\zeta - T_{\zeta'} - T_\xi + T_{\xi'})} \right\rangle_E \quad (5.3.26)$$

To go to higher orders the symmetrized correlation function is more useful, but, because of the extra factors, we need to track the trajectories for each structure. Each link is traversed by two of the four trajectories and if we record which ones, and how the trajectories cross the encounters, we can again separate the contribution into links and encounters. Generating the permissible structures and summing over their contribution can be done by a computer program. Nevertheless, it is still interesting to briefly explore the leading order term and check that this method does indeed give the same end result.

Starting from the symmetrized correlation function, the diagonal approximation $\zeta = \xi'$, with the leading order channel factor, becomes

$$\tilde{C}_2^{\mathrm{diag}}(\eta, M) \approx \frac{\kappa M^2}{T_{\mathrm{H}}^2} \int_0^\infty \int_0^\infty \mathrm{d}T_\zeta \mathrm{d}T_\xi\ \mathrm{e}^{-\mu(T_\zeta + T_\xi)} \mathrm{e}^{\frac{\mathrm{i}\eta}{\hbar}(T_\zeta - T_\xi)} \mathrm{e}^{\frac{\mathrm{i}(\epsilon_1 + \epsilon_2)}{2\hbar}(T_\zeta + T_\xi)} \quad (5.3.27)$$

which can be evaluated as

$$\tilde{C}_2^{\mathrm{diag}}(\eta, M) \approx \frac{\kappa \mu^2}{\mu^2 + \left(\frac{\eta}{\hbar}\right)^2 + \mathrm{i}\mu(\epsilon_1 + \epsilon_2) - \left(\frac{\epsilon_1 + \epsilon_2}{2\hbar}\right)^2} \quad (5.3.28)$$

This changes the result to the following

$$\tilde{R}_2^{\mathrm{diag}}(\eta, M) \approx \frac{\kappa}{2T_{\mathrm{H}}^2} \frac{3\mu^4 - \left(\frac{\eta\mu}{\hbar}\right)^2}{\left[\mu^2 + \left(\frac{\eta}{\hbar}\right)^2\right]^3} \quad (5.3.29)$$

The trajectory quadruplet corresponding to Figure 5.4 gives a contribution (with the leading order channel factor) to the correlation function of

$$\frac{2\kappa M^3}{T_{\mathrm{H}}^2} \int_0^\infty \mathrm{d}t_1 \mathrm{d}t_2 \mathrm{d}t_3 \mathrm{d}t_4 \, \mathrm{e}^{-\mu(t_1+t_2+t_3+t_4)} \mathrm{e}^{\frac{\mathrm{i}\eta}{\hbar}(t_2-t_4)} \mathrm{e}^{\frac{\mathrm{i}\epsilon_1}{2\hbar}(2t_1+t_2+t_4)} \mathrm{e}^{\frac{\mathrm{i}\epsilon_2}{2\hbar}(2t_3+t_2+t_4)}$$

$$\times \int \mathrm{d}\boldsymbol{s}\, \mathrm{d}\boldsymbol{u}\, \frac{\mathrm{e}^{-\left(\mu-\frac{\mathrm{i}}{\hbar}(\epsilon_1+\epsilon_2)\right)t_{\mathrm{enc}}}}{\Omega t_{\mathrm{enc}}} \mathrm{e}^{\frac{\mathrm{i}}{\hbar}\boldsymbol{su}} \tag{5.3.30}$$

When we evaluate the integrals, we find that the contribution to the time delay correlation function is given by

$$\kappa \, \frac{-\mu^4 + 5\left(\frac{\eta\mu}{\hbar}\right)^2 + 2\left(\frac{\eta}{\hbar}\right)^4}{T_{\mathrm{H}}^2 \left[\mu^2 + \left(\frac{\eta}{\hbar}\right)^2\right]^3} \tag{5.3.31}$$

In Table 5.3 we also give the contribution from the main diagrams in Figure 5.5, including the leading order channel factor M^4 (and the factor 2 for the relevant diagrams). When we add all these terms, and include the extra diagrams for the

5.5a	5.5b	5.5c
$\dfrac{-\mu^4-9\left(\frac{\eta\mu}{\hbar}\right)^2-2\left(\frac{\eta}{\hbar}\right)^4}{2T_{\mathrm{H}}^2\left[\mu^2+\left(\frac{\eta}{\hbar}\right)^2\right]^3}$	$\dfrac{8\left(\frac{\eta}{\hbar\mu}\right)^2\left[\mu^2+\left(\frac{\eta}{\hbar}\right)^2\right]}{T_{\mathrm{H}}^2\left[\mu^2+\left(\frac{\eta}{\hbar}\right)^2\right]^2}$	$\dfrac{2\mu^2-2\left(\frac{\eta}{\hbar}\right)^2-8\left(\frac{\eta}{\hbar\mu}\right)^2\left[\mu^2+\left(\frac{\eta}{\hbar}\right)^2\right]}{T_{\mathrm{H}}^2\left[\mu^2+\left(\frac{\eta}{\hbar}\right)^2\right]^2}$

Table 5.3: Contribution of different types of trajectory quadruplets to the two-point correlation function of the symmetric time delay.

orthogonal case, we again retrieve the leading order result of

$$\tilde{R}_2^{\mathrm{lo}}(\eta, M) = \frac{2\kappa}{T_{\mathrm{H}}^2} \frac{\mu^2 - \left(\frac{\eta}{\hbar}\right)^2}{\left[\mu^2 + \left(\frac{\eta}{\hbar}\right)^2\right]^2} \tag{5.3.32}$$

It is interesting to note that even though each structure gives a different contribution for the usual and the symmetrized time delay, in both cases the diagonal term cancels the terms from Figures 5.4 and 5.5a, while Figures 5.5b and 5.5c contain both terms that cancel as well as terms which leave the desired result.

As a final remark, note that if we set $\epsilon_1 = \epsilon_2 = 0, \eta = 0$ in $\tilde{C}_2(\eta, M)$ we are effectively calculating the semiclassical approximation to

$$\left(\mathrm{Tr}\left[S(E)S^\dagger(E)\right] - M\right)^2 \tag{5.3.33}$$

which should be zero because of the unitarity of the scattering matrix. We have checked this, to all orders, by using the formulae for the conductance variance given in Müller et al. (2007), but with the appropriate channel factors given in this section. The result is indeed 0, and the unitarity of the scattering matrix is preserved by the semiclassical approximation if all the semiclassical contributions are included.

5.4   Periodic orbit terms

We have previously noticed, the Wigner time delay is interesting because there are two semiclassical pictures of it. As we can express the time delay equally in terms of open trajectories and trapped periodic orbits, there should be a semiclassical equivalence between the two pictures (equations (5.1.3) and (4.1.3)), and the following should hold

$$
\frac{1}{MT_{\mathrm{H}}} \sum_{a,b} \sum_{\zeta,\zeta'(a\to b)} T_\zeta A_\zeta A_{\zeta'}^* \mathrm{e}^{\frac{\mathrm{i}}{\hbar}(S_\zeta - S_{\zeta'})} \mathrm{e}^{-\frac{\mathrm{i}\pi}{2}(\nu_\zeta - \nu_{\zeta'})} \approx \bar{\tau}_{\mathrm{W}} + \frac{1}{M} \sum_{\gamma,d} \left[A_{\gamma,r} \mathrm{e}^{\frac{\mathrm{i}}{\hbar} r S_\gamma(E)} + \mathrm{c.c.} \right]
$$

(5.4.1)

The left hand side is the sum over scattering trajectories, while the right hand side includes an average part and a sum over trapped periodic orbits. We have seen in section 5.3.1 that correlated open trajectories with self-encounters recreate the average time delay. We shall now show how, by considering the contribution in the semiclassical limit of pairs of correlated trajectories, from the sum on the left, we can also recreate the periodic orbit terms on the right.

The types of correlated trajectory pair we will consider have local motion around the trapped periodic orbits which is similar to the motion of periodic orbits that accumulate on homoclinic orbits (see Ozorio de Almeida, 1989), except they will enter and leave the region around the periodic orbit rather than looping back around. As such they will approach the trapped orbit closely (nearly following the stable manifold) follow it for a certain number of periods and then leave (nearly along the unstable manifold). A representation of such a trajectory is shown in Figure 5.6. If the trajectory follows the periodic orbit γ then, as we saw in section 1.1.2, we
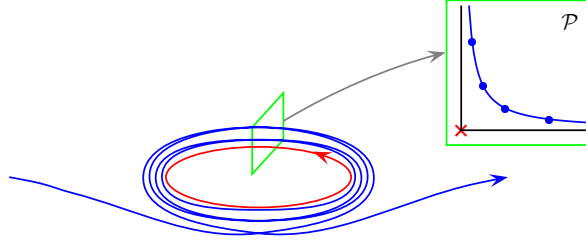
Figure 5.6: A schematic picture of a trajectory that approaches an unstable periodic orbit, follows it a number of times and leaves it again. In a Poincaré map transverse to the periodic orbit the trajectory moves along the invariant hyperbola $\boldsymbol{su} = \text{const}$.

can find $f - 1$ pairs of stable and unstable coordinates in the Poincaré section of a point along the periodic orbit. In the linearized approximation, the motion follows a hyperbola in each pair of coordinates (labelled by i)

$$u_i' = |\Lambda_{\gamma,i}|u_i, \quad s_i' = |\Lambda_{\gamma,i}^{-1}|s_i \tag{5.4.2}$$

where the point (u_i, s_i) is mapped to (u_i', s_i') after following the periodic orbit once and piercing the Poincaré section again. $|\Lambda_{\gamma,i}|$ are the stretching factors of the periodic orbit, which are the (modulus of the) expanding eigenvalues of the stability matrix M_γ. They are related to the Lyapunov exponents $\lambda_{\gamma,i}$ of the periodic orbit by $|\Lambda_{\gamma,i}| = e^{\lambda_{\gamma,i}T_\gamma}$. These coordinates however are not necessarily invariant along the periodic orbit, and we will need to consider the stable and unstable directions of the real eigenvalue pairs and the loxodromic quartets separately. Hence we will now restrict ourselves to systems with 2 degrees of freedom and consider higher dimensional systems in Appendix C.

We consider a trajectory ζ that approaches the periodic orbit γ and follows it a number of times before leaving. To make the calculation as similar as possible to previous work (as discussed in Chapter 2) we define an encounter using a small constant c. We fix a Poincaré section at a point along the periodic orbit, and we count the intersection points of the trajectory whose stable and unstable coordinates remain smaller than c. We say that a trajectory follows the orbit k times if it has k intersection points in the region bound by c. In the Poincaré section we can thus
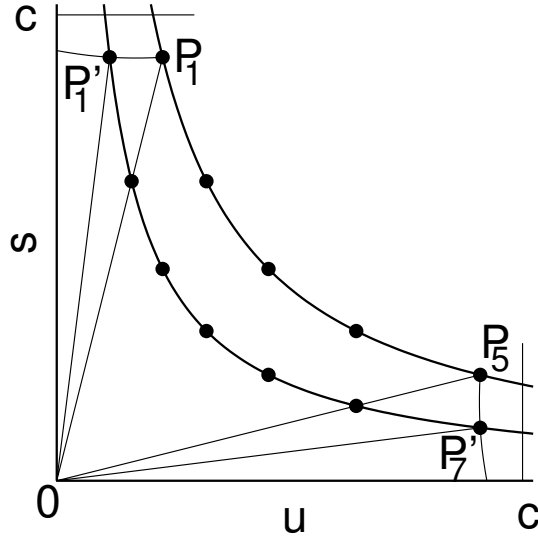
Figure 5.7: Two trajectories which follow the periodic orbit at O five and seven times within a region in the Poincaré section bounded by the constant c. The action difference $S_\zeta - S_{\zeta'}$ is the area of the two triangles $OP_1'P_1$ and OP_5P_7' minus twice the action of the periodic orbit S_γ

map $k - 1 = \tilde{k}$ times from the first intersection point, P_1, to the last, P_k.

The partner trajectory ζ' enters very close to ζ, (almost) along the stable manifold, but winds around the periodic orbit an additional r times before leaving close to ζ along the unstable manifold. The coordinates of its intersection points can be found by moving from P_1 approximately along the unstable direction until we reach a unique point P_1' whose $(\tilde{k}+r)$-th iterate under the mapping in the Poincaré section, P_{k+r}', has approximately the same unstable coordinate as P_k and only really differs in the stable direction. This is illustrated for positive Λ_γ in Figure 5.7, where the original trajectory ζ winds around the periodic orbit 5 times, moving from point P_1 to point P_5, while its partner ζ' winds an additional 2 times, from the point P_1' to P_7'. We consider in the next section the contribution of these types of trajectories to the Wigner time delay.

5.4.1 Action differences

To calculate the action difference between the two trajectories $\Delta S = S_\zeta - S_{\zeta'}$ we split the trajectories into parts and use the Poincaré–Cartan theorem, as in sec-

134

tion 2.2.2. For the initial part, the trajectories start in the lead, with the correct initial conditions, and then approach the periodic orbit (almost) along the stable manifold, while a small difference in the unstable direction grows to the difference between the first piercing points P_1 and P_1'. There is a curve given by a family of trajectories with differing unstable coordinates that joins the two points, and the action difference ΔS_I of the initial part of the trajectories is given by the action integral along the curve (cf Figure 2.6)

$$\Delta S_I = \int_{P_1'}^{P_1} p \, \mathrm{d}q \tag{5.4.3}$$

Similarly, the action difference ΔS_F of the final parts of the trajectories from the last piercing points to the lead, where they exit with the correct final conditions, is given by

$$\Delta S_F = \int_{P_k}^{P_{k+r}'} p \, \mathrm{d}q \tag{5.4.4}$$

During the central part of each trajectory, we compare the action of each trajectory with that of the periodic orbit. For example, for the trajectory ζ, the action along the hyperbola linking the first and last piercing points is the same as the action calculated along a curve, formed by a family of trajectories, joining the point P_1 to the periodic orbit, then along $\tilde{k}$ repetitions of the orbit and finally back to the point P_k (along the image of the curve from the orbit to P_1)

$$\int_{P_1}^{P_k} p \, \mathrm{d}q = \int_{P_1}^{O} p \, \mathrm{d}q + \tilde{k} S_\gamma + \int_{O}^{P_k} p \, \mathrm{d}q \tag{5.4.5}$$

where the integrals are along the curves described above. If we do the same for the partner trajectory ζ' we obtain

$$\int_{P_1'}^{P_{k+r}'} p \, \mathrm{d}q = \int_{P_1'}^{O} p \, \mathrm{d}q + (\tilde{k} + r) S_\gamma + \int_{O}^{P_{k+r}'} p \, \mathrm{d}q \tag{5.4.6}$$

The action difference between ζ and ζ' is then given by action integrals along the edges of the triangles $OP_1'P_1$ and OP_kP_{k+r}' and we obtain the term $-rS_\gamma$ from

135

the extra repetitions of the periodic orbit performed by the longer trajectory. The action integrals along the edges of the triangles give their symplectic areas which are invariant under a change of coordinates, and also as points are transported around the periodic orbit (eg from one piercing in the Poincaré section to the next). The triangles $OP_1'P_1$ and OP_kP_{k+r}' are also represented in Figure 5.7. In the linearized approximation, the sides of the triangles are straight lines and we can calculate their area simply from the coordinates of the piercing points. If P_1 occurs at the point (u, s) then after $\tilde{k} = k - 1$ iterations we arrive at the point $P_k \approx (u\Lambda_\gamma^{\tilde{k}}, s\Lambda_\gamma^{-\tilde{k}})$. P_1' has approximately the same stable coordinate as P_1 and takes r more iterations to arrive at the same unstable coordinate as P_k, so it should have coordinates $P_1' \approx (u\Lambda_\gamma^{-r}, s)$ and hence $P_{k+r}' \approx (u\Lambda_\gamma^{\tilde{k}}, s\Lambda_\gamma^{-(\tilde{k}+r)})$. We can now obtain the area of the triangles and thus the approximation of the action difference

$$S_\zeta - S_{\zeta'} \approx su(1 - \Lambda_\gamma^{-r}) - rS_\gamma \tag{5.4.7}$$

We can see that the action difference has a part which depends on the distance between the piercing points of ζ and the periodic orbit, which can be small on the scale of $\hbar$, as well as a semiclassically large part from the extra repetitions of the periodic orbit. If the eigenvalue is negative, the coordinates are still given as above and the result for the action difference is the same, but the points are reflected between each piercing in the Poincaré section. If r is odd then P_1' lies on the opposite side of the s-axis with respect to P_1, and P_{k+r}' on the other side of the u-axis with respect to P_k.

5.4.2 Trajectory differences

As well as the action difference, there are other differences between the two trajectories. The longer trajectory revolves around the periodic orbit an additional r times, so its time will be longer by approximately r times the period of the orbit

$$T_{\zeta'} \approx T_\zeta + rT_\gamma \tag{5.4.8}$$

136

For chaotic cavities with leads attached, the stability amplitude of a trajectory is proportional to $\frac{1}{\sqrt{|M_{21}|}}$, where M_{21} is an element of the stability matrix M of the whole trajectory (Richter and Sieber, 2002). As stability matrices are multiplicative, we can separate the stability matrix of the trajectory ζ into a product of the matrices corresponding to its initial part up to the first piercing point, the part where it follows the periodic orbit k times, and then its final part to the exit lead

$$M_\zeta \approx M_F M_\gamma^{\tilde{k}} M_I \tag{5.4.9}$$

Here we have approximated the stability matrix of the trajectory as it follows the periodic orbit k times by the stability matrix of the periodic orbit itself. The same approximation holds for the longer trajectory ζ', except we have an additional r repetitions of the orbit. We can express the stability matrix of the periodic orbit using its eigenbasis as

$$M_\gamma^k = \Lambda_\gamma^k P_u + \Lambda_\gamma^{-k} P_s \tag{5.4.10}$$

where P_u is the projector onto the unstable eigenvector and P_s onto the stable one. For large k the unstable part dominates and we can get the leading order approximation to the stability amplitudes

$$A_{\zeta'} \approx \frac{A_\zeta}{|\Lambda_\gamma|^{\frac{r}{2}}} \tag{5.4.11}$$

For the Maslov type indices, we can use the geometric interpretation from Creagh et al. (1990) to obtain a simple relation between $\nu_{\zeta'}$ and ν_ζ. Along a periodic orbit, the Maslov index is the number of times the stable and unstable manifolds rotate by half a turn (plus twice the number of reflections on hard walls with Dirichlet boundary conditions). After each loop along the periodic orbit, the manifolds are back where they started and the Maslov index must be an integer. As long as both ζ and ζ' are close enough to the periodic orbit they will rotate with the manifolds of the orbit and ζ' will pick up r times the Maslov index of the orbit γ over the

trajectory ζ. Outside of the encounter, both trajectories should be close and have the same index, giving

$$\nu_{\zeta'} = \nu_\zeta + r\mu_\gamma \tag{5.4.12}$$

All of these approximations become more accurate the larger k becomes, and the closer the trajectories get to the periodic orbit. As was the case previously, the semiclassical contribution comes from the region of small stable and unstable separations, which in this case means near the periodic orbit itself, and this provides a justification of the use of these approximations.

We now have the elements we need to include trajectory pairs, that follow a trapped periodic orbit γ as described above, into the correlation function of the scattering matrix (equation (5.1.6))

$$C^{\gamma,r}(\epsilon) \approx \sum_{a,b} \frac{e^{-\frac{i}{\hbar}rS_\gamma}e^{\frac{i\pi}{2}r\mu_\gamma}e^{\frac{i\epsilon}{2\hbar}rT_\gamma}}{T_H|\Lambda_\gamma|^{\frac{r}{2}}} \sum_{\zeta(a\to b)} |A_\zeta|^2 e^{\frac{i}{\hbar}su(1-\Lambda_\gamma^{-r})}e^{\frac{i\epsilon}{\hbar}T_\zeta} + (r \to -r) \tag{5.4.13}$$

The $(r \to -r)$ denotes a term derived from exchanging the two trajectories ζ and ζ', which gives a similar contribution, but with r replaced by $-r$.

5.4.3 Probability of encounters

We can perform this sum in a similar way to the sums in section 5.3.1 by thinking of the approach as an encounter with the orbit. We then split the trajectory into three parts, a section from the lead (channel a) to a coordinate $\approx c$ along the stable manifold of the periodic orbit, the encounter with the orbit following a hyperbola, and then a final section where the trajectory leaves, after its unstable coordinate grows larger than the constant c, and travels back to the lead (channel b). We let the three parts have times t_1, t_{enc}^γ and t_2 respectively, with total time

$$T_\zeta = t_1 + t_{enc}^\gamma + t_2 \tag{5.4.14}$$

138

Trajectories, if long enough, will cover the available phase space uniformly because of ergodicity. Strictly speaking we consider trajectories as uniform over the energy shell (of the closed system), and we then weight each trajectory with its average probability of survival. We can then define a weight function that is the density that a trajectory approaches the periodic orbit closely. This means that the trajectory pierces the Poincaré section of the orbit within a small region $\mathrm{d}u\mathrm{d}s$ of a point (u, s), where both coordinates are bounded by the small constant c. With uniformity, the probability that the trajectory pierces the Poincaré section between times t_1 and $t_1 + \mathrm{d}t_1$ is given by

$$\frac{\mathrm{d}u\mathrm{d}s\mathrm{d}t_1}{\Omega} \tag{5.4.15}$$

The time of the first link is free to vary between 0 and $T_\zeta - t_{\mathrm{enc}}^\gamma$ so the total density of an encounter is

$$\int_0^{T_\zeta - t_{\mathrm{enc}}^\gamma} \mathrm{d}t_1 \frac{\mathrm{d}u\mathrm{d}s}{\Omega} \tag{5.4.16}$$

However, in the fixed Poincaré section we would count the trajectory k times, once for each time that it winds round the periodic orbit, so we should divide by this number to compensate for overcounting. k itself is given by the number of iterations in the Poincaré section where the point (u, s) remains bounded by the constant c

$$k \approx \frac{1}{\lambda_\gamma T_\gamma} \ln \frac{c}{|s|} + \frac{1}{\lambda_\gamma T_\gamma} \ln \frac{c}{|u|} \tag{5.4.17}$$

The encounter time is approximately k times the period of the periodic orbit, and so it is given by

$$t_{\mathrm{enc}}^\gamma \approx kT_\gamma \approx \frac{1}{\lambda_\gamma} \ln \frac{c}{|su|} \tag{5.4.18}$$

This equation has the same form that we had previously for self-encounters, and in fact this allows us to use similar methods with only minor modifications. Importantly we can therefore use the semiclassical result of equation (2.2.25). The weight function, once we correct for the overcounting by a factor of $k \approx \frac{t_{\mathrm{enc}}^\gamma}{T_\gamma}$, is given by

$$w_{\gamma,T}(s,u) = \int_0^{T-t_{\text{enc}}^\gamma} dt_1 \frac{T_\gamma}{\Omega t_{\text{enc}}^\gamma} \qquad (5.4.19)$$

where T is the time of the trajectory T_ζ. The coordinates of the weight function are the stable and unstable separations between the piercing point and the periodic orbit.

5.4.4 Semiclassical contribution

By using the weight function of equation (5.4.19) and the analogue of the Hannay–Ozorio de Almeida sum rule for open systems (equation (5.2.5)), we can now replace the sum over trajectories in equation (5.4.13) with the following

$$\sum_{\zeta(a\to b)} |A_\zeta|^2 \dots \approx \int dT \int dsdu\, w_{\gamma,T}(s,u) e^{-\mu T_{\text{exp}}} \dots \qquad (5.4.20)$$

Since the encounter is with a trapped periodic orbit, the trajectory will not leave the system while it winds around the periodic orbit (for small enough c) and so the exposure time does not include the encounter time, but only the time spent in the links

$$T_{\text{exp}} = t_1 + t_2 \qquad (5.4.21)$$

By substituting into the correlation function (equation (5.4.13)), and making a change of integration variable from T to t_2, we can again separate the contribution into encounters and links

$$
\begin{aligned}
C^{\gamma,r}(\epsilon) \quad \approx \quad & \sum_{a,b} \frac{T_\gamma e^{-\frac{i}{\hbar} r S_\gamma} e^{\frac{i\pi}{2} r \mu_\gamma} e^{\frac{i\epsilon}{2\hbar} r T_\gamma}}{T_{\text{H}} |\Lambda_\gamma|^{\frac{r}{2}}} \int dsdu\, \frac{e^{\frac{i}{\hbar} su(1-\Lambda_\gamma^{-r})} e^{\frac{i\epsilon}{\hbar} t_{\text{enc}}^\gamma}}{\Omega t_{\text{enc}}^\gamma} \\
& \times \prod_{i=1}^{2} \int_0^\infty dt_i\, e^{-\left(\mu - \frac{i\epsilon}{\hbar}\right) t_i} + (r \to -r) \qquad (5.4.22)
\end{aligned}
$$

We can now perform the integral over s and u using exactly the equation (2.2.25) that we have used in the context of self-encounters. Note that this integral automatically sums over all the different values of the winding number k, which in turn depends

on the phase space separations. Only terms where the t_{enc}^{γ} cancel in the numerator and denominator contribute, and when we perform all the integrals we obtain the following result

$$C^{\gamma,r}(\epsilon) \approx \frac{M(M-\kappa+1)}{T_{\text{H}}^2 \left(\mu - \frac{\mathrm{i}\epsilon}{\hbar}\right)^2} \frac{\mathrm{i}\epsilon}{\hbar} \left[\frac{T_\gamma \mathrm{e}^{\frac{\mathrm{i}\pi}{2}r\mu_\gamma} \mathrm{e}^{\frac{\mathrm{i}\epsilon}{2\hbar}rT_\gamma}}{|\Lambda_\gamma|^{\frac{r}{2}}|1-\Lambda_\gamma^{-r}|} \mathrm{e}^{-\frac{\mathrm{i}}{\hbar}rS_\gamma} + \text{c.c.} \right] \tag{5.4.23}$$

where the complex conjugate comes from exchanging r and $-r$. When we differentiate at $\epsilon = 0$, to get the contribution to the time delay, we obtain

$$\tau_{\text{W}}^{\gamma,r} \approx \frac{(M-\kappa+1)}{M^2} \left[\frac{T_\gamma \mathrm{e}^{\frac{\mathrm{i}\pi}{2}r\mu_\gamma}}{|\Lambda_\gamma|^{\frac{r}{2}}|1-\Lambda_\gamma^{-r}|} \mathrm{e}^{-\frac{\mathrm{i}}{\hbar}rS_\gamma} + \text{c.c.} \right] \tag{5.4.24}$$

If we recall the expression for the stability amplitude of a periodic orbit (equation (1.3.17))

$$A_{\gamma,r} = \frac{T_\gamma \mathrm{e}^{-\mathrm{i}r\mu_\gamma\frac{\pi}{2}}}{\sqrt{|\det(M_\gamma^r - 1)|}} \tag{5.4.25}$$

and use the identity $\sqrt{|\det(M_\gamma^r - 1)|} = |\Lambda_\gamma|^{\frac{r}{2}}|1-\Lambda_\gamma^{-r}|$, then one can see that we indeed recreate the contribution of the r-th repetition of the periodic orbit γ in the time delay. For systems without time reversal symmetry we recreate its contribution exactly while for systems with time reversal symmetry, the channel factor is slightly different, as it was for the average time delay (section 5.3.1). This is because we have so far only allowed the possibility of a single encounter with a periodic orbit. To get full agreement, we need to include self-encounters and combinations of self- and periodic orbit encounters which we do in the next section.

5.4.5 Combinations of self- and periodic orbit encounters

In order to combine periodic orbit encounters and self-encounters, we explore the diagrammatic rules which simplify the calculation of the contribution of trajectories to the correlation function. As we have seen, we can separate the contribution into encounters and links, and for each link we have the integral

141

$$\int_0^\infty \mathrm{d}t_i \, \mathrm{e}^{-\left(\mu - \frac{\mathrm{i}\epsilon}{\hbar}\right)t_1} = \frac{1}{\left(\mu - \frac{\mathrm{i}\epsilon}{\hbar}\right)} \tag{5.4.26}$$

If we define $\tilde{\epsilon} = \frac{\epsilon}{\hbar\mu}$, and remove the Heisenberg time factor, then for each the link we obtain a factor of $\frac{1}{M(1-\mathrm{i}\tilde{\epsilon})}$. Each l-encounter gives the following contribution

$$\int \mathrm{d}^{l_\alpha - 1} s_\alpha \, \mathrm{d}^{l_\alpha - 1} u_\alpha \frac{\mathrm{e}^{-\mu(1-\mathrm{i}\tilde{\epsilon}l_\alpha)t_{\mathrm{enc}}^\alpha}\mathrm{e}^{\frac{\mathrm{i}}{\hbar}\sum_j s_{\alpha j}u_{\alpha j}}}{\Omega^{l_\alpha - 1}t_{\mathrm{enc}}^\alpha} \tag{5.4.27}$$

which reduces (without the Heisenberg time) to the factor $-M(1 - \mathrm{i}l\tilde{\epsilon})$. In the previous section, from the periodic orbit encounter, we also had

$$\frac{T_\gamma \mathrm{e}^{-\frac{\mathrm{i}}{\hbar}rS_\gamma}\mathrm{e}^{\frac{\mathrm{i}\pi}{2}r\mu_\gamma}\mathrm{e}^{\frac{\mathrm{i}\tilde{\epsilon}\mu}{2}rT_\gamma}}{T_{\mathrm{H}}|\Lambda_\gamma|^{\frac{r}{2}}} \int \mathrm{d}s\mathrm{d}u \, \frac{\mathrm{e}^{\frac{\mathrm{i}}{\hbar}su(1-\Lambda_\gamma^{-r})}\mathrm{e}^{\mathrm{i}\tilde{\epsilon}\mu t_{\mathrm{enc}}^\gamma}}{\Omega t_{\mathrm{enc}}^\gamma} + (r \to -r) \tag{5.4.28}$$

providing a factor of

$$2\mathrm{i}\tilde{\epsilon}\mu|A_{\gamma,r}|\cos\left(-\frac{1}{\hbar}rS_\gamma + \frac{\pi}{2}r\mu_\gamma + \frac{\tilde{\epsilon}\mu}{2}rT_\gamma\right) \tag{5.4.29}$$

The diagrammatic rules described above are recorded in the first three lines of Table 5.4.

Now we consider the contribution of a family of trajectory pairs, with self-encounters, that are described by a vector $\boldsymbol{v}$, and that additionally have a periodic orbit encounter. The latter can occur either during one of the links, or at the same time as one of the self-encounters. First we consider the case where the periodic orbit encounter occurs during one of the $(L + 1)$ links. The encounter will divide the link in which it occurs into three parts, the encounter itself and two new links, so that the total number of links increases to $(L + 2)$. The weight function can be expressed as an integral

$$w_{\gamma,T}(\boldsymbol{s}, \boldsymbol{u}) = \int' \mathrm{d}t_1 \ldots \mathrm{d}t_{L+1} \frac{T_\gamma}{\Omega^{L+1-V}t_{\mathrm{enc}}^\gamma \prod_{\alpha=1}^V t_{\mathrm{enc}}^\alpha} \tag{5.4.30}$$

where all the link times must be positive (including the remaining link not in the

integral) and this restriction is denoted by the prime. The vectors $\boldsymbol{s}$ and $\boldsymbol{u}$ record the $L - V$ stable and unstable separations of the encounters along the trajectory, as well as the phase space separation between the piercing point of the trajectory in the Poincaré section of the periodic orbit and the orbit itself. With the open sum rule (equation (5.2.5)), and a change of variables from the trajectory time T to the last link time t_{L+2}, we can separate the contribution into links and encounters. Using the diagrammatic rules, we can calculate the contribution to the correlation function. To leading order we find

$$
\begin{aligned}
C_{\mathrm{I}}^{\boldsymbol{v},\gamma,r}(\tilde{\epsilon}) \quad \approx \quad & (L+1)\frac{M(M+\kappa-1)}{M^{L-V+2}}N(\boldsymbol{v})(-1)^V 2\mathrm{i}\tilde{\epsilon}\mu|A_{\gamma,r}|\cos\left(-\frac{1}{\hbar}rS_\gamma + \frac{\pi}{2}r\mu_\gamma\right) \\
& +O(\tilde{\epsilon}^2)
\end{aligned}
\tag{5.4.31}
$$

where the factor $(L+1)$ comes from the fact that we can place the periodic orbit encounter on any of the original $(L+1)$ links.

We can also have the situation where a periodic orbit encounter occurs at the same time as a self-encounter, or in other words that a self-encounter occurs in the vicinity of a periodic orbit. The simplest scenario, for systems with time reversal symmetry, is when we have a trajectory with a single 2-encounter that is a short distance away from the periodic orbit. Such a trajectory would enter from the lead, wander uniformly and then have its first encounter with the periodic orbit by winding around k_1 times. It then leaves the periodic orbit and later loops back to follow the periodic orbit an additional k_2 times in the other direction before exiting through the lead. Such a trajectory is depicted in the Poincaré section of the periodic orbit in Figure 5.8 by the full lines. In the Figure we have $k_1 = 5$ and $k_2 = 3$ and we have used the time reverse of the intersection points for the second encounter stretch, as it travels in the opposite direction to the first. The intersection points lie on hyperbolae, and the direction of travel is indicated by the arrows.

In section 2.2.2, for periodic orbits in closed systems, we considered the partner orbit to an orbit with a single 2-encounter. There we had a Poincaré section with only two piercing points from the two encounter stretches of the original orbit. If we
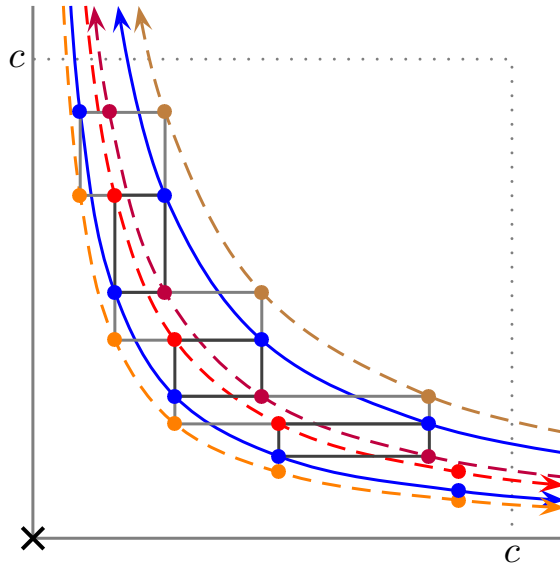
Figure 5.8: A representation of a trajectory (full line) with two encounter visits and examples of two partner trajectories (dashed lines). The partner trajectories are formed using rectangles based on piercing points of the original trajectory. Several images of each rectangle (leading to the same partner trajectory) can be found inside the encounter.

drew a rectangle in the stable and unstable directions whose opposite corners were the piercing points, then the coordinates of the other two corners were those of the partner encounter stretches, in the linearized approximation. Here we have many piercing points (k_1 and k_2) and we could make rectangles and partner trajectories by combining any pair of them. However, as each partner also winds around the periodic orbit, we get several images of the same rectangle in the Poincaré section, and these are also illustrated in Figure 5.8. The number of images, k, corresponding to the same trajectory pair is given by

$$k \approx \frac{1}{\lambda_\gamma T_\gamma} \ln \frac{c}{\max_j |u_j|} + \frac{1}{\lambda_\gamma T_\gamma} \ln \frac{c}{\max_j |s_j|} \qquad (5.4.32)$$

where we take the maximum over the stable and unstable coordinates of the corners of each rectangle. As we overcount by this factor, we will need to divide by it later to compensate. By analogy with equation (2.2.14), this suggests the following definition for the encounter time

144

$$t_{\text{enc}}^{\gamma,\alpha} \approx kT_\gamma \approx \frac{1}{\lambda_\gamma} \ln \frac{c^2}{\max_i |s_i| \times \max_j |u_j|} \qquad (5.4.33)$$

We can also understand the occurrence of multiple partner trajectories by considering how the partner follows the periodic orbit. The original trajectory follows the periodic orbit k_1 times on the first encounter, and k_2 times on the second. The partner trajectory could follow the periodic orbit a different number of times on each visit, as long as the total number of traversals is the same. For example it could follow the orbit $k_1 + m > 0$ times on the first visit and $k_2 - m > 0$ times on the second, for any integer m that keeps the number of traversals positive. These choices of piercing points lead to a single 2-encounter near a periodic orbit, but we are interested in different type of encounter with further traversals of the periodic orbit. Therefore we choose a partner trajectory ζ' that traverses the periodic orbit an additional r times in total, for example it follows the orbit $k_1 + r + m > 0$ times on the first visit and $k_2 - m > 0$ times the second for some integer m. The action difference will then include these additional r traversals of the periodic orbit. We consider now the action difference for a general l-encounter combined with a periodic orbit encounter, where the partner trajectory has an additional r traversals of the periodic orbit.

From the original l-encounter we found the encounter stretches of the partner trajectory by reconnecting the entrance and exit ports of the encounter. If the original encounter stretches (or their time reverse) pierce the Poincaré section of the periodic orbit at (u_i, s_i), for $i = 1 \ldots l$, then the partner trajectory stretches pierce at $\approx (u_{\pi(i)}, s_i)$ where $\pi(i)$ records the permutation. The action difference from the encounter reconnections was (see equation (2.2.11))

$$\Delta S_\alpha = \sum_{j=1}^{l-1} (s_{\pi^j(1)} - s_{\pi^{(j-1)}(1)})(u_{\pi^j(1)} - u_1) \qquad (5.4.34)$$

Note that we can also include the term $j = l$ in the sum without changing the value of the sum, as $\pi^l(1) = 1$. With this term included, u_1 multiplies all the stable

145

coordinates on the l-cycle, with both a positive and negative sign, and therefore it cancels and we can rewrite the action difference as

$$\Delta S_\alpha = \sum_{j=1}^{l} (s_{\pi^j(1)} - s_{\pi^{(j-1)}(1)}) u_{\pi^j(1)} \tag{5.4.35}$$

Next we also include an extra r traversals of the periodic orbit in the partner trajectory. These traversals can be separated into l parts so that we have an extra r_i for each stretch i, as long as the total number of extra traversals from all the stretches is r

$$\sum_{i=1}^{l} r_i = r \tag{5.4.36}$$

The action difference between an encounter stretch that passes through $(u_{\pi(i)}, s_i)$ and one that takes an extra r_i traversals is (see equation (5.4.7))

$$s_i u_{\pi(i)} (1 - \Lambda_\gamma^{r_i}) - r_i S_\gamma \tag{5.4.37}$$

so that the total action difference between the two trajectories from all the encounter stretches is

$$\Delta S_{\alpha,\gamma,r} = \sum_{j=1}^{l} s_j (u_j - u_{\pi(j)} \Lambda_\gamma^{-r_j}) - r S_\gamma \tag{5.4.38}$$

where we have made a change of index for the first product of stable and unstable coordinates. If we record the l coordinates in the stable and unstable directions in vectors $\boldsymbol{s}$ and $\boldsymbol{u}$ then we can rewrite the action difference in a matrix form

$$\Delta S_{\alpha,\gamma,r} = \boldsymbol{u}^{\mathrm{T}} D \boldsymbol{s} - r S_\gamma \tag{5.4.39}$$

The matrix D can be separated, $D = I + \tilde{D}$, where $\tilde{D}$ has elements $\tilde{D}_{ij} = -\delta_{i\pi(j)} \Lambda_\gamma^{-r_j}$. Because the permutation matrix of the left and right ports consists of a single cycle of length l, we have the relation $\det D = 1 + \det \tilde{D}$. We can diagonalise $\tilde{D}$ with $(l-1)$ column exchanges, and hence $\det \tilde{D} = -\Lambda_\gamma^r$ and $\det D = 1 - \Lambda_\gamma^r$.

146

If the trajectory has no further self-encounters, so that we only have one l-encounter α in the vicinity of a periodic orbit γ, then the weight function is given by

$$w_{\gamma,T}(\boldsymbol{s},\boldsymbol{u}) = \int' \mathrm{d}t_1 \ldots \mathrm{d}t_l \, \frac{T_\gamma}{\Omega^l t_{\mathrm{enc}}^{\gamma,\alpha}} \tag{5.4.40}$$

where we have divided by the factor $k \approx \frac{t_{\mathrm{enc}}^{\gamma,\alpha}}{T_\gamma}$ to compensate for the overcounting. We can now put this type of trajectory pair into the correlation function and the contribution again factorises as

$$\sum_{a,b} \frac{T_\gamma \mathrm{e}^{-\frac{\mathrm{i}}{\hbar}rS_\gamma + \frac{\mathrm{i}\pi}{2}r\mu_\gamma} \mathrm{e}^{\frac{\mathrm{i}\tilde{\epsilon}\mu}{2}rT_\gamma}}{T_{\mathrm{H}} \, |\Lambda_\gamma|^{\frac{r}{2}}} \int \mathrm{d}\boldsymbol{s} \, \mathrm{d}\boldsymbol{u} \, \frac{\mathrm{e}^{\frac{\mathrm{i}}{\hbar}\boldsymbol{u}^{\mathrm{T}}D\boldsymbol{s}} \mathrm{e}^{\mathrm{i}l\tilde{\epsilon}\mu t_{\mathrm{enc}}^{\gamma,\alpha}}}{\Omega^l \, t_{\mathrm{enc}}^{\gamma,\alpha}} \prod_{i=1}^{l+1} \int_0^\infty \mathrm{d}t_i \mathrm{e}^{-\mu(1-\mathrm{i}\tilde{\epsilon})t_i} + (r \to -r) \tag{5.4.41}$$

For the integral over $\boldsymbol{s}$ and $\boldsymbol{u}$ we use the result

$$\int \mathrm{d}\boldsymbol{s} \, \mathrm{d}\boldsymbol{u} \, \frac{\mathrm{e}^{\frac{\mathrm{i}}{\hbar}\boldsymbol{u}^{\mathrm{T}}D\boldsymbol{s}} \mathrm{e}^{\mathrm{i}l\tilde{\epsilon}\mu t_{\mathrm{enc}}^{\gamma,\alpha}}}{\Omega^l \, t_{\mathrm{enc}}^{\gamma,\alpha}} \approx \frac{\mathrm{i}l\tilde{\epsilon}\mu}{T_{\mathrm{H}}^l |\det D|} \tag{5.4.42}$$

which is an extension of equation (2.2.25). If we recall that $\det D = 1 - \Lambda_\gamma^r$, we can extract the diagrammatic rule for the contribution of a combination of an l-encounter and a periodic orbit encounter, and complete Table 5.4

$$2\mathrm{i}l\tilde{\epsilon}\mu|A_{\gamma,r}| \cos\left(-\frac{1}{\hbar}rS_\gamma + \frac{\pi}{2}r\mu_\gamma + \frac{\tilde{\epsilon}\mu}{2}rT_\gamma\right) \tag{5.4.43}$$

contribution of each link	$\frac{1}{M(1-\mathrm{i}\tilde{\epsilon})}$
contribution of each l-encounter	$-M(1 - \mathrm{i}l\tilde{\epsilon})$
r-th contribution of a periodic orbit encounter	$2\mathrm{i}\tilde{\epsilon}\mu|A_{\gamma,r}| \cos\left(-\frac{1}{\hbar}rS_\gamma + \frac{\pi}{2}r\mu_\gamma + \frac{\tilde{\epsilon}\mu}{2}rT_\gamma\right)$
r-th contribution of a periodic orbit plus l-encounter	$2\mathrm{i}l\tilde{\epsilon}\mu|A_{\gamma,r}| \cos\left(-\frac{1}{\hbar}rS_\gamma + \frac{\pi}{2}r\mu_\gamma + \frac{\tilde{\epsilon}\mu}{2}rT_\gamma\right)$

Table 5.4: Diagrammatic rules for the different contributions to the correlation function $C(\tilde{\epsilon})$.

The contribution does not depend on how the repetition number r is split into

147

parts $r_1, \ldots, r_l$, and the different ways are included in the integral over the $\boldsymbol{s}$ and $\boldsymbol{u}$ coordinates. Each way has several copies in the Poincaré section and this over-counting was compensated for with the division by the encounter time.

If the original trajectory ζ has many self-encounters, described by a vector $\boldsymbol{v}$, then we could have a periodic orbit encounter combined with any of them. When we include this possibility, we finally obtain the second part of the contribution to the correlation function

$$
\begin{aligned}
C_{\text{II}}^{\boldsymbol{v},\gamma,r}(\tilde{\epsilon}) &\approx -\sum_{\alpha=1}^{V} l_\alpha \frac{M(M+\kappa-1)}{M^{L-V+2}} N(\boldsymbol{v})(-1)^V 2\mathrm{i}\tilde{\epsilon}\mu|A_{\gamma,r}|\cos\left(-\frac{1}{\hbar}rS_\gamma + \frac{\pi}{2}r\mu_\gamma\right) \\
&\quad +O(\tilde{\epsilon}^2)
\end{aligned}
\tag{5.4.44}
$$

This expression differs from $C_{\text{I}}^{\boldsymbol{v},\gamma,r}(\tilde{\epsilon})$ in the prefactor, where $(L+1)$ has been replaced by $-\sum_\alpha l_\alpha = -L$. When we add the two possibilities of combining self-encounters with a periodic orbit encounter, this factor becomes one, leaving the following end result

$$
C^{\boldsymbol{v},\gamma,r}(\tilde{\epsilon}) \approx \frac{M(M+\kappa-1)}{M^{L-V+2}} N(\boldsymbol{v})(-1)^V 2\mathrm{i}\tilde{\epsilon}\mu|A_{\gamma,r}|\cos\left(-\frac{1}{\hbar}rS_\gamma + \frac{\pi}{2}r\mu_\gamma\right) + O(\tilde{\epsilon}^2)
\tag{5.4.45}
$$

Finally we sum over all possible vectors $\boldsymbol{v}$, and also include the contributions from section 5.4.4 (which can be thought of as corresponding to a vector with $L = V = 0$ and $N(\boldsymbol{v}) = 1$)

$$
\begin{aligned}
C^{p,r}(\epsilon) &\approx (M+\kappa-1)\sum_{n=1}^{\infty} \sum_{\boldsymbol{v}}^{L-V+1=n} \frac{N(\boldsymbol{v})(-1)^V}{M^n} \frac{2\mathrm{i}\epsilon}{\hbar}|A_{\gamma,r}|\cos\left(-\frac{1}{\hbar}rS_\gamma + \frac{\pi}{2}r\mu_\gamma\right) \\
&\quad +O(\epsilon^2) \\
&\approx \frac{2\mathrm{i}\epsilon}{\hbar}|A_{\gamma,r}|\cos\left(-\frac{1}{\hbar}rS_\gamma + \frac{\pi}{2}r\mu_\gamma\right) + O(\epsilon^2)
\end{aligned}
\tag{5.4.46}
$$

which reproduces exactly the term of the r-th repetition of the trapped periodic orbit γ in the Wigner time delay, for both symmetry classes.

In total, the leading order result for the correlation function $C(\epsilon)$ derived from

summing over all trapped periodic orbits and their repetitions, and including the average part (equation (5.3.8)) is

$$C(\epsilon) \approx M \left(1 + \frac{\mathrm{i}\epsilon}{\hbar} \bar{\tau}_{\mathrm{W}} \right) + \frac{\mathrm{i}\epsilon}{\hbar} \sum_{\gamma,r} \left[A_{\gamma,r} \mathrm{e}^{\frac{\mathrm{i}}{\hbar} r S_\gamma} + \mathrm{c.c.} \right] + O(\epsilon^2) \qquad (5.4.47)$$

so that we recreate the right hand side of equation (5.4.1) when we differentiate at $\epsilon = 0$ (as in equation (5.1.7)).

A nice property of the types of trajectory pairs, with a periodic orbit encounter, that we have considered is that if the periodic orbit they traverse escapes, so too do the trajectories. They would have a zero survival probability and therefore there is no contribution from the periodic orbits that escape.

We have so far considered all the types of correlated trajectories that allow us to recreate the second picture of the Wigner time delay. Trajectories with self-encounters recreate the average time delay, while trajectories that also have a single periodic orbit encounter recreate the term of that periodic orbit in the time delay. However the consideration here of combinations of self-encounters and periodic orbit encounters suggests that there are other correlations. For example we could have n periodic orbit encounters with different periodic orbits. From the diagrammatic rules, we can see that these would give a contribution of order ϵ^n and would not contribute to the time delay. Multiple encounters with the same periodic orbit could be the combination with a self-encounter that we have considered in this section, but they could also, depending on the direction of the traversals, and whether the system has time reversal symmetry or not, be independent. One example is a trajectory that follows a periodic orbit in the same direction both times it has an encounter with it, and has no further self-encounters. Then we could not make all the reconnections and partners we have seen above, but we could still have all the possible different numbers of traversals in both encounters of the partner trajectory that keep the total number of traversals constant. Another interesting type of correlation involves the trajectory pairs where a self-encounter coincides with a periodic orbit encounter that we have considered in this section, but with $r = 0$. We have not examined

149

these types of correlations yet, but it would be interesting to consider them, both in the context of the time delay, and also in the context of periodic orbit correlations of closed system.

When we let ϵ tend to zero, then the correlation function $C(\epsilon)$ becomes

$$\lim_{\epsilon \to 0} C(\epsilon) = M = \text{Tr}\left[S(E)S^\dagger(E)\right] \qquad (5.4.48)$$

When we take the limit in our semiclassical result (equation (5.4.47)) then we see that it does satisfy the unitarity of the S matrix, as all the periodic orbit contributions tend to 0 in this limit. This has implications for the conductance and other related quantities. The difference between the conductance and $C(0)$ lies in the channel factor, and this result suggests that periodic orbit contributions would also vanish for the conductance to leading semiclassical order. This does not completely rule out the possibility of periodic orbit terms in the conductance, for example trajectories with encounters with particular periodic orbits might favour certain channel combinations, and contribute preferentially to the conductance or reflectance. Of course, if any periodic orbit terms exist in the conductance they would also need to appear with the opposite sign in the reflectances, as the transmission and reflectance sum to the constant number of channels in the respective lead.

Conclusion

The first main result of this thesis was the extension of recent developments in semiclassical periodic orbit expansions for chaotic systems. A commonly studied quantity is the form factor $K(\tau)$ which is given semiclassically by a sum over orbit pairs. A method based on correlated orbit pairs, of Müller et al. (2004, 2005), involves considering all periodic orbits with self-encounters, or regions where the orbit approaches itself closely. For quantum chaotic systems, the series expansion obtained from those orbits for the form factor for small τ, was shown to agree with the expansion obtained from RMT. In this thesis we have shown that similar methods can be applied in more general situations, and that the expansions so obtained indeed also agree with small τ RMT predictions.

The first case we considered was parametric correlations, where we compare the density of states at two slightly different values of an external parameter (as well as at different energy values). This parameter preserves the symmetry of the system, and we assume that the parametric velocities of long periodic orbits follow a Gaussian distribution (Goldberg et al., 1991; Ozorio de Almeida et al., 1998). It is important to stress however that encounters, where encounter stretches are close together, have to be treated carefully. The stretches will all be affected by the parameter in almost the same way, and therefore we can not treat them as being uncorrelated, as we assume for the links between the encounters. This leads to a small difference, of the order of the encounter time (which itself is of the order of the Ehrenfest time), which nevertheless turns out to affect the result significantly and bring it in line with RMT.

The second case we considered was the extension to open systems, and we examined the form factor of the Wigner time delay for chaotic cavities. The time delay can be expressed in terms of the trapped periodic orbits of the system, and hence treated in a similar way. However, as the period of the orbits increases, the fraction of the orbits (of the closed system) that remain inside the system decreases exponentially. This effect is included in the Hannay–Ozorio de Almeida sum rule as an exponentially decreasing term which represents the average survival probability of the periodic orbits. Again a small correction arises due to the encounters, as for each encounter we have several orbit stretches that are close together. If one stretch escapes it is reasonable to assume that all of the stretches will also escape, and likewise if it survives then all should survive (Heusler et al., 2006). This dependence means that the time during which the orbit can escape is reduced by the encounters and the survival probability slightly increased. Despite being a small effect, this correction turns out to be important in the semiclassical limit and again it means that the result agrees with RMT. Taking one step further, we can also include parametric correlations, by treating each effect independently, and again obtain results for small τ that agree with the RMT expansions.

The assumption of independence allows us to consider an even more general case for open systems, where we include the effect of a symmetry breaking parameter (due to a magnetic field) and also compare our system at different values of a non-symmetry breaking parameter. The effect of the symmetry breaking parameter is also evaluated using the assumption that the parametric phases follow a Gaussian distribution, but now the contribution depends on the length of time that a periodic orbit and its partner spend travelling in opposite directions. This most general case, for a form factor $K(\tau, x, y, M)$ dependent on all three effects, encompasses all the other cases that we considered. Setting $y = 0$ preserves the time reversal symmetry, while the limit $y \to \infty$ breaks it. We can remove the parametric correlations by setting $x = 0$, and we can close the system by setting $M = 0$.

In all cases, for small τ, we find that periodic orbits with self-encounters allow us to recreate the universal form of the form factor in agreement with RMT and

in line with the conjecture of Bohigas et al. (1984). There is also an interesting analogue between our semiclassical expansions and the RMT ones. For each extra parameter we include, we add an extra factor to the augmented weight, dependent on the encounters and links. Likewise, for the RMT results, we also include an extra factor in the random matrix integrals.

In order to calculate our semiclassical periodic orbit expansions, we make the assumption that we can treat different effects independently, along with the approximations that are used for the spectral form factor $K(\tau)$ (see Müller et al., 2004, 2005). The fact that using the same methods we recreate RMT results boosts the idea that it is genuinely capturing the semiclassical contributions, even though a rigorous justification is lacking. One difficulty is to show that no other types of periodic orbit correlation contribute for small τ. However, if we wish to recreate RMT results for $\tau > 1$ directly from periodic orbits we would need additional types of correlated orbits.

One of the interesting properties of the Wigner time delay is that there are two semiclassical pictures of it - one in terms of the trapped periodic orbits and a second in terms of scattering trajectories that enter and subsequently leave the system. As one of the main results of this thesis, we showed that these two pictures agree with each other at the semiclassical level. Starting from the semiclassical picture in terms of pairs of scattering trajectories, we were able to recreate the average time delay by considering correlated trajectories with self-encounters, using a method which is analogous to the strategy adopted in previous work for the conductance (Heusler et al., 2006).

Obtaining the periodic orbit terms, however, required the evaluation of a new type of trajectory correlation that has not been treated before. This allowed us to complete the semiclassical agreement between the two pictures of the time delay. The key idea involved considering pairs of trajectories that are linked to the trapped periodic orbits, and which were shown to recreate the contribution of the orbits in the time delay. If we take a trajectory that approaches a periodic orbit closely, in that it follows the orbit for several traversals before leaving, we can find a partner trajectory

that follows almost the same path, but follows the orbit an additional r times. Formally, we define such an interaction as a 'periodic orbit encounter', and this type of encounter has surprisingly similar properties to the self-encounters considered previously. By treating such trajectory pairs with a periodic orbit encounter, we were able to show that they recreate the contribution of the r-th repetition of the trapped periodic orbit in the time delay. A nice feature of this calculation is that we get no contribution from the periodic orbits that escape, as any trajectory that tried to wind around them would also escape.

For systems with time reversal symmetry we actually needed to include the possibility that the trajectory has a periodic orbit encounter plus additional self-encounters to obtain exact agreement between the two pictures (this possibility can also occur without time reversal symmetry, but the contributions cancel). The most interesting of these situations is when the self-encounter occurs near the periodic orbit, so that we have multiple encounter stretches that are close to the orbit and each stretch follows the orbit some number of times. We only considered the situation where the total number of traversals of the partner trajectory is r more than the original trajectory, but this type of encounter suggests that there may be other types of correlated trajectories. For example, the situation where $r = 0$ has a form which would suggest that it may contribute to the average part, rather than a periodic orbit term. Multiple encounters with the same periodic orbit (without also being a self-encounter) are also of interest.

The next place to study these new types of correlation is the semiclassical sum rule of Berry (1985), which is derived from a property of delta functions. If we give a delta function some width ϵ, square it and renormalize, then in the limit $\epsilon \to 0$ this recreates a delta function. As the density of states has a delta spike at each energy level of the quantum system, the same property should hold for the density of states as long as the energy levels are not degenerate. Explicitly, if we give the delta functions widths, by approximating with a Lorentzian function, we have the following relation

$$\lim_{\epsilon \to 0} 2\pi\epsilon d_\epsilon^2(E) = \bar{d}(E) + d^{\mathrm{osc}}(E)$$

Starting with the Gutzwiller trace formula, semiclassically this sum rule means that a double sum over periodic orbits recreates both the average density of states and a single sum over periodic orbits. This relation for periodic orbits is similar to equation (5.4.1) for the time delay. It is worth noting that the analogue of this relation for the zeros of the Riemann zeta function has been obtained by using the Hardy-Littlewood conjecture for correlations between prime numbers (see Connors, 1998).

The periodic orbits analogous to trajectories that encounter a trapped periodic orbit are those that accumulate on the homoclinic points of shorter periodic orbits in closed systems (Ozorio de Almeida, 1989). It is interesting to speculate whether a treatment of these types of orbits can recreate the periodic orbit terms of the above equation. A more speculative task would be to try and recreate the average density of states from periodic orbits, and to consider whether a new type of correlation, of which multiple encounters with $r = 0$ seems the most likely candidate, can allow us to do so. This result would provide the large τ behaviour of the spectral form factor as it implies that $K(\tau) \to 1$ as $\tau \to \infty$.

As well as the semiclassical demonstration of equation (5.4.1), we checked the agreement between the two pictures for the irreducible two-point correlation function of the time delay. From the quadruple sum over trajectories, we were able to extend the diagonal approximation (Lewenkopf and Vallejos, 2004a) to calculate the leading order result. Interestingly there are quadruplets with encounters that contribute at the same order as the diagonal approximation. Hence these quadruplets are needed to establish agreement with the leading order term calculated from the periodic orbit picture, which in turn agrees with the RMT result. We also showed that the unitarity of the semiclassical scattering matrix is preserved when all trajectories with encounters are included.

The demonstration in this thesis of equation (5.4.1) for the time delay, and the semiclassical sum rule, are examples of semiclassical relations that are outside the

remit of RMT. Although we have remained in a regime where universal RMT results are expected to hold, so that we can use the property of uniformity to simplify the calculations, these relations should also hold in other regimes. Treating these regimes, especially the border between the system specific and the universal (for example Ehrenfest time corrections for scattering trajectories examined by Whitney and Jacquod, 2006; Brouwer and Rahav, 2006), we effectively have to consider the fringes of the encounters. There we have trajectory stretches that remain reasonably close together before they decouple completely and start to wander uniformly. It is an interesting, though demanding, challenge to treat self- and periodic orbit encounters in this regime, but an ability to do so would add power to the semiclassical methods. Not only would periodic orbit expansions give an intuitive explanation of the universal quantum fluctuation statistics of individual chaotic systems, but they would also provide information beyond that available from the ensemble averages of RMT.

A   Recursion relations

In this Appendix, which is reproduced from Kuipers and Sieber (2007a), we are considering the parametric form factor for systems without time reversal symmetry. We will show here that all terms from correlated periodic orbits cancel, apart from the highest order terms from orbit pairs with only 2-encounters. We start with the augmented weight function of equation (3.1.24), where the exponentials have been expanded to first order

$$\frac{z_T(\boldsymbol{s}, \boldsymbol{u})}{L} \approx \frac{\mathrm{e}^{-\beta T} T (T - \sum_\alpha l_\alpha t_{\mathrm{enc}}^\alpha)^{L-1} \prod_\alpha (1 - l_\alpha (l_\alpha - 1) \beta t_{\mathrm{enc}}^\alpha)}{L! \Omega^{L-V} \prod_\alpha t_{\mathrm{enc}}^\alpha} \qquad (\mathrm{A.1})$$

The contribution of orbits with different types of encounters can then be calculated using the recipe given in section 2.2.5. First we need to find the term in the above equation where the encounter times cancel in the numerator and the denominator. To obtain a product of the V different encounter times in the numerator we can take r of them from the product over α and $V - r$ of them from the bracket with the exponent $L - 1$. The corresponding coefficient is obtained by combinatorial considerations. Then we sum over all values of r from 0 to V, and the result is

$$\frac{z_T(\boldsymbol{s}, \boldsymbol{u})}{L} \quad \Longrightarrow \quad \frac{\mathrm{e}^{-\beta T} T}{L! \Omega^{L-V}} \sum_{r=0}^{V} \frac{T^{L-V+r-1} \beta^r (L-1)! (-1)^V \prod l^{v_l}}{(L-V-1+r)! r!}$$

$$\times \sum_{\substack{\alpha_1, \dots, \alpha_r \\ \text{distinct}}} (l_{\alpha_1} - 1) \dots \times (l_{\alpha_r} - 1) \qquad (\mathrm{A.2})$$

We can now substitute this coefficient into equation (2.2.33), and evaluate the integrals using the semiclassical result in equation (2.2.25), to find the contribution to

157

the form factor of

$$
K_{\boldsymbol{v}}(\tau, x) \quad \sim \quad \kappa N(\boldsymbol{v}) \frac{e^{-B\tau}}{L} \sum_{r=0}^{V} \frac{\tau^{L-V+r+1} B^r (-1)^V \prod l^{v_l}}{(L-V-1+r)!\, r!}
$$
$$
\times \sum_{\substack{\alpha_1,\ldots,\alpha_r \\ \text{distinct}}} (l_{\alpha_1} - 1) \times \ldots \times (l_{\alpha_r} - 1) \tag{A.3}
$$

where we sum over all vectors $\boldsymbol{v}$ to obtain the semiclassical approximation to the parametric form factor.

We now proceed to derive the full expansion of the parametric form factor for small τ for the case of systems without time reversal symmetry. For this purpose we write the semiclassical expansion as $K(\tau, x) = \tau e^{-B\tau} + \sum_{n=2}^{\infty} K_{\boldsymbol{v}}(\tau, x)$ with $K_{\boldsymbol{v}}(\tau, x)$ from equation (A.3) expressed in the following form

$$
K(\tau, x) = \tau e^{-B\tau} + \sum_{n=2}^{\infty} \frac{e^{-B\tau}}{(n-2)!} \sum_{r=0}^{n-1} S_n[f_r(\boldsymbol{v})] \tau^{n+r} B^r \tag{A.4}
$$

where

$$
S_n[f_r(\boldsymbol{v})] = \sum_{\boldsymbol{v}}^{L-V+1=n} f_r(\boldsymbol{v}) \tilde{N}(\boldsymbol{v}), \qquad \tilde{N}(\boldsymbol{v}) = \frac{N(\boldsymbol{v})\,(-1)^V}{L} \prod_l l^{v_l} \tag{A.5}
$$

and the functions $f_r(\boldsymbol{v})$ are given by

$$
f_r(\boldsymbol{v}) = \frac{(L-V-1)!}{(L-V-1+r)!\, r!} \sum_{\substack{\alpha_1,\ldots,\alpha_r \\ \text{distinct}}} (l_{\alpha_1} - 1) \times \ldots \times (l_{\alpha_r} - 1) \tag{A.6}
$$

The first two functions are $f_0(\boldsymbol{v}) = 1$ and $f_1(\boldsymbol{v}) = 1$. We need to evaluate the quantities $S_n[f_r(\boldsymbol{v})]$ for $r < n$ and we now show that the quantities $S_n[f_r(\boldsymbol{v})]$, defined in equations (A.5) and (A.6), vanish for $r \leq n - 1$. The function $f_r(\boldsymbol{v})$ are defined in terms of a restricted sum in which all summation indices are distinct. As a first step this sum is expressed by unrestricted sums. How to do this by combinatorial sieving is discussed, for example, in Section 4 of Rudnick and Sarnak (1996). We first introduce some notation. A set partition $\boldsymbol{F}$ of the set of integers $\{1, 2, \ldots r\}$ is a

decomposition of this set into disjoint subsets $[F_1, \ldots, F_\nu]$. Then $|F_1| + \ldots + |F_\nu| = r$ where $|F_i|$ is the number of elements in the set F_i. Let us define a generalization of the Kronecker delta-function

$$
\delta^{\boldsymbol{F}}_{\alpha_1, \ldots, \alpha_r} = \begin{cases} 1 & \text{if } \alpha_i = \alpha_j \text{ for all } i \text{ and } j \text{ such that } i, j \in F_k \text{ for some } k \\ 0 & \text{otherwise} \end{cases} \tag{A.7}
$$

Then

$$
\sum_{\substack{\alpha_1, \ldots, \alpha_r \\ \text{distinct}}} [\ldots] = \sum_{\boldsymbol{F}} \mu(\boldsymbol{F}) \sum_{\alpha_1, \ldots, \alpha_r} \delta^{\boldsymbol{F}}_{\alpha_1, \ldots, \alpha_r} [\ldots] \tag{A.8}
$$

where the first sum of the right-hand side runs over all set partitions of the set of r integers, and the corresponding Möbius function is given by

$$
\mu(\boldsymbol{F}) = \prod_{i=1}^{\nu} (-1)^{|F_i| - 1} (|F_i| - 1)! \tag{A.9}
$$

If we apply this to the functions $f_r(\boldsymbol{v})$ we obtain

$$
f_r(\boldsymbol{v}) = \frac{(L - V - 1)!}{(L - V - 1 + r)! r!} \sum_{\boldsymbol{F}} \mu(\boldsymbol{F}) g_{\boldsymbol{F}}(\boldsymbol{v}) \tag{A.10}
$$

where

$$
g_{\boldsymbol{F}}(\boldsymbol{v}) = \left(\sum_k v_k (k - 1)^{|F_1|} \right) \times \ldots \times \left(\sum_k v_k (k - 1)^{|F_\nu|} \right) \tag{A.11}
$$

The expansion of the form factor $K(\tau)$ was evaluated in Müller et al. (2004, 2005) by using recurrence relations for the number of structures $N(\boldsymbol{v})$ corresponding to a vector $\boldsymbol{v}$. These recurrence relations were obtained by relating orbits with L links to orbits with $L - 1$ links by considering all possible ways of removing a link (i.e. letting its size shrink to zero). For systems without time reversal symmetry the relevant recurrence relation is

$$
v_2 \tilde{N}(\boldsymbol{v}) + \sum_{k \geq 2} v_{k+1}^{[k, 2 \to k+1]} k \tilde{N}(\boldsymbol{v}^{[k, 2 \to k+1]}) = 0 \tag{A.12}
$$

Here the vector $\boldsymbol{v}^{[k,2\to k+1]}$ is obtained from the vector $\boldsymbol{v}$ by decreasing the components v_k and v_2 by one and increasing the component v_{k+1} by one. Hence $L(\boldsymbol{v}^{[k,2\to k+1]}) = L(\boldsymbol{v}) - k - 2 + (k+1) = L(\boldsymbol{v}) - 1$ and $V(\boldsymbol{v}^{[k,2\to k+1]}) = V(\boldsymbol{v}) - 1$. In order to obtain the coefficient of the form factor expansion one has to sum over the numbers $N(\boldsymbol{v})$ for all vectors for which $L(\boldsymbol{v}) - V(\boldsymbol{v}) + 1 = n$. The recurrence relation may be used for this purpose, because one can show that for each k

$$\sum_{\boldsymbol{v}}^{L-V+1=n} v_{k+1}^{[k,2\to k+1]} h(\boldsymbol{v}^{[k,2\to k+1]}) = \sum_{\boldsymbol{v}'}^{L'-V'+1=n} v_{k+1}' h(\boldsymbol{v}') \tag{A.13}$$

where $h(\boldsymbol{v})$ is some function of $\boldsymbol{v}$. One condition is that $v_1 = v_1^{[k,2\to k+1]} = 0$, because the vectors describe encounter regions which contain at least two orbit stretches. Summing the recurrence relation in equation (A.12) over $\boldsymbol{v}$ yields

$$0 = S_n \left[v_2 + \sum_{k\geq 2} v_{k+1} k \right] = S_n[L - V] = (n-1)S_n[1] \tag{A.14}$$

This shows, for example, that all off-diagonal terms of the form factor $K(\tau, 0)$ vanish (Müller et al., 2004, 2005).

We want to show in the following that $S_n[g_{\boldsymbol{F}}(\boldsymbol{v})] = 0$ if $r < n - 1$. We consider first the case when the partition consists of only one subset F_1 with $|F_1| = r$. Then $g_{\boldsymbol{F}}(\boldsymbol{v}) = g_r(\boldsymbol{v})$ where

$$g_r(\boldsymbol{v}) = \sum_k v_k (k-1)^r \tag{A.15}$$

We show that $S_n[g_r(\boldsymbol{v})] = 0$ if $r < n - 1$ by induction. The statement is true for $r = 0$, because $S_n[1] = 0$ by equation (A.14). Now we fix a value of $r < n - 1$ and assume that the statement is true for all smaller values of r. From the definition in equation (A.15), it follows that

$$g_r(\boldsymbol{v}^{[k,2\to k+1]}) = g_r(\boldsymbol{v}) - h_r(k), \quad h_r(k) = (k-1)^r - k^r + 1 \tag{A.16}$$

Points that will be important in the following are that $h_r(1) = 0$ and that $h_r(k)$ is

160

given by a finite power series in k whose highest order term is $-rk^{r-1}$.

Multiplying equation (A.12) by $g_r(\boldsymbol{v})$ and using relation in equation (A.16) we obtain

$$0 = v_2\, g_r(\boldsymbol{v})\, \tilde{N}(\boldsymbol{v}) + \sum_{k\geq 2} v'_{k+1} k g_r(\boldsymbol{v}')\tilde{N}(\boldsymbol{v}') + \sum_{k\geq 2} v'_{k+1} k h_r(k)\tilde{N}(\boldsymbol{v}') \qquad (A.17)$$

where $\boldsymbol{v}' = \boldsymbol{v}^{[k,2\to k+1]}$. In the last sum we can start the sum at $k = 1$, because $h_r(1) = 0$, and then change the summation index $k \to k-1$. After summing over all vectors $\boldsymbol{v}$ we obtain

$$
\begin{aligned}
0 &= S_n\left[v_2 g_r(\boldsymbol{v}) + \sum_{k\geq 2} v_{k+1} k g_r(\boldsymbol{v}) + \sum_{k\geq 2} v_k(k-1)h_r(k-1)\right] \\
&= S_n\left[(L-V)g_r(\boldsymbol{v}) - \sum_{k\geq 2} v_k r(k-1)^r + \dots\right] \qquad (A.18)
\end{aligned}
$$

In the second line we used that $v_2 + \sum_{k\geq 2}^{\infty} v_{k+1} k = \sum_{l\geq 2} v_l(k-1) = L - V$, and we wrote only the highest order term of $h_r(k-1)$. The lower order terms, denoted by the dots, involve powers $(k-1)^m$ with $m < r$ and can be neglected due to our induction assumption. Hence we find that

$$(n - r - 1)S_n[g_r(\boldsymbol{v})] = 0 \qquad (A.19)$$

so that indeed $S_n[g_r(\boldsymbol{v})] = 0$ if $r < n-1$. The proof for general $g_{\boldsymbol{F}}(\boldsymbol{v})$ is very similar. We consider the general form

$$g_{\boldsymbol{F}}(\boldsymbol{v}) = \prod_{i=1}^{\nu} g_{|F_i|}(\boldsymbol{v}) \qquad (A.20)$$

and we use again induction to prove that $S_n[g_{\boldsymbol{F}}] = 0$ if $r < n-1$. The statement is true for $r = 0$, and we fix a value of r and assume that it is true for all smaller values of r. In order to use the recurrence relation in equation (A.12) we note that

$$g_{\boldsymbol{F}}(\boldsymbol{v}) = \prod_{i=1}^{\nu} (g_{|F_i|}(\boldsymbol{v}^{[k,2\to k+1]}) + h_{|F_i|}(k)) \tag{A.21}$$

We multiply equation (A.12) by $g_{\boldsymbol{F}}(\boldsymbol{v})$ and use equation (A.21) to obtain

$$
\begin{aligned}
0 \;=\;& v_2 g_{\boldsymbol{F}}(\boldsymbol{v}) \tilde{N}(\boldsymbol{v}) + \sum_{k\geq 2} v'_{k+1} k g_{\boldsymbol{F}}(\boldsymbol{v}') \tilde{N}(\boldsymbol{v}') \\
&+ \sum_{k\geq 2} v'_{k+1} k \left(\prod_{i=1}^{\nu} (g_{|F_i|}(\boldsymbol{v}') + h_{|F_i|}(k)) - \prod_{i=1}^{\nu} g_{|F_i|}(\boldsymbol{v}') \right) \tilde{N}(\boldsymbol{v}')
\end{aligned} \tag{A.22}
$$

where $\boldsymbol{v}' = \boldsymbol{v}^{[k,2\to k+1]}$, as before, and we have added an additional term and subtracted it again. In the second sum we can start the sum at $k = 1$, because $h_i(1) = 0$ for all i, and then change the summation index $k \to k-1$. After summing over all vectors $\boldsymbol{v}$ we obtain

$$
\begin{aligned}
0 \;=\;& S_n \left[v_2 g_{\boldsymbol{F}}(\boldsymbol{v}) + \sum_{k\geq 2} v_{k+1} k g_{\boldsymbol{F}}(\boldsymbol{v}) \right. \\
&\left. + \sum_{k\geq 2} v_k (k-1) \left(\prod_{i=1}^{\nu} (g_{|F_i|}(\boldsymbol{v}) + h_{|F_i|}(k-1)) - \prod_{i=1}^{\nu} g_{|F_i|}(\boldsymbol{v}) \right) \right] \\
\;=\;& S_n \left[(L-V) g_{\boldsymbol{F}}(\boldsymbol{v}) + \sum_{k\geq 2} v_k (k-1) \sum_{j=1}^{\nu} (-|F_j|(k-1)^{|F_j|-1}) \prod_{i\neq j} g_{|F_i|}(\boldsymbol{v}) + \ldots \right]
\end{aligned} \tag{A.23}
$$

In the step from the first to the second line we expanded the first product, inserted the power series for the functions $h_{|F_i|}(k-1)$ and wrote only those terms that do not vanish due to the induction assumption. We obtain further

$$
\begin{aligned}
0 \;=\;& S_n \left[(L-V) g_{\boldsymbol{F}}(\boldsymbol{v}) - \sum_{j=1}^{\nu} |F_j| g_{|F_i|}(\boldsymbol{v}) \prod_{i\neq j} g_{|F_i|}(\boldsymbol{v}) + \ldots \right] \\
\;=\;& (n-1-r) S_n[g_{\boldsymbol{F}}(\boldsymbol{v})]
\end{aligned} \tag{A.24}
$$

which concludes the proof that $S_n[g_{\boldsymbol{F}}(\boldsymbol{v})] = 0$ for $r < n-1$.

As we have now shown that $S_n[f_r(\boldsymbol{v})] = 0$ for $r < n-1$, the only non-vanishing

162

terms in the expansion of equation (A.4) are those with $r = n - 1$. Since r satisfies $r \leq V$ we have $V \geq n - 1$. Together with the condition $L - V = n - 1$ we find that $2V \geq L$. This is only satisfied for orbit pairs with V 2-encounters for which $\boldsymbol{v} = (2)^V$ and $L = 2V$. The contribution of these orbit pairs to the form factors can be calculated explicitly. We obtain from equations (A.5) and (A.6) with $r = V = n - 1$, $L = 2V$, and $l_\alpha = 2$ for all α

$$S_n[f_{n-1}(\boldsymbol{v})] = \frac{(L - V - 1)!}{(L - V + n - 2)!}\tilde{N}(\boldsymbol{v}) = \frac{(-1)^{n-1}2^{n-1}(n-2)!}{(2n-2)!}N(\boldsymbol{v}) \qquad \text{(A.25)}$$

The number $N(\boldsymbol{v})$ for orbits with only 2-encounters was given in equation (3.1.27) and hence we obtain $S_n[f_{n-1}(\boldsymbol{v})] = 1/n!$ for odd n (and zero for even n). The complete expansion of the form factor is ($n = 2m + 1$)

$$K(\tau, x) = \tau e^{-B\tau} + e^{-B\tau} \sum_{m=1}^{\infty} \frac{\tau^{4m+1}B^{2m}}{(2m+1)!} = \frac{\sinh(B\tau^2)}{B\tau}e^{-B\tau} \qquad \text{(A.26)}$$

B Parametric correlation function

In this Appendix we consider the parametric two-point correlation function of the density of states. A recursion relation result of Nagao et al. (2007) will allow us to obtain the full parametric form factor for systems without time reversal symmetry. As well as providing a different way of arriving at the expansion to all orders, the treatment presented here ties in with the application of semiclassical methods to correlated scattering trajectories, which we considered in Chapter 5. In fact this connection was noticed by Müller et al. (2006) starting from their work on scattering trajectories (Heusler et al., 2006; Braun et al., 2006). The real advantage of this approach, however, is that the semiclassical contribution coming from the links and encounters can be separated.

Here we will start by recalling an observation from the Appendix of Müller et al. (2006), that the correlation function of the density of states can be written as the derivative of the correlation function of the staircase function

$$
\begin{aligned}
\tilde{R}_2(\omega, x) &= \left\langle \frac{d^{\mathrm{osc}}\left(E + \frac{\omega}{2\bar{d}} + \frac{x\rho}{2\sigma}, X + \frac{x}{2\sigma}\right) d^{\mathrm{osc}}\left(E - \frac{\omega}{2\bar{d}} - \frac{x\rho}{2\sigma}, X - \frac{x}{2\sigma}\right)}{\bar{d}^2} \right\rangle_{E,X} \\
&= -\frac{\mathrm{d}^2}{\mathrm{d}\omega^2} \left\langle N^{\mathrm{osc}}\left(E + \frac{\omega}{2\bar{d}} + \frac{x\rho}{2\sigma}, X + \frac{x}{2\sigma}\right) \right. \\
&\qquad \left. \times N^{\mathrm{osc}}\left(E - \frac{\omega}{2\bar{d}} - \frac{x\rho}{2\sigma}, X - \frac{x}{2\sigma}\right) \right\rangle_{E,X}
\end{aligned}
\tag{B.1}
$$

This relationship derives from the following. When we perform the derivatives we get

two terms which are the product of the oscillating part of the staircase function and its second derivative, and a third term which is the product of the oscillating parts of the density of states (like in the first line of equation (B.1)). Because of the average over an energy interval, which we can perform as an integral, we can integrate the mixed terms by parts to rewrite them in terms of the correlation function of the density of states, which results in the above relationship. The oscillating part of the staircase function can be written as a sum over the periodic orbits of the system

$$N^{\mathrm{osc}}(E) = \mathrm{Im}\frac{1}{\pi}\sum_{\gamma,r}\tilde{A}_{\gamma,r}\mathrm{e}^{\frac{\mathrm{i}}{\hbar}rS_\gamma(E)} \tag{B.2}$$

where γ labels the primitive periodic orbits and r their repetitions. The orbits have action S_γ and amplitudes $\tilde{A}_{\gamma,r} = \frac{A_{\gamma,r}}{T_\gamma}$. Here we take the imaginary part of the sum as opposed to the real part for the oscillating part of the density of states. When we make the usual semiclassical approximations, and ignore the repetitions of the primitive orbits, we can write the two point correlation function as the following second derivative of a double sum

$$\tilde{R}_2(\omega,x) = -\frac{\mathrm{d}^2}{\mathrm{d}\omega^2}\frac{1}{4\pi^2}\sum_{\gamma,\gamma'}\left[\tilde{A}_\gamma\tilde{A}_{\gamma'}^*\mathrm{e}^{\frac{\mathrm{i}}{\hbar}(S_\gamma-S_{\gamma'})}\mathrm{e}^{\frac{\mathrm{i}x}{2\sigma\hbar}(Q_\gamma+Q_{\gamma'})}\mathrm{e}^{\frac{\mathrm{i}\omega}{2\hbar\bar{d}}(T_\gamma+T_{\gamma'})} + \mathrm{c.c.}\right] \tag{B.3}$$

When we perform the sum over the orbit pairs, we are considering correlated pairs with $T_\gamma \approx T_{\gamma'}$, so if we differentiate before summing we arrive at the correlation function of the density of states.

The advantage of using the staircase function and differentiating later, that Müller et al. (2006) noticed, is that, by removing the period from the prefactor, the contribution from each orbit pair can be separated into a product of contributions from the encounter regions and the links. We will follow their argument and include parametric correlations. Firstly we make the usual approximations for two correlated orbits with self-encounters, that they have the same Maslov indices and approximately the same period, so their contribution to the correlation function reduces to

166

$$\tilde{R}_2(\omega, x) = -\frac{\mathrm{d}^2}{\mathrm{d}\omega^2} \frac{1}{4\pi^2} \sum_\gamma \left[|\tilde{A}_\gamma|^2 \mathrm{e}^{\frac{\mathrm{i}}{\hbar}(S_\gamma - S_{\gamma'})} \mathrm{e}^{\frac{\mathrm{i}x}{\sigma\hbar}} Q_\gamma \mathrm{e}^{\frac{\mathrm{i}\omega}{\hbar\bar{d}}T_\gamma} + \text{c.c.} \right] \qquad \text{(B.4)}$$

For orbits of a particular structure, we find their contribution by considering the probability that an orbit will have a certain phase space separation (and action difference) using the weight function and then averaging over all orbits of a particular period using the equidistribution theorem. We then sum over all structures corresponding to the same vector $\boldsymbol{v}$ to find the contribution of that vector. For convenience we state the Hannay–Ozorio de Almeida sum rule for the sum over the stability amplitudes of orbits of period T

$$\sum_\gamma |\tilde{A}_\gamma|^2 \delta_\epsilon (T - T_\gamma) \sim \frac{1}{T}, \quad T \to \infty \qquad \text{(B.5)}$$

For the correlation function we then need to sum over all periods by integrating over all period times

$$\tilde{R}_2^{\boldsymbol{v}}(\omega, x) = -\frac{\mathrm{d}^2}{\mathrm{d}\omega^2} \frac{\kappa N(\boldsymbol{v})}{4\pi^2} \left[\int_0^\infty \mathrm{d}T \, \frac{\mathrm{e}^{\frac{\mathrm{i}\omega}{\hbar\bar{d}}T}}{T} \int \mathrm{d}\tilde{\boldsymbol{s}} \, \mathrm{d}\tilde{\boldsymbol{u}} \, \frac{w_T(\tilde{\boldsymbol{s}}, \tilde{\boldsymbol{u}})}{L} \mathrm{e}^{\frac{\mathrm{i}}{\hbar}\tilde{\boldsymbol{s}}\tilde{\boldsymbol{u}}} \mathrm{e}^{\frac{\mathrm{i}x}{\sigma\hbar}} Q_\gamma + \text{c.c.} \right]$$
$$\text{(B.6)}$$

When we recall the definition of the weight function

$$\frac{w_T(\tilde{\boldsymbol{s}}, \tilde{\boldsymbol{u}})}{L} = \frac{\int_0^T \mathrm{d}t_L \int_0^{T-t_{\text{enc}}} \mathrm{d}t_{L-1} \dots \int_0^{T-t_{\text{enc}}-t_{L-1}\dots-t_2} \mathrm{d}t_1}{L\Omega^{L-V} \prod_\alpha t_{\text{enc}}^\alpha} \qquad \text{(B.7)}$$

we see that it is contains $L - 1$ integrals over the different link lengths (or, equivalently, piercing points) and a factor T from the first integral over the different possible starting points. Müller et al. (2006) spotted that this factor T cancels with the factor $\frac{1}{T}$ from the Hannay–Ozorio de Almeida sum rule. Through a change of variables, the integral over the period time T can be re-expressed as an integral over the last link time. With the weight factor, the contribution now includes integrals over all the links times t_i. The orbit time is simply

$$T = \sum_{i=1}^{L} t_i + \sum_{\alpha=1}^{V} l_\alpha t_{\text{enc}}^\alpha \tag{B.8}$$

and with parametric correlations we also need to include the factor

$$\left\langle e^{\frac{ix}{\sigma\hbar}Q_\gamma} \right\rangle = e^{-\beta \sum_{i=1}^{L} t_i} e^{-\beta \sum_{\alpha=1}^{V} l_\alpha^2 t_{\text{enc}}^\alpha} \tag{B.9}$$

Then we can separate the integrals over the links and the phase space separations (on which the encounter times depend)

$$\tilde{R}_2^{\boldsymbol{v}}(\omega, x) \approx -\frac{d^2}{d\omega^2} \frac{\kappa N(\boldsymbol{v})}{4\pi^2 L} \left[\prod_{\alpha=1}^{V} \int d^{l_\alpha-1} \boldsymbol{s}_{\alpha j} \, d^{l_\alpha-1} \boldsymbol{u}_{\alpha j} \, \frac{e^{-\left(\beta l_\alpha - \frac{i\omega}{\hbar \bar{d}}\right) l_\alpha t_{\text{enc}}^\alpha}}{\Omega^{l_\alpha-1} t_{\text{enc}}^\alpha} e^{\frac{i}{\hbar} \sum_j \boldsymbol{s}_{\alpha j} \boldsymbol{u}_{\alpha j}} \right.$$

$$\left. \times \prod_{i=1}^{L} \int_0^\infty dt_i \, e^{-\left(\beta - \frac{i\omega}{\hbar \bar{d}}\right) t_i} + \text{c.c.} \right] \tag{B.10}$$

Now we can see why this factorization is so useful. The integral over each link simply gives a factor $\frac{1}{\left(\beta - \frac{i\omega}{\hbar \bar{d}}\right)}$, while the integral over each encounter, performed using equation (2.2.25), gives a factor of $\left(\beta l_\alpha - \frac{i\omega}{\hbar \bar{d}}\right) l_\alpha$. When we substitute $B = \beta T_{\text{H}}$, $T_{\text{H}} = 2\pi\hbar\bar{d}$, the contribution becomes

$$\tilde{R}_2^{\boldsymbol{v}}(\omega, x) \approx -\frac{d^2}{d\omega^2} \frac{\kappa N(\boldsymbol{v})}{4\pi^2 L} (-1)^V \left[\frac{\prod_{\alpha=1}^{V} (B l_\alpha - 2\pi i\omega) l_\alpha}{(B - 2\pi i\omega)^L} + \text{c.c.} \right] \tag{B.11}$$

because the Heisenberg times mutually cancel. The cancellation of the Heisenberg times allows us to specify simple diagrammatic rules for the parametric correlation function: each of the L links gives a factor $(B - 2\pi i\omega)$ in the denominator, while each encounter α gives a factor $(B l_\alpha - 2\pi i\omega) l_\alpha$ in the numerator. The contribution of orbits described by any vector $\boldsymbol{v}$ can then be calculated directly using these rules, and this is the real advantage of the factorization into links and encounters.

With the substitutions $B = 0$ and $\epsilon = \pi\omega$ in equation (B.11), this equation coincides with the result given by Müller et al. (2006). Performing the differential and summing over vectors, this leads to the non-parametric form factor $K(\tau)$ result

found previously by Müller et al. (2004, 2005)

When we sum over different structures, we want to look at the sum from orbits with the same value of $L - V$, as they contribute to the same powers of τ in the form factor. If we set $n = L - V$, then we can see that for a fixed n the structures with the most encounters will have n 2-encounters and a denominator of $(B - 2\pi\mathrm{i}\omega)^{2n}$. To compare the contributions of orbits with different vectors and the same n we will put them over the same denominator

$$\tilde{R}_2^n(\omega, x) \approx -\frac{\mathrm{d}^2}{\mathrm{d}\omega^2} \frac{\kappa}{4\pi^2} \left[\frac{Z_n}{(B - 2\pi\mathrm{i}\omega)^{2n}} + \text{c.c.} \right] \tag{B.12}$$

where the numerator Z_n is given by the following sum

$$Z_n = \sum_{\boldsymbol{v}}^{L-V=n} \frac{N(\boldsymbol{v})}{L}(-1)^V (B - 2\pi\mathrm{i}\omega)^{n-V} \prod_{\alpha=1}^{V} l_\alpha (Bl_\alpha - 2\pi\mathrm{i}\omega) \tag{B.13}$$

When the system does not have time reversal symmetry, we can evaluate this sum exactly using recursion relations. First we rewrite the sum as

$$\begin{aligned}
Z_n &= (B - 2\pi\mathrm{i}\omega)^n \sum_{\boldsymbol{v}}^{L-V=n} \frac{N(\boldsymbol{v})}{L}(-1)^V \prod_{\alpha=1}^{V} l_\alpha \frac{(Bl_\alpha - 2\pi\mathrm{i}\omega)}{(B - 2\pi\mathrm{i}\omega)} \\
&= (B - 2\pi\mathrm{i}\omega)^n \sum_{\boldsymbol{v}}^{L-V=n} \tilde{N}(\boldsymbol{v}) \prod_{\alpha=1}^{V} (1 + (l_\alpha - 1)z)
\end{aligned} \tag{B.14}$$

where $\tilde{N}(\boldsymbol{v}) = \frac{N(\boldsymbol{v})}{L}(-1)^V \prod_\alpha l_\alpha$ and $z = \frac{B}{(B - 2\pi\mathrm{i}\omega)}$.

From the recursion relations of Müller (2005), which link the number of structures with L links to the number of structures with one fewer link, Nagao et al. (2007) derived the recursion relations when parametric correlation terms are included. These extra terms, like the product in Z_n, make the sum over vectors $\boldsymbol{v}$ more difficult, but Nagao et al. (2007) noticed that when this sum is differentiated with respect to the variable z it satisfies the following equation

$$\left(n - z\frac{\partial}{\partial z} \right) \sum_{\boldsymbol{v}}^{L-V=n} \tilde{N}(\boldsymbol{v}) \prod_{\alpha=1}^{V} (1 + (l_\alpha - 1)z) = 0 \tag{B.15}$$

by using the recursion relation on the terms in the sum and then summing the result over all vectors and relabelling the indices. As the sum satisfies the above differential equation, it must be proportional to z^n. The only term with this power comes from a vector with V 2-encounters, and all other terms therefore cancel. The number of structures corresponding to this vector is given by the formula (of Müller, 2003) in equation (3.1.27). As such Nagao et al. (2007) were able to evaluate the following

$$\sum_{\boldsymbol{v}}^{L-V=n} \tilde{N}(\boldsymbol{v}) \prod_{\alpha=1}^{V} (1 + (l_\alpha - 1)z) = \begin{cases} \frac{(2n-1)!}{(n+1)!} z^n & \text{if } n \text{ even,} \\ 0 & \text{if } n \text{ odd} \end{cases} \tag{B.16}$$

from which it follows directly that

$$Z_n = \begin{cases} \frac{(2n-1)!}{(n+1)!} B^n & \text{if } n \text{ even,} \\ 0 & \text{if } n \text{ odd} \end{cases} \tag{B.17}$$

This means that the contribution to the correlation function of all orbits of fixed even n is given by

$$\tilde{R}_2^n(\omega, x) \approx -\frac{\mathrm{d}^2}{\mathrm{d}\omega^2} \frac{1}{4\pi^2} \left[\frac{(2n-1)!B^n}{(n+1)!(B-2\pi\mathrm{i}\omega)^{2n}} + \text{c.c.} \right] \tag{B.18}$$

which gives

$$\tilde{R}_2^n(\omega, x) \approx \left[\frac{(2n+1)!B^n}{(n+1)!(B-2\pi\mathrm{i}\omega)^{2n+2}} + \text{c.c.} \right] \tag{B.19}$$

This result also incorporates the diagonal approximation if we set $n = 0$. Each term is exactly the Fourier transform of

$$K^n(\tau, x) \approx \mathrm{e}^{-B\tau} \frac{B^n \tau^{2n+1}}{(n+1)!} \tag{B.20}$$

So when we sum over all even n this gives the following full result, for small τ

$$K(\tau, x) = \sum_{m=0} K^{2m}(\tau, x) = \frac{\sinh(B\tau^2)}{B\tau} \mathrm{e}^{-B\tau} \tag{B.21}$$

170

C   Periodic orbit encounters when $f > 2$

In this Appendix we show that we obtain the same diagrammatic rules in Table 5.4 for systems with more than two degrees of freedom ($f > 2$). This result means that we recover equation (5.4.47) and therefore show the semiclassical agreement of the two pictures of the time delay for systems with higher degrees of freedom. For such systems, the ($2f - 2$) eigenvalues of the stability matrix M_γ of the periodic orbit γ can either come in real pairs or loxodromic quartets. If we have m real pairs and n loxodromic quartets, these numbers satisfy the relation $m + 2n = f - 1$. For each of the real pairs i, with an eigenvalue $\Lambda_{\gamma,i}$ (where $|\Lambda_{\gamma,i}| > 1$) and its inverse, we have a stable direction s_i and an unstable one u_i. If the original trajectory ζ pierces the plane spanned by each pair of stable and unstable directions at the coordinates (u_i, s_i), then for each pair the action difference between it and the trajectory ζ', which traverses the periodic orbit an additional r times can be calculated as in section 5.4.1. The total action difference, from all m pairs, which can be calculated from the area of the triangles obtained connecting the first and last piercing points of ζ and ζ' and the periodic orbit is

$$\sum_{i=1}^{m} s_i u_i (1 - \Lambda_{\gamma,i}^{-r}) \tag{C.1}$$

With each loxodromic quartet j, where we have four eigenvalues of the form $\mathrm{e}^{\pm\lambda_{\gamma,j}T_\gamma \pm \mathrm{i}\phi_{\gamma,j}}$, the situation is more complicated. There is an eigenvalue $\Lambda_{\gamma,j}$ with

magnitude $|\Lambda_{\gamma,j}| > 1$ and its complex conjugate, as well as both their inverses. In the following we will use $\tilde{\Lambda}_{\gamma,j}$ to represent the magnitude ($\tilde{\Lambda}_{\gamma,j} = |\Lambda_{\gamma,j}| = e^{\lambda_{\gamma,j}T_\gamma}$). We have a stable plane, spanned by the real and imaginary parts of the stable eigenvector s_{1j} and s_{2j}, and likewise an unstable one with the directions u_{1j} and u_{2j}. As well as contracting in the stable plane and expanding in the unstable one, points are rotated in both planes as they are transported around the periodic orbit (Ozorio de Almeida, 1988). In these coordinates, the stable and unstable directions rotate by an angle of $\phi_{\gamma,j}$ clockwise as they move around the periodic orbit, and thus between each piercing of the Poincaré section. In general, the symplectic area of a rectangle bound by the piercing points (u_{1j}, u_{2j}) and (s_{1j}, s_{2j}) of the trajectory ζ in the Poincaré section, and the periodic orbit itself, is given by $s_{1j}u_{1j} + s_{2j}u_{2j}$, and is invariant under successive mappings from the Poincaré section to itself. To simplify matters, we will choose coordinates that rotate with the original trajectory ζ, so that both products $s_{1j}u_{1j}$ and $s_{2j}u_{2j}$ are invariant under transport around the periodic orbit.

To calculate the action difference, in these loxodromic coordinates, between the trajectory ζ which follows the periodic orbit k times and a partner that follows the orbit $k+r$ times, we examine the first and last piercing points of both trajectories. If the first piercing point of ζ, P_1, is at $(u_{1j}, u_{2j}, s_{1j}, s_{2j})$, it has coordinates (u_{1j}, u_{2j}) in the unstable plane directions at the first traversal of the Poincaré section of the periodic orbit. The partner trajectory, ζ', must have approximately the same unstable coordinates after an additional r traversals of the periodic orbit, so that it can leave almost along the same trajectory as ζ. Thus, if we map the point (u_{1j}, u_{2j}) backwards r times we have the approximate unstable coordinates of ζ', while since ζ' arrives almost along the same trajectory as ζ it has the same stable coordinates. To map (u_{1j}, u_{2j}) backwards r times, we rotate anticlockwise by $r\phi_{\gamma,j}$ and shrink by a factor $\tilde{\Lambda}_{\gamma,j}^r$, which we can write in matrix form as follows

$$\begin{pmatrix} u'_{1j} \\ u'_{2j} \end{pmatrix} \approx \tilde{\Lambda}_{\gamma,j}^{-r} \begin{pmatrix} \cos(r\phi_{\gamma,j}) & -\sin(r\phi_{\gamma,j}) \\ \sin(r\phi_{\gamma,j}) & \cos(r\phi_{\gamma,j}) \end{pmatrix} \begin{pmatrix} u_{1j} \\ u_{2j} \end{pmatrix} \qquad \text{(C.2)}$$

The first piercing point of ζ', P_1', is then $\approx (u_{1j}', u_{2j}', s_{1j}, s_{2j})$. The symplectic area of the triangle $OP_1'P_1$ is given by

$$\frac{1}{2}s_{1j}(u_{1j} - u_{1j}') + \frac{1}{2}s_{2j}(u_{2j} - u_{2j}') \tag{C.3}$$

which can also be written in matrix form

$$\frac{1}{2}\begin{pmatrix} u_{1j} & u_{2j} \end{pmatrix} \begin{pmatrix} 1 - \tilde{\Lambda}_{\gamma,j}^{-r}\cos(r\phi_{\gamma,j}) & -\tilde{\Lambda}_{\gamma,j}^{-r}\sin(r\phi_{\gamma,j}) \\ \tilde{\Lambda}_{\gamma,j}^{-r}\sin(r\phi_{\gamma,j}) & 1 - \tilde{\Lambda}_{\gamma,j}^{-r}\cos(r\phi_{\gamma,j}) \end{pmatrix} \begin{pmatrix} s_{1j} \\ s_{2j} \end{pmatrix} \tag{C.4}$$

To arrive at the final piercing point of ζ, P_k, we map the first point $\tilde{k}$ times, but because we rotate the coordinates as we do so, its unstable coordinate is approximately $(\tilde{\Lambda}_{\gamma,j}^{\tilde{k}}u_{1j}, \tilde{\Lambda}_{\gamma,j}^{\tilde{k}}u_{2j})$ while its stable coordinate is $\approx (\tilde{\Lambda}_{\gamma,j}^{-\tilde{k}}s_{1j}, \tilde{\Lambda}_{\gamma,j}^{-\tilde{k}}s_{2j})$. The final piercing point of ζ', P_{k+r}', has approximately the same unstable coordinates as P_k, but its stable coordinates have been mapped an additional r times. In matrix form, it has the stable coordinates given by

$$\begin{pmatrix} s_{1j}' \\ s_{2j}' \end{pmatrix} \approx \tilde{\Lambda}_{\gamma,j}^{-r} \begin{pmatrix} \cos(r\phi_{\gamma,j}) & \sin(r\phi_{\gamma,j}) \\ -\sin(r\phi_{\gamma,j}) & \cos(r\phi_{\gamma,j}) \end{pmatrix} \tilde{\Lambda}_{\gamma,j}^{-\tilde{k}} \begin{pmatrix} s_{1j} \\ s_{2j} \end{pmatrix} \tag{C.5}$$

The symplectic area covered by the triangle OP_kP_{k+r}' is the same as the triangle $OP_1'P_1$ (equation (C.4)). In total the area of both of them is

$$\hat{\boldsymbol{u}}_j^{\mathrm{T}} K_{\gamma,j}^{-r} \hat{\boldsymbol{s}}_j \tag{C.6}$$

where $\hat{\boldsymbol{s}}_j = (s_{1j}, s_{2j})$ and $\hat{\boldsymbol{u}}_j = (u_{1j}, u_{2j})$ and the matrix $K_{\gamma,j}^{-r} = 1 - \tilde{K}_j^{-r}$, where

$$\tilde{K}_{\gamma,j}^{-r} = \tilde{\Lambda}_{\gamma,j}^{-r} \begin{pmatrix} \cos(r\phi_{\gamma,j}) & \sin(r\phi_{\gamma,j}) \\ -\sin(r\phi_{\gamma,j}) & \cos(r\phi_{\gamma,j}) \end{pmatrix} \tag{C.7}$$

When we integrate later over these stable and unstable coordinates, the determinant of $K_{\gamma,j}^{-r}$ will be important (cf equation (5.4.42)), and it is given by

$$\det K_{\gamma,j}^{-r} = \left(1 - \tilde{\Lambda}_{\gamma,j}^{-r} \cos(r\phi_{\gamma,j})\right)^2 + \left(\tilde{\Lambda}_{\gamma,j}^{-r} \sin(r\phi_{\gamma,j})\right)^2 = |1 - \Lambda_{\gamma,j}^{-r}|^2 \qquad \text{(C.8)}$$

In fact, by diagonalising the matrix, we can effectively treat the loxodromic quartet as two pairs of coordinates, each of which provides an action difference term of $s_{ij} u_{ij} |1 - \Lambda_{\gamma,j}^{-r}|$, for $i = 1, 2$.

As we obtain an area from each loxodromic quartet, in total the action difference between ζ and ζ' is

$$S_\zeta - S_{\zeta'} = \sum_{i=1}^{m} s_i u_i (1 - \Lambda_{\gamma,i}^r) + \sum_{j=1}^{n} \hat{\boldsymbol{u}}_j^{\mathrm{T}} K_{\gamma,j}^{-r} \hat{\boldsymbol{s}}_j - r S_\gamma \qquad \text{(C.9)}$$

We can simplify this equation using the coordinate $(\boldsymbol{u}, \boldsymbol{s})$ of the piercing point of ζ. If the components are in order first along the m real eigenvalue pair directions then along the $2n$ loxodromic quartet direction, we can write this action difference as

$$S_\zeta - S_{\zeta'} = \boldsymbol{u}^{\mathrm{T}} K_\gamma^{-r} \boldsymbol{s} - r S_\gamma \qquad \text{(C.10)}$$

where the matrix $K_\gamma^{-r} = I - \tilde{K}_\gamma^{-r}$, and $\tilde{K}_\gamma^{-r}$ has 'diagonal' entries, first of the m values $\Lambda_{\gamma,i}^{-r}$, then the n (2×2) matrices $\tilde{K}_{\gamma,j}^{-r}$

$$\tilde{K}_\gamma^{-r} = \begin{pmatrix} \Lambda_{\gamma,1}^{-r} & \cdots & & & \\ \vdots & \ddots & & & \\ & & \Lambda_{\gamma,m}^{-r} & & \\ & & & \tilde{K}_{\gamma,1}^{-r} & \cdots \\ & & & \vdots & \ddots \end{pmatrix} \qquad \text{(C.11)}$$

The determinant of K_γ^{-r} will enter into our result, and satisfies

$$|\det K_\gamma^{-r}| = \prod_{i=1}^{m} |1 - \Lambda_{\gamma,i}^{-r}| \prod_{j=1}^{n} |1 - \Lambda_{\gamma,j}^{-r}|^2 \qquad \text{(C.12)}$$

In higher dimensions, the other trajectory differences between ζ and ζ' remain

the same, apart from the stability amplitudes of the trajectories. Expanding in the eigenbasis, to leading order in k we obtain

$$A_{\zeta'} \approx \frac{A_{\zeta}}{\prod_{i=1}^{m} |\Lambda_{\gamma,i}|^{\frac{r}{2}} \prod_{j=1}^{n} |\Lambda_{\gamma,j}|^{r}} \tag{C.13}$$

The contribution to the correlation function (cf equation (5.4.22)) then becomes

$$\begin{aligned}
C^{\gamma,r}(\epsilon) &\approx \sum_{a,b} \frac{T_{\gamma} \mathrm{e}^{-\frac{\mathrm{i}}{\hbar} r S_{\gamma}} \mathrm{e}^{\frac{\mathrm{i}\pi}{2} r \mu_{\gamma}} \mathrm{e}^{\frac{\mathrm{i}\epsilon}{2\hbar} r T_{\gamma}}}{T_{\mathrm{H}} \prod_{i=1}^{m} |\Lambda_{\gamma,i}|^{\frac{r}{2}} \prod_{j=1}^{n} |\Lambda_{\gamma,j}|^{r}} \int \mathrm{d}\boldsymbol{s}\, \mathrm{d}\boldsymbol{u}\, \frac{\mathrm{e}^{\frac{\mathrm{i}}{\hbar} \boldsymbol{u}^{\mathrm{T}} K_{\gamma}^{-r} \boldsymbol{s}} \mathrm{e}^{\frac{\mathrm{i}\epsilon}{\hbar} t_{\mathrm{enc}}^{\gamma}}}{\Omega t_{\mathrm{enc}}^{\gamma}} \\
&\quad \times \prod_{i=1}^{2} \int_{0}^{\infty} \mathrm{d}t_{i}\, \mathrm{e}^{-(\mu - \frac{\mathrm{i}\epsilon}{\hbar}) t_{i}} + (r \rightarrow -r)
\end{aligned} \tag{C.14}$$

where the integral over the phase space coordinates can be written in terms of the components

$$\mathrm{d}\boldsymbol{s}\, \mathrm{d}\boldsymbol{u} = \prod_{i=1}^{m} \mathrm{d}s_{i} \mathrm{d}u_{i} \prod_{j=1}^{n} \mathrm{d}\hat{\boldsymbol{s}}_{j} \mathrm{d}\hat{\boldsymbol{u}}_{j} \tag{C.15}$$

When we perform the integrals over $\boldsymbol{s}$ and $\boldsymbol{u}$, the result includes the term

$$\frac{\mathrm{i}\epsilon}{\hbar} \left[\frac{T_{\gamma} \mathrm{e}^{\frac{\mathrm{i}\pi}{2} r \mu_{\gamma}} \mathrm{e}^{\frac{\mathrm{i}\epsilon}{2\hbar} r T_{\gamma}}}{\prod_{i=1}^{m} |\Lambda_{\gamma,i}|^{\frac{r}{2}} |1 - \Lambda_{\gamma,i}^{-r}| \prod_{j=1}^{n} |\Lambda_{\gamma,j}|^{r} |1 - \Lambda_{\gamma,i}^{-r}|^{2}} \mathrm{e}^{-\frac{\mathrm{i}}{\hbar} r S_{\gamma}} + \mathrm{c.c.} \right] \tag{C.16}$$

By using the identity

$$\sqrt{|\det(M_{\gamma}^{r} - 1)|} = \prod_{i=1}^{m} |\Lambda_{\gamma,i}|^{\frac{r}{2}} |1 - \Lambda_{\gamma,i}^{-r}| \prod_{j=1}^{n} |\Lambda_{\gamma,j}|^{r} |1 - \Lambda_{\gamma,i}^{-r}|^{2} \tag{C.17}$$

we can rewrite equation (C.16) as

$$2 \frac{\mathrm{i}\epsilon}{\hbar} |A_{\gamma,r}| \cos\left(-\frac{1}{\hbar} r S_{\gamma} + \frac{\pi}{2} r \mu_{\gamma} + \frac{\tilde{\epsilon}\mu}{2} r T_{\gamma} \right) \tag{C.18}$$

This is the same diagrammatic rule we found for systems with 2 degrees of freedom, which was recorded in the third line of Table 5.4, and now we have seen that it also holds for systems with higher degrees of freedom.

When we allow a trajectory with self-encounters to also encounter a trapped

periodic orbit, the periodic orbit encounter can occur during one of the links, or at the same time as the self-encounter. When the periodic orbit encounter occurs in the links, we use the first three diagrammatic rules from Table 5.4, and we recover equation (5.4.31) for systems with higher degrees of freedom. When the periodic orbit encounter occurs at the same time as an l-encounter, we recall the action difference from the l piercing points $(\boldsymbol{u}_i, \boldsymbol{s}_i)$ of the self-encounter (equation (2.2.11) modified to the form of equation (5.4.35))

$$\Delta S_\alpha = \sum_{j=1}^{l} (\boldsymbol{s}_{\pi^j(1)} - \boldsymbol{s}_{\pi^{(j-1)}(1)}) \boldsymbol{u}_{\pi^j(1)} \tag{C.19}$$

The extra r_i traversals of the periodic orbit added to the encounter stretch that passes through $(\boldsymbol{u}_{\pi(i)}, \boldsymbol{s}_i)$ add an action difference of

$$\boldsymbol{u}_{\pi(i)}^{\mathrm{T}} K_\gamma^{-r_i} \boldsymbol{s}_i - r_i S_\gamma \tag{C.20}$$

so that the total action difference between the two trajectories is

$$\Delta S_{\alpha,\gamma,r} = \sum_{j=1}^{l} \boldsymbol{u}_j \boldsymbol{s}_j + \boldsymbol{u}_{\pi(j)}^{\mathrm{T}} \tilde{K}_\gamma^{-r_j} \boldsymbol{s}_j - r S_\gamma \tag{C.21}$$

where we have again made a change of index labels. Recording the l coordinates in the stable and unstable directions in vectors $\tilde{\boldsymbol{s}}$ and $\tilde{\boldsymbol{u}}$, this is equivalent to

$$\Delta S_{\alpha,\gamma,r} = \tilde{\boldsymbol{u}}^{\mathrm{T}} D \tilde{\boldsymbol{s}} - r S_\gamma \tag{C.22}$$

We can view the matrix D as an $l \times l$ matrix, whose elements are themselves matrices following

$$\tilde{D}_{ij} = \delta_{ij} I - \delta_{i\pi(j)} \tilde{K}_\gamma^{-r_j} \tag{C.23}$$

Because the permutation matrix is a single l-cycle, the determinant of D is simply given by

$$|\det D| = \prod_{i=1}^{m} |1 - \Lambda_{\gamma,i}^{-r}| \prod_{j=1}^{n} |1 - \Lambda_{\gamma,i}^{-r}|^2 \tag{C.24}$$

and we indeed recreate the diagrammatic rule in the last line of Table 5.4 for systems with higher degrees of freedom. When the self-encounter occurs at the same time as a periodic orbit encounter, we therefore recover equation (5.4.44), and hence our final semiclassical result (equation (5.4.47)).

Bibliography

Balian R. and Bloch C. (1974): 'Solution of the Schrödinger equation in terms of classical paths', *Ann. Phys.*, **85**, 514–545.

Baranger H.U., Jalabert R.A. and Stone A.D. (1993a): 'Weak localization and integrability in ballistic cavities', *Phys. Rev. Lett.*, **70**, 3876–3879.

Baranger H.U., Jalabert R.A. and Stone A.D. (1993b): 'Quantum-chaotic scattering effects in semiconductor microstructures', *Chaos*, **3**, 665–682.

Barth M., Kuhl U. and Stöckmann H.-J. (1999): 'Global versus local billiard level dynamics: The limits of universality', *Phys. Rev. Lett.*, **82**, 2026–2029.

Berry M.V. (1981): 'Quantizing a classically ergodic system: Sinai's billiard and the KKR method', *Ann. Phys.*, **131**, 163–216.

Berry M.V. (1985): 'Semiclassical theory of spectral rigidity', *Proc. Roy. Soc. A*, **400**, 229–251.

Berry M.V. and Tabor M. (1977): 'Level clustering in the regular spectrum', *Proc. Roy. Soc. A*, **356**, 375–394.

Bertelsen P., Ellegaard C., Guhr T., Oxborrow M. and Schaadt K. (1999): 'Measurement of parametric correlations in spectra of resonating quartz blocks', *Phys. Rev. Lett.*, **83**, 2171–2174.

Blümel R. and Smilansky U. (1990): 'Random-matrix description of chaotic scattering: Semiclassical approach', *Phys. Rev. Lett.*, **64**, 241–244.

Bohigas O., Giannoni M.J. and Schmit C. (1984): 'Characterization of chaotic quantum spectra and universality of level fluctuation laws', *Phys. Rev. Lett.*, **52**, 1–4.

Bowen R. (1972): 'The equidistribution of closed geodesics', *Am. J. Math.*, **94**, 413–423.

Braun P., Heusler S., Müller S. and Haake F. (2006): 'Semiclassical prediction for shot noise in chaotic cavities', *J. Phys. A: Math. Gen.*, **39**, L159–L165.

Brouwer P.W. and Rahav S. (2006): 'Semiclassical theory of the Ehrenfest time dependence of quantum transport in ballistic quantum dots', *Phys. Rev. B*, **74**, 075322.

Casati G., Valz-Gris F. and Guarneri I. (1980): 'On the connection between quantization of nonintegrable systems and statistical theory of spectra', *Lett. Nuovo Cimento*, **28**, 279–282.

Connors R.D. (1998): *Classical periodic orbit correlations and quantum spectral statistics*, Ph.D. thesis, University of Bristol.

Creagh S.C., Robbins J.M. and Littlejohn R.G. (1990): 'Geometrical properties of Maslov indices in the semiclassical trace formula for the density of states', *Phys. Rev. A*, **42**, 1907–1922.

Cvitanović P., Artuso R., Mainieri R., Tanner G. and Vattay G. (2005): *Chaos: Classical and Quantum*, Niels Bohr Institute, Copenhagen, `http://ChaosBook.org`.

Cvitanović P. and Eckhardt B. (1991): 'Periodic orbit expansions for classical smooth flows', *J. Phys. A: Math. Gen.*, **24**, L237–L241.

Dietz B., Heine A., Richter A., Bohigas O. and Leboeuf P. (2006): 'Spectral statistics in an open parametric billiard system', *Phys. Rev. E*, **73**, 035201.

Doron E., Smilansky U. and Frenkel A. (1990): 'Experimental demonstration of chaotic scattering of microwaves', *Phys. Rev. Lett.*, **65**, 3072–3075.

Eckhardt B. (1993): 'Correlations in quantum time delay', *Chaos*, **3**, 613–617.

Eckhardt B., Fishman S., Keating J., Agam O., Main J. and Müller K. (1995): 'Approach to ergodicity in quantum wave functions', *Phys. Rev. E*, **52**, 5893–5903.

Feynman R.P. (1948): 'Space-time approach to non-relativistic quantum mechanics', *Rev. Mod. Phys.*, **20**, 367–387.

Fisher D.S. and Lee P.A. (1981): 'Relation between conductivity and transmission matrix', *Phys. Rev. B*, **23**, 6851–6854.

Friedel J. (1952): 'The distribution of electrons round impurities in monovalent metals', *Phil. Mag.*, **43**, 153–189.

Fyodorov Y.V., Savin D.V. and Sommers H.-J. (1997): 'Parametric correlations of phase shifts and statistics of time delays in quantum chaotic scattering: Crossover between unitary and orthogonal symmetries', *Phys. Rev. E*, **55**, 4857–4860.

Fyodorov Y.V. and Sommers H.-J. (1996): 'Parametric correlations of scattering phase shifts and fluctuations of delay times in few-channel chaotic scattering', *Phys. Rev. Lett.*, **76**, 4709–4712.

Fyodorov Y.V. and Sommers H.-J. (1997): 'Statistics of resonance poles, phase shifts and time delays in quantum chaotic scattering: Random matrix approach for systems with broken time-reversal invariance', *J. Math. Phys.*, **38**, 1918–1981.

Gaspard P., Rice S.A., Mikeska H.J. and Nakamura K. (1990): 'Parametric motion of energy levels: Curvature distribution', *Phys. Rev. A*, **42**, 4015–4027.

Goldberg J., Smilansky U., Berry M.V., Schweizer W., Wunner G. and Zeller G. (1991): 'The parametric number variance', *Nonlinearity*, **4**, 1–14.

Gutzwiller M.C. (1967): 'Phase-integral approximation in momentum space and the bound state of an atom', *J. Math. Phys.*, **8**, 1979–2000.

Gutzwiller M.C. (1971): 'Periodic orbits and classical quantization conditions', *J. Math. Phys.*, **12**, 343–358.

Gutzwiller M.C. (1990): *Chaos in Classical and Quantum Mechanics*, Interdisciplinary Applied Mathematics, Springer, New York.

Haake F. (2000): *Quantum signatures of chaos*, Springer, Berlin, second edition.

Hannay J.H. and Ozorio de Almeida A.M. (1984): 'Periodic orbits and a correlation function for the semiclassical density of states', *J. Phys. A: Math. Gen.*, **17**, 3429–3440.

Heusler S. (2003): *Universal spectral fluctuations in the Hadamard-Gutzwiller model and beyond*, Ph.D. thesis, Universität Duisburg-Essen.

Heusler S., Müller S., Altland A., Braun P. and Haake F. (2007): 'Periodic-orbit theory of level correlations', *Phys. Rev. Lett.*, **98**, 044103.

Heusler S., Müller S., Braun P. and Haake F. (2004): 'Universal spectral form factor for chaotic dynamics', *J. Phys. A: Math. Gen.*, **37**, L31–L37.

Heusler S., Müller S., Braun P. and Haake F. (2006): 'Semiclassical theory of chaotic conductors', *Phys. Rev. Lett.*, **96**, 066804.

Hlushchuk Y., Kohler A., Bauch Sz., Sirko L., Blümel R., Barth M. and Stöckmann H.-J. (2000): 'Autocorrelation function of level velocities for ray-splitting billiards', *Phys. Rev. E*, **61**, 366–370.

Hussein M.S., Malta C.P., Pato M.P. and Tufaile A.P.B. (2002): 'Effect of symmetry breaking on level curvature distributions', *Phys. Rev. E*, **65**, 057203.

Jung C. (1986): 'Poincaré map for scattering states', *J. Phys. A: Math. Gen.*, **19**, 1345–1353.

Jung C. and Scholz H.J. (1987): 'Cantor set structures in the singularities of classical potential scattering', *J. Phys. A: Math. Gen.*, **20**, 3607–3617.

Keating J.P. and Müller S. (2007): 'Resummation and the semiclassical theory of spectral statistics', *Proc. Roy. Soc. A*, **463**, 3241–3250.

Kuipers J. and Sieber M. (2007a): 'Semiclassical universality of parametric spectral correlations', *J. Phys. A: Math. Theor.*, **40**, 935–948.

Kuipers J. and Sieber M. (2007b): 'Semiclassical expansion of parametric correlation functions of the quantum time delay', *Nonlinearity*, **20**, 909–926.

Kuipers J. and Sieber M. (2007c): 'The semiclassical relation between open trajectories and periodic orbits for the Wigner time delay', Preprint, arXiv:0711.4537.

Leboeuf P. and Sieber M. (1999): 'Universality in quantum parametric correlations', *Phys. Rev. E*, **60**, 3969–3972.

Lehmann N., Savin D.V., Sokolov V.V. and Sommers H.-J. (1995): 'Time delay correlations in chaotic scattering: random matrix approach', *Physica D*, **86**, 572–585.

Lewenkopf C.H., Müller A. and Doron E. (1992): 'Microwave scattering in an irregularly shaped cavity: Random-matrix analysis', *Phys. Rev. A*, **45**, 2635–2636.

Lewenkopf C.H. and Vallejos R.O. (2004a): 'Open orbits and the semiclassical dwell time', *J. Phys. A: Math. Gen.*, **37**, 131–136.

Lewenkopf C.H. and Vallejos R.O. (2004b): 'Classical-quantum correspondence for the scattering dwell time', *Phys. Rev. E*, **70**, 036214.

Lewenkopf C.H. and Weidenmüller H.A. (1991): 'Stochastic versus semiclassical approach to quantum chaotic scattering', *Ann. Phys.*, **212**, 53–83.

McDonald S.W. and Kaufman A.N. (1979): 'Spectrum and eigenfunctions for a Hamiltonian with stochastic trajectories', *Phys. Rev. Lett.*, **42**, 1189–1191.

Mehta M.L. (2004): *Random matrices*, Pure and Applied Mathematics, Elsevier, Amsterdam, third edition.

Miller W.H. (1975): 'The classical S-matrix in molecular collisions', *Adv. Chem. Phys.*, **30**, 77–136.

Mucciolo E.R., Capaz R.B., Altshuler B.L. and Joannopoulos J.D. (1994): 'Manifestation of quantum chaos in electronic band structures', *Phys. Rev. B*, **50**, 8245–8251.

Müller J. (2003): 'On a mysterious partition identity', Preprint.

Müller S. (2005): *Periodic-orbit approach to universality in quantum chaos*, Ph.D. thesis, Universität Duisburg-Essen.

Müller S., Heusler S., Braun P. and Haake F. (2006): 'Semiclassical approach to chaotic quantum transport', Preprint, arXiv:cond-mat/0610560.

Müller S., Heusler S., Braun P. and Haake F. (2007): 'Semiclassical approach to chaotic quantum transport', *New J. Phys.*, **9**, 12.

Müller S., Heusler S., Braun P., Haake F. and Altland A. (2004): 'Semiclassical foundation of universality in quantum chaos', *Phys. Rev. Lett.*, **93**, 014103.

Müller S., Heusler S., Braun P., Haake F. and Altland A. (2005): 'Periodic-orbit theory of universality in quantum chaos', *Phys. Rev. E*, **72**, 046207.

Nagao T., Braun P., Müller S., Saito K., Heusler S. and Haake F. (2007): 'Semiclassical theory for parametric correlation of energy levels', *J. Phys. A: Math. Theor.*, **40**, 47–63.

Ozorio de Almeida A.M. (1988): *Hamiltonian systems: Chaos and quantization*, Cambridge University Press, Cambridge.

Ozorio de Almeida A.M. (1989): 'On the quantisation of homoclinic motion', *Nonlinearity*, **2**, 519–540.

Ozorio de Almeida A.M., Lewenkopf C.H. and Mucciolo E.R. (1998): 'Semiclassical limit of universal parametric density correlations', *Phys. Rev. E*, **58**, 5693–5703.

Parry W. and Pollicott M. (1990): 'Zeta functions and the periodic orbit structure of hyperbolic dynamics', *Astérisque*, **187–188**.

Pato M.P., Schaadt K., Tufaile A.P.B., Ellegaard C., Nogueira T.N. and Sartorelli J.C. (2005): 'Universality of rescaled curvature distributions', *Phys. Rev. E*, **71**, 037201.

Percival I.C. (1973): 'Regular and irregular spectra', *J. Phys. B*, **6**, L229–L232.

Richter K. (2000): *Semiclassical theory of mesoscopic quantum systems*, Springer, Berlin.

Richter K. and Sieber M. (2002): 'Semiclassical theory of chaotic quantum transport', *Phys. Rev. Lett.*, **89**, 206801.

Robbins J.M. (1991): 'Maslov indices in the Gutzwiller trace formula', *Nonlinearity*, **4**, 343–363.

Rudnick Z. and Sarnak P. (1996): 'Zeros of principal L-functions and random matrix theory', *Duke Math. J.*, **81**, 269–322.

Saito K. and Nagao T. (2006): 'Spectral form factor for chaotic dynamics in a weak magnetic field', *Phys. Lett. A*, **352**, 380–385.

Schaadt K. and Kudrolli A. (1999): 'Experimental investigation of universal parametric correlators using a vibrating plate', *Phys. Rev. E*, **60**, 3479–3482.

Shushin A. and Wardlaw D.M. (1992): 'Properties of time delay and S-matrix for chaotic scattering on a leaky surface of constant negative curvature', *J. Phys. A: Math. Gen.*, **25**, 1503–1515.

Sieber M. (2000): 'Spectral statistics in chaotic systems with a point interaction', *J. Phys. A: Math. Gen.*, **33**, 6263–6278.

Sieber M. (2002): 'Leading off-diagonal approximation for the spectral form factor for uniformly hyperbolic systems', *J. Phys. A: Math. Gen.*, **35**, L613–L619.

Sieber M. (2003): 'Semiclassical approach to spectral correlation functions', Preprint.

Sieber M. and Richter K. (2001): 'Correlations between periodic orbits and their rôle in spectral statistics', *Phys. Scr.*, **T90**, 128–133.

Simons B.D. and Altshuler B.L. (1993a): 'Universal velocity correlations in disordered and chaotic systems', *Phys. Rev. Lett.*, **70**, 4063–4066.

Simons B.D. and Altshuler B.L. (1993b): 'Universalities in the spectra of disordered and chaotic systems', *Phys. Rev. B*, **48**, 5422–5438.

Simons B.D., Hashimoto A., Courtney M., Kleppner D. and Altshuler B.L. (1993): 'New class of universal correlations in the spectra of hydrogen in a magnetic field', *Phys. Rev. Lett.*, **71**, 2899–2902.

Smith F.T. (1960): 'Lifetime matrix in collision theory', *Phys. Rev.*, **118**, 349–356.

Spehner D. (2003): 'Spectral form factor of hyperbolic systems: leading off-diagonal approximation', *J. Phys. A: Math. Gen.*, **36**, 7269–7290.

Stöckmann H.-J. (1999): *Quantum chaos: An introduction*, Cambridge University Press, Cambridge.

Szafer A. and Altshuler B.L. (1993): 'Universal correlation in the spectra of disordered systems with an Aharonov-Bohm flux', *Phys. Rev. Lett.*, **70**, 587–590.

Turek M. and Richter K. (2003): 'Leading off-diagonal contribution to the spectral form factor of chaotic quantum systems', *J. Phys. A: Math. Gen.*, **36**, L455–L462.

Turek M., Spehner D., Müller S. and Richter K. (2005): 'Semiclassical form factor for spectral and matrix element fluctuations of multidimensional chaotic systems', *Phys. Rev. E*, **71**, 016210.

Vallejos R.O., Ozorio de Almeida A.M. and Lewenkopf C.H. (1998): 'Quantum time delay in chaotic scattering: a semiclassical approach', *J. Phys. A: Math. Gen.*, **31**, 4885–4897.

von Oppen F. (1994): 'Exact distribution of eigenvalue curvatures of chaotic quantum systems', *Phys. Rev. Lett.*, **73**, 798–801.

von Oppen F. (1995): 'Exact distributions of eigenvalue curvatures for time-reversal-invariant chaotic systems', *Phys. Rev. E*, **51**, 2647–2650.

Wardlaw D.M. and Jaworski W. (1989): 'Time delay, resonances, Riemann zeros and chaos in a model quantum scattering system', *J. Phys. A: Math. Gen.*, **22**, 3561–3575.

Whitney R.S. and Jacquod Ph. (2006): 'Shot noise in semiclassical chaotic cavities', *Phys. Rev. Lett.*, **96**, 206804.

Wigner E.P. (1955): 'Lower limit for the energy derivative of the scattering phase shift', *Phys. Rev.*, **98**, 145–147.

Wilkinson M. (1988): 'Statistical aspects of dissipation by Landau-Zener transitions', *J. Phys. A: Math. Gen.*, **21**, 4021–4037.

Wilkinson M. (1989): 'Statistics of multiple avoided crossings', *J. Phys. A: Math. Gen.*, **22**, 2795–2805.

Wilkinson M. (1990): 'Diffusion and dissipation in complex quantum systems', *Phys. Rev. A*, **41**, 4645–4652.